

FORMULATION AND PHYSICO-CHEMICAL CHARACTERISATION OF NOVEL FILMS AND WAFERS FOR MUCOSAL DRUG DELIVERY

By

Farnoosh Kianfar {Pharm-D, MSc (Enterprise in Bioscience)}

A thesis submitted in partial fulfilment of the requirements of the University of Greenwich
for the Degree of Doctor of Philosophy

November, 2011

School of Science
University of Greenwich, Medway Campus,
Chatham Maritime,
Kent ME4 4TB, UK



the
UNIVERSITY
of
GREENWICH

DECLARATION

“I certify that this work has not been accepted in substance for any degree, and is not concurrently being submitted for any purpose, other than that of the PhD thesis being studied at the University of Greenwich. I also declare that this work is the result of my own investigations except where otherwise identified by references and that I have not plagiarised another’s work”.

_____ Ms F. Kianfar (Candidate)

.....

Thesis Supervisors

_____ Dr. J. S. Boateng (First Supervisor)

_____ Dr. M. A. Antonijevic (Second Supervisor)

_____ Prof. B. Z. Chowdhry (RAE Supervisor)

30/11/2011

ACKNOWLEDGMENT

Firstly, I would like to express my sincere gratitude to Dr J.S. Boateng, Dr M.A. Antonijevic and Prof. B.Z. Chowdhry for their dedicated support during my research studies.

Most importantly, I wish to express my heartfelt gratitude to my mother, and family for their continuous support throughout my studies.

DEDICATION

This thesis is dedicated to:

my precious twin sons

ARYA & SAM

and my supportive parents

ABSTRACT***FORMULATION AND PHYSICO-CHEMICAL CHARACTERISATION OF NOVEL FILMS AND WAFERS FOR MUCOSAL DRUG DELIVERY***

Development of novel drug delivery systems has become a major research endeavour in the pharmaceutical industry. Drug administration via the traditional oral route (GIT) presents certain challenges including enzymatic and acid break down of labile drugs and first pass metabolism in the liver.

The research reported in this thesis involved the development of solvent cast films and freeze-dried wafers for the potential delivery of drugs via the buccal mucosa. The formulations were prepared from two polymers (κ -carrageenan (CAR) 911 and poloxamer 407 (P407)), two types of plasticizers (glycerol (GLY)) and various grades of polyethylene glycol (PEG) using paracetamol (PM), ibuprofen (IBU) and indomethacin (IND) as model drugs. The investigations involved extensive evaluation/characterisation of the initial formulation components and their optimum combinations to obtain the desired formulation by employing various physico-chemical characterisation techniques. Texture analysis was used to investigate the tensile properties (percent elongation and elastic modulus) of the films, the resistance of the films upon stretching as well as the behaviour of the films during handling. In the case of the wafers, texture analysis was used to determine the compressibility as well as *in vitro* mucoadhesive characteristics. The stability of both the initial components and within the formulated films or wafers was studied using thermal analysis (HSM, TGA and DSC). Thermogravimetric analysis (TGA) was used to estimate the residual water content of both formulations. XRPD was used to assess the different forms (amorphous or crystalline) of the various components, including the model drugs. Scanning electron microscopy provided topographic information with regard to surface architecture of the films and wafers. The drug loaded films and wafers were further characterised for chemical stability of the drugs, after storage at room temperature for twelve months and drug dissolution profiles using simulated saliva as dissolution medium.

The results of the preliminary development and optimization experiments showed that gels prepared with 2.5% (w/w) CAR 911, in combination with 4% (w/w) P407 and 5.5% (w/w) PEG 600 produced a flexible film with 'ideal' characteristics and was selected for drug incorporation. However, the concentration of PEG was increased to 6% (w/w) in the presence

of 1.6% w/w PM, and 6.5% (w/w) PEG with 0.6% (w/w) IND and 0.8% w/w IBU (concentrations relative total drug weight of film matrix).

The initial results from the wafers demonstrated that a flexible wafer, obtained by freeze-drying (incorporating an annealing step), could be produced from a gel containing 2% (w/w) CAR 911 in combination with 4% (w/w) P407 and 4.4% (w/w) PEG 600. Addition of 0.8% (w/w) IBU also increased the flexibility of the wafer approximately two fold, whilst the flexibility of 1.8% (w/w) PM and 0.6% (w/w) IND loaded wafers was slightly reduced. TGA experiments indicated a water content of approximately 5% and 1% for films and wafers, respectively. SEM experiments revealed an even surface without any macroscopic pores for the film whilst the microstructure of the wafer was observed as being porous. The data from DSC experiments demonstrated interactions between P407 and PEG 600 during film formation. Furthermore, the conversion of the originally added model crystalline drugs into the amorphous form within the film and wafers was ascertained by DSC and confirmed by XRPD.

Farnoosh Kianfar {Pharm-D, MSc (Enterprise in Bioscience)}

CONTENTS

DECLARATION.....	II
ACKNOWLEDGMENT.....	III
ABSTRACT.....	IV
CONTENTS.....	VI
ABBREVIATIONS.....	XI
Summary of project aims & objectives.....	XII
Chapter 1 : General introduction.....	1
1.1 Drug delivery systems.....	2
1.2 Classification of dosage forms.....	2
1.3 Routes of drug administration.....	3
1.3.1 Oral route.....	4
1.3.2 Injectable dosage forms.....	6
1.3.3 Topical route.....	7
1.4 Novel drug delivery systems.....	8
1.4.1 Site specific delivery systems.....	9
1.4.2 Time directed delivery.....	10
1.4.3 Alternative delivery routes.....	10
1.5 Mucosal dosage forms.....	11
1.5.1 Buccal drug delivery.....	12
1.5.2 The buccal mucosa.....	15
1.5.3 Drug absorption via buccal route.....	17
1.6 Hydrogel based systems.....	18
1.7 Drug release kinetics.....	20
1.8 Mechanism of drug release from hydrogels.....	21
1.9 Erodible systems.....	25
1.9.1 Molecular basis of polymer dissolution.....	26

1.10	Solvent cast films.....	27
1.10.1	Film forming techniques	29
1.11	Freeze dried wafers.....	31
1.11.1	Freeze-drying	32
1.11.2	Advantages of freeze-drying.....	35
1.12	Physical properties of polymeric dosage forms.....	36
1.12.1	Mechanical (tensile) characteristics	36
1.12.2	Bioadhesivity	38
1.13	Drugs in the solid state	41
1.13.1	Thermal properties of amorphous compounds	43
1.13.2	Glass transition.....	43
1.13.3	Determination of glass transition temperature	44
1.13.4	Factors affecting the glass transition temperature	45
1.14	Thermal analysis techniques (TA).....	45
1.15	Polymers	46
1.15.1	Poloxamer 407 (P407)	46
1.15.2	Carrageenan	47
	Chapter 2 : Experimental.....	52
2.1.	Materials and equipment	52
2.1.1	Chemicals.....	52
2.1.2	Equipment & instruments	53
2.1.3	Consumables	54
2.2	DSC analysis of physical mixtures of starting materials.....	54
2.3	Formulation development of solvent cast films	55
2.3.1	Gel preparation.....	55
2.3.2	Drug loading into optimized films.....	57
2.3.3	Film formation	57
2.4	Characterisation of solvent cast films	59
2.4.1	Texture analysis	59
2.4.2	Hot stage microscopy (HSM)	61

2.4.3	Thermogravimetry (TGA)	63
2.4.4	Differential scanning calorimetry (DSC).....	66
2.4.5	Scanning electron microscopy (SEM)	70
2.4.6	X-ray powder diffraction (XRPD).....	72
2.4.7	Stability test by high performance liquid chromatography (HPLC).....	74
2.5	Formulation development of freeze-dried wafers	75
2.5.1	Gel preparation.....	75
2.5.2	Drug loading into optimized gels.....	76
2.5.3	DSC analysis to determine optimized freeze-drying cycle incorporating an annealing step.....	77
2.5.4	Preparation of freeze-dried wafers.....	77
2.6	Characterisation of freeze-dried wafers	80
2.6.1	Texture analysis	80
2.6.2	Hot stage microscopy (HSM)	81
2.6.3	Thermogravimetry (TGA)	81
2.6.4	Differential scanning calorimetry (DSC).....	82
2.6.5	Scanning electron microscopy (SEM)	82
2.6.6	X-ray powder diffraction (XRPD).....	82
2.6.7	Stability test by HPLC	83
2.7	Hydration, dissolution and mucoadhesion of the films and wafers	83
2.7.1	Hydration and swelling studies.....	83
2.7.2	Drug dissolution studies.....	84
2.7.3	Mucoadhesion studies for films and wafers.....	85
2.8.	Statistical analysis	86
Chapter 3 : DSC studies of interaction between starting materials (physical mixtures).....		87
3.1	Study of the interaction between PEG 600 and P407	87
3.2	DSC analysis for interaction between the compounds in films	94
3.3	Effect of polymers on model drug.....	95

Chapter 4 : Development and characterisation of films.....	99
4.1 Film development.....	99
4.1.1 Gel formulation.....	99
4.1.2 Drying time.....	100
4.1.3 Visual evaluation of initial gels and resulting films.....	101
4.1.4 Evaluation of drug loaded films.....	102
4.1.5 Poloxamer and carrageenan ratios.....	102
4.1.6 Films plasticised with GLY or PEG.....	104
4.1.7 Drug loading results.....	107
4.2 Characterisation of physical and mechanical properties of films.....	107
4.2.1 Texture analysis.....	107
4.2.2 HSM results.....	110
4.2.3 TGA results (water content).....	110
4.2.4 DSC results (melting point, glass transition).....	112
4.2.5 SEM results.....	118
4.2.6 XRPD results.....	121
4.2.7 Stability studies.....	128
Chapter 5 : Lyophilized wafer development and characterisation.....	130
5.1 Formulation development.....	130
5.1.1 Gel formation.....	130
5.1.2 DSC application to develop the freeze drying cycle.....	130
5.1.3 Freeze-drying process.....	133
5.1.4 Results after freeze-drying.....	135
5.1.5 Visual evaluation of wafers.....	136
5.2 Wafer characterisation.....	138
5.2.1 Texture analysis results.....	138
5.2.2 TGA results (water content).....	142
5.2.3 DSC results.....	144
5.2.4 SEM results.....	148
5.2.5 XRPD results.....	151

5.2.6	Stability studies	155
Chapter 6 : Comparison of hydration, dissolution and mucoadhesive properties of solvent cast films and freeze-dried wafers		
		157
6.1	Hydration\swelling profile	157
6.1.1	Films hydration and swelling	157
6.1.2	Wafer hydration and swelling	160
6.2	Drug dissolution profile	165
6.2.1	Film drug dissolution profiles	166
6.2.2	Wafer drug dissolution profiles	171
6.3	<i>In-vitro</i> mucoadhesivity	175
6.3.1	Film mucoadhesion	176
6.3.2	Wafer mucoadhesion	177
Chapter 7 : Conclusions & future work.....		
		181
7.1	Conclusions	181
7.2	Future work	183
Chapter 8 : References.....		
		184
Chapter 9 : Appendix.....		
		199
9.1	Published Manuscripts	199
9.2	Oral presentations.....	199
9.3	Conference posters	200
9.4	Supplementary results	207

ABBREVIATIONS

Symbol	Description
AF	Adhesion force
CAR	Carrageenan
CF	Compression force
DSC	Differential scanning calorimetry
GLY	Glycerol
HPLC	High Performance Liquid Chromatography
IBU	Ibuprofen
IND	Indomethacin
IM	Intra muscular
IV	Intra venous
PM	Paracetamol
PEG	Polyethylene glycol
P407	Poloxamer
SEM	Scanning electron microscopy
T_g	Glass transition temperature
TGA	Thermogravimetric analysis
UV	Ultra-violet
WOA	Work of adhesion
WOC	Work of compression
XRPD	X-ray powder diffraction

Summary of project aims & objectives

The aim of this project was to design and formulate novel mucosal drug delivery systems in the form of polymer (CAR and P407) based solvent cast films and freeze-dried wafers as potential matrices to deliver drugs via the buccal mucosa.

Objectives include:

- design and formulation of hydrogel based films and wafers with optimum mucoadhesive characteristics. To achieve the foregoing, the choice of optimum ratios of drug and excipients were investigated in order to design the desired dosage form. This will potentially aid in effective delivery of active pharmaceutical agents via the buccal tissues.
- employing a range of analytical techniques (texture analysis, DSC, TGA, XRPD, SEM, dissolution studies and HPLC) to investigate the properties of starting materials and their corresponding formulations. Furthermore, the stability and possible transitions during gel formulation, solvent casting or freeze-drying and storage under a variety of stress conditions (which may cause alterations in the properties of the dosage form), will be evaluated. These will be followed by evaluation of the swelling, drug release and mucoadhesion properties of the final selected formulations.
- the development of dosage forms with improved dissolution and drug delivery properties based upon observations achieved from testing various formulations and investigating their physico-chemical properties.

Chapter 1 : General introduction

Active pharmaceutical ingredients are largely administered by two common routes i.e. oral or injection. However, previous studies have frequently demonstrated that these administration routes are not effective in all cases, and are also considered to have numerous side effects and disadvantages (Saxena, *et al.*, 2004; Morales and McConville, 2011; Table 1.1)

Table 1.1 Advantages and disadvantages of various pharmaceutical dosage forms (adapted from Fred, 1994).

Dosage forms	Solids	Liquids	Semi-solids
Advantages	<ul style="list-style-type: none"> ❖ More stable than liquids, with longer expiration dates ❖ Ease of shipping and handling ❖ Less shelf space needed ❖ No preservation requirements ❖ Accurate dosage (single dose) ❖ Suitable for sustained release formulations 	<ul style="list-style-type: none"> ❖ Faster action than solid dosage form as dissolution step is avoided ❖ Has more dosing flexibility in comparison to other forms ❖ May be more practical to administer than solids 	<ul style="list-style-type: none"> ❖ Localizes the drug at the site of action ❖ Undesired side effects are minimized ❖ Easy to administer ❖ Risk of over dosage is very low ❖ Easy application
Disadvantages	<ul style="list-style-type: none"> ❖ Concerns raised regarding the dissolution profile 	<ul style="list-style-type: none"> ❖ May have shorter expiry time ❖ May have unpleasant taste on tongue ❖ Not convenient as it requires careful measurement 	<ul style="list-style-type: none"> ❖ Not appropriate for systemic treatments ❖ Need to administer frequently as it is wiped off the skin quickly

In recent years, significant efforts have been made by pharmaceutical scientists to improve upon traditional and existing dosage forms by extensive research into alternative (novel) drug delivery systems. These vary from modifications of the existing formulations such as film (enteric) coated tablets to more sophisticated versions such as liposomes and nanoparticles to target specific routes or sites of action.

1.1 Drug delivery systems

Drug delivery involves the process of administering a pharmacological compound to attain a therapeutic effect in humans or animals. Most drug delivery systems consist of non-invasive peroral (via the mouth), topical (skin) or invasive parenteral (injections) dosage forms. However, as noted above, they have the disadvantage of lacking site specificity and eventual drug action at the target organ. The need for targeting drugs to particular tissues, thereby decreasing the level of undesired side effects, has led pharmaceutical formulators to explore alternative routes of drug administration or employ novel technologies to deliver active pharmacological agents to the site of action with minimal losses (Ansel, *et al.*, 1993., Loth, *et al.*, 2007).

One of the main objectives in novel drug delivery technology is protecting the patents of formulation technologies which include amending drug release profile, uptake, target organ disposition and elimination to improve efficacy and safety of the drug and patient convenience (Vogelson, *et al.*, 2001).

1.2 Classification of dosage forms

A dosage form is the physical form of a dose of a chemical compound which can be employed as a drug or medication. They are designed to transfer drug molecules to the site of action the drug induces the desired physiological/pharmacological action. There are several types of dosage forms commonly available including tablets, capsules, syrups, aerosol or inhaler, liquid injection, pure powder or solid crystal and natural or herbal forms obtained from plant or food sources (FDA, 2004). Each of these dosage forms can be further classified into three main groups based on their physical state i.e. solid, liquids and semi-solids (Table 1.1). They are employed to deliver a particular active compound, as various medical conditions require different routes of administration. Besides, a specific dosage form may be required for certain types of drugs, as a consequence of different factors such as chemical stability or pharmacokinetics (Breuer, *et al.*, 2009). Each type of dosage form has specific advantages and disadvantages (Table 1.1) that need to be addressed and considered in order to select the most appropriate dosage form and minimize side effects (Allen, 2004).

1.3 Routes of drug administration

The route of administration is, from a pharmacological perspective, the specific path via which a drug, fluid, poison, or other substance is transported into the body. A chemical compound should be transferred from the point of entry to the part of the body called the site of action where the desired action occurs and the role of the body's transport mechanisms to achieve this purpose is very important. Any kind of pharmacokinetic characteristics of a drug from absorption to distribution and elimination are vitally related and influenced by the route of administration (Breuer, *et al.*, 2009).

Table 1.2 Routes of drug administration (adapted from Merck manual, 2007).

Route of administrations			
Oral	Enteral/ digestive tract	Solids	Capsule · Pill · Tablet · Orally disintegrating tablet · Film · OROS (osmotic controlled release capsule)
		Liquids	Elixir · Emulsion · Suspension · Syrup · Tincture
	Respiratory tract	Inhaler (Metered-dose, Dry powder) · Nebulizer	
	Circulatory system	Sublingual administration	
Eye/ENT	Eye drop · Ear drop · Intranasal		
Transdermal	Emulsion (Ointment · Cream · Lotion · Gel · Paste · Film) · Medicated shampoo · Transdermal implant · Transdermal patch		
Injection/ parenteral	Subcutaneous (sc) · Intravenous (iv) · Intramuscular (im) · Intraosseous · Intraperitoneal (ip) · Intrathecal · Intracavernosal		
Vaginal	Pessary (vaginal suppository) · Vaginal ring · Douche · Intrauterine device		
Rectal	Suppository · Enema		

According to the FDA (2010), routes of administration can broadly be divided into three categories:

- 1) **topical**; local effect, substance is applied directly to the desired site of action.
- 2) **enteral**; the desired effect is systemic (non-local), drug is given via the digestive tract.
- 3) **parenteral**; desired effect is systemic, substance is given by routes (e.g. iv, im) other than the digestive tract

Other classifications and site specific drug administration routes are listed in Table 1.2. In recent years, there have been significant advances in the field of pharmacology and biopharmaceutics related to the administration of drugs to treat various conditions. Despite such improvements a significant proportion of pharmacological agents are still administered by the two common routes, (orally or by injection).

1.3.1 Oral route

The most common route of administering pharmacological agents is oral and generally formulated as tablet, capsule or a liquid based dosage forms which need to be swallowed (Liekweg, *et al.*, 2004). The oral route comprises the buccal cavity through the oesophagus and the gastrointestinal tract (GIT). The advantages and disadvantages of this route are summarised below.

Advantages

- 1) It is the most commonly used route.
- 2) The prices are considerably low and very economical.
- 3) Administration does not require special skills.
- 4) Self-medication is possible.
- 5) This route is convenient.
- 6) This route is painless (Aronson, 2009).

Disadvantages

- 1) Paediatric and geriatric patients have difficulty in swallowing.

- 2) Swallowing the medication requires fluids and gastric volume enhancement and therefore the probability of nausea and vomiting is increased in the case of patients with GI problems.
- 3) Absorption rate of the drug into the bloodstream after swallowing varies depending on how fast the drug moves from the stomach to small (i.e. gastric emptying rate) or large intestines, differs from patient to patient and not exactly predictable. Intestinal and stomach secretions and pH are other factors which can interfere with the absorption process (Figure 1.1). In certain cases such as anxiety and stress, GI movements and secretions, are significantly reduced which prevents or reduces the intended effects of the drug, and causes delay in onset of drug action (Metcalf &, 2010).
- 4) Therapeutic peptides and proteins administered orally will be deactivated by the presence of a strong acidic (stomach) environment and proteolytic enzymes in the GI tract (Werle, *et al.*, 2009).
- 5) First pass effect. As the veins from the stomach and the small and large intestines pass directly through the liver, most drugs which are administered orally are instantly metabolized and about sixty percent of most drugs (hundred percent of certain drugs) are removed before reaching the systemic circulation (Figure 1.2). This causes an extra metabolic load for the liver and kidneys as they eliminate high levels of drug in the bloodstream especially in chronic treatment with a resultant risk of hepatic or renal disorders (Paediatrics, 2007).

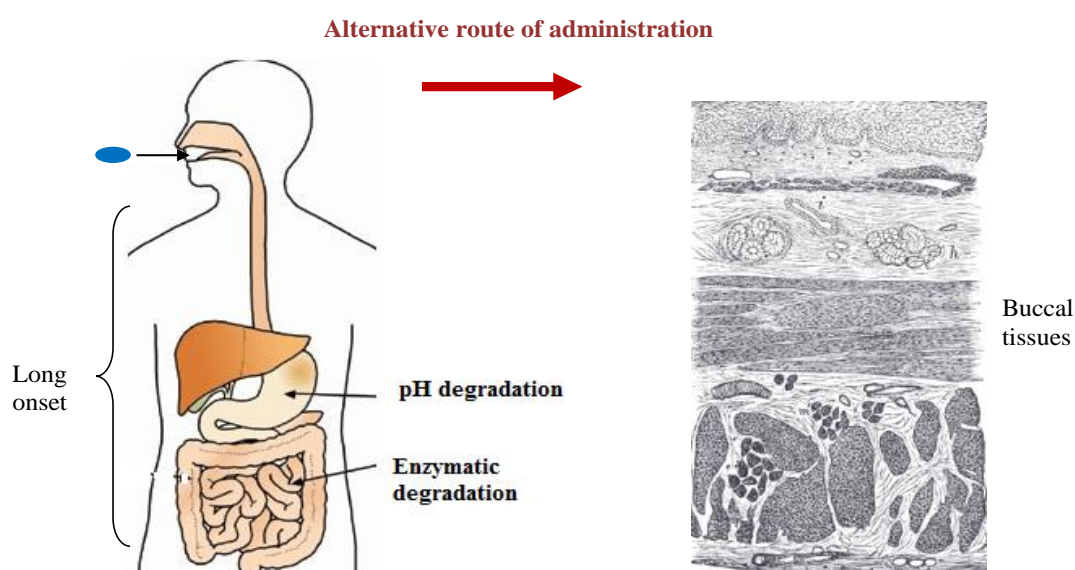


Figure 1.1 Mucosal delivery as an alternative to oral drug delivery.

1.3.2 Injectable dosage forms

To eliminate and overcome some of the challenges involved in oral administration, injections have been frequently used. Drugs are commonly injected either intravenously or intramuscularly.

Advantages

- 1) A rapid access of drug to the site of action without the risk of first pass metabolism in the liver.
- 2) A smaller amount of drug is required in comparison to the oral route.
- 3) Drug rapidly disperses to various part of the patient's body before experiencing first pass effect in the liver.

Disadvantages

- 1) Most patients, predominantly infants and geriatrics, do not readily accept injections because of pain. This resistance is sometimes very obvious and causes a serious psychological stress which can make the patient's condition worse. Occasionally, it is undesirable to use injections where the patient is seriously ill and going through an unstable condition or injury.
- 2) The metabolic rate varies from patient to patient and to prevent any possibilities of overdosing (especially drugs with central nervous system effect), the injection route is utilised with a lower than average dose and then an additional dose administered as required. However, this repeated injection process can increase the stress level in patients (Aronson, 2009).

There are new strategies to develop delivery devices such as pre-filled syringes, pens, auto-injectors and needle-free devices to reduce the problem of self-administration and improve patient compliance. In addition, development of micro-needles (Ji, *et al.*, 2006) or employing nanoparticles compensate for some of the disadvantages of parenteral dosage forms (Joshi & Müller, 2009). However, the possibility of skin irritation, allergy, toxicity and cost effectiveness are a cause of concern for dissolvable needles (Prausnitz, 2004) and necessitates the need for alternative administration routes such as mucosal surfaces.

1.3.3 Topical route

The topical route is commonly used for dermal dosage forms which are a convenient means of delivering drugs locally to the skin surface. Patients do not need to be trained or use special applicators during use. The advantages and disadvantages of this route are summarised as follows.

Advantages

- 1) It is a practical approach for local application to treat skin conditions.

Disadvantages

- 1) Formulating a drug in a dermal base does not always enable medication to penetrate deeply in order to provide a systemic effect. The rate of drug uptake across the skin is slow and in an emergency situation when the level of drug in the blood stream is expected to be high, this route cannot be employed.
- 2) The skin surface is in continuous contact with air and its constituents which is a huge concern because either oxidation (i.e. hydroquinone creams) or contamination can change the properties of the drug and consequently may not have the desired effects.

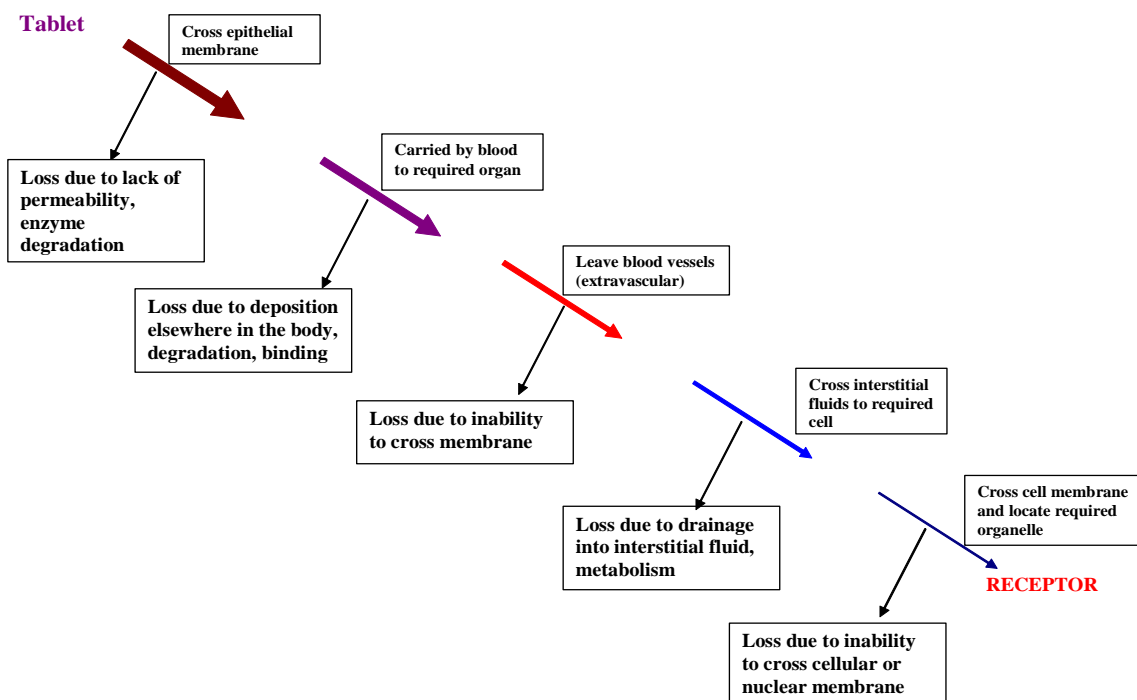


Figure 1.2 The various stages of loss encountered by a drug delivered in the form of an oral tablet.

Even though traditional dosage forms are useful and continue to be used extensively, their major disadvantages and obstacles as discussed above have necessitated the need for designing a new generation of drug delivery systems. The combined effects of the shortcomings of the above formulations have been the driving force for researchers to design novel dosage forms (Figure 1.3, Figure 1.4) which will deliver drugs to the site of action in an ideal time and with minimum losses while providing the desired effect (Merck manual, 2007).

1.4 Novel drug delivery systems

Current efforts in the area of drug delivery also include modifications of existing drug delivery systems to overcome some of the barriers encountered by traditional dosage forms, as illustrated in Figure 1.2 for a typical oral tablet. For example, new generations of oral dosage forms have been developed including pH-controlled (release under specified pH conditions), time-controlled (release from coated dosage forms typically occurs after a pre-determined lag time) and osmotic pressure-induced (water penetrates through the pores of a semi-permeable outer film, created by a pore-forming agent). Others include enzyme-controlled (release in specific enzymatic condition) or biodegradable polymeric coating (release occurs following degradation in the body) (Sato, *et al.*, 2010, Nunthanid, *et al.*, 2007) release methods. However, even though the new developments have resulted in further improvements, they still have not resolved major disadvantages such as first pass effect and onset delay (Sun, *et al.*, 2007).

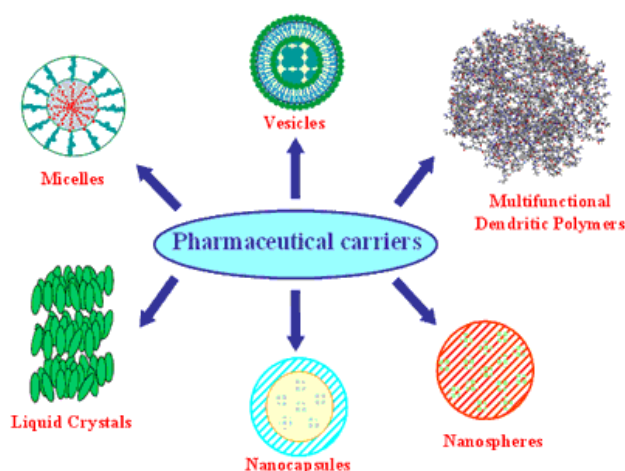


Figure 1.3 Examples of novel pharmaceutical carriers (Copyright AZoM.com Pty Ltd).

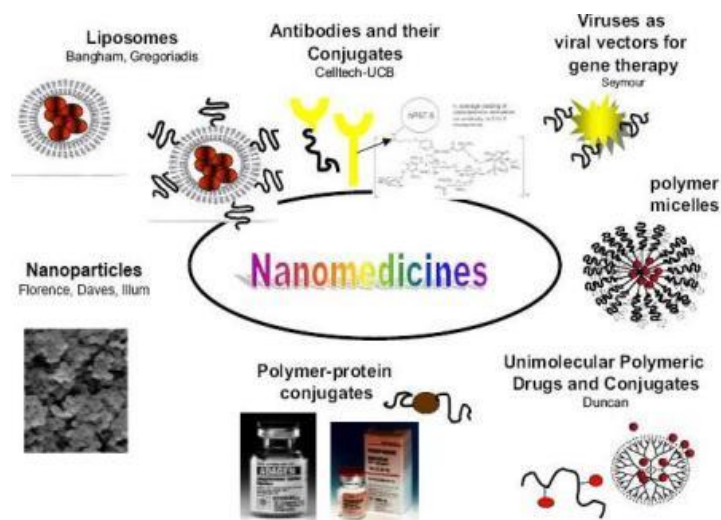


Figure 1.4 New nanomedicines in the pharmaceutical market (Prof. Duncan presentation, www.ruthduncan.co.uk/#/recent-lectures/4551764748).

Following the improvements in designing novel drug delivery systems, other innovative techniques (Figure 1.3) have been employed to enhance drug efficacy. Many attempts have been made to develop several pharmaceutical carriers with the ability to protect and transfer the drug molecules while controlling the release of the drug (Kiparissides, *et al.*, 2008). Other advanced novel drug delivery systems (nanomedicines) are shown in Figure 1.4.

1.4.1 Site specific delivery systems

The aim of this type of delivery system is to activate the drug in the target area of the body (for example, in cancerous tissues) by transferring active ingredient to the specific target cells without causing unwanted side-effects in other parts of the body and thereby eliminating the disadvantages of non-specific traditional dosage forms (Kiparissides, *et al.*, 2008). Site-specific targeting is a complicated subject and involves factors such as limiting administration route opportunities, decreasing the amount of active component in the formulation to reduce side effects, eliminating/minimizing toxicity and enhancing safety (Ahmad, *et al.*, 2009). Usually, physiological conditions of the target area cause conformational changes in the carrier material, which results in the release of the drug. One of the most applicable materials with high molecular weight and ability to deliver drugs properly and selectively are polymers.

According to Kiparissides, *et al* (2008), two main mechanisms which control drug release at the desired site in the case of cancer are: (1) passive and (2) active targeting. Passive targeting is the specific accumulation of a chemotherapeutic compound in solid tumours as a consequence of increase in their vascular permeability in comparison to healthy tissue. Active targeting, on the other hand, is based on surface functionality of ligands present in drug carriers that are selectively distinguished by receptors located on the surface of the target cells. Ligand–receptor interactions can be extremely selective; which causes a more precise targeting of the particular site (Husseini, *et al*, 2008).

1.4.2 Time directed delivery

This refers to any sort of sustained release of the drug from the administered dosage form in which the amount of drug released can be adjusted to decline or remain constant over a long period of time or even released frequently at precise time intervals. This could be achieved by using for example swellable and degradable polymers. It is possible to prolong the release of a drug, up to weeks; by prolonging degradation of the polymer matrix (e.g. use of block copolymers and hydrogels). Various types of sustained release formulations including liposomes, biodegradable microspheres with incorporated drug, drug polymer conjugates and medical devices (Serra, *et al*, 2010); can be considered as time directed.

Potential mechanisms that will provide sustained drug release are desorption of surface-bound/adsorbed drugs, diffusion throughout the carrier matrix, diffusion (e.g. nanocapsules) through the carrier wall, carrier matrix erosion or a combination of erosion/diffusion processes.

1.4.3 Alternative delivery routes

Administering and transferring drugs to the site of action is desirable; however, as noted earlier, the choice of drug is often influenced by the drug administration route. This has led to exploration of systems for drug delivery via alternative routes. These types of formulations are more desirable and have the potential to eliminate the problems encountered with traditional dosage forms and achieve desired efficiency in treatment of chronic conditions such as asthma (where steroid therapy can be over a prolonged period) via steady level of

medication while reducing side-effects and thereby enhance patient convenience and compliance.

Table 1.3 Potential advantages and disadvantages of controlled-release therapy (Adapted from Lin, *et al.*, 2006, Yang & Alexandridis 2000).

Advantages	Disadvantages
<ul style="list-style-type: none"> ❖ Reduction in administration frequency increases the patient compliance ❖ Minimum drug loading ❖ Minimize or eliminate side effects ❖ Reduce the chance of drug accumulation by frequent administration ❖ Efficacy of treatment is improved ❖ Minimizing the fluctuation in drug levels ❖ Improvement in bioavailability ❖ Special effects can be achieved e.g. sustained release helps the morning relief of arthritis by administering the drug before bedtime. 	<ul style="list-style-type: none"> ❖ Potentially expensive ❖ Unpredictable and usually poor <i>in-vitro in-vivo</i> correlations and dose dumping ❖ Not applicable for rapid systemic availability

The new routes of administration include:

- ❖ Oral transmucosal (buccal, sublingual)
- ❖ Transdermal patches
- ❖ Transmucosal (rectal, nasal, vaginal)

1.5 Mucosal dosage forms

Mucosal routes include areas of the body where mucosal tissues are present such as the mouth, pharynx, oesophagus and nasal regions. Both the buccal and nasal mucosa is well vascularised and able to absorb hydrophobic drugs with small molecular size with high efficiency. However, the nasal mucosa has specific disadvantages such as potential irritation, ciliary action of nasal cavity might be irreversibly damaged and there are significant

variations in mucosal secretion. Therefore, one of the most routes that have gained a lot of interest in recent years for drug delivery is the buccal mucosa.

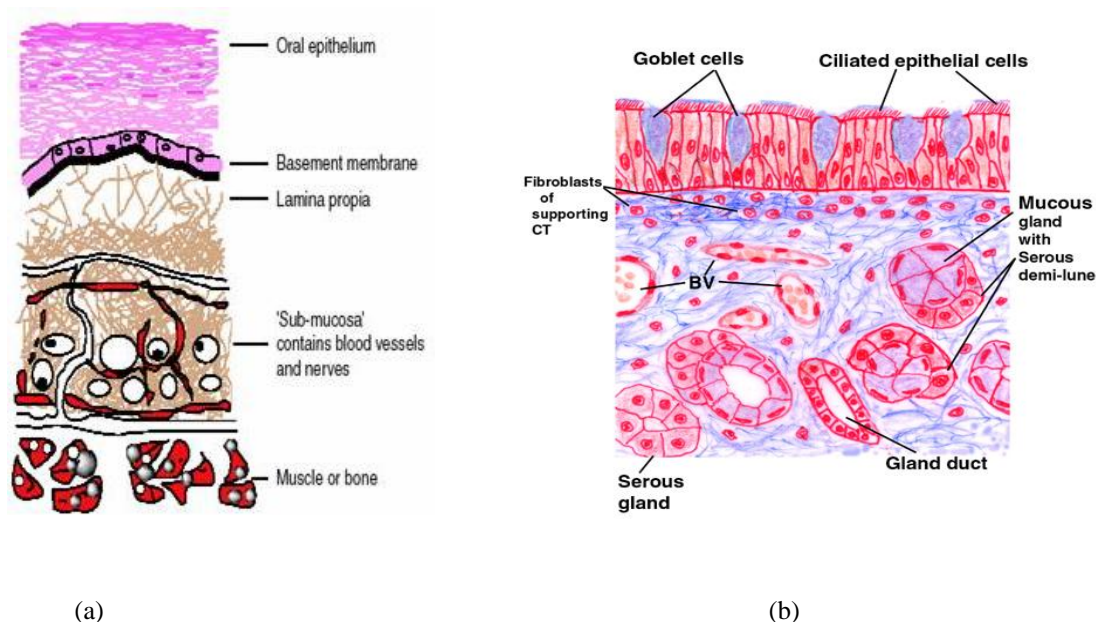


Figure 1.5 Cross-sectional representations of (a) the oral mucosa (www.pharmainfo.net/reviews/currentstatus-buccal-drug-delivery-system) and (b) the nasal mucosa tissues (www.vetmed.vt.edu/education/curriculum).

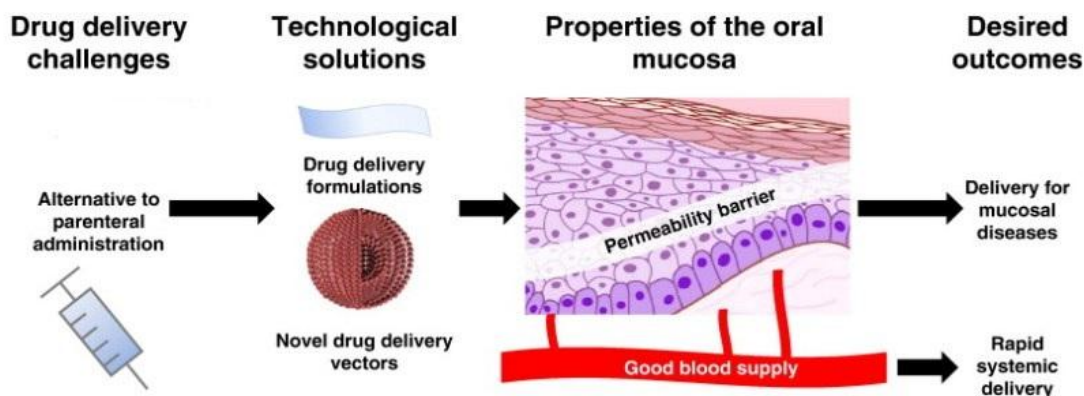


Figure 1.6 Mucosal delivery as an alternative to parenteral delivery (Hearnden *et al.*, 2011).

1.5.1 Buccal drug delivery

The first attempts at buccal drug delivery involved manufacturing conventional medicated candy products by adding therapeutic agents to a molten candy mass.

However, during the formulation process such as addition of the candy mass at high temperatures, decomposition of the therapeutic agent could occur. Furthermore, many available medicated candy lozenges will disintegrate when placed in the mouth and hence mucosal tissues do not obtain uniform release of the drug. In addition, patients mostly chew and swallow lozenges resulting in most of the drug reaching the bloodstream through the GI tract and subsequent first pass metabolism in the liver. Therefore, lozenges are not considered desirable for administering potent, fast-acting drugs including those that affect the central nervous system, respiratory, cardiovascular and renal systems. This is because therapeutic bioavailability is critical and significantly lower levels of drug in the blood circulation can be life threatening (Degim, *et al.*, 2006).

Advantages of buccal dosage forms include avoiding the first pass effect and exposure of the drug to gastric and intestinal fluids thereby increasing their bioavailability. It also improves patient compliance by avoiding pain and the formulation can be removed if medication needs to be discontinued. In addition, the chance of accidental choking in the respiratory tract is diminished (Paediatrics, 2007). Compared with other routes, such as transdermal, mucosal surfaces do not have a stratum corneum, hence the main barrier to drug transport is removed and therefore provides quicker onset of drug action.

The buccal route is a promising route for administering drugs which have high first-pass metabolism, low dose, log P value in the range of 1.60–3.30 and small molecular size. A selection of dosage forms for buccal delivery of small molecules reported in the literature are summarised in Table 1.4.

The critical factors that need to be considered in mucosal dosage forms include stability, solubility, bioadhesion and bioavailability. In some cases the main objective is the gradual release of drug over a long time period to maintain therapeutic levels of the drug in the systemic circulation to prevent frequent administration. To achieve this goal, various forms of buccal dosage forms have been designed such as patches, gels and ointments, films and tablets (Dixit, *et al.*, 2009). Commercialized buccal delivery systems available in the market in the form of thin film include ZuplenzTM (approved by FDA), BenadrylTM (diphenhydramine) and Gas-X (simethicone). In addition, insulin buccal spray or hydrocortisone buccal tablets are available.

Table 1.4 Selected buccal drug delivery systems reported in the scientific literature within the last decade.

Type	Drug	Authors	Year
Double-layered mucoadhesive tablets by HPMC and carbomer	Nystatin	Labot <i>et al.</i>	2002
Mucoadhesive microcapsules for glipizide	Glipizide	Chowdary & Rao	2003
Buccal liposomal delivery	Silymarin	El-Samaligy <i>et al.</i>	2006
Release of naltrexone on buccal mucosa	Naltrexone	Giannola <i>et al.</i>	2007
Complexes of omeprazole with native and chemically modified b-cyclodextrin	Omeprazole	Figueiras <i>et al.</i>	2007
Fenugreek gum /polycarbophil transmucosal disc	Sumatriptan	Amarjit Singh <i>et al.</i>	2009 (US Patent)

Labot, *et al* (2002) developed double-layered mucoadhesive tablets containing nystatin as API and various polymers as excipients including lactose (direct compression), carbomer and hydroxypropylmethylcellulose (HPMC). The formulation demonstrated sustained release profile over 6 hours. In addition, Chowdary and Rao (2003) formulated glipizide microcapsules coated with alginate and a mucoadhesive polymer such as carboxymethylcellulose, methylcellulose, HPMC, carbopol and was prepared by an orifice-ionic gelation process. These mucoadhesive microcapsules showed suitability for controlled release of glipizide in the oral cavity. As mentioned before, in transmucosal drug delivery systems, absorption is a major limitation which has an impact on drug bioavailability. Giannola, *et al.*, 2007 assessed the ability of naltrexone hydrochloride (NLX) to penetrate the human buccal mucosa by histological approaches. Other factors that should be considered include pH conditions within the mouth which may affect the administration of certain lipophilic and hydrophilic drugs.

Previous studies have shown that maximum drug uptake through the mucosal tissues normally occurs when the drug is in the unionized form and pH variation alters the percentage of unionized drug at a particular point in time (Değim, *et. al.* 2006). This affects the absorption of the drug across the mucosal membrane and subsequently systemic bioavailability. The optimum pH of saliva is between 6.2 and 6.9; hence drugs readily absorbed by mucosal tissues are those with a high pK_a (Sasaki, *et al.*, 1997).

Most of the drugs are either weak acids or weak bases hence; they are part ionized and part unionized. The extent to which a drug is in its ionized and non-ionized forms at a certain pH is very important. pH (hydrogen ion concentration), affects the physical and chemical properties linked to absorption, such as solubility of the drug, lipid/water partition coefficient, electrical membrane potential, permeability of the membrane, and chemical reactivity. The ionized ratio is charged and attracts water molecules to form large complexes. They cannot cross the membranes due to less lipid solubility. Therefore, the ionized part of the drugs cannot cross the membrane and drugs are better absorbed in unionized form. Henderson-Hasselbalch equation determines the relative concentration of the ionic and the molecular moieties of a drug at a certain pH (Aronson, 2009).

$$pH = \text{Log} \frac{[A^-]}{[HA]} + pK_a \quad \text{Eqn 1}$$

The rapid elimination of drugs due to the flushing action of saliva or the ingestion of food materials may cause the need for frequent dosing in case of local delivery. Furthermore, the distribution of drugs in saliva is non-uniform due to uneven release from solid or semi-solid formulations which may result in lower amounts being absorbed by the mucosal tissues and subsequently the systemic circulation (Mizrahi and Domb, 2008).

1.5.2 The buccal mucosa

The buccal area forms part of the oral cavity bounded by the lips and the cheeks, as well as medially by the teeth and/or gums.

The oral mucosa consists of a non-keratinized area (sublingual and buccal mucosa) and the keratinized area (the gum or gingiva, the palatal mucosa, and the inner side of the lips), with

the non-keratinized regions generally more permeable compared to the keratinized areas (Veuillez *et al.*, 2001).

The oral cavity offers a large surface area for absorption (100– 200 cm²), is richly vascularized with blood reaching the buccal mucosa via the maxillary artery at a faster and richer blood flow rate (2.4 ml/min/cm²) than that in the other regions of the mouth cavity which facilitates passive diffusion of drug molecules across the mucosa. The buccal mucosa is composed of several layers of different cells as shown in figure 1.5 (b). The epithelium is about 40–50 cell layers thick and is similar to stratified squamous epithelia found in the rest of the body. Lining the epithelium of the buccal mucosa is the non-keratinized stratified squamous epithelium that has a thickness of about 500–800 μm and surface area of 50.2 cm². The rough textured buccal mucosa is thus suitable for retentive delivery systems (Rathbone *et al.*, 1996). Basement membrane and lamina propria followed by the submucosa are found below the epithelial layer (Gandhi & Robinson, 1988). The lamina propria is rich with blood vessels and capillaries (20ml/min/100 gr of tissue) which open to the internal jugular vein. Lipids present in the buccal tissues include phospholipid (76.3%), glucosphingolipid (23.0%) and ceramide NS (0.72%) (Hearnden, *et al.*, 2011; Sudhakar, *et al.*, 2006). The buccal epithelium is primarily designed to offer protection of the underlying tissue. In non-keratinized regions, lipid-based permeability barriers in the outer epithelial layers protect the underlying tissues against fluid loss and entry of potentially harmful environmental agents such as antigens, carcinogens, microbial toxins and enzymes from foods and beverages (Squier & Finkelstein, 1989). Based on the structure, the oral mucosa is classified into three main types:

1. masticatory mucosa,
2. lining mucosa,
3. specialized mucosa.

Masticatory mucosa is keratinized and similar to epidermis of skin in its pattern of maturation and lined up on the gingival and the hard palate area and is necessary due to mechanical forces of mastication such as abrasion and stress. The lining mucosa is non-keratinized and the thickness differs substantially in different parts of the oral cavity.

Generally, their thickness is more than the masticatory mucosa though more permeable due to their non-keratinized texture. Buccal and sublingual regions are covered with this form of

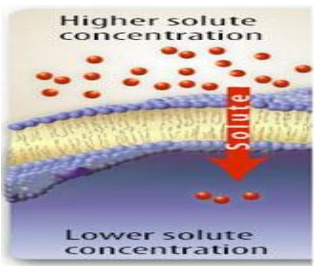
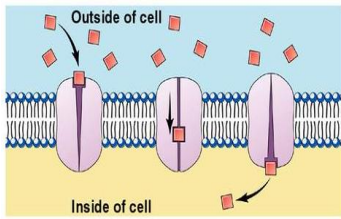
epithelium. Specialized mucosa is found on the surface of the tongue with the characteristics of both masticatory and lining mucosa and is not effective for drug absorption purposes.

The proportion of different types of oral mucosa differs in the oral cavity. Masticatory mucosa is about 25%, lining mucosa 60%, and specialized mucosa approximately 15% of the total surface area of oral lining. Small molecules with molecular weight less than 75–100 Da can cross the oral mucosa readily. Scientifically, as the molecular size of the drug increases, the permeability decreases (Sudhakar, *et al.*, 2006).

1.5.3 Drug absorption via buccal route

As stated previously, drug permeation is one of the most critical parameters which need to be addressed and evaluated. The absorption rate of drugs from the buccal mucosa is 4-4000 times higher than skin. However, this depends on the different parts of the oral mucosae (described above) which exhibit differences in permeability rates (Patil & Sawant, 2008). The various mechanisms of drug absorption through the oral mucosal cells are summarised below in (Table 1.5).

Table 1.5 Mechanism of drug absorption in buccal tissues.

Absorption	Mechanism of absorption	Schematic view
Passive diffusion via para-cellular & trans-cellular route	The driving force in the process of passive diffusion is the concentration gradient of the molecule which controls the transfer of molecules across the membrane. Diffusion occurs following the accumulation of a high concentration in a region which induces molecules to pass through membranes until it reaches the lower concentration region.	
Facilitated passive diffusion	If the drug molecule transfers through the membrane with the help of a carrier protein, the process is called facilitated passive diffusion. However it is limited to particular types of molecules as the carrier proteins only bind to specific molecules. This process is entirely dependent upon the accessibility of carriers as in particular stages during transport, the carrier might be saturated.	

1.6 Hydrogel based systems

In recent years, attention has turned to hydrogel polymers and their use in pharmaceutical products as a desirable drug delivery system. These substances have numerous advantages including their functional characteristics such as hydrophilicity, high water content and absorption capacity. Hydrogels are three-dimensional polymeric systems with the ability to absorb high amounts of water or biological fluids. This hydration is polymer related and occurs to various degrees (occasionally reaching more than 90% w/w of original weight) though it depends on the nature of the aqueous environment and polymer structure. Hydrogels consist of cross-linked polymeric chains with very high viscosity, in contrast to others such as microgels with lower viscosity.

The similarity between the physical properties of hydrogels and body tissues in terms of structure makes them suitable as effective drug delivery systems in comparison to other synthetic polymers. These characteristics include high water content, soft and rubbery conformation, and low interfacial tension with water or biological fluids. Although they are able to absorb high amounts of water, they swell in an aqueous environment instead of being dissolved following critical cross-linking (Li, *et al.*, 2010) and their slow solution response allows prolonged drug release (Casolaro, *et al.*, 2006).

Covalent, hydrogen bonds and van der Waals interactions or physical entanglements are the fundamental reasons for the cross-links in the polymer network. Currently, various hydrogel systems consisting of natural or synthetic polymers have been introduced and their characteristics studied. Since the release mechanism of any loaded drug from a hydrogel matrix is complicated, regardless of the type of polymer, the main factors controlling drug release i.e. swelling of the hydrogel matrix and chemical reactivity of the drug/matrix must be considered.

In order to design novel hydrogel systems, pre-formulation studies and determination of the physicochemical properties as well as knowledge of polymer chemistry is required. In addition, the structure of polymers, interaction parameters, disintegration/release kinetics and the chain's movement phenomena are fundamentally critical and require quantitative determination (Hoare and Kohane, 2008).

Hydrogels are classified according to their characteristics including:

- 1) the nature of side groups which can be neutral or ionic,
- 2) mechanical and structural features,
- 3) method of preparation: whether they will be formulated individually or with another polymers (co-polymer),
- 4) physical structure: there are several forms of polymers such as amorphous, semi-crystalline, hydrogen bonded, super molecular and hydrocolloids and
- 5) reaction to physiological stimulants such as changes in pH, ionic strength, temperature and electromagnetic radiation.

Temperature and pH are two common factors amongst physical and chemical stimuli for biomedical purposes to deliver drugs via the hydrogel based systems to the particular site of the body (He, *et al.*, 2008).

The critical point in the pH-sensitive polymers system is the presence of ionizable weakly acidic or basic groups attached to a hydrophobic back bone. Following their ionization, the coiled chains extend dramatically, reacting to the electrostatic repulsions of the produced charges (anions or cations). In temperature stimuli systems there is a balance between hydrophobic-hydrophilic structures. Therefore small temperature changes around the critical temperature will collapse or expand the chains in response to the new adjustments of the hydrophobic and hydrophilic interactions between the polymeric chains and the aqueous media (Meng, *et al.*, 2009).

Several characteristic advantages make stimuli-sensitive block copolymers a desirable choice for novel drug delivery. These include:

- ❖ simplicity of drug formulation and administration procedures,
- ❖ no requirement for organic solvent,
- ❖ site-specificity,
- ❖ demonstrating prolonged drug release behaviour,
- ❖ considerably lower systemic toxicity, and
- ❖ the ability to distribute both hydrophilic and hydrophobic drugs in the body.

1.7 Drug release kinetics

The mechanism of drug release is affected by various factors, including diffusion through a rate-controlling membrane or a matrix, osmosis, ion exchange or degradation of the whole/partial matrix. Employing biodegradable devices to control the drug delivery mechanism has considerable advantages as it avoids the need to remove the system from the site of action following the completion of drug release. The most common polymers used to formulate systemic drug delivery systems are bioresorbable polymers. They are suitable due to degradation to lower molecular weight fragments which are readily removed from the body. The kinetics of drug release from hydrogel based dosage forms can be determined by finding the best fit of the percentage release *vs* time data to distinct models. Examples of such models include the following.

(1) Korsmeyer- Peppas model:

$$\ell_n(Q_t / Q_\infty) = \ell_n k + n \ell_n t \quad (\text{Korsmeyer- Peppas equation}) \quad \text{Eqn 2}$$

In this equation Q_t is the amount of drug released at a given time (t), Q_∞ is the amount of drug present initially, while k is a constant (which reflects the structural and geometric characteristics of the formulation) and n is the release exponent.

(2) Higuchi model:

$$Q_t = k_H t^{1/2} \quad (\text{Higuchi equation}) \quad \text{Eqn 3}$$

Q_t is the amount of drug released at time (t) and k_H is a constant (the Higuchian release rate).

(3) Zero order model:

$$Q_t - Q_0 = k_0 t \quad (\text{Zero order equation}) \quad \text{Eqn 4}$$

Q_t is again, the amount of drug released in time (t) while Q_0 is the amount of drug dissolved at time zero, and k_0 is the zero-order release constant.

(4) First order model:

$$\ell_n(Q_\infty / Q_1) = k_1 t \quad (\text{First order equation}) \quad \text{Eqn 5}$$

Q_1 is the amount of remaining drug at time (t), Q_∞ is the initial amount of drug which exists in the system and k_1 is the first-order rate constant.

(5) Hixson–Crowell model:

Eqn 6

$$Q_0^{1/3} - Q_t^{1/3} = K_{HC} t$$

Where, Q_t is the amount of drug released in time t , Q_0 is the initial amount of the drug in sample and K_{HC} is the rate constant for Hixson-Crowell rate equation.

1.8 Mechanism of drug release from hydrogels

Drug molecules with varying sizes and characteristics are released from hydrogels by different mechanisms. Drug molecules may diffuse out of hydrogel matrix during handling and storage which need to be considered and addressed. In addition, hydrogels are highly hydrophilic and behave differently from hydrophobic polymers in terms of releasing drug. Hydrogels control drug release occurs by three main mechanisms: diffusion-controlled, swelling-controlled and chemically-controlled (Lin, *et al.*, 2006).

❖ Diffusion-controlled

The most common mechanism is diffusion–controlled which is based on Fick’s first law. Diffusion controlled systems can be classified into two as follows.

1) Reservoir

In this system, an inert membrane encapsulates the drug core and the rate of drug diffusion via the polymer membrane is the rate-limiting step (Figure 1.7). By choosing various types of polymers to achieve the desirable diffusion and partition coefficients of the drug in the polymer, the release rates are predictable (Park & Shaly, 1993).

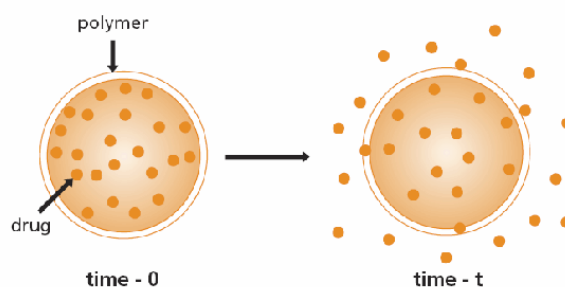


Figure 1.7 Schematic view of reservoir diffusion.

2) Monolithic

In this system, the drug is dispersed homogeneously in the wetted matrix (Figure 1.8) and therefore this system is called mono-bloc.

The Higuchi model is commonly used to describe drug release from this system and states that “if sink conditions are maintained in the dissolution medium, the amount of drug released is related to the square root of time” (Miyajima, *et al.* 1998).

For poorly water soluble drugs, this system enhances the rate of drug release in the human body in comparison to the other conventional dosage forms since the drug is molecularly dispersed rather than crystalline or amorphous aggregates which need to be disrupted prior to drug dissolution. To achieve high solubility, a fast hydrating hydrogel is important because the macromolecular network of the matrix former shouldn't have any significant hindrance on drug release. This should however, be balanced by a parallel consideration of long term stability during storage and formation of thermodynamically stable crystalline form (Rathbone, *et al.*, 2007). The rate of diffusion from a hydrogel matrix is entirely dependent on the pore sizes within the matrix and this factor is also related to the degree of cross-linking and chemical structure of the monomers. In addition, the type of monomers and the strength of external stimulants are important factors.

The porosity in the matrix directly affects various characteristics such as mechanical strength, degradability, diffusivity and other physical properties of a hydrogel network (Hamidi, *et al.*, 2008).

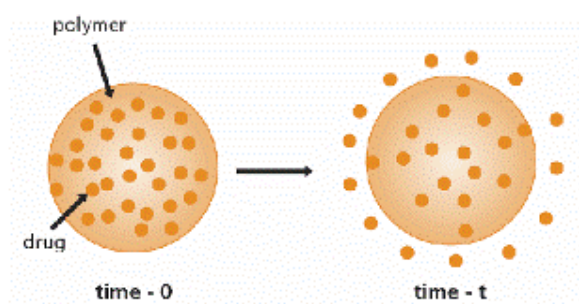


Figure 1.8 Schematic view of monolithic diffusion.

❖ Swelling- controlled

If the rate of drug diffusion is significantly higher than swelling, the mechanism of drug release is swelling-controlled; with the rate of swelling being the rate limiting step. In swelling controlled release systems, the dosage form is initially dry.

Following the placement of polymeric matrix in the body, the swelling process begins by the ingress of water or body fluids. In the early stages, water penetrates the drug delivery system as a consequence of a concentration gradient which results in enhanced mobility of the polymer chains and drug molecules followed by an increase in macromolecular mobility at a specific polymer-water concentration point.

This process is termed polymer chain relaxation. Consequently, the water content and polymer network mesh size within the formulation increases allowing the drug to diffuse via the swollen network and into the external environment (dissolution medium). Subsequently, the swollen polymer chain dissolves (erodes) in the surrounding fluid and eventually, the end-to-end distance of the individual polymer molecules will increase (Boateng, *et al.*, 2008). It has been shown that in an aqueous environment, a polymer chain relaxation procedure takes place which induces the hydrated polymer to undergo direct erosion or dissolution (Ritger, *et al.*, 1987). A large number of materials used to formulate swelling controlled release systems are capable of swelling spontaneously without a requirement for dissolution while in contact with water or biological fluids.

As noted earlier, such polymers are usually cross-linked which makes them resistant to complete disintegration. This polymeric network causes the progression of swelling until the equilibrium state is attained where elastic and osmotic swelling forces are balanced. It is possible to achieve different types of drug release profiles, based on the ratio of the drug diffusion rate to polymer swelling rate.

If polymer structural rearrangement, due to solvent penetration, occurs faster than drug diffusion, the dominant diffusion release will be Fickian or first order release (i.e. uncross-linked polymers) (Kydonieus, 2004). Drug release from swollen hydrogels follows Fick's law and Fick's equation helps to calculate the rate of drug release from an equilibrated slab device.

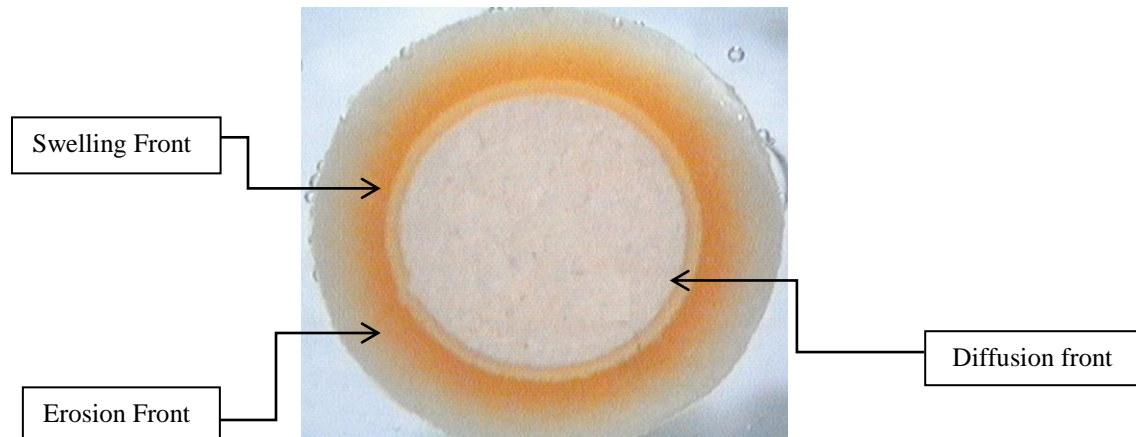


Figure 1.9 Schematic view of swelling, erosion and diffusion fronts of a hydrogel matrix.

This system is referred to as monolithic (as described above) where the drug is dispersed in the polymer medium.

$$M_t / M_0 = 4 (D_t / \pi h^2)^{1/2} \quad \longrightarrow \quad \text{Fick's Law} \quad \text{Eqn 7}$$

M_t = amount of drug released, in time t

M_0 = total mass of the drug incorporated into the device

D = diffusion coefficient of the drug

$\pi = 3.14$

h = thickness of the device

$$M_t / M_0 = 1 - (8 / \pi^2) \exp [(- \pi^2 D_t) h^2] \quad \text{Eqn 8}$$

In monolithic devices with high drug loadings, drug release behaviour is modified by the shape of the device and the loading dose. Hence when the concentration of drug is lower than 5 volume percent, the Higuchi equation is the most suitable model to describe the rate of drug release from the polymer slab.

$$M_t = A [DC_s (2C_0 - C_s)^2]^{1/2} = A (2DC_s C_0 t)^{1/2} \quad \longrightarrow \quad \text{Higuchi Model} \quad \text{Eqn 9}$$

M_t = amount of drug released, in time t

D = diffusion coefficient of a drug

C_s = drug solubility in the polymer matrix

C_0 = initial total drug concentration (includes both dissolved and dispersed drug)

A = area of polymer slab

The Higuchi equation is also the most appropriate method to calculate drug release in some systems where drug release from a polymeric system occurs following the penetration of fluid into the network rather than relaxation of the polymeric chain. In these systems, fluid penetration rate called swelling rate is the dominant mechanism that controls the drug release stage (Perioli, *et al.*, 2004).

❖ Chemically- controlled

In chemically controlled release systems, the controlling mechanism of drug release is the rate of dissolution of the polymeric matrix during the drug diffusion process. This system is comparable to swelling controlled-release systems but mass erosion is replaced by the phase erosion (moving front). However, additional factors such as enzymes or biochemicals may induce the hydrolysis process.

In general, bioerosion is distinctive from biodegradation; bioerosion is the fragmentation of the polymer by a chemical reaction that is occurring in the dissolution media (Chiellini, 2001). During chemical bioerosion, the polymer will be fragmented into smaller molecular weight components attached to drug molecules and dispersed throughout the dissolution environment while in a biodegradable system, the large particle sizes of micro-spherical drug may be dispersed but not necessarily molecularly dispersed. The main parameter which controls the release process is chemical reaction taking place at the surface. This reaction produces oligomers and molecules with smaller molecular weight due to break down of the polymer until no further change in geometry occurs. At this point smaller polymer molecules plus drug that was incorporated in the remaining segment will be free to dissolve and diffuse. In addition, the geometric shape of the device in most chemically controlled systems play the main role in drug release. Other mechanisms such as polymer dissolution or reaction and the ratio of polymer surface degradation are contributing factors controlling drug release (Ranade, 1990).

1.9 Erodible systems

This term is used to describe water soluble polymers or very small molecules from water-insoluble polymers which can occur in different parts of the compound or just limited to the surface area and referred to as bulk (homogenous) erosion or surface (heterogenous) erosion,

respectively. Bioerodible polymers in contact with physiological fluids will dissolve instead of disintegrating (Gijpferich, 1996).

The drug-release mechanism occurs principally following the surface erosion although various mechanisms such as water diffusion, polymer hydration, disentanglement and dissolution are involved.

An erodible matrix in contact with any available water will erode although it will be desirable to prevent water ingress into the matrix until the system reaches the critical release point. This is possible by eliminating hydrolysis, diffusion and reducing the effects of enzymes. In sustained-release systems erosion has some advantages compared with more conventional delivery systems including:

- 1) capability of delivering poorly water-soluble drugs,
- 2) release mechanism by zero-order equation demonstrating that the rate of release depends on gastrointestinal motility and availability of water,
- 3) simplicity in modification of dosage to achieve the most desirable release profile by changing size, width, and matrix composition of API and excipients.

Both films and freeze-dried wafers, which are the subject of this study, can be classified as erodible systems and discussed further in the ensuing chapters.

1.9.1 Molecular basis of polymer dissolution

Structural molecules within polymers are arranged in a network and pulling them apart requires a considerable amount of energy. When the chain attachments are very strong, separation is actually difficult especially when the arrangement is straight, stiff, and lined up next to each other. This causes slower flow rate during dissolution, due to slower movement of long chains, (Li, *et al.*, 2010). The rate determining steps implicated in this process are polymer swelling followed by the dissolution step. After addition of polymer to the solvent, two main forces namely attraction and dispersion begin to act between polymer sections based on their polarity, chemical properties and solubility parameter. When a high polymer-solvent interaction is achieved compared with polymer-polymer attraction forces, molecules start absorbing solvent molecules.

Consequently the volume of the matrix increases resulting in a loss of polymer coil shape and production of a solvated polymer instead of aggregated (in solid phase). The entire process of solvation-unfolding-swelling is time dependent and affected by interactions between polymer and solvent molecules and stirring does not alter the time (Balaji and Peppas, 1996).

The loosened coils disperse out of the swollen polymer, dissolving into a solution followed by stirring which results in further disintegration of the swollen polymer and an increase in the rate of drug dissolution. During the dispersion section in the solvent phase, polymer chains still have their fully solvated coiled structure. However spherical or ellipsoid shapes form due to the solvent molecules ingress between the spaces of the loosened sections and polymer coils which fill the hydrodynamic volume of the polymer coil (Miller-Chou and Koenig, 2003).

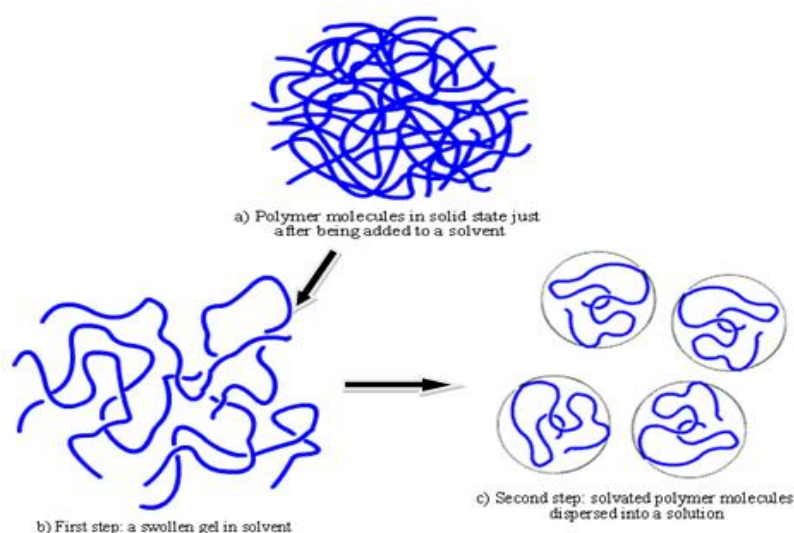


Figure 1.10 Schematic view of polymer molecule dissolution (adapted from Mississippi university website <http://pslc.ws/macrog/property/solpol/ps3.htm>, date accessed 21.04.2010).

1.10 Solvent cast films

Films are thin sheets, usually prepared from polymers and depending upon the type of application might be transparent or opaque. They have been widely employed in the pharmaceutical industry for various purposes.

Initially films were used as packaging materials and coatings for tablets to prevent any sort of undesirable side effects such as gastrointestinal disturbance, and protect the drug from environmental factors such as light, moisture and air. The coating application has been employed to produce film coated mucosal tablets (Dirim, *et al.*, 2004; Sarbach, *et al.*, 1996).

Films are formulated as an alternative to oral dosage forms that have been broadly employed in pharmaceutical industries as a consequence of demonstrating reliable drug delivery characteristics. Boateng *et al.*, 2008 and 2009, designed and formulated solvent cast films as a potential for wound healing dressings or mucosal drug delivery systems. General ideal characteristics of films included ease of administration and removal without any trauma or damage to the sensitive mucosal tissues. Formulation of films are based on initial preparation of aqueous gels or organic suspensions, emulsions or dispersions with appropriate flexibility (elasticity) and resistance to stress during handling, storage or even following administration. Fundamentally, the properties of a film depend on the composition of the initial materials and the preparation technique. Therefore, the initial development of films is important and several steps and processes are involved in designing an optimum formulation.

The method of preparation and investigation of physico-mechanical characteristics before and after formulation should be considered carefully (Boateng, *et al.*, 2009). In addition, polymer selection is an important and functional characteristic factor that should be considered based on the application of the film. Other ideal properties which should be considered while formulating films include (Jones, 2004):

- ❖ low toxicity and ease of removal from the body,
- ❖ low chemical reactivity, compatibility with a broad range of drugs/excipients and be thermodynamically stable,
- ❖ sufficient mechanical strength i.e. flexibility/stiffness,
- ❖ a high drug loading capacity and readily dispersed in aqueous solvents,
- ❖ suitable viscosity and optimum bioadhesivity (mucoadhesivity),
- ❖ glass transition (T_g) temperature should be controllable.

By employing an appropriate combination of polymers, the physic-chemical properties of films can be predictable. For example insoluble polymers can be combined with soluble polymers which help to control release of drug from the polymeric film.

Uniform drug content is required for all dosage forms, mainly those with low doses of very high potency drugs (Morales and McConville, 2011).

1.10.1 Film forming techniques

Various methods can be employed to produce films including solvent casting, hot melt extrusion and spray coating. In solvent casting (Boateng, *et al.*, 2002), solvent evaporates from a solution or dispersion (gel) of polymer and produces a continuous layer of polymeric film while in spray coating technique the polymer solution is sprayed on a Teflon plate. According to the type of solvent employed, two main types of films can be obtained: solvent and water-based films. There has been a recent shift from organic solvent to aqueous based films (Kamada, *et al.*, 2009).

The main disadvantages of organic solvent-based films, for pharmaceutical purposes, are the complexity in eliminating the solvents entirely; rigorous regulations on exposure to these organic solvents, and increased public concern regarding ecological issues such as discharge into water bodies. The critical factors that should be considered during film preparation include temperature and humidity which impact upon the physical and mechanical characteristics of polymeric films (Boateng, *et al.*, 2009; Donhowe & Fennema 1993).

For example, the mechanical properties of films such as flexibility can be affected by handling (Boateng, *et al.*, 2003). The simplicity of application is an important factor, as it influences clinical acceptance. In fact some of the characteristics such as brittleness can cause irritation to newly formed tissue during wound healing, for example, which can prolong clinical treatment and therefore lead to patient non-compliance. It is, therefore, important to formulate films with optimum plasticity to avoid tissue damage or contact irritation when applied.

❖ Film casting from solution

In this method, polymeric solution or gel is produced by mixing polymer and other additives with solvent, either aqueous or organic. Dissolution of polymer occurs by hydration and swelling of the polymers in the aqueous media.

Homogenising (stirring) also affects polymer dissolution especially with high speed overhead stirring, though the rate of stirring should be controlled to prevent excessive generation of air bubbles in the system. To eliminate the air bubbles, pressure techniques can be employed prior to pouring into casting moulds. After obtaining a clear and transparent solution a weighed amount of viscous solution is transferred into a clean glass plate or Petri dish. Occasionally, to achieve a uniform thickness film, the thick and jelly-like solution is spread by a glass rod moving over the surface and left at a precise temperature to remove solvent. Evaporation rate and process conditions significantly affect the film characteristics. In the case of very rapid evaporation, air bubbles or semi-crystalline precipitates can be formed in the final film (Averineni, *et al*, 2009).

Some important points to consider during film formation include the following.

- 1) Replacement of the glass plate with poly tetrafluroethylene film can help overcome the challenge of the final film sticking to the casting surface.
- 2) Film thickness can be controlled by changing the volume of polymer solution and using a Gardner knife (a device with a micrometer adjustment) on the casting surface.
- 3) By covering the casting surface with a removable lid the rate of solvent evaporation can be controlled
- 4) Removing organic solvent from the system by locating the sample in a hood assembly can be easier and faster than placing on the normal bench (Siemann, 2005).

❖ Film casting by spraying the solution

In this technique, a thin layer of polymeric solution is sprayed onto a Teflon sheet and incubated to allow solvent evaporation at a suitable temperature until the film is formed. As soon as the film is dried it can be peeled off and stored in a controlled environment such as a desiccator. Film forming solutions create an alternative film technique although they are directly sprayed onto the body and organic solvents evaporate rapidly and film adheres to the skin or body part, e.g. locoryle nail solution (Weuts, *et al.*, 2010).

❖ Films by hot melt extrusion (HME)

Another technique used to generate films is hot melt extrusion. By employing this technique poorly water soluble drugs can be formulated as films because the film is produced using a solid melt solution instead of a liquid solution.

In this technique all components (polymer, drug and any additives used) are mixed, and to obtain a uniform mixture (they should be blended in a blender at 100 rpm) before transferring them to the single screw extruder (Morales and McConville, 2011). Screw extruder machines have various segments known as feeding, melting and the metering segments.

When the mixture is injected into the machine, via the feeding section, it passes through a melting segment and steadily melts before entering the metering segment where the melted mixture is pumped through a die in the form of a film. The extruded film is cooled by passing through a chill roll. HME can be a useful technique because of speed, economy, safety and ability to produce a broad range of film based (and other controlled) drug delivery systems as well as ability to mask bitter taste of drugs (Andrews, *et al.*, 2009, Maniruzzaman, *et al.*, 2012).

1.11 Freeze dried wafers

Freeze-dried wafers are porous polymeric matrices produced by freeze-drying of polymer gels in solution or dispersion form. They have been used in different novel drug delivery systems including fast dissolving tablets e.g. Zydis and wound healing dressings (Boateng, *et al.*, 2010., Matthews, *et al.*, 2006). This novel drug delivery system is a practical way to formulate proteins due to avoiding high temperature during desorption of solvent from the systems (Grant, *et al.*, 2009).

Alfadhel, *et al.* (2011) also developed a polymeric lyophilized matrix in order to act as a bacteriophage carrier for the treatment of *Staphylococcus aureus* infections.

Maintaining all relevant quality characteristic of the freeze-dried product is a critical issue. The glass transition of frozen systems must be analysed and considered in detail due to its significant effect on collapse, formation of eutectic mixture and crystallization following the temperature rise during the primary drying stage of freeze drying (Kasper and Friess, 2011).

It is feasible to make slight changes in composition of the formulation, for instance adjust the pH of the formulation, use buffer salts, vary the drug concentration, or add a suitable excipient to achieve an optimum product (Nail, *et al.*, 2002).

According to the most recent formulation studies on various hydrogel polymers, lyophilised wafers are able to produce stable and efficient formulations of insoluble therapeutic agents to deliver the drug directly to the site of action (Matthews, *et al.*, 2008). The wafer should be able to absorb specific amount of fluid and maintain an appropriate high viscosity matrix to prolong retention and drug release by reducing the flow of polymeric matrix (Matthews, *et al.*, 2006).

1.11.1 Freeze-drying

Freeze drying or lyophilisation is a technique used to dry a solution to produce a solid product. This method provides the means to dry heat-sensitive drugs or specimens at low temperatures due to reduction of the decomposition or deactivation of such products. Because of large surface area, a freeze-dried product is able to absorb solvent (typically) upon its reconstitution. This is useful for solubilizing freeze-dried vaccines and antibodies during reconstitution for injections (Tang and Pikal, 2004).

Lyophilisation involves three separate, unique and interdependent stages with each step being critical to the final quality of the product. These comprise freezing the formulation and reduction of the solvent (usually water) content by sublimation (primary drying process). This is followed by desorption (secondary drying process) to a residual solvent level that will no longer support biological activity or chemical reactions (Jennings, 2000).

At industrial scale, the freezing stage is usually performed by use of a freeze-drying machine though the material should be cooled below its eutectic point in advance using a freezer or liquid nitrogen. At temperatures lower than the eutectic point, the possibility of solid and liquid material coexisting will be reduced which is desirable. The length of the freezing cycle can be altered as a consequence of the following:

- ❖ Freezing and annealing procedures encourage crystallization while maximizing the size of the crystals and reducing drying rates.

- ❖ The length of the freezing procedure is affected by the thickness of the sample which leads to water vapour molecules experiencing resistance while escaping from the dried portion of the gel.

Therefore reducing the thickness of the starting material (e.g. gels) reduces the resistance to vapour flow; hence the drying process is faster (Tsinontides, et al., 2004).

Freeze drying cycle

i) Freezing or freeze-annealing

The freezing cycle can be performed either by freezing sample continuously at a certain temperature while the drying process is on-going, or freezing coupled with annealing. During freezing and annealing the liquid sample is cooled until pure crystalline ice forms from part of the liquid and the residue of the sample is freeze-concentrated into a glassy state which possesses high viscosity and prevents further crystallization.

ii) Primary drying

During the primary drying step, the majority of the sample's water content present in the form of ice crystals is removed which require specific pressure (vacuum) conditions in the freeze dryer instrument. Sublimation is the basic mechanism of water removal from the substrate (e.g. gels) during freeze drying and occurs by escape of free ice crystals through the frozen gel during the primary drying step. Primary drying or sublimation is a time consuming process, taking place at cooler temperatures and completed safely below the substrate's critical temperature (eutectic point of the formulation). It also requires heat energy to initiate the sublimation process. To obtain the maximum drying yield during the primary drying, several parameters should be considered.

- ❖ Samples must be cooled down to at least 5°C below the critical temperature.
- ❖ The shelf temperature during whole the process should be monitored.
- ❖ The chamber pressure must be selected between one third and one half of the vapour pressure of ice at the freezing temperature.

- ❖ The temperature must be monitored and correlated with the stability point of the sample to ensure that it will not exceed the critical temperature.
- ❖ Temperature and/or pressure should be adjusted accordingly, to control the energy input to the samples.

Primary drying begins when a vacuum is applied to the sealed chamber, and pure frozen ice starts to sublime. The frozen ice, in the ice channels surrounding the interstitial area, is detached during primary drying.

During the removal of these ice channels, critical temperature consideration is extremely important. Within the frozen system, the dense ice in the ice channels provides physical support to the frozen system and act as a scaffold to which other components are attached (Schewgman, 2009).

Following the ice removal through sublimation, residual components within the interstitial area should have sufficient strength to preserve their own weight as the ice scaffolding is removed; otherwise they will collapse and produce a non-porous structure which remains at the bottom of the container.

The critical temperatures, such as eutectic (T_{eu}) and glass transition (T_g), demonstrate different phases from a rigid solid which is capable of supporting their own structure, to a rubbery product that will collapse after ice removal during primary drying. As a consequence, the product temperature should stay below the T_g , T_{eu} or T_c (critical temperature) to retain interstitial space in the solid phase with ability to support its own weight after the ice removal (Schneid and Gieseler, 2009).

As the heat input to the product is increased, evaporative cooling retains the temperature of the product below the temperature of its surrounding atmosphere. After the completion of primary drying, the temperature of the product rises and reaches the shelf temperature an indication of a successful primary drying process with desirable yield (Barley, 2009).

iii) Secondary drying

After the sublimation phase all the ice will have disappeared from the sample and the product's temperature starts rising and approaches the shelf temperature although the product

is not completely dry to remain stable during long term storage. The water content in most products after the primary drying state varies from 5% to 7%.

In secondary drying, the product enter desorption phase and the last traces of water vapour are removed as well as the traces of the “bound” water within the freeze-dried matrix.

The goal is a reduction in the residual water content of the product to acceptable levels of about 1-3% for long term storage and imparts several benefits such as preventing the product from being denatured. In addition it avoids chemical or enzymatic changes by reducing water content to lower levels. Therefore:

- ❖ the starting point for secondary drying should be “ambient” temperature, except when the product is unstable, e.g. proteins which aggregate.
- ❖ during secondary drying an appropriate balance between time against final moisture level is important (Schwegman, 2010).

1.11.2 Advantages of freeze-drying

The advantages of freeze-drying include the following.

1. Increase the potential to protect the product from microorganisms and enzymes.
2. Prevents degradation of the active compound as a consequence of water content reduction.
3. The possibility of damaging the sample by heating at high temperature during drying of the product is considerably reduced.
4. The appearance of the product does not change because of shrinkage or toughening effects as well as smell or flavouring properties of the product.
5. This technique is not only a practical choice to remove water but also other solvents such as acetic acid and alcohols.
6. Rehydration will be rapid because of the existence of microscopic pores in the freeze-dried products.

7. As a consequence of sublimation of ice crystals, and retaining gaps or pores in their place, freeze dried products have pharmaceutical applications because their shelf life can be prolonged for many years (www.biopharma.co.uk- date accessed 27/05/2011).

1.12 Physical properties of polymeric dosage forms

1.12.1 Mechanical (tensile) characteristics

Mechanical properties indicate the physical integrity of the dosage form. To determine the mechanical properties of pharmaceutical film formulations, tensile tests are employed. The relevant tensile properties that are measured include tensile strength, elastic modulus, percent strain at break, and the work done to break.

The tensile strength of a film is defined as the resistance of the material to a force tending to tear it apart, normally identified as the maximum stress in the stress–strain curve (Shah, *et al.*, 2010). The tensile strength reflects how strong the film is mechanically (including brittleness). To enhance the abrasion resistance (in film coatings), higher values of tensile strength of the films are desirable. The type of polymer and its molecular weight are the main determinants of tensile strength. The relationship between film thickness, width and the level of applied force (Alanazi, *et al.*, 2007) can be expressed as:

$$\text{Tensile strength} \left(\frac{\text{N}}{\text{mm}^2} \right) = \frac{\text{Force at break (N)}}{\text{Initial cross – sectional area of sample (mm}^2\text{)}} \quad \text{Eqn 10}$$

Although the aforementioned factors are determined in tensile strength calculations, they are not always reliable in predicting the functional performance of the films.

Elastic modulus on the other hand is a fundamental physical parameter that affects the mechanical characteristics of a film. Elastic modulus or flexibility evaluates the stiffness of the film or how the film deforms in the elastic region. Elastic modulus is also defined as the initial linear elastic phase of deformation and obtained from the ratio of applied stress and corresponding strain (Perumal, *et al.*, 2008).

$$\text{Elastic modulus} \left(\frac{\text{N}}{\text{mm}^2} \right) = \frac{\text{Force corresponding stress (N)}}{\text{Cross - sectional area (mm}^2\text{)} \times \text{corresponding strain}} \quad \text{Eqn 11}$$

Rigid materials exhibit a high elastic modulus, therefore to produce an acceptable strain more stress will be required. Different polymers can possess similar or different elastic modulus and flexibility properties (Cilurzo, *et al.*, 2008).

Another parameter that is measured by the tensometer is tensile elongation which is the eventual elongation of a material (the percentage enhancement in length that takes place before it breaks under stress). The elongation at break is a measure of the ultimate deformation of the film before tearing apart. In general, elongation (or strain) will increase with the addition of suitable plasticizing agents in a formulation.

$$\% \text{ Elongation} = \frac{\text{Increase in length (mm)}}{\text{Original length of the sample}} \times 100 \quad \text{Eqn 12}$$

Shah, *et al* (2010) have explained that soft and weak polymers have a low tensile strength, low elastic modulus, and low elongation at break; while a soft and strong polymer demonstrates adequate tensile strength, elastic modulus and a high elongation at break. Desired mechanical properties will vary depending on the formulation goals and the method selected. Most of the polymers used for film coating of pharmaceutical dosage forms demonstrate brittle characteristics under humid conditions and at ambient temperature. In addition, the strain and type of deformation under stress can fluctuate due to effect of the surrounding atmosphere. The presence of a plasticizer in an aqueous polymeric dispersion minimizes such deformation behaviour.

There is a universal standard method introduced by the American Society for Testing and Materials (ASTM) to define tensile properties of thin plastic sheets which involves measurement of the ductility and brittleness of a film and is associated with elongation of the film at the breaking point. Calculation of the elastic modulus is by measuring the slope of the initial linear portion of the stress-strain curve. A firm and rigid film that is hard to break has a high elastic modulus, however the presence of plasticizers such as water or glycerol alters the elastic modulus, as is the case for the tensile strength. Plasticizers such as glycerol, act by increasing the free volume between the polymer chains, reduce the interactions between the

chains and provide flexibility to the polymer(s). The brittleness will be decreased due to the polymer chains sliding easily as a result of the decrease in tensile strength (Perumal, *et al.*, 2008). To run the test and measure the force required for breaking sample apart, a tensometer is employed (Figure 1.11).

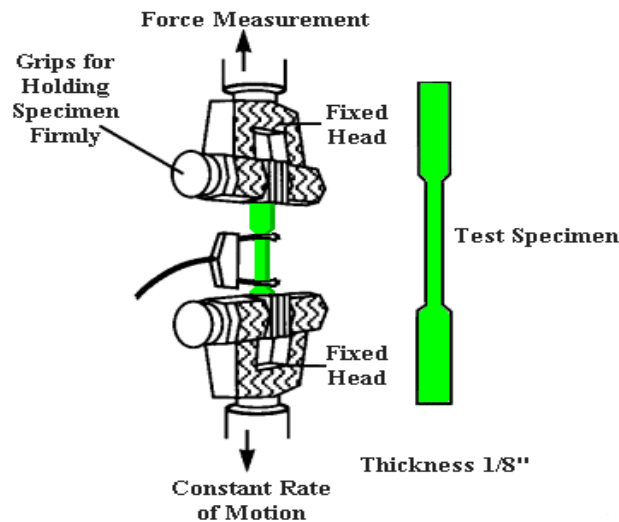


Figure 1.11 Schematic view of tensometer (texture analyser).

This instrument exerts a force on the sample from both ends whilst the elongation and resistance is measured simultaneously in the samples before they break (De Moura, *et al.*, 2009).

The resistance of the solid formulation such as wafers to deformation following the application of pressure is called “hardness”, which is measured in units of force per unit area. It shows the brittleness or wafer’s mechanical strength (upon hydration) and elastic behaviour which is used to characterise the material (Boateng *et al.*, 2010).

1.12.2 Bioadhesivity

Bioadhesivity involves the process whereby polymers (synthetic or bio materials) adhere to biological tissues and if the attachment occurs with mucus or a mucosal membrane, this phenomenon is referred to as mucoadhesion (Smart, 2005). Adhesivity is defined as the essential free energy required for removing a bioadhesive polymer from the body surfaces where it is attached and can be measured using texture analysis. The adhesive force depends on several parameters such as hydrophilicity (reported to progress bioadhesion), stage of

hydration and rate of polymer erosion after being in contact with the hydrating surface (Patel, *et al.*, 2009).

Smart (2005) explained that the mucoadhesion bonds formation depends on the nature of the mucous membrane and mucoadhesive material, formulation type, the attachment procedure and the environment of the bond. The mucoadhesion occurs as a consequence of various adhesive bonds at the interface of mucosal membrane and mucoadhesive agent.

These bonds include (1) ionic bonds: where two oppositely charged ions attract each other via electrostatic interactions and a strong bond will be formed (e.g. in a salt crystal); (2) covalent bonds which are very strong bonds in which electrons are shared in space, between the bonded atoms in order to fill the orbitals; (3) hydrogen bonds: here a hydrogen atom, when covalently bonded to an electronegative atom such as oxygen, fluorine or nitrogen, carries a slight positively charge and hence, is attracted to electronegative atoms. The mucosal membrane and mucoadhesive share the hydrogen atom though this bond is usually weaker than ionic or covalent bonds; (4) van-der-Waals forces: these are some of the weakest forms of interaction that arise from dipole–dipole and dipole-induced dipole attractions in polar molecules, and dispersion forces with non-polar substances; (5) hydrophobic forces: give rise to the hydrophobic effect and occur when non-polar groups are present in an aqueous solution (Laidler, *et al.*, 2003). The process of adhesion to mucosal cells can be summarized in three steps.

❖ Wetting and swelling of polymer

The wetting and swelling steps happen following the spread of a polymer on the surface of the biological substrate or mucosal membrane (e.g. oral cavity or vagina) to facilitate the development of a close contact with the substrate. Bioadhesives stick to biological tissues as a consequence of the surface tension and forces existing at the site of adsorption or contact. Swelling of polymers takes place because their constituent molecular components have an affinity for water which results in hydration (Semalty, *et al.*, 2008).

❖ Interpenetration between the polymer chains and the mucosal membrane

The surface of mucosal membranes is composed of glycoproteins which are high molecular weight polymers. The bioadhesive polymer chains and the mucosal glycoprotein chains interact and entangle together to produce an adhesive bond. The strength of these bonds will

be affected by the level of inter-penetration between the two groups of polymer. To obtain strong adhesive bonds, one polymer group should be soluble in the other and both polymers should have similar chemical structure (Shaikh, *et al.*, 2011; Figure 1.12).

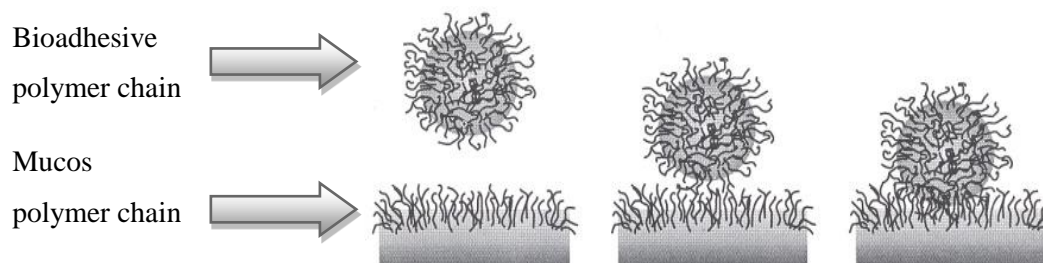


Figure 1.12 Schematic view of the interaction between the bioadhesive and mucosal tissues (Nangia, 2008).

❖ Formation of chemical bonds between the entangled chains

The formation of weak chemical bonds between the entangled polymer chains occurs after the second step (Figure 1.13). Various types of bonds formed between the chains are primary bonds such as covalent bonds and weaker secondary interactions such as van-der-Waals forces and hydrogen bonds.

Primary or secondary bonds are employed to achieve bioadhesive formulations where strong adhesions between polymers are produced (Semalty, *et al.*, 2008, Shaikh, *et al.*, 2011).

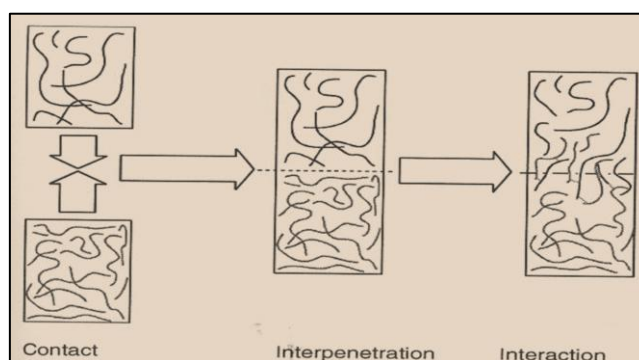


Figure 1.13 Final adhesion between bioadhesive polymer and the mucosal tissues (Shaikh, *et al.*, 2011).

Bioadhesive polymers are expected to possess certain 'ideal' characteristics to make them suitable for their role as mucosal formulations (Smart, 2005).

1) Flexibility- the flexibility of bioadhesive polymers is important since it determines the extent of the interpenetration between the polymers and mucosal/epithelial surfaces.

- 2) Hydrophilicity – hydrophilic polymers are able to form stronger adhesive bonds with mucosal membranes as the mucus layer retains significant amounts of water.
- 3) Hydrogen bonding – hydrogen bonding between the entangled polymer chains creates strong adhesive bonds, hence the existence of hydrogen bond – forming groups such as OH and COOH groups are essential.
- 4) Molecular weight – high molecular weight polymers are more desirable since more bonding sites are available.
- 5) Surface tension – this is necessary to widen the bioadhesive polymer into the mucosal layer epithelial surface (Smart, 2005).

According to the theories; generation of mucoadhesion force is based on the ability of bioadhesive polymers to form non-covalent bonds with mucin glycoprotein. Scientifically, ionisable polymers existing in their unionized form are able to form non-covalent bonds with mucus glycoprotein. Also in acidic polymers, pH plays a critical role to predict binding behaviour. The pH should be around or lower than their corresponding pKa values and the reverse is true for basic polymers. Unionized amino and carboxyl groups on polymers are important for polymer structures and formation of weak chemical bonds with mucus glycoproteins (Sigurdssona, *et al.*, 2001).

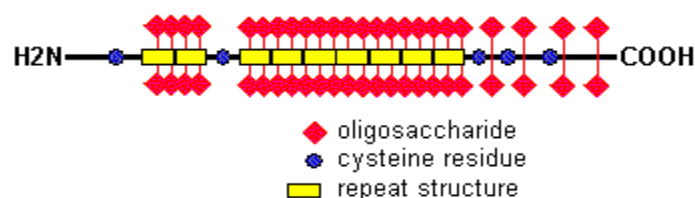


Figure 1.14 The generic structure of mucin monomer.

1.13 Drugs in the solid state

Based on their structure, there are two types of solids (crystalline, amorphous) and each form exhibits different physical and chemical properties such as colour, morphology, stability, dissolution, and bioavailability. Therefore monitoring the polymorph of the drug during the various stages of drug development is critically important (Graeser, 2009). Amorphous forms of a drug do not possess long-range order of molecular packing or well-defined molecular

conformation therefore far less energy is needed to dissolve them and consequently solubilise more quickly in comparison to the crystalline and hydrated forms of a drug (Yu, 2000).

The ‘apparent solubility’ and dissolution advantage provided by these systems is a means to improve bioavailability of poorly water soluble drugs (Murdande, *et al.*, 2010). However, amorphous systems present certain limitations which include physical instability and higher chemical reactivity with a tendency to convert to the crystalline form. This often leads to limited use in pharmaceutical formulations. Therefore, it is vital to determine the molecular and thermodynamic characteristic that contributes to the solubility and stability of amorphous drugs.

Drugs in crystalline state may exist in several molecular arrangements (morphs). Such phenomenon is called polymorphism and it is defined as the ability of a material to be present in two or more arrangements or conformations of molecules in the crystal lattice. The most important pharmaceutical issues which are related to polymorphism are bioavailability and toxicity. The chemical reactivity in the solid state is related to the nature of the crystalline state (Giron, 2001b). Therefore, during pre-formulation studies characterisation of the polymorphic nature of the initial materials is essential.

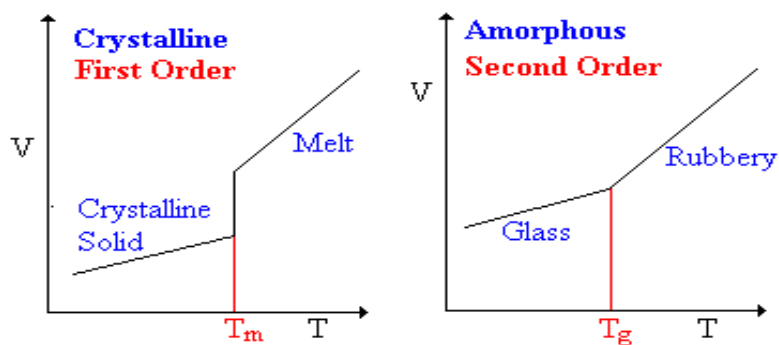


Figure 1.15 Schematic view of melting point of crystalline (left) and glass transition of amorphous (right).

A glassy material is an amorphous solid that exhibits a “glass transition” into the rubbery state (Figure 1.15) upon heating in contrast to crystalline which show melting point. Therefore, all glasses are amorphous, but not all amorphous materials are glasses. Glass is classified as an amorphous solid with the energy level of a solution and a liquid-like structure but their high viscosity is not as observed for liquids (Angell, 2008).

1.13.1 Thermal properties of amorphous compounds

As mentioned above, potential changes in the properties of amorphous systems during storage need to be ascertained. These changes include e.g. physical ageing, chemical reactions, crystallization and protein unfolding (i.e., destabilization). Such changes usually decrease and alter the potency and/or quality of the drug formulation therefore, those changes should be systematically studied (Yu, 2000).

Thermo-analytical techniques and microcalorimetry are the most common techniques used for determination of the thermodynamic relationships between different phases of a compound of interest and the use of different thermo-analytical techniques e.g. differential scanning calorimetry (DSC), hot stage microscopy (HSM) and thermogravimetry (TGA) with X-ray diffraction (XRD) is complimentary (Giron, 2001b).

1.13.2 Glass transition

Forming amorphous material is possible if the cooling rate of a liquid is fast enough to prevent crystallization which would otherwise take place if time had been sufficient for the compound to reach equilibrium at each temperature (Royall, 1998).

By cooling a liquid slowly, the material (substance) of interest can crystallize which causes a reduction in the specific volume as a consequence of the first-order phase transition (Figure 1.16). When the liquid is cooled first (crystallization prevented) and material reaches a temperature T below the melting point (T_m) then it is called a super-cooled liquid. The specific volume and thermodynamic characteristics of a super-cooled liquid at lower temperature can be extrapolated according to the characteristics of the liquid above T_m (Angell, 2008).

When a super-cooled liquid goes beyond the glass transition point and the system falls out of energy equilibrium, a glassy state is obtained (Edinger, *et al.*, 1996). However, the crystalline form is invariably the thermodynamically stable form. Hence, there is a high possibility for the transition from glassy state with high energy and non-equilibrium meta-stable phase to a low energy level phase to occur (Wu, 2009).

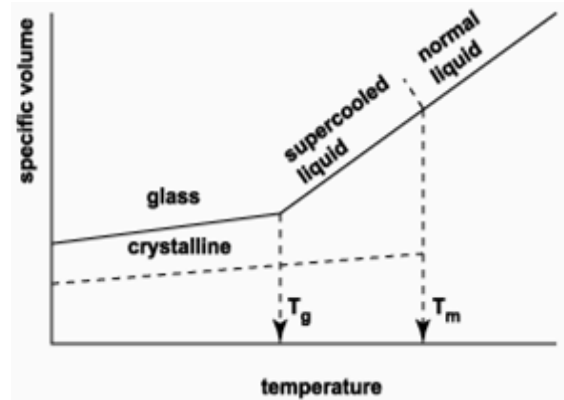


Figure 1.16 Plot showing the transition from liquid to super-cooled liquid and glassy state.

Glasses are generally produced with a constant cooling of the liquid state and frequently followed by an annealing stage, in that existing stresses during the vitrification are eliminated (Angell, 1995). Apart from fast cooling of the liquid form, the glassy state can be obtained practically by vapour-phase deposition, desolvation and *in situ* chemical reactions (Figure 1.17).

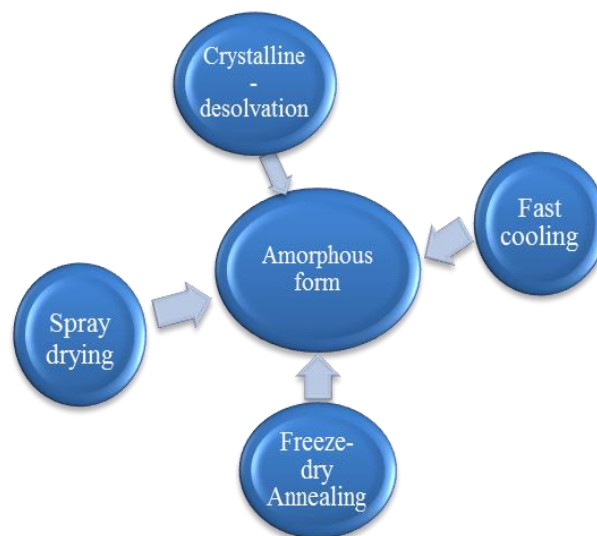


Figure 1.17 Different methods used to obtain amorphous material.

1.13.3 Determination of glass transition temperature

Amorphous polymers go through the glassy state to the rubbery state as temperature increases and the glass transition temperature is the temperature at which this phase change occurs.

There are several properties of a compound which are affected by the glass transition temperature including stability, swelling and elastic modulus (Figure 1.15). The variations in glass transition temperature values reported depend on the broad range of techniques selected to measure it as well as the choice of industrial polymers used. The most common method to determine T_g is specific volume. In this method a curve is plotted by measuring the specific volume as a function of temperature (Figure 1.16). The glass transition will occur and the corresponding accurate temperature is estimated by analytical methods such as differential scanning calorimetry (Ediger et al., 1996).

1.13.4 Factors affecting the glass transition temperature

- ❖ Molecular weight and its distribution can affect T_g because the mobility of the molecules decrease with increasing molecular weight and therefore a higher energy will be required to achieve the desired mobility level.
- ❖ The fraction of free volume in the polymer will be affected by pressure. Increasing pressure causes a reduction in the free volume fraction which directly decreases the glass transition (Craig, 1995).
- ❖ Size of the polymer pendant side chain can affect density variation and depends on how regular the arrangement of the pendant group is. When the arrangement of the pendant group is random, the density is lower than when the pendant arrangement is in a regular array. Consequently, the glass transition temperature is lower for polymers with lower density. If the density is not changed significantly (> than 2%) by the regularity of the polymer chain pendant, the glass transition temperature for ordered or random pendant structures will be similar (Menczel & Prime, 2009).
- ❖ Other factors include rigidity of the backbone, branching, cross-linking, symmetry and polarity (Angell, 2000).

1.14 Thermal analysis techniques (TA)

The pharmaceutical industry utilizes a wide range of techniques to analyse, design and produce compounds with therapeutic efficacy. Physical properties of solid dosage forms are evaluated and utilized in early stages of the drug development process.

The final results of the characterization are critical in determining whether the examined component is nominated for further development and formulated into a commercial product. The characterization of hydrates and solvates are very important in determining the behaviour of polymorphs and pseudopolymorphs within a system. Some specific thermal analytical methods such as hot stage microscopy, DSC, TGA are used for analysis. Although TA techniques are fast and a convenient means of characterisation, the heat applied is considerably higher in comparison to actual storage conditions. To obtain reliable information, the data produced should be extrapolated to the real condition to predict the compound's stability (Glass, *et al.*, 2004).

In some cases, heating may result in new phases, including eutectics and solid solutions as well as the possibility of chemical interactions such as “host-guest” complexation (Glass, *et al.*, 2004). Determination of all potential interactions is sometimes very complicated and requires use of various techniques and correlating the information obtained in order to arrive at a valid conclusion.

1.15 Polymers

1.15.1 Poloxamer 407 (P407)

P407 (Figure 1.18) is a block copolymer synthesized by sequential addition of ethylene oxide to propylene oxide in the presence of hydroxide ions in an inert and anhydrous atmosphere in a high pressure environment. The main sources of P407 are natural gas and oil.

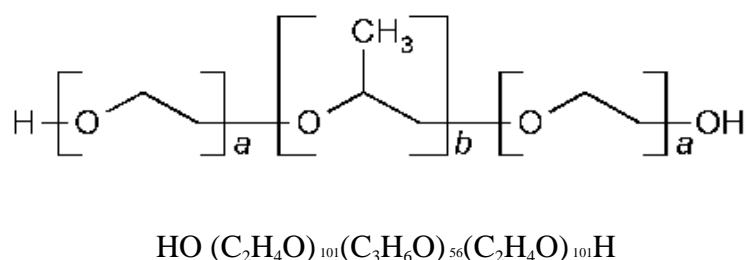


Figure 1.18 Chemical structure of P407.

Pharmaceutical applications

This compound is classified as a non-ionic surfactant and its low toxicity properties allow it to be employed in oral dosage forms.

P407 also function as emulsifiers and viscosity stabilizers in dermatological creams and pastes. In addition, they have been added to drug formulations to control the particle size and as solubilising agents for hydrophobic drugs (Klang, *et al.*, 1994). P407 is present in most mouth washes, except natural cleansing products. In addition, hydrogel-based microparticles containing thermo-gelling P407 with cross-linked alginate demonstrated potential as a controlled protein delivery system (Gong, *et al.*, 2009).

An *in situ* ocular gelling sustained release system formulated with P407 and containing IND showed the ability to release drugs over eight hours (Balasubramaniam, *et al.*, 2003). As a consequence of their properties, such as ordered micellar packing structure and inter-micellar entanglement, P407 gels exhibit high viscosity and partial rigidity and therefore incorporation of hydrophilic and hydrophobic drugs will be enhanced (He, *et al.*, 2008). Extensive investigations have confirmed the use of P407 to formulate gels that can provide a potential controlled release drug delivery system with the ability to target drugs to particular sites in the body; which has attracted a great deal of attention (Yang and Alexandridis, 2000). In addition other potential clinical applications include stimulatory effects on the immune response; protection of human vein grafts during storage and uses in cleaning wounds Dumortie, *et al.* (2006) and Barichello, *et al.* (1999). This will provide the opportunity to use films or wafers on the buccal wounds as well.

1.15.2 Carrageenan

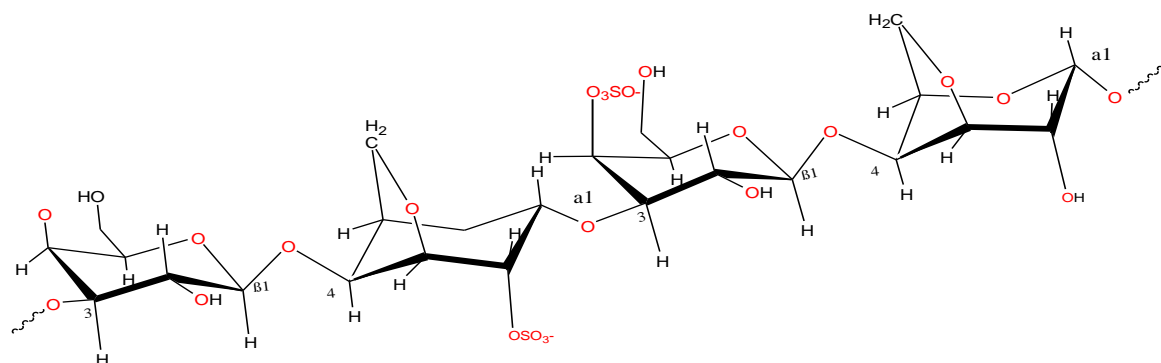


Figure 1.19 Chemical structure of kappa-carrageenan.

Kappa Carrageenan (Figure 1.19) is an anionic sulphated polysaccharide produced from red seaweed (*Rhodophyceae*).

According to the number of sulphate groups per repeat unit of polysaccharide, carrageenan is classified into three main types: kappa (κ), iota (ι) and lambda (λ) with one, two or three sulphate groups, respectively. They can occur as sodium, potassium, magnesium, calcium or mixed cation forms.

In aqueous solution, kappa and iota types exhibit a thermoreversible sol-gel transition and retain pseudoplastic properties with some degree of ‘yield value’ structure. Water dispersion is as a consequence of random coil formation in the sol stage. All solutions demonstrate a reversible decrease in viscosity upon temperature increase, while addition of electrolytes results in a decrease in viscosity. Carrageenan solution is stable at pH between 6 and 10. In addition low temperature causes galactose sequences to twist in a double helix manner (Yughuchi, *et al.*, 2002, Thommes, *et al.*, 2006 & 2008). Anderson, *et al.* (1973) proposed the theory of gel formation of carrageenan which is related to the formation of double helix structure. This image (Figure 1.20) was obtained by X-ray powder diffraction (Gabriele, *et al.*, 2009).

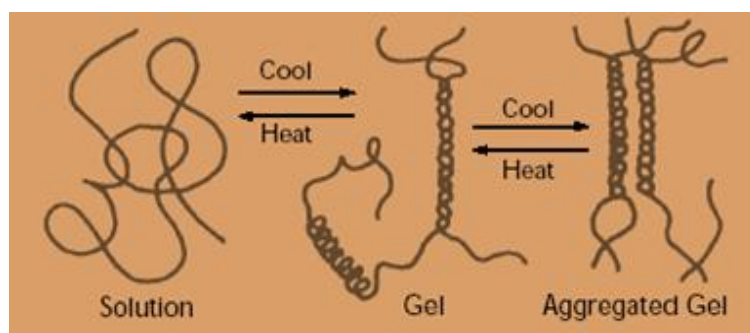


Figure 1.20 Schematic view of mechanism of gelation of carrageenan.

Various grades of carrageenan obtained from different sources were used in the experimental part of the project and exhibited specific characteristics (Table 1.6). Also the physico-chemical properties for each of the grades depend on the chemical structure and the salt content. κ -carrageenan is produced by alkaline elimination from μ -carrageenan isolated mostly from the tropical seaweed *Kappaphycus alvarezii*.

Kappa carrageenan easily binds to water and forms strong and rigid gels. Formation of the firm gel essentially occurs due to the presence of potassium salts. Increasing the level of potassium therefore results in formation of a gel with a tight cumulative structure.

Table 1.6 Characteristics of various grades of carrageenan.

Product name	Carrageenan type	Viscosity	Gel characteristics	Water solubility	Use level	Examples of use
Gelcarin GP-379 NF	Iota	High thixotropic	Elastic medium strength	Hot	0.3-1.0%	Creams, suspension, useful for freeze drying protein reactive
Gelcarin GP-812 NF	Kappa	Low	Brittle Strong	Hot	0.3-1.0%	Stronger gels than GP-911 Note: syneresis higher than GP-911
Gelcarin GP-911 NF	Kappa	Low	Brittle Firm	"Hot partial cold"	0.25-2.0%	Encapsulation/delivery systems protein reactive

(Adapted from FMC Biopolymer corporate website)

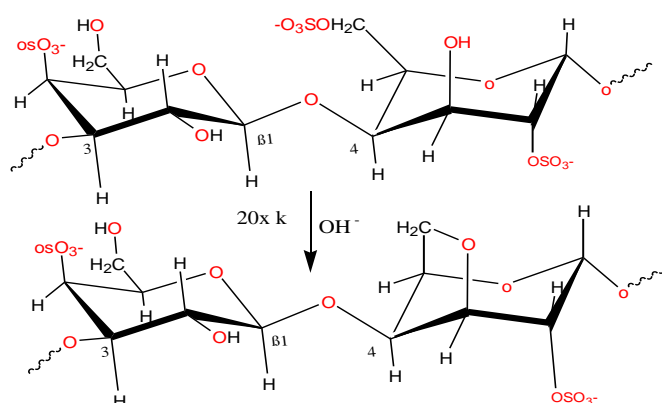


Figure 1.21 κ -Carrageenan rearrangement.

ι -carrageenan is produced by alkaline elimination from ν -carrageenan isolated mostly from the Philippines seaweed *Eucheuma denticulatum* (also called Spinosum).

Iota carrageenan binds to water as well; however, the gel is dry and elastic, mainly due to the presence of calcium salts (BASF, 2009). The effect of divalent calcium ions induces bond formation between the carrageenan chains to produce helices.

The two sulphate group on the exterior of the iota carrageenan molecule prevents the helices from aggregating to the same extent as kappa carrageenan, although it forms additional bonds via interaction with calcium. Therefore resultant gels are more elastic, dry but have excellent stability in freeze/thaw dosage form (Schmidt, *et al.*, 2003).

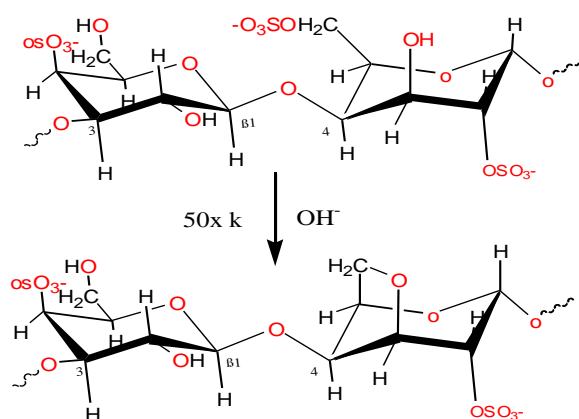


Figure 1.22 ι -carrageenan rearrangement.

Addition of kappa-carrageenan causes an increase in drug bioavailability (Thommas, *et al.*, 2009) and has been reported for use in microencapsulation Suzuki and Lim (1994). Carrageenan is known as a bioadhesive agent due to the anionic nature which helps to bind to mucosal tissues more effectively. Besides, anionic polymers with sulphate groups bind more effectively to mucosal tissues compared to those with carboxylic groups. In addition, polyanions are much safer than polycations in terms of binding potential and toxicity (Rajput, 2010). Carrageenan has been widely employed in the food industry as a gel or viscose base. However, it is used less widely in the pharmaceutical industry although it has been shown to exhibit physiological effects such as anti-tumour activity (Yughuchi, *et al.*, 2002).

Eudragit, polyethylene glycol and glycerol

Eudragit L100 has been used in the pharmaceutical industry as a film coating agent and demonstrated acceptable properties as well as adequate safety. Eudragit L100 is an anionic copolymer based on methacrylic acid and methyl methacrylate (Figure 1.23). It has good solubility in a mixture of methanol, ethanol, 3% water in isopropyl alcohol and acetone.

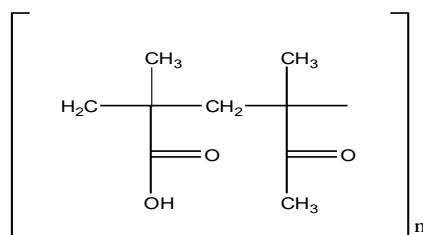


Figure 1.23 Chemical structure of Eudragit L100.

Polyethylene glycol is a well-known precipitant for protein crystallization and also been used in toothpastes as a dispersing agent. In the current project, the main use in the formulations is as plasticizer. Polyethylene glycols (PEGs) are water soluble synthetic polymers with monomers of oxyethylene and general structure of H-[-O-CH₂-CX-]_n-OH. In this structural formula n is the number of repeat units. PEGs have a wide range of molecular weights, starting from (PEG 200-600) which are liquids at room temperature to semi-solids with 1500 Da molecular weight, (PEG 3000-20,000) which are semi-crystalline solids as well as resinous solids with higher than 100,000 Da molecular weight.

The various biopharmaceutical advantages of PEGs such as ability to attach to the surface of liposomes to prevent recognition by the immune system, binding to proteins and to allow fusion with cells has contributed to the significant interests shown in these compounds (Craig, 1995). In addition these polymers have been used in several pharmaceutical products, so there is adequate evidence of its safety. Glycerol has been used in pharmaceutical products mainly to improve smoothness, providing lubrication in tooth pastes, skin care products and in solid dosage forms such as tablets as a binding agent. According to the FDA there is no concern regarding safety issues.

Chapter 2 : Experimental

2.1. Materials and equipment

2.1.1 Chemicals

Excipients	Supplier	Batch number
κ-Carrageenan (Gelcarin GP 911)	Honeywill & Stein Ltd Surrey, UK	50102070
κ-Carrageenan (Gelcarin GP 812)	Honeywill & Stein Ltd Surrey, UK	80402170
ι-Carrageenan(Gelcarin GP 379)	Honeywill & Stein Ltd Surrey, UK	40021170
Polyethylene glycol 600	Aldrich, Gillingham, UK	25398PJ-139
Polyethylene glycol 2000	Aldrich, Gillingham, UK	1415570
Polyethylene glycol 6000	Aldrich, Gillingham, UK	0001409391
Polyethylene glycol 20000	Aldrich, Gillingham, UK	1382603
Poloxamer 407	Sigma, Gillingham, UK	038k0071
Glycerol	Fluka, Gillingham, UK	RB12720
Eudragit L100	Degussa, Gillingham, UK	B071003084
Model drugs	Supplier	Batch number
Ibuprofen	Sigma, Gillingham, UK	026H1368
Indomethacin	Sigma, Gillingham, UK	088K0666
Paracetamol	Aldrich, Gillingham, UK	RB16652

2.1.2 Equipment & instruments

Equipment	Supplier
Homogenizer-IKA; RW20 digital	Camlab, London, UK
Texture analyser-HTI Hounsfeild	Deutschland, Germany
Heating magnetic stirrer up to 370°C- T.ARE (VELP scientific)	Rhys Scientific, Chorley, UK
Vortex up to 40 Hertz- Top Mix FB15024	Fisher, Loughborough, UK
Oven up to 250°C	Genlab, Widnes, UK
Balance d=0.001 Max=200g	Denver Instrument SI 230, USA
Hi resolution TGA 2950	TA Instruments, Crawley, UK
DSC 823e	Mettler Toledo, Leicester, UK
Hot Stage Microscopy FP90 central processor	Mettler Toledo, Leicester, UK
Setaram TGA	Thron Scientific Services, Surrey, UK
Balance XS 105 dual range Max=41gr/120gr, d=0.01mg/0.1mg	Mettler Toledo, Leicester, UK
D8 Advance XRD	Brucker, Coventry, UK
JSM5310LV SEM	Jeol, Tokyo, Japan
HPLC, G1329A Agilent-1200 series	Agilent Technologies Ltd, Wokingham, UK
Varian Cary 100 UV/Vis spectrophotometer,	Varian, Yarnton, UK
DSC Q2000	TA Instruments, Crawley, UK
AdVantage Freeze-Dryer	Biopharma Process Systems, Winchester, UK

2.1.3 Consumables

Consumable	Supplier
75µl Aluminium crucibles	Setaram, Ashtead, UK
Magnetic stirrer	Fisher, Gillingham, UK
40µl Aluminium crucibles	Mettler Toledo, Coventry, UK
Aluminium lids	Mettler Toledo, Coventry, UK

2.2 DSC analysis of physical mixtures of starting materials

Prior to the formulation development step extensive DSC studies were conducted in order to evaluate the thermal characteristics of pure components and their physical mixtures corresponding to the amounts present in the films and wafers. Specifically, melting transition (T_m) and glass transition point (T_g) were determined as well as any possible interactions between the starting materials during gel formation. Initial mixtures were prepared by addition of two starting components to deionized water with heating up to 40-50°C and continuous stirring. Samples were analysed using a Q2000 instrument (TA Instruments, Crawley, UK) calibrated with indium and sapphire under a nitrogen atmosphere. T zero aluminium pans (75 µL) were packed with 3-10 mg of sample and hermetically sealed. The samples were cooled before heating, dynamically using the heating cycles below:

1st heating: -80 to 180°C at a rate of 10°C/min.

2nd heating: -80 to 180°C at a rate of 10°C/min.

Cooling after each heating cycle was immediately undertaken at a rate of -10°C/min.

The foregoing steps were conducted in order to ensure that any physico-chemical changes (interactions/degradation) occurring during gel formulation could be detected. To evaluate the interaction between PEG 600 and P407 additional DSC studies were performed. This

study was based on the possible interaction between PEG 600 and P407 which had been observed for the films during DSC analysis.

The investigation involved preparation of various mixtures of P407 and PEG 600. They were physically mixed, melted and solidified before DSC analysis. Samples were prepared by heating the physical mixtures of PEG 600 and P407 at ratios of (0/100) up to (100/0) % w/w of PEG/ P407, respectively at 10% increments followed by solidification. 3-10 mg of the mixtures were loaded into the T zero DSC pans and DSC analysis were performed as follows:

1st heating -40°C to 80°C at 10°C/min

2nd heating -40°C to 80°C at 10°C/min

3rd heating -40°C to 80°C at 10°C/min

Cooling after each heating cycle was at - 10°C/min

2.3 Formulation development of solvent cast films

Different polymers were initially used to formulate solvent cast films. The films were evaluated in terms of transparency, satisfactory elasticity and ability to incorporate drug and selected for further development. Stability, during handling and storage was ascertained for blank and drug loaded films. The polymers used were P407, CAR (κ or ι), Eudragit L100 and 4 grades of polyethylene glycol (PEG 600, 2000, 6000, 20000). Different grades of PEG were used to evaluate the plasticity of the films and the most appropriate one based on the physical criteria mentioned above, chosen for further formulation development. This procedure was performed just for solvent casting.

2.3.1 Gel preparation

Prior to film casting, aqueous gels of the polymers were prepared. Formulation development to obtain the optimum gel involved three strategies (A1, A2 and B).

A. The preliminary method employed to produce gels involved adding the polymers to warm deionised water and heating to 70°C. The percentage of PEG or glycerol, as plasticiser, was dependent upon the amount of CAR using three different ratios of

carrageenan: plasticiser of 1:2, 2:3 and 1:3, respectively. Producing a transparent gel with acceptable viscosity characteristics was conducted by two methods.

1. CAR (κ or ι) or Eudragit L100 was added to magnetically stirred hot deionised water (60-70°C) in a beaker until a clear, swollen and homogeneous gel was obtained. P407 and PEGs or glycerol were then added together to the resulting gel and heated with continuous stirring for 30 minutes.
 2. The required amount of deionized water was divided into two equal portions. One portion was heated to 60°C and CAR or Eudragit L100 added with continuous stirring for 10 minutes. P407 and plasticizer (PEG 600 or glycerol) were dissolved in the second portion, stirred for 5 minutes to produce a clear solution and then gently added to the initially prepared CAR or Eudragit gel.
- B. P407 was added to cold water and left for two hours at room temperature before adding κ -CAR powder to the resulting gel. This mixture was incubated at room temperature overnight to allow complete hydration of the CAR after which the gel was heated up to 40-50°C to ensure a homogeneous mixture was obtained. The remaining components i.e. plasticiser (PEGs or glycerol) and model drug were added and mixing continued for a further 5-10 min.

Initially, the gels generated were examined visually to evaluate their physical characteristics such as trapped air bubble, transparency, acceptable flexibility and viscosity (ease of pouring).

Drying procedure for cast films

The gels were poured into Petri dishes (90 mm diameter) to a height of 10 mm and placed in a vacuum oven at 60°C to remove excess moisture and help the drying procedure. The length of drying was investigated for optimum duration in the oven by measuring the weight at 24 hour intervals until it remained constant.

2.3.2 Drug loading into optimized films

Investigation of drug loading into the films was performed after selection of the optimised films. The purpose was to determine the maximum amount of drug that could be incorporated into the films whilst maintaining the ideal physical characteristics in terms of flexibility and transparency.

This was achieved by formulating films using increasing concentrations of drugs until beyond the optimum amount; drug re-crystallization occurs and is visible on the surface of the films. Two strategies were evaluated based on the maximum amount of drug that could be loaded without being visible (to the naked eye) on the film surface.

1. IBU (0.3-1.0% w/w), IND (0.1-0.8% w/w) or PM (1-2% w/w) were added to the P407 solution 4% (< 15°C), kept for 2 hours before addition of 2.5% w/w CAR 911 and plasticizer (PEG 600 5.0 - 6.5% w/w) or glycerol (4.5-5.5% w/w) and incubated for 24 hours. This was done with the aim of increasing drug incorporation based on the surfactant properties of P407.
2. The second strategy was employed to increase the loading of the less soluble drugs IND and IBU based on the work reported by Watkinson *et al* (2009) observations. The model drug (IND or IBU) was dissolved in 2 mL of ethanol and the resulting solution added to the gel comprising 2.5% w/w CAR 911, 4% w/w P407 and 5.0-6.5% w/w PEG 600 or glycerol (4.5-5.5% w/w) prepared as in (B) above.

2.3.3 Film formation

Various films with different ratios of κ and ι -CAR were prepared in the presence of P407 and glycerol or different grades of PEG as plasticizers (Table 2.1). Subsequently, the blank films were evaluated to determine the composition that gave the most flexible film before loading with IBU (Table 2.2).

Table 2.1 Composition of gels containing P407 with various grades of carrageenan (CAR 812, 911, or 379), PEG 600 or glycerol (GLY)

CAR (% w/w)	P407 (% w/w)	Plasticiser (% w/w)
2.5 (911)	4	3.5 PEG 600
1.5 (812, 911, 379)	2	4.5 PEG 600
1.5 (812, 911, 379)	3	4.5 PEG 600
1.5 (812, 911)	5	4.5 PEG 600
1.5 (812,911)	6	4.5 PEG 600
1.5 (812, 911)	7	4.5 PEG 600
2.5 (812, 911)	4	5.0 PEG 600
1.5 (812, 911)	4	5.5 PEG 600
2.5 (812, 911)	4	5.5 PEG 600
2.5 (812, 911)	4	6.0 PEG 600
2.5 (812)	4	6.5 PEG 600
2.5 (911)	4	6.5 PEG 600
1.5 (812, 911)	4	5.0 GLY
1.5 (812, 911)	4	5.5 GLY
2.5 (812, 911)	4	5.0 GLY
2.5 (812, 911)	4	5.5 GLY
4.0 (911,812)	8	5.0 PEG 600
3.0 (812, 911, 379)	8	5.5 PEG 600
1.5 (812, 911, 379)	2	5.0 PEG 600
2.0 (812,911, 379)	2	2.0 PEG 20000
1.5 (812, 911, 379)	2	3.0 PEG 20000
1.5 (812, 911, 379)	3	4.5 PEG 2000
1.5 (812, 911)	2	4.5 PEG 2000
2.5 (812,911)	4	5.5 PEG 6000
2.5 (812, 911)	4	5.5 PEG 2000
2.5 (812, 911)	4	5.5 PEG 20000
2.0 (812, 911)	4	4.5 PEG 600
2.0 (812, 911)	4	5.5 PEG 600
2.5 (911, 812)	4	3.5 GLY
2.5 (911, 812)	4	4.0 GLY
2.5 (911, 812)	8	4.5 GLY
2.5 (911, 812)	8	3.5 GLY

Following the initial investigations with IBU, the procedure was repeated using various concentrations of IND and PM.

Table 2.2 Composition of the IBU loaded gels prepared during film formulation development and optimization process.

Total dry weight of CAR (% w/w)	P407 (% w/w)	Plasticiser (% w/w)	Model drugs (% w/w)
2.5 (911)	4	5.0 PEG	0.3 IBU
2.5 (812)	4	5.0 PEG	0.3 IBU
2.5 (911)	4	5.0 PEG	0.4 IBU
2.5 (812)	4	5.0 PEG	0.4 IBU
2.5 (812, 911)	4	5.5 PEG	0.3 IBU, IND
2.5 (812, 911)	4	5.5 PEG	0.4 IBU, IND
2.5 (911)	4	5.5 PEG	1.0 PM
2.5 (911)	4	5.5 PEG	0.8 IBO
2.5 (911)	4	5.5 PEG	1.4 PM
2.5 (911)	4	5.5 PEG	1.6 PM
2.5 (911)	4	5.5 PEG	1.0 IBU
2.5 (911)	4	5.5 PEG	1.2 PM
2.5 (911)	4	5.5 PEG	0.6 IND
2.5 (911)	4	6.5 PEG	0.6 IND
2.5 (911)	4	6.5 PEG	0.8 IBO
2.5 (911)	4	6.5 PEG	1.0 IBU, IND
2.5 (812, 911)	4	4.5 GLY	0.3 IBU
2.5 (812)	4	5.0 GLY	0.3 IBU
2.5 (911)	4	5.0 GLY	0.3 IBU
2.5 (812)	4	5.0 GLY	0.3 IBU
2.5 (911)	4	5.0 GLY	0.3 IBU
2.5 (812, 911)	4	5.5 GLY	0.4 IBU
2.5 (812, 911)	4	5.5 GLY	0.8 IBU
2.5 (812, 911)	4	5.5 GLY	1.0 IBU

2.4 Characterisation of solvent cast films

2.4.1 Texture analysis

Texture analysis was employed to measure the tensile properties of the films including tensile strength, elastic modulus, elongation and “work done to break” the films. This technique was used to determine the effect of polymer, plasticiser and drug concentration on the tensile properties of the films and the resulting data used to select the most appropriate formulations for further development and drug release studies. For this purpose a texture analyser HD-plus with Exponent software to plot and interpret the data from the tensometer was employed. Before tensile measurements, the thickness of the films was measured by micro screw-meter

in five different areas of each sample (four edges and one in the middle) and showed thickness ranging from 0.33-0.37 mm which was considered quite uniform.

The thickness of each particular specimen was entered into the texture analyser software prior to stretching. The films were cut into dumb-bell shapes prior to stretching (Figure 2.1).

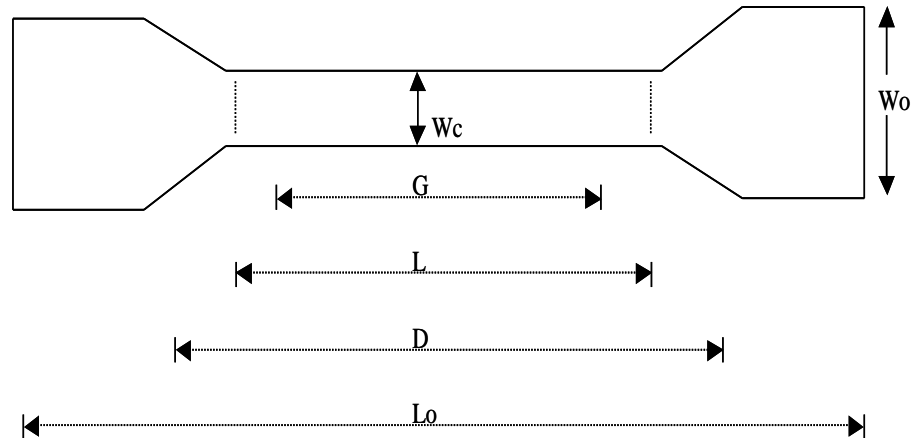


Figure 2.1 Schematic diagram of typical dumb-bell shaped sample for tensile testing of thin films.

W_c = the width of the narrow section.

G = gauge length, the film specimen is expected to break within this distance, or else a particular test is rejected. It is defined as the original length of that portion of the specimen over which change in length is determined.

L = the length of the narrow section. The tensile force per unit area (stress) is greatest along this length and the test is centred within this section.

D = the distance between the grips holding the films. This represents the portion of the whole film subjected to tensile stress.

L_0 = the overall length of the film.

The dumb-bell shape specimens were clamped between two tensile grips and stretched till breaking point using the settings summarised below. The maximum force which the film could tolerate before break was measured as well as the maximum strain.

Test mode: Tension

Trigger type: Auto (Force)

Load Range: 10 N

Gauge length: 30 mm

Pre-test speed: 0.2 mm/min

Trigger force: 0.1 N

Target mode: Distance

Preload: 0 N

Extensions: 25 mm

Test speed: 10 mm/min

Post-test speed: 0.1mm/min



Figure 2.2 Texture analyser instrument showing the on-going elongation tests.

2.4.2 Hot stage microscopy (HSM)

One of the preliminary analytical methods used to explore phase transitions in crystalline materials is hot stage microscopy and its development is based on light microscopy. The hot stage produces a high amount of heat which leads to thermal convection and conductive heat transfer that can be detected (Figure 2.3). HSM can be used to provide controlled temperature conditions for *in-situ* specimen investigation, while still protecting the microscope from damage due to excessive heat (Hanke, 2010).

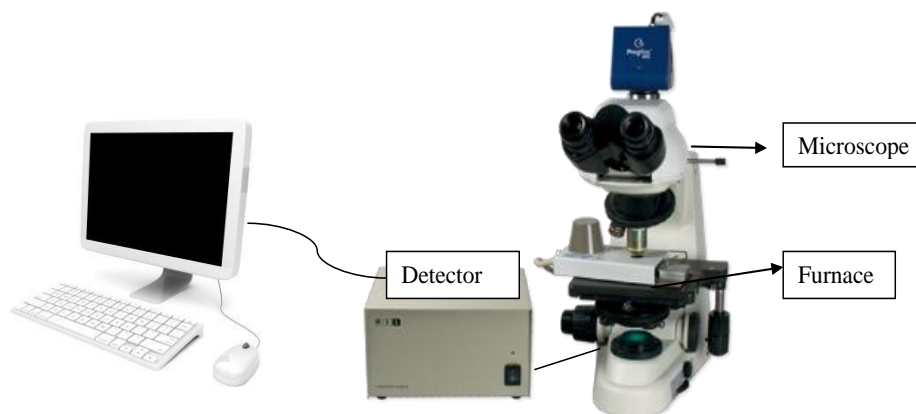


Figure 2.3 Schematic set up of hot stage microscope (adapted from Mettler Toledo, date accessed 5.02.2010).

In the pharmaceutical industry, HSM is employed in a variety of ways to validate transitions detected by other techniques. These include solid-state characterization of bulk drugs as well as evaluation of crystal forms and their hydrates (Shah, *et al*, 2006). The capability of this method to detect solvates by observing the evolution of a gas or liquid from a crystal can identify new polymorphic forms. This is feasible either by transition of one form to another following a high temperature exposure or recrystallization from the melt. To improve the sensitivity of HSM technique, vibrational spectroscopy or DSC can be coupled to the instrument. HSM was determined the experimental parameters for the TGA and DSC techniques with regard to the thermodynamic behaviour of pure compounds and films, with or without different model drugs (Figure 2.4). A known amount of the sample was placed on a glass slide located on the microscope stage. The lens should be clear and bright before running the HSM programme.



Figure 2.4 Hot stage microscopy instrument used in the analysis.

HSM experiments to determine the thermodynamic properties of films were conducted three times with one of the following dynamic heating settings:

30 to 300°C at a scan rate of 10°C/min

30 to 300°C at a scan rate of 5°C/min

100 to 250°C at a scan rate of 2°C/min

2.4.3 Thermogravimetry (TGA)

Thermogravimetric analysis is one of the most common analytical techniques used to characterise pharmaceutical products. The main purpose of performing TGA test on samples is to detect and identify stability and degradation. The reliability of this type of analysis depends entirely on the level of accuracy of measuring the weight and temperature changes (Bugay, 2001). The similarity in most of the weight loss curves necessitates the need for transformation of the results prior to interpretation. To obtain the best interpretation, a derivative plot of the weight loss curve can act as a guide to identify the most likely point at which the weight loss is noticeable and significant. Furthermore, accurate interpretation requires additional modifications and deconvolution of overlapping peaks (Rodriguez-Spong, *et al.*, 2004).

Mechanism of operation during TGA measurements

The main part of a TGA instrument is the high-precision balance and a pan, usually made of platinum, in which the sample is loaded. The measurement of temperature, with maximum accuracy, is achieved by means of a small thermocouple placed close to the sample pan. To prevent oxidation or any other undesired reactions that may affect the experimental results, an inert gas such as nitrogen or argon can be pumped throughout the system. To enhance the reliability of results, the carrier gas can be a mixture of ambient gas and oxygen (1 to 5% O₂ in N₂ or He) to reduce the oxidation rate (Reed, *et al.*, 1994). All the above parameters are operated by computer to control functions of the instrument. Analysis is performed by increasing the temperature and plotting the data as a curve showing weight change against the temperature (Reed, *et al.*, 1994).

Some specific instruments not only detect weight changes but also record the temperature difference between the sample and reference pans which means that these instruments are coupled with (differential thermal analysis, DTA) or (differential scanning calorimetry, DSC) to compare the heat flow into the sample pan relative to the reference pan. Sometimes TGA tests may be run in controlled heating rate mode; however, the determination of the percentage weight loss following heating to a certain temperature is the main purpose. This loss is the non-combusted residual water at the highest temperature (Tatavarti, *et al.*, 2002).

Applications of TGA

- ❖ Determine the exact degradation temperature, amount of absorbed water and the ratio of organic and inorganic content in a product
- ❖ Solvation points of volatiles and residual solvents present in the product can be identified
- ❖ Compositional analysis of multi-component materials or blends
- ❖ Thermal stability
- ❖ Oxidative stability
- ❖ Estimation of product lifetime
- ❖ Decomposition kinetics
- ❖ Effects of reactive atmospheres on materials
- ❖ Filler content of materials
- ❖ Moisture and volatile content

TGA enables researchers to test and determine characteristic properties such as decomposition that occur following the release of volatile products from compounds such as low molecular weight polymers. Overall, the main application of TGA is the determination of the percentage of volatile components by plotting the weight loss change as the sample is heated and directly related to stability of the whole system. Sometimes this technique is used to analyse the kinetics of deterioration following oxidation due to high temperature (Rodri'guez-Spong, *et al.*, 2004).

In the current project, TGA was used to measure the residual water in the films and wafers, since water molecules act as plasticizers and have an effect on the glass transition of amorphous compounds, which directly affects the stability, drug release and other physico-chemical properties of the films such as tensile strength. By coupling TGA with DSC the degradation temperature of the films or pure compounds was also ascertained in order to evaluate their stability.

About 3-10 mg of sample was weighed, placed in the T-Zero aluminium pans and weight loss determined using a high resolution TGA 2950 instrument (TA Instruments, Crawley- UK) (Figure 2.5a). The settings employed to measure the water content were as follows:

isothermal: 25°C for 5 min, and

dynamic heating from 25- 150°C at a scan rate of 10°C/min.

To confirm the results a SETARAM TGA Instrument (Figure 2.5b) combined with DSC was employed; 3-10 mg of sample was placed into the aluminium pans (100 μ L) on the tared balance and analysed. Subsequently, the instruments were programmed to heat the samples using two different heating cycles to determine degradation point as well as the residual water content.

To detect the degradation point the following parameters were used:

isothermal: 25°C for 5 min, and dynamic heating from 25-500°C at a scan rate of 10°C/min.

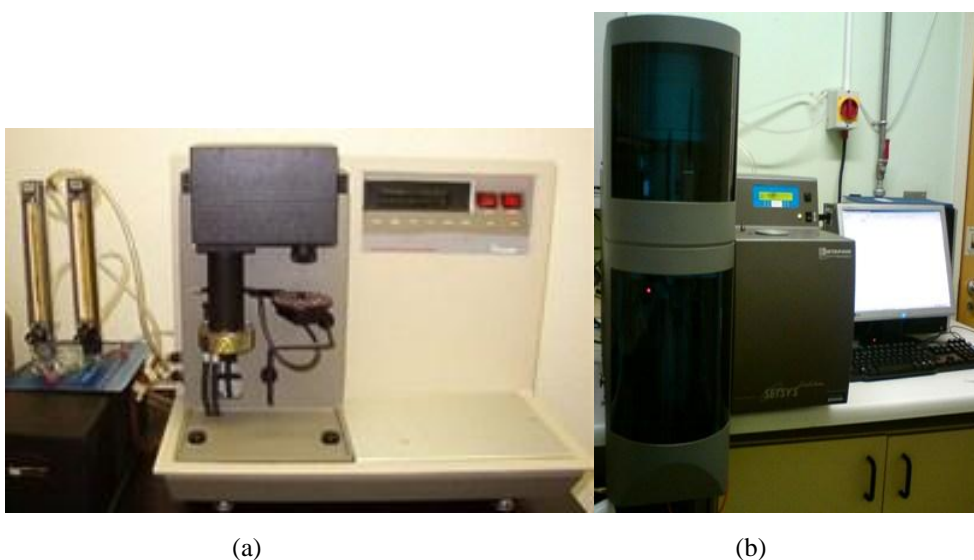


Figure 2.5 (a) 2950 TGA instrument and (b) Setaram TGA Instrument.

2.4.4 Differential scanning calorimetry (DSC)

Differential scanning calorimetry (DSC) measures the amount of energy absorbed or released during heating, cooling or holding the sample at constant temperature. The fundamental principle behind the technique is measuring the difference in heat flow between a standard (reference) material and an unknown material (sample). The two main types of DSC systems are described below.

❖ Power compensation

In this system two separate but identical furnaces independently control the temperature of the sample and reference (Figure 2.6). During analysis, the sample and reference pans are heated to the same temperature and the difference in the amount of input energy to the two furnaces detected.

This difference is a measure of the enthalpy or heat capacity difference in the sample in comparison to the reference. Therefore, power compensation DSC is based on the “Zero Balance Principle”, by maintaining the sample and reference at the same temperature, measuring the difference in power supplied to them and then directly recording it as signal ΔQ ($\Delta Q = \text{heat}$).

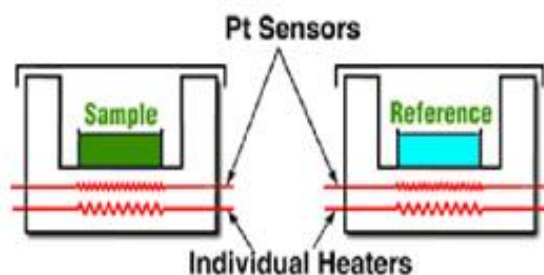


Figure 2.6 Schematic view of power compensation DSC instrument (adapted from institute of inorganic chemistry, http://www.chtf.stuba.sk/kach/lab_538.php, date accessed 12.10.2009).

Hence, an individual signal (d_H/d_t which is the normalized heat generated per time unit or normalized heat flow) is proportional to the difference of heat input between sample and reference (Marsh & Boyd, 2008).

❖ Heat flux

In this method, both pans are located on a tiny slab of material with an identified (calibrated) heat resistance K (Figure 2.7). The temperature of the calorimeter is increased linearly with time (scanned) while the heating rate ($d_T/d_t = \beta$) is maintained constant. The same heating power is applied to the sample and reference pans and the temperature difference (ΔT) between the two is measured. The output signal is obtained by converting ΔT to ΔQ (heat difference).

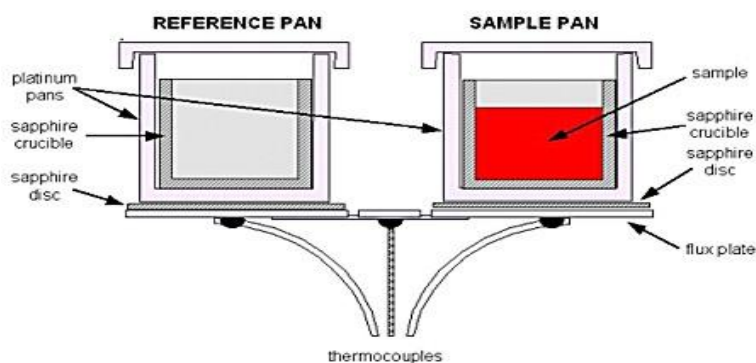


Figure 2.7 Schematic view of a heat flux DSC instrument (adapted from evitherm website, <http://www.evitherm.org/default.asp?lan=1&ID=982&Menu1=982>, date accessed 24.07.2009).

The time linearity needs well designed and (computerized) temperature control; however this might function as a controlled cooling and isothermal experiment (Sabau & Porter, 2007).

Mechanism of DSC

The DSC mechanism is that heat flows into the two pans by conduction. The flow of heat into the sample is greater because of its heat capacity, C_p . The variation in flow d_q/d_t creates a small temperature difference ΔT across the specimen which is measured by a thermocouple.

The heat capacity is determined as:

$$\Delta T = K \, dq/dt = K C_p \, \beta \quad \text{Eqn 13}$$

where the symbols represent the following:

d_q/d_t = heat flow

ΔT = temperature variation

C_p = heat capacity

T = temperature

K = heat resistance

t = time

β = heating rate

In addition, an enthalpy or heat capacity difference causes a change in the temperature between sample and reference. The difference in temperature between the sample and reference is detected and recorded according to the enthalpy change in the sample, based on calibration experiments.

Using this data (Figure 2.8) the enthalpies of transitions can be calculated by integrating the peak using the following equation:

$$\Delta H = KA \quad \text{Eqn 14}$$

ΔH is the enthalpy of transition, K is the calorimetric constant, and A is the area under the curve. The calorimetric constant will differ from instrument to instrument, and can be determined by analysing a well-characterised standard sample (sapphire or indium) with identified enthalpies of transition (Skoog, 1997).

To clarify the stability relationship between polymorphs, DSC is one of the most useful techniques. However, in some cases when the sample degrades following the heating process, this method might be confusing since decomposed product can recrystallize and modify the melting point of the compound. That notwithstanding, it is still an appropriate technique to characterize polymer and excipient interactions and also to estimate the percentage composition of each phase following a precipitation process (Barreiro-Iglesias, *et al*; 2002).

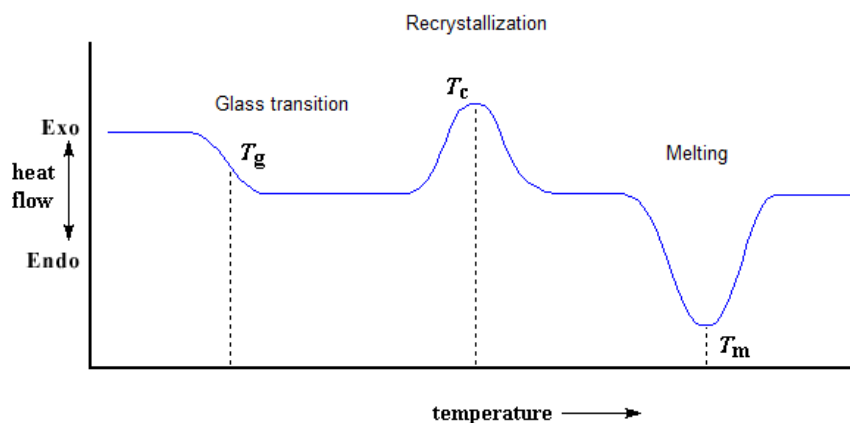


Figure 2.8 DSC curve representing different phase transitions in a solid material.

Applications of DSC

DSC is used to measure melting temperature, enthalpy of melting, percentage crystallinity, glass transition temperature, softening, crystallization, presence of recyclates/regrinds, effect of plasticisers and polymer blends (presence, composition and compatibility). The information provided by the measurements helps formulators to design new drug delivery systems with adequate stability and appropriate solubility *in-vivo* to obtain the ultimate goal of drug administration which is improving the bioavailability at the site of action (Chieng, 2011).

Following the initial DSC studies, optimized films were analysed using a Q2000 DSC instrument. 3-10 mg of each film were placed in T zero aluminium pans (75 μ L) and hermetically sealed.

The sample was cooled to -80°C before heating dynamically:

1st heating from -80 to 180°C at a rate of $10^{\circ}\text{C}/\text{min}$,

2nd heating from -80 to 180°C at the rate of $10^{\circ}\text{C}/\text{min}$, and cooling after each heating cycle at a rate of $-10^{\circ}\text{C}/\text{min}$.

In addition, experiments were performed in order to investigate the effect of polymers on drug transformation from crystalline to amorphous form during formulation process.



(a)



(b)

Figure 2.9 (a) TA and (b) Mettler Toledo DSC instruments.

A new set of samples were prepared by addition of the same weight of PM and each polymer (CAR 911, P407 and PEG 600) individually to the same amount of deionized water. Subsequently, the samples were heated to the same temperature as used during gel formation to simulate the formulation conditions. The gels or solutions were poured into Petri dishes and incubated in an oven at 60°C for 24 hours to remove the solvent. The samples were then analysed individually by DSC using the same method as for the films described above.

2.4.5 Scanning electron microscopy (SEM)

SEM (Figure 2.10) is used widely due to its ability to provide morphological information of biological and physical materials. Applications of SEM in the pharmaceutical industry include the following.

- ❖ Deposits and wear debris analysis
- ❖ Particle sizing and characterization
- ❖ Determine the shape and the distribution statistics of particles
- ❖ Quality control check
- ❖ Failure analysis
- ❖ Contaminant analysis (Mueller, 2002).

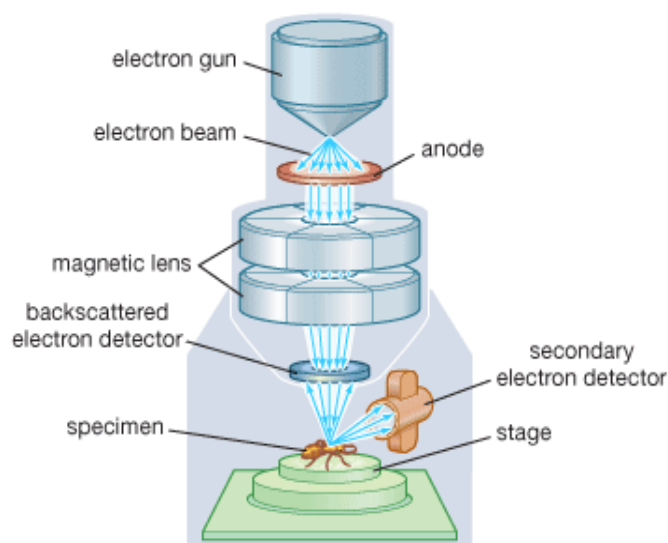


Figure 2.10 Scanning electron microscopy (Adapted from Encyclopaedia Britannica, date accessed 18.08.2010).

Mechanism of SEM imaging. The fundamental theory behind the scanning electron microscope (SEM) instrument is imaging the surface of the sample following scanning with high-energy beam of electrons in a raster scan pattern. After interaction between electron signals and atoms in a specimen, various signals are generated which provide information corresponding to the specimen's surface topography and properties such as conductivity and composition.

Secondary electrons. During SEM analysis, a beam of electrons is focused on a spot volume of the sample, causing energy transfer to the spot. These bombarding electrons, known as primary electrons, consequently emit secondary electrons from the sample.

A positively charged grid or detector attracts the emitted electrons which are then converted into a signal. To construct the SEM image, the electron beam moves across the target area to generate lots of signals. These signals are then amplified, analysed and transformed into topographic images (Hanke, 2010).

Back scattered electrons. The primary electron beam also results in the emission of backscattered (or reflected) electrons from the sample and these have a higher energy level and specific direction in comparison to secondary electrons.

The secondary electron detector is unable to collect the back scattered electron beam unless the detector is located directly in their path. All emissions above 50 eV are classified as backscattered electrons. This method is useful for chemical analysis of compounds as the backscattered electrons have a direct relation with the atomic number of the sample which helps to differentiate between samples with at least 3 atomic number differences (Cosslett, 1986).

SEM was used to evaluate the topographic characteristics and the surfaces properties of the films with or without the model drugs. An S360 Cambridge SEM instrument was employed to image the surface properties of the film by the secondary electron method. Each sample was gold plated before placing in the high vacuum chamber (50 Pa). The image was captured using x 50 magnification, acceleration voltage of 5 kV and at a working distance of 10 mm.



Figure 2.11 Scanning electron microscopy instrument.

2.4.6 X-ray powder diffraction (XRPD)

In this technique, the position of numerous peaks demonstrates periodic spacing of atoms in the solid state. Since various lattice constants in novel batch crystallizer, can be utilized coincidentally with dispersive X-ray diffraction to study solution crystallization *in situ*, this method is one of the best approaches to investigate polymorph characteristics. Molecular and crystalline structure is the most important information for crystalline solids existing as polymorphs and solvates. This data can be obtained by single-crystal X-ray diffractometry.

Applications of powder X- ray diffraction

The most common application of powder X-ray diffractometry is providing solid phase “fingerprints” which occasionally might be used to determine crystal structure (Vippagunta, *et al.*, 2001). To evaluate and determine the presence of solvent molecules in the lattice or changes in density between polymorphs, a comparison between the cell volume and other crystalline forms will be beneficial.

Unique X-ray powder diffraction (XRPD) patterns of polymorphs and screening different phases or polymorphs in a particular compound can differentiate one form from another. Determination of amorphous versus crystallinity by XRPD can be performed via calculation of percentage crystallinity. The measurement and determination depends on volume concentration of amorphous filler to crystalline active matrix in a drug's dosage form

(Mathkar, *et al.*, 2009). Percentage crystallinity is a critical parameter since it can influence a drug's processing behaviour and its pharmacological performance. All these tests provide information regarding stability. It can present unambiguous information about the formation of polymorphs or hydrates under different environmental (storage or processing) conditions. Conditions such as increasing temperature and/or humidity during transport or storage could have a harmful effect on a drug's performance and toxicity. The non-destructive nature of XRPD makes it a useful technique for systematic drug-excipient analysis in pre-formulation studies (Maccaroni *et al.*, 2009).

Careful excipient selection and evaluation of the drug-excipient interactions, is critical to obtain reliable release and bioavailability data. It assists in preventing any unexpected stability problems during early formulation or final stages of formulation development.

In addition, qualitative phase analysis by XRPD and polymorph screening can provide extended and full quantitative data which is valuable in optimizing pharmaceutical formulations (www.panalytical.com) (date accessed 17/09/2011).



Figure 2.12 D8 XRD instrument.

Experiments were performed to determine the structure of all the pure components and those present in the films, with or without model drug, with the aim of determining the various forms (crystalline or amorphous) of components that existed within the formulation. The films were cut into small pieces to allow loading onto the sample holder. Powdered samples were spread on the sample holder and compressed to ensure an even surface.

2θ values were entered manually between 5 and 42. A D8 Advance XRPD diffractometer (Bruker, Coventry, UK) equipped with a Lyn X– Iris detector and 6.5 mm slit size was employed to obtain results in reflection and transmission modes. The instrument parameters were set at 40 kV and 40 mA with primary solar slit of 4° and a secondary solar slit of 2.5 mm while the scattered slit was 0.6 mm. Samples were scanned at a speed of 0.02° , 2θ step size every 0.1 seconds. Similar experiments were conducted using pure PEG 600, P407 and their physical mixtures before and after heating on the DSC.

2.4.7 Stability test by high performance liquid chromatography (HPLC)

An Agilent 1200 HPLC instrument was employed to quantify the amount of drug present in the films to determine the stability of the drugs in the films after storage under two sets of conditions. Samples were placed in humidity controlled desiccators (45% relative humidity) and at room temperature and the stability was studied for 12 months.



Figure 2.13 High performance liquid chromatography.

Films were wrapped in paraffin film to prevent moisture absorption by CAR, which is a hygroscopic polymer. Prior to analysing the drug content in the films a 0.5 mg/mL standard solution of IBU, and IND and 1 mg/mL PM was prepared, serially diluted and analysed by HPLC to obtain their calibration curves.

The weighed samples were dissolved in deionised water (mixed with 2 mL of ethanol in the case of IND and IBU loaded films to ensure complete solubility of the two hydrophobic drugs) and injected onto an ODS C₁₈ reverse phase column (Hichrom H50DS-3814) and eluted with the respective mobile phases which were methanol: water: ortho-phosphoric acid (74:24:2), methanol: water: glacial acetic acid (74:24:2) and methanol: water: ortho-phosphoric acid (25:75:3 (V/V %)) for IBU, IND and PM, respectively. The flow rate of the mobile phase was 1.5 mL/min for IND and IBU and 1 mL/min for PM containing samples. A diode array UV detector at 230, 214 and 242 nm was used for IND, IBU and PM samples, respectively.

2.5 Formulation development of freeze-dried wafers

2.5.1 Gel preparation

As one of the main aims of the project was the development of two related buccal dosage forms and comparison of their mucoadhesion, swelling and dissolution characteristics, wafer development was performed on the basis of preliminary films evaluations. In order to produce freeze-dried wafers, similar optimised gels were prepared as for films containing various ratios of κ -CAR (1.5, 2, 2.5% w/w), 4% (w/w) P407, with or without the presence of PEG 600.

Initially P407 was added to cold water then incubated for two hours at room temperature before adding CAR 911 to the solution. This mixture was left overnight at room temperature to allow complete hydration of the CAR after which the gel was heated to 40-50°C to ensure a homogeneous mixture. The remaining components i.e. plasticiser (PEG 600) and model drugs were added and mixing continued for a further 5-10 min. 10 g of the clear gels were poured into a six well plate and placed in the freeze-drier.

Table 2.3 Composition of the gels prepared during formulation development and optimization process for wafers.

CAR 911 (% w/w)	P407 (% w/w)	PEG 600 (% w/w)
1.5	4	-----
1.5	4	3.3
1.5	4	5.5
2	4	-----
2	4	4.4
2	4	5.5
2.5	4	-----
2.5	4	5.5

2.5.2 Drug loading into optimized gels

This step was performed by formulating wafers initially containing varying amounts of drug {0.6-0.7% (w/w) IND, 0.8-0.9 % (w/w) IBU and 1.6-1.9% (w/w) PM} within the gel. The procedure was continued until the drug concentration exceeded the optimum amount with a consequent collapse in the porous texture of the wafer.

Table 2.4 Composition of the gels prepared during formulation development and optimization process for wafers.

CAR 911 (% w/w)	P407 (% w/w)	PEG 600 (%w/w)	Drug (% w/w)
2.5	4	4.4	0.6 IND
2.5	4	5.0	0.6 IND
2.5	4	5.5	0.6 IND
2.5	4	4.4	0.8 IBU
2.5	4	5.0	0.8 IBU
2.5	4	5.5	0.8 IBU
2.5	4	4.4	1.8 PM
2.5	4	5.0	1.8 PM
2.5	4	5.5	1.8 PM
2.5	4	4.4	0.7 IND
2.5	4	4.4	0.9 IBU
2.5	4	4.4	1.9 PM
2.5	4	4.4	0.6 PM
2.5	4	4.4	0.6 IBU

Drug loading studies were performed by either directly adding the drug to the aqueous gel or first adding to ethanol. Ethanol was employed to dissolve hydrophobic model drugs (IND and IBU) to increase the amount incorporated into the aqueous gels. The amount of CAR 911 and PEG 600 was 2% w/w and 4.4-5.5% w/w, respectively in the presence of 4% (w/w) P407.

The various formulations prepared are summarised in Table 2.4.

2.5.3 DSC analysis to determine optimized freeze-drying cycle incorporating an annealing step

Identification of critical gel temperatures, such as the eutectic point (T_{eu}), were used to ascertain the maximum temperature to which the gel could be heated during the primary drying phase and the glass transition (T_g). The T_g of the gel indicates the ultimate temperature of the cooling step. To detect the critical temperatures 3-10 mg of the gels were placed in a DSC crucible and heated from -80 to 180°C at a scan rate of 10°C/min.

2.5.4 Preparation of freeze-dried wafers

The first few attempts were conducted by simply freezing the gel in liquid nitrogen initially and then continuing freezing (at -55°C under 100 mTorr) and eventually the primary drying stage on the older freeze-dryer version (Heto Power dry LL3000, Biopharma Process Systems Ltd. Winchester, UK). Although several cycles with various time scales (24 up to 96 hours) were conducted, the physical characteristics of the wafers did not meet the required criteria.

Subsequently, freeze-drying was pursued with the more modern AdVantage freeze dryer. Two modes, manual or automatic, can be used for the freeze drying process on the AdVantage instrument; the automatic mode was used because it is considerably easier and saves time. Using automatic mode, the freeze drying procedure was carried out by programming the freezing and primary/ secondary drying cycles for different time periods and temperatures.

Freeze-drying cycles comprising freezing, primary and secondary drying were developed with the help of the DSC results from section 2.5.3 and consideration of the critical points (T_c). Further attempts were made to produce wafers using an annealing procedure, to increase the porosity of the wafers, by increasing the size of ice crystals during the freezing cycle.



Figure 2.14 AdVantage Freeze-dryer used in this project.

(a) The first annealing process was performed according to the procedure shown in Figure 2.15. The gel (previously kept in room temperature, 5°C and -5°C for 30 minutes each) was slowly cooled to -35°C and kept at this temperature for 30 minutes before increasing the temperature to -10°C for 2 hours and returned again to the initial temperature of -35°C (annealing). Sample was maintained at -35°C for 2 hours and subsequently primary drying started by turning on the vacuumed pump to remove the ice crystals from the surface of the sample by sublimation. During the primary drying, the temperature was increased to -10°C for 3 hours, -5°C for 2 hours and finally reached 0°C and maintained for 2 hours.

The secondary drying stage involved heating from 0 to 5°C kept for 1 hour and consequently 25°C to reach room temperature.

Visual evaluation of the wafers produced with the cycle shown in Figure 2.15 confirmed that the process was not suitable due to product collapse from melt back and/or incomplete ice removal. Because, the product temperature must be maintained below the T_{eu} (eutectic temperature) to retain interstitial space in the solid phase and make it capable of supporting

its own weight after the ice removal and preserve the wafer's structure, a new freeze-drying cycle was required. The new freeze drying cycle was planned based on the requirement of lower freezing and annealing temperature with a consequent increase in cycle time.

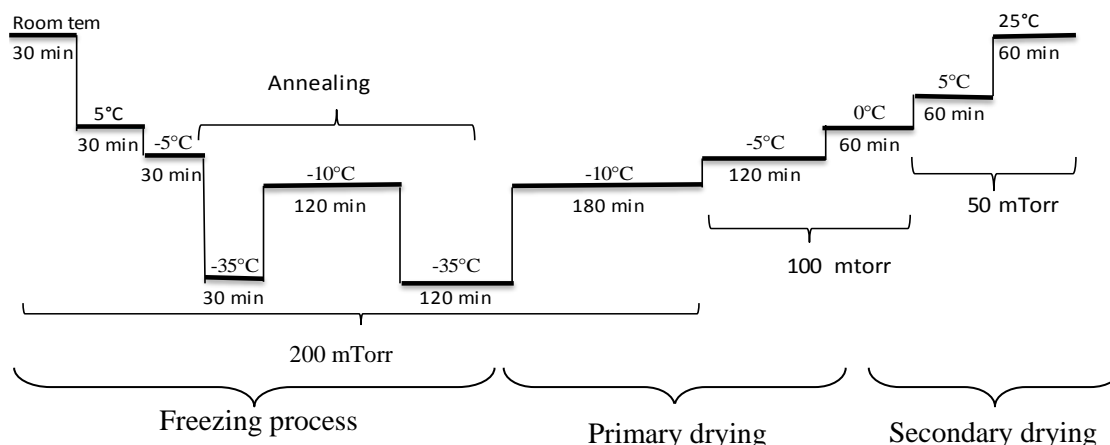


Figure 2.15 Schematic of the freeze- drying process comprising freezing, primary and secondary drying.

(b) DSC analysis determined the eutectic point (12.8°C) of the mixture hence; the initial freeze-drying cycle involved cooling gels gradually from room temperature to 5°C , maintained for, cooled to 0°C and maintained for 40 minutes, and cooled finally to -55°C and maintained for 1 hour. Subsequently, annealing was performed by increasing the temperature to -35°C . The annealing process lasted 3 hours to provide adequate time for large ice crystal formation. The temperature was returned to the initial temperature and maintained for 2 hours before primary drying was initiated.

During primary drying, as the ice crystals were sublimed, the temperature was increased from -55°C to -10°C and eventually 0°C (5°C lower than the eutectic point) to prevent melt back and preserve the stability of all the components. The whole primary drying procedure was 8 hours at -10°C followed by 6 hours at -0°C . To increase the stability of the freeze-dried wafers at room temperature, secondary drying was performed to further reduce residual water content. During all stages of the freeze drying process, from freezing to drying cycles, the

pressure was adjusted according to the temperature and with the aid of information provided from the manufacturer of the freeze-dryer to achieve the most desirable wafer with acceptable water content and flexibility. Based on the optimisation, gels comprising 2% w/w CAR, 4% w/w P407 and 4.4% w/w PEG 600 were prepared according to Figure 2.16.

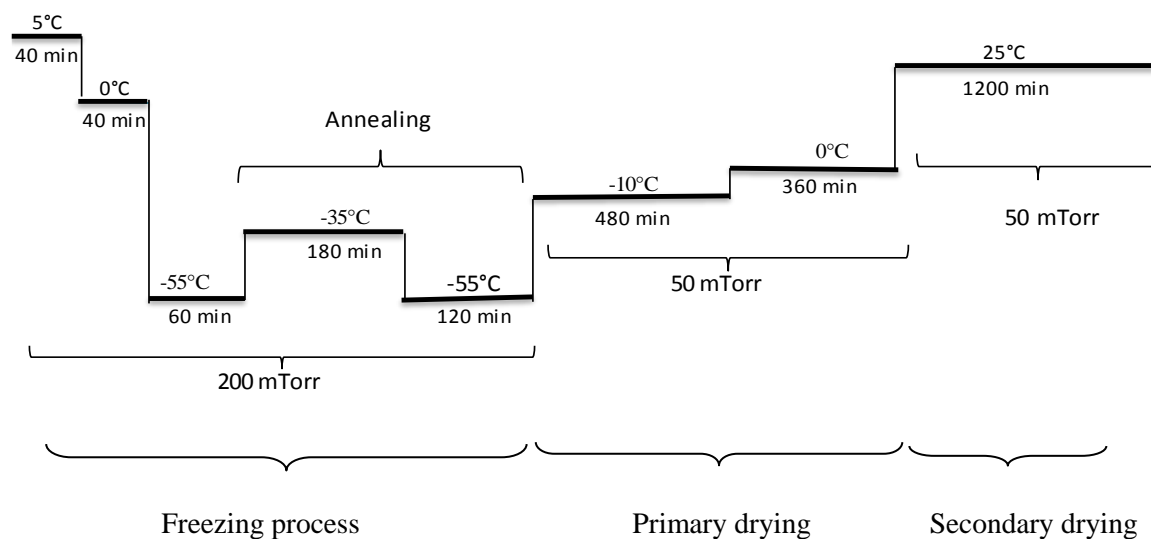


Figure 2.16 Schematic of the final freeze- drying process that produced wafers with appropriate characteristics.

2.6 Characterisation of freeze-dried wafers

2.6.1 Texture analysis

Texture analysis was employed to measure the mechanical strength of the wafers by measuring textural parameters including resistance to compression. The instrument employed was a “Texture analyser HD-plus” with Exponent software to plot and display the data. The experiments were used to select optimized wafers with acceptable flexibility for drug loading as well as to determine the effect of increasing drug content. A P6 (6 mm) cylindrical stainless steel probe was used to compress the wafers.

Before compression measurements, the thickness of the wafer was measured by micro screw-meter in five different areas of each sample (four edges and one in the middle) and showed

thicknesses ranging from 3.5-3.7 mm which was considered uniform. The exact thickness of each specific specimen was entered into the texture analyser software prior to compression. A force was applied by the probe to compress the wafer to a depth of 2 mm. The software plots force *vs* distance data and the area under the curve which is a measure of the work of compression. Instrumental settings to measure the compressibility were as follows:

Test mode: Compression	Pre-test speed: 0.1 mm/sec
Test speed: 0.1 mm/sec	Post-test speed: 1 mm
Hold time: 2 Sec	Trigger type: 2 Sec
Trigger force: 0 gr	Target mode: Distance
Distance: 2 mm	Break mode: Off
Stop plot: Target distance	Advance option: On

2.6.2 Hot stage microscopy (HSM)

HSM was used to provide complimentary data to the results obtained by TGA and DSC with regard to the thermodynamic behaviour of pure compounds and wafers with or without the presence of model drugs.

A small amount of the wafer was placed on a glass slide located on the microscope stage. The same experimental settings were employed for wafers as previously stated for films in section 2.4.2.

2.6.3 Thermogravimetry (TGA)

TGA was employed to measure the residual water in the wafers and the degradation temperature/stability of wafers or pure compounds by coupling the TGA instrument with the DSC. About 3-10 mg of each wafer was weighed, placed in aluminium pans (100 μ L) and the weight loss determined by using a high resolution TGA 2950 or a SETARAM TGA instrument. The experimental parameters used to evaluate the water content, was the same as for option 1 (section 2.4.3) while for degradation studies option 2 (section 2.4.3) was used.

2.6.4 Differential scanning calorimetry (DSC)

As previously stated DSC experiments were used to ascertain the thermodynamic profile of pure compounds and the Q2000 instrument used to detect the melting point and glass transition point of the wafers, as well as to investigate any possible interactions between wafer components. T zero aluminium pans (75 μ L) were packed with 3-10 mg of sample and hermetically sealed and the same method employed as for the DSC film experiments (section 2.4.4).

2.6.5 Scanning electron microscopy (SEM)

SEM experiments involved the topographic investigation of the blank wafers produced with different ratios of κ - CAR 911 and 4% (w/w) P407, with or without PEG 600 as a plasticizer. In addition the optimized gel was loaded with 0.6% (w/w) IND, 0.8% (w/w) IBU or 0.6/1.8% (w/w) PM and SEM images of the wafers obtained.

The samples, which were not gold coated, were placed in a low vacuum (20Pa) SEM chamber. SEM images were obtained using a Jeol instrument (Tokyo, Japan) with an accelerating voltage of 20Kv, magnification of x 50 and back scattered electron technique with artificial shadowing.

2.6.6 X-ray powder diffraction (XRPD)

XRPD was employed not only to evaluate the diffraction profiles of all the pure components in the wafers, but also to analyse wafers with or without model drugs.

The aim was to investigate the various forms (crystalline or amorphous) of drug components that existed in the formulation.

The wafers were broken up into smaller pieces and placed in the sample holder in order to obtain transmission mode XRPD data at the 5 and 42(2 θ) range. All the other parameters and instrumental settings were the same as those employed for XRPD analysis of the films (section 2.4.6).

2.6.7 Stability test by HPLC

HPLC (Agilent 1200 Technology) was used to check the stability of the drugs remaining in the freeze-dried wafers during storage at room temperature (about 15°C) and 45% RH for 6 months. Wafers were wrapped in paraffin to prevent moisture absorption by CAR. Prior to analysing the drug content in the wafers a 0.5 mg/mL standard solution of IBU or IND or 1 mg/mL PM was prepared, serially diluted and analysed by HPLC to plot the calibration curves. The samples were dissolved in deionised water (PM) or ethanol/ deionised water 4:100 by volume (for IND and IBU loaded wafers only) to ensure the two hydrophobic drugs were completely dissolved. The sample solutions were then injected onto an ODS C₁₈ reverse phase column (Hichrom H50DS-3814) and eluted with mobile phases. The experimental conditions used were the same as for film stability tests (section 2.4.7).

2.7 Hydration, dissolution and mucoadhesion of the films and wafers

2.7.1 Hydration and swelling studies

Before performing the dissolution studies, the behaviour of the films or wafers under aqueous conditions were investigated. Hence, hydration tests were conducted using two different media at 37°C temperature and the results obtained were correlated with the dissolution profiles. Medium 1 was 0.9% sodium chloride solution, to mimic biological fluids.

Since the secretion of saliva is 0.3 ml/min (Eliasson, *at al.*, 2009), the volume of medium 1 used was 42 mL so that films or wafers were immersed for 140 minutes.

The other medium used was phosphate buffer which was prepared by the addition of 100 mL of KH₂SO₄ (0.1 M) to 13 mL of NaOH (0.1 M) and final pH confirmed with a pH meter and maintained at 6.2 (mimicking the buccal mucosa and saliva pH).

The swelling capacity of polymeric films and wafers were determined by immersing samples of films and wafers cut to 3 cm×3 cm in size in buffer solution (pH=6.2) or sodium chloride solution in a 100 mL beaker. Samples of film or freeze-dried wafer were weighed before placing in the saline or phosphate buffer solution. The sample was taken out of the solution

every 20 minutes and reweighed and the procedure was continued for 140 minutes; and results were plotted as weight changes versus time. Calculation of % swelling (% weight change) for the polymeric matrices was determined using equation (15) below, where W_0 and W_t are the weights of the films or wafers initially and after swelling at time t respectively. Each data point represents the mean (\pm s.d) of three replicates.

$$\% \text{ Swelling} = \frac{W_0 - W_t}{W_0} \times 100 \quad \text{Eqn 15}$$

2.7.2 Drug dissolution studies

To determine the drug dissolution profiles of the films and freeze-dried wafers a Varian UV spectrometer was employed. Before performing dissolution studies, the actual content of IBU, IND and PM in the film or freeze-dried wafer specimens was calculated, based on amounts initially loaded. Dissolution studies were performed using two different dissolution media deionised water as a control and buffer solution mimicking saliva pH conditions:

- a. Saline solution (0.9% sodium chloride) with measured pH of = 5.6 and 37°C.
- b. Buffer solution with pH= 6.2 to simulate that of saliva and 37°C.

As a control, equal amounts of model drugs in the wafer or film specimen were weighed and dispersed separately in two 100 mL beakers containing 40 mL buffer solution and 40 mL deionised water, at 37°C with continuous stirring and the same procedure repeated for the wafer specimens.

The drug released from the polymeric films and wafers was measured using samples cut in 3 cm×3 cm size and immersed in buffer solution (pH = 6.2). Each data point represents the mean \pm s.d. of three replicates. Dissolution media were sampled at 5 minutes intervals starting from time zero and UV absorbance measured using a Varian Spectrophotometer (Yarnton, UK). The absorbance at 318 nm for IND (Malamataris, 1990), 221 nm for IBU (Kislalioglu, *et al.*, 2006) and 245 nm for PM (Di Martino, *et al.*, 1996) loaded films and freeze-dried wafers which was dissolved in the deionized water/ethanol was measured. Amount of drug released (mg) was calculated from the UV calibration curve and % release

versus time profile plotted. The kinetics of drug release from the films and wafers was evaluated by finding the best fit of the dissolution data to zero and first order, Higuchi and Korsmeyer–Peppas equations.

2.7.3 Mucoadhesion studies for films and wafers

Mucoadhesivity tests were conducted by employing a P/75 (75 mm diameter) probe with films or wafers specimen fixed on the surface of probe using double sided adhesive tape. A Petri dish containing agar gel was employed as the mucosal substrate equilibrated with 200 μ L of buffer solution (pH = 6.2) to simulate pH conditions in the buccal environment. The sample was then placed on the agar surface and contact maintained for one minute to allow water absorption and adhering to the surface (Figure 2.17). The texture analyser settings summarised below were applied to pull the sample and detach it from the agar surface and the peak force of detachment measured.

Test mode: Tension

Pre-test speed: 0.5 mm/sec

Target mode: Distance

Trigger type: Auto (Force)

Trigger force: 1 N

Break mode: Off

Stop plot at: Target distance

Tare mode: Off

Advance: on

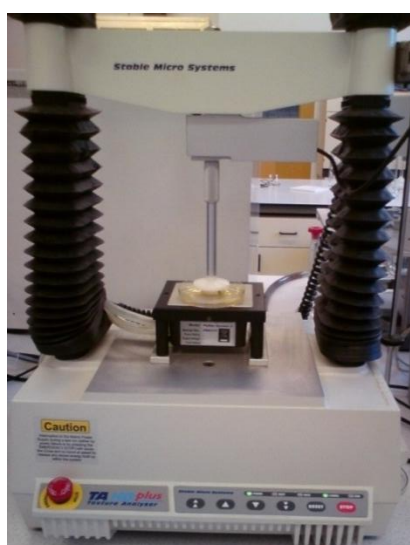


Figure 2.17 Texture analyser instrument showing the on-going adhesion tests.

2.8. Statistical analysis

To compare the dissolution and mucoadhesion results (WOA and stickiness) statistical analyses were employed. All measurements were performed in triplicate in each experiment and the results are presented as the mean \pm standard deviation (s.d).

To test for significant differences between means, statistical analysis was performed by one-way ANOVA. The results were considered statistically significant if the p value of < 0.05 was obtained. To compare the dissolution profiles for films and wafers variables, additional investigations were performed using the modified Moore and Flanner equation (Eqn 16) by calculating the similarity (f_2) factors. The dissolution profiles of the pure crystalline drug were used as a reference in calculating the similarity factors (f_2), where n is the number of time points, R is the dissolution value of the reference t (pre-change) batch at time t , and T is the dissolution value of the test batch at time t (post-change).

$$f_2 = 50 \times \log \left\{ \left(1 + \frac{1}{n} \sum_{j=1}^n |R_j - T_j|^{-0.5} \right) \right\} \times 100 \quad \text{Eqn 16}$$

The similarity factor is a logarithmic reciprocal square root transformation of the sum of squared error and is a measurement of the similarity in the percent (%) of dissolution between the film and wafer drug release curves. For curves to be considered similar, f_2 values should be close to 100. Generally, f_2 values greater than 50 (50-100) imply similarity of the two curves (i.e. the performance of the test (post-change) and reference (pre-change) products) (<http://www.fda.gov/cder/guidance.htm>).

Chapter 3 : DSC studies of interaction between starting materials (physical mixtures)

Chemical interactions between various ingredients alter the stability of pharmaceutical products. Investigating the interaction between starting materials is a pre-requisite to develop a stable high quality pharmaceutical formulation. Changes in melting point directly influence the stability of a product. One of the fundamental changes that might modify the melting point of a compound and consequently alter the stability of the system is the interaction between excipient(s) and API(s). The formation of a mixture, following the interaction between component compounds, influences the characteristics of the system which therefore need to be determined. The aim of the study was to evaluate the interactions between PEG 600 and P407 prior to their use in a pharmaceutical formulation. In addition, the effects of existing polymers on crystalline-amorphous habits of models drug were evaluated.

3.1 Study of the interaction between PEG 600 and P407

The DSC results of films and wafers made by mixing PEG 600 and P407 showed additional melting transition which appeared between the melting peaks belonging to PEG 600 and P407. These observations led to further examination to explore possible interactions between P407 and PEG 600 (Bely, *et al.*, 2010).

DSC analysis was conducted using method described in section 2.2. Results were evaluated by comparing the melting transition of pure P407 and PEG 600 with the detected melting transitions from the first and second heating cycle of the mixtures. All of the mixtures contained P407 and PEG 600 but comprising different ratio of two components. Initial analysis showed a wide melting transition over temperature range of 40.0 to 63.0°C meaning pure P407 is in crystalline form (Figure 3.1). Similar result for pure PEG 600 (Figure 3.2) was observed at temperature range of -10.0 to 22.0°C. However, the normalized melting peaks were detected at around 51.4°C and 6.2°C for P407 and PEG 600, respectively.

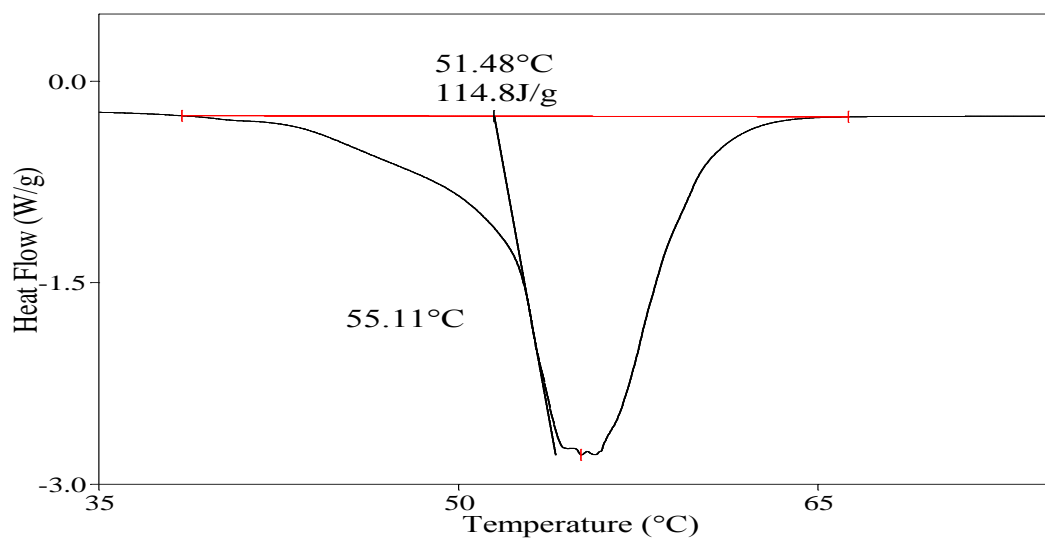


Figure 3.1 DSC results for P407.

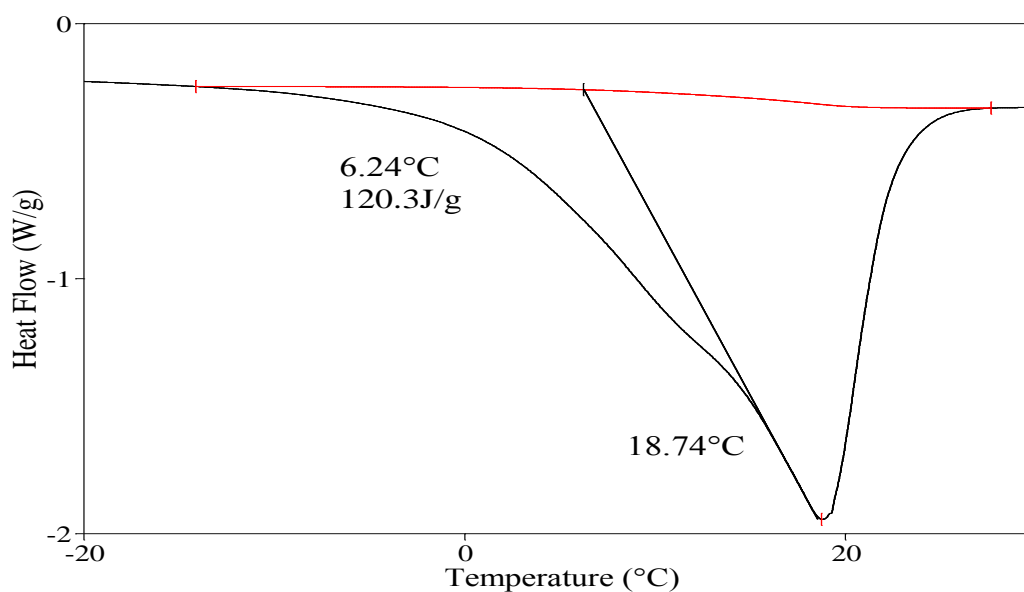


Figure 3.2 DSC results for PEG 600.

The DSC studies involved two heating cycles. When examining physical mixture of PEG 600/P407 (ratio 58/42) the results after the first heating cycle showed the first melting transition onset point corresponding to PEG 600 at 0.4°C and the second one for P407 at 42.8°C (Figure 3.3). The results showed a significant difference between the detected melting points of the pure compounds and mixtures. However the difference is more significant after the second heating cycle.

As Figure 3.4 shows, the thermal events from the second heating cycle appeared at 3.6°C for PEG 600 and 41.1°C for P407 plus an additional melting point transition appeared at 23.4°C. The current observation explains the reason for the DSC profile of the film exhibiting three separate melting transitions instead of two transitions corresponding to PEG 600 and P407 (Figure 3.1). In addition, the results clearly demonstrate that by mixing PEG 600 and P407 sharper peaks for the melting points of individual components were detected which may suggest that molecules of different chain length from the majority of molecules for both PEG and P407 may be involved in that interaction.

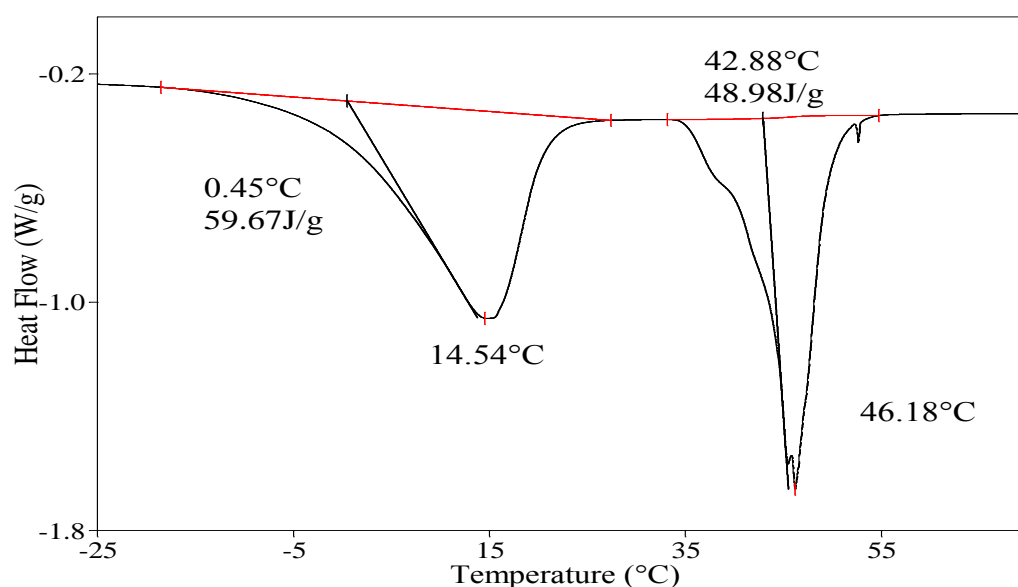


Figure 3.3 DSC results of the first heating cycle for a physical mixture of P407/ PEG 600 (ratio 58/42).

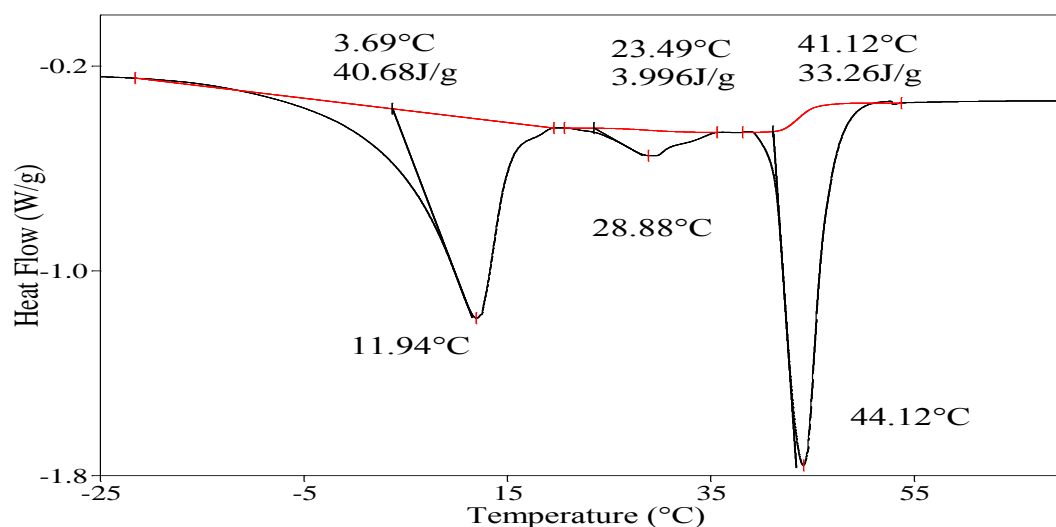


Figure 3.4 DSC results of the second heating cycle for a physical mixture of P407/ PEG 600 (ratio 58/42).

It is plausible therefore that a mixture of P407 and PEG 600 is formed within the film which has a direct modifying effect on the melting point of each compound (Figure 3.5).

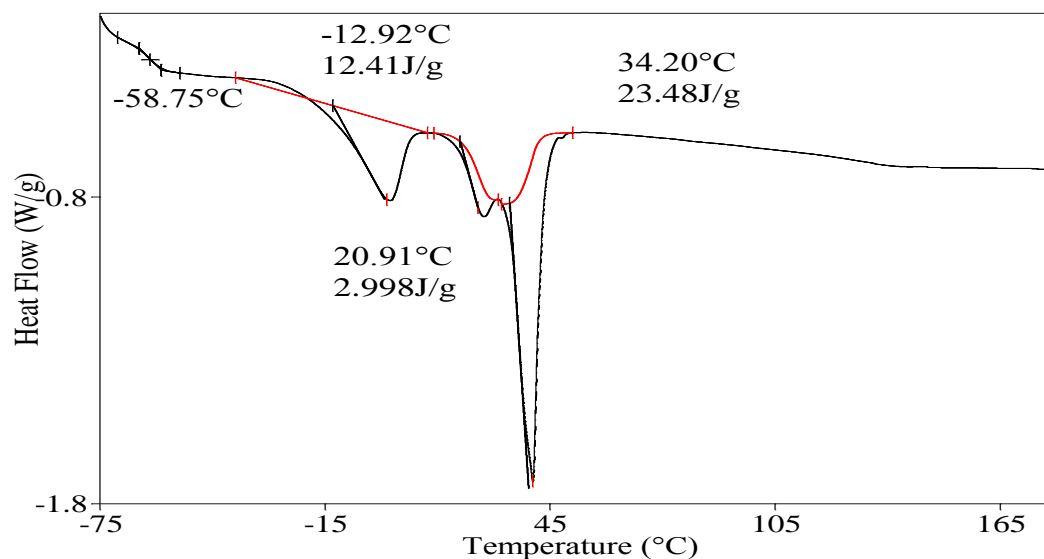


Figure 3.5 DSC results of film comprising 2.5% CAR+ 4% P407+ 6.5% PEG and 0.8% IBU within the initial gel.

Figure 3.6 shows the melting point values for a series of PEG/ P407 mixtures. It is evident that with an increase in percentage of P407, the melting point of PEG is decreased from 14.2°C to 0.7°C for pure PEG 600 and 10/90 mixture (PEG 600/P407), respectively. However, the same effect has not been observed with the change in melting point of P407.

After addition of 20% of PEG 600, P407 reached its minimum melting point of 41.2°C and remained fairly constant with further increase of PEG 600/P407 ratio. The most interesting finding is the formation of what is believed to be a complex (mixture) of PEG/P407 at ratios of 30/70; 40/60 up to 80/20 with the melting point of the complex being relatively uniform (26.7°C). This additional transition confirms that not only do the two compounds physically interact but also form a unique entity that has characteristic properties i.e. melting behaviour.

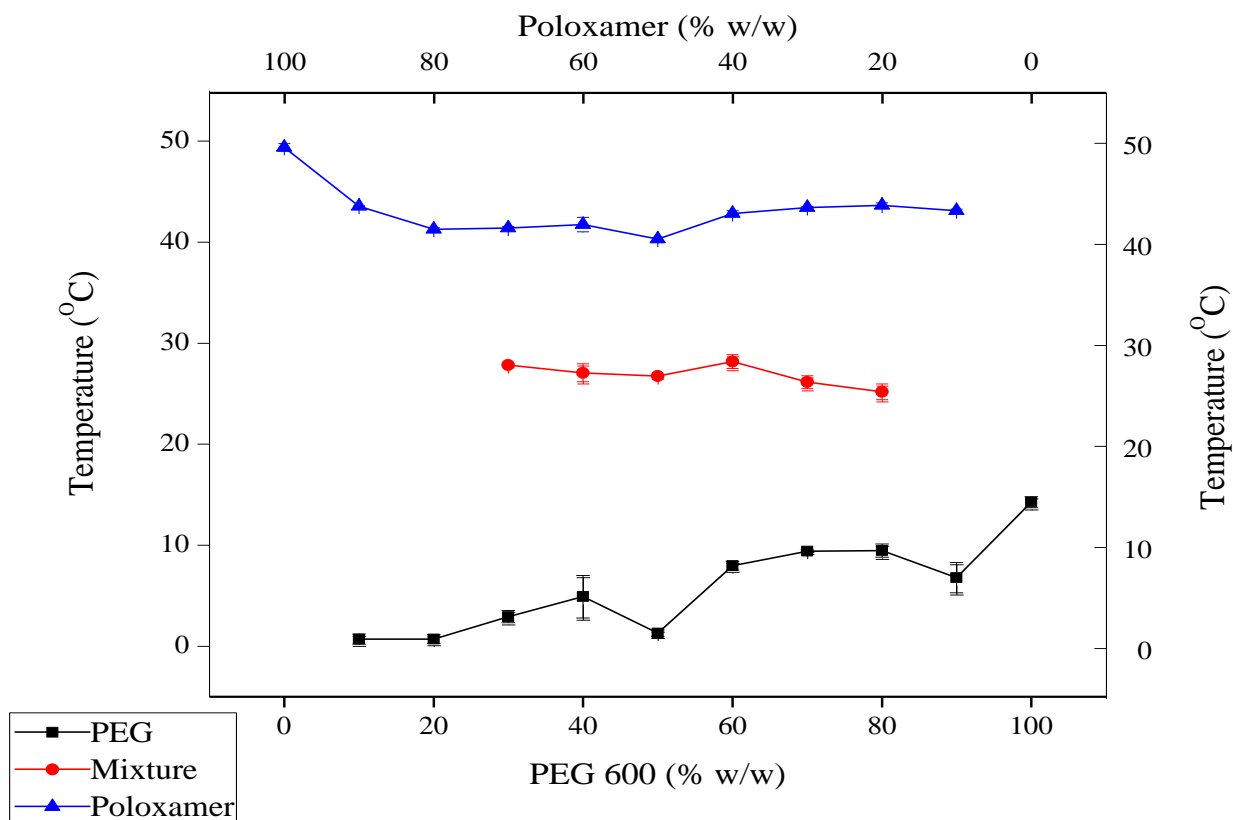


Figure 3.6 DSC transition onset values for a mixture of 0/100 (% w/w) to 100/0 (% w/w) of PEG 600/ P407 {mean \pm s.d, (n=3)}.

According to the DSC results significant changes in melting points values between the individual samples of PEG 600 and P407 and the mixture were detected (Table 3.1).

Thus, this finding confirms that an interaction occurs between the two polymers. However, the extent of interaction varies and depends on the ratios of the two compounds in the various mixtures. Subsequent to the evaluations of DSC thermograms in terms of the transition point onset additional investigations were conducted to scrutinize the enthalpy values and the changes for each transition and the results are summarised in Table 3.2. However, the result related to the mixture of 50/50% of P407/PEG 600 didn't follow the same trend for PEG 600 melting point with a sudden decrease in the onset at this point.

Table 3.1 Melting transition values for PEG 600, P407 and the new entity phase.

Runs	1 st Heating				2 nd Heating					
	PEG 600		P407		PEG 600		Mixture		P407	
T _m Peaks	Onset °C	Peak °C	Onset °C	Peak °C	Onset °C	Peak °C	Onset °C	Peak °C	Onset °C	Peak °C
100% PEG	6.8± 0.1	20.2± 0.6	—	—	14.2± 0.5	20.2± 0.4	—	—	—	—
(90/10)% PEG/P407	14.7± 0.2	25.4± 0.2	49.4± 0.6	57.1± 0.7	9.5± 1.0	16.5± 0.9	—	—	43.1± 0.1	44.1± 0.2
(80/20)% PEG/P407	5.0± 0.3	18.9± 0.7	46.7± 0.4	56.4±	9.4± 0.6	15.9± 0.5	25.2±0.4	32.8±0.3	43.6± 0.3	45.9± 0.2
(70/30)% PEG/P407	10.0± 0.1	20.4± 0.1	47.8± 0.5	57.3± 0.6	5.0± 0.1	17.9± 0.2	26.1±0.1	37.6±0.2	43.4± 0.1	45.4± 0.2
(60/40)% PEG/P407	11.8± 0.4	24.6± 0.6	44.2± 0.7	59.2± 0.8	7.8± 0.4	18.6± 0.3	28.8±0.2	37.9±0.3	42.8± 0.3	46.2± 0.3
(50/50)% PEG/P407	9.1± 0.5	17.2± 0.4	47.5± 0.5	54.3± 1.1	1.3± 0.3	12.4± 0.3	26.7±0.2	38.0±0.5	40.3± 0.2	45.3± 0.3
(40/60)% PEG/P07	8.9± 0.3	16.5± 0.9	48.5± 0.1	59.5± 0.7	5.2± 2.0	21.6± 0.3	27.1±0.2	37.9±0.4	41.7± 0.7	47.2± 0.6
(30/70)% PEG/P407	55.1± 0.4	58.2± 1.0	50.1± 0.2	59.7± 0.1	3.1± 0.6	17.2± 0.5	27.9±0.6	37.3±0.3	41.4± 0.2	46.8± 0.3
(20/80)% PEG/P407	—	—	45.3± 0.2	54.3± 0.2	0.7± 0.4	12.2± 0.3	—	—	41.3± 0.2	46.3±0.5
(10/90)% PEG/P407	—	—	51.8± 0.0	59.9± 0.1	0.7± 0.5	11.5± 0.6	—	—	43.6± 0.0	49.9± 0.1
100% P407	—	—	55.1± 0.4	58.2± 0.4	—	—	—	—	49.4± 0.4	50.2± 0.4

During the second heating cycle and after the interaction a similar trend was observed for either P407 or PEG 600 enthalpy values as an increase in the ratio of one component caused a decrease in enthalpy value of the other compound (Table 3.2).

However, at exceptional point of (50/50 w/w) the enthalpy value of PEG 600 didn't show the same trend as melting point. Instead the sudden increase in enthalpy value at (70/30) % PEG 600/P407 ratio might be due to stimulation effect of mixture in recrystallizing the PEG 600, however this requires further investigations.

Table 3.2 Enthalpy values for PEG 600, P407 and the new entity phase transition peaks.

DSC Runs	1 st Heating		2 nd Heating		
	PEG 600 enthalpy (J/g)	P407 enthalpy (J/g)	PEG 600 enthalpy (J/g)	Mixture (J/g)	P407 enthalpy (J/g)
100% PEG600	92.1±1.8	—	90.5±0.8	—	—
(90/10)% PEG600/P407	84.0±2.3	108.0±2.8	84.3±1.2	—	8.2±0.4
(80/20)% PEG600/P407	83.3±1.8	103.8±1.3	59.7±0.9	—	16.9±0.7
(70/30)% PEG600/P407	92.7±2.9	91.2±1.0	75.5±0.5	7.3±0.6	36.1±1.3
(60/40)% PEG600/P407	53.5±1.1	85.4±0.9	37.1±1.4	11.8±0.8	36.7±0.9
(50/50)% PEG600/P407	49.9±1.2	63.6±1.6	40.6±0.9	13.0±1.1	35.7±1.7
(40/60)% PEG600/P407	30.4±0.6	85.4±1.3	23.3±1.7	2.8±0.4	64.4±1.9
(30/70)% PEG600/P407	23.2±1.6	91.2±1.1	14.3±0.9	15.6±0.9	71.9±0.9
(20/80)% PEG600/P407	7.3±0.7	103.8± 0.8	3.1±0.5	8.3±0.7	89.3±0.4
(10/90)% PEG600/P407	2.1± 1.5	108.0±1.8	1.0±0.2	—	96.0±1.4
100% P407	—	113.9±0.5	—	—	111.5±0.6

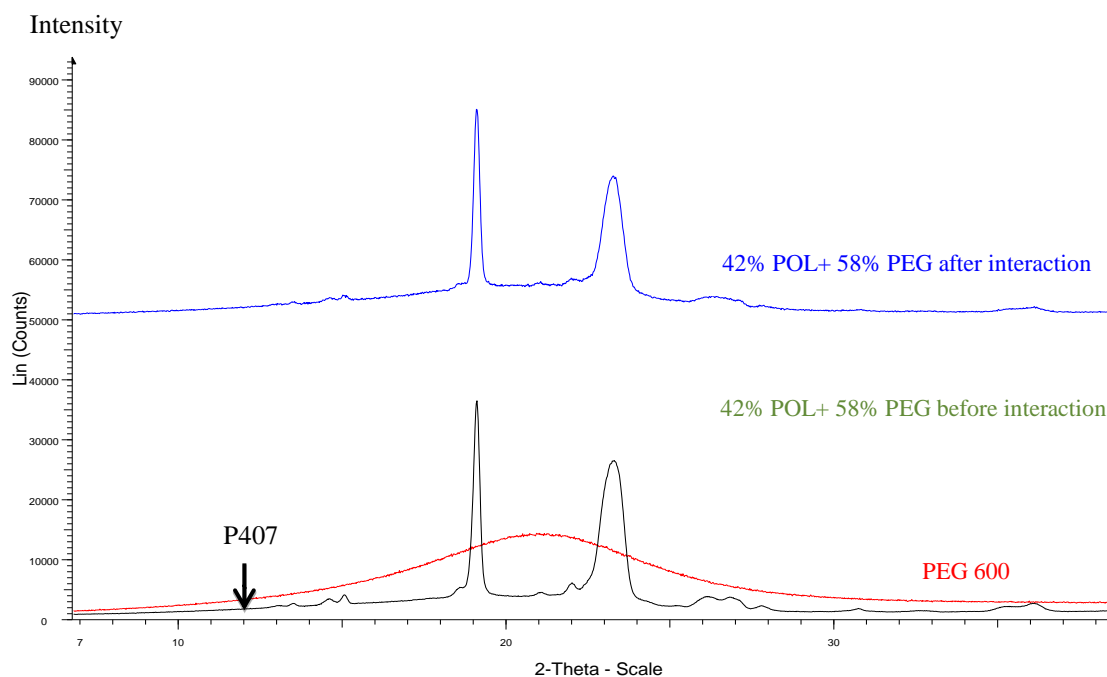


Figure 3.7 XRPD profiles showing combined diffractograms for PEG 600, P407 and mixture of PEG 600/P40 before and after interaction.

Figure 3.7 presents the results of additional XRPD studies conducted to investigate and support the DSC observations (results enclosed in appendix chapter). The results confirmed the presence of crystalline P407 plus amorphous form of PEG 600 within the sample. By evaluating DSC and XRPD results feasibility of co-crystallisation or production of new crystalline form is unlikely. Therefore, there are two possible explanations with regards to the identity of the new entity within the film matrix and discussed in the section below.

3.2 DSC analysis for interaction between the compounds in films

As mentioned above there are two explanations including the solubilisation of P407 in the PEG 600 which could result in formation of micelles of P407 in the core surrounded by PEG 600 in the shell. However, the comparison of XRPD diffractogram (Figure 3.7) for pure PEG 600 and P407 and their mixtures before and after heating in DSC demonstrates that this explanation is unlikely to be true as PEG 600 is predominantly present in amorphous form in the system. Furthermore, the DSC results and the above hypothesis relate to the non-drug loaded films but not the physical mixtures or drug loaded films and therefore cannot account

for the incorporation of model drug within the micelles. Although a shift in the melting transition of P407 and PEG 600 was observed, it did not have any effect on the thermal characteristics of IBU. Therefore it can be concluded that the model drug was not incorporated in micelles comprising PEG 600 and P407.

Furthermore, the chemical structure of P407 shows that it comprises 79% PEG and 21% PPG (polypropylene oxide). PEG has the ability to form inter-chain hydrogen bonding as well as hydrogen bonding with water. It is therefore possible that the presence of water may promote greater interaction of the PEG chains of P407 and PEG 600 through greater hydrogen bonding. Consequently increase in the residual water promotes greater interaction of the PEG chains of P407 and PEG 600 through greater hydrogen bonding.

In addition, the comparison between the enthalpies of PEG 600 and P407 demonstrated that the enthalpies variation was negligible which confirmed the probability of inter chain hydrogen bonding occurring (Sawatari and Kondo, 1999).

3.3 Effect of polymers on model drug

DSC analysis revealed new data which explained the reason for drug transformation from initial crystalline to amorphous form. Additional DSC analysis was conducted to evaluate the effect of various polymers on one of the model drugs (PM) during film formation. According to Figure 3.8 PM has two polymorphs including monoclinic polymorph ($T_m = 168.6^\circ\text{C}$). This form is the initial form and due to fast cooling it can produce amorphous form with glass transition point at around 21.8°C . However amorphous form is unstable and recrystallization can be initiated upon heating and resulting in the orthorhombic form ($T_m = 158.1^\circ\text{C}$).

According to Figure 3.9 the sharp melting transition at 168.5°C was observed for pure PM film showing the presence of monoclinic polymorph. Similarity of the results with melting transition value of the initial form of PM demonstrates that applied temperature during film formation process did not have any effect on the physical properties of the PM.

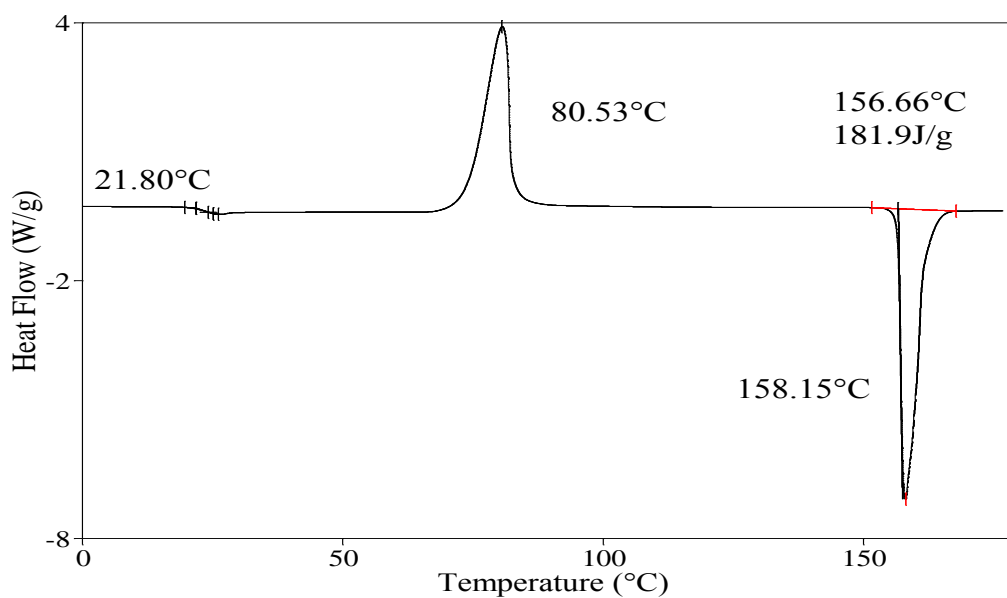


Figure 3.8 Amorphous PM, recrystallization and converted orthorhombic polymorph.

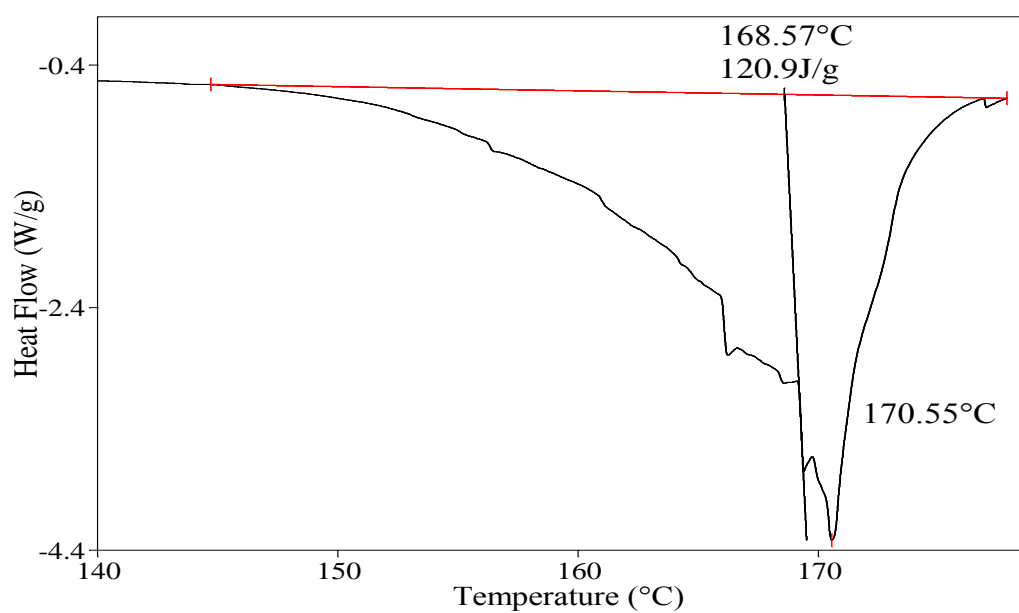


Figure 3.9 DSC results for solvent cast film prepared from PM and film.

In addition, the melting thermal event was still detected after addition of the P407 and CAR 911. However, due to addition of CAR 911 the monoclinic polymorph ($T_m=168.5^\circ\text{C}$) of PM was converted to orthorhombic form with melting transition onset at 158.0°C . Though such

phenomena confirmed that, CAR doesn't have any impact on formation of amorphous form of PM (Figure 3.10).

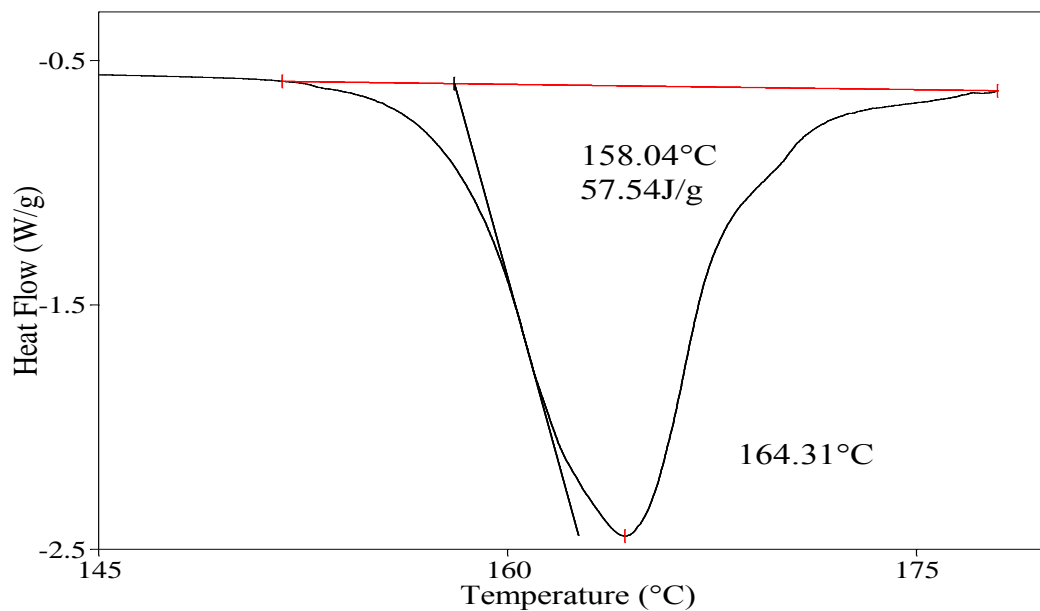


Figure 3.10 DSC results for film prepared from PM, CAR and water.

According to Figure 3.11 addition of P407 could have an effect on the physical properties of PM and produced polymorphs, however did not impart on formation of the amorphous form.

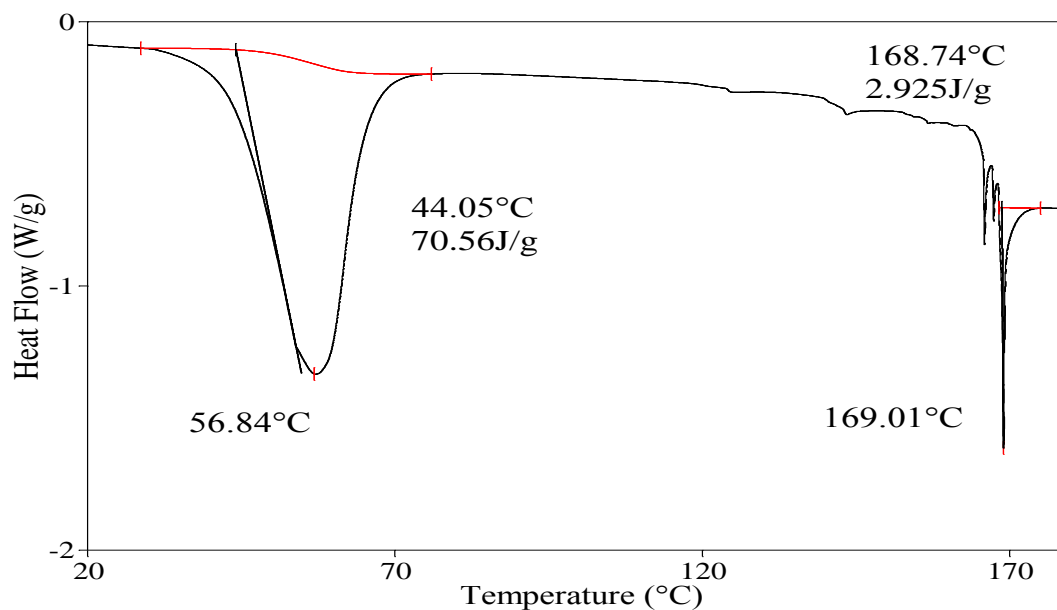


Figure 3.11 DSC results for film prepared from PM, P407 and water.

Furthermore, results from DSC analysis of combination of PEG 600 and PM (Figure 3.12) demonstrated the recrystallization of PEG 600 at -14.5°C . Subsequently, this crystalline form melted at two different temperatures -4.6°C and 66.7°C .

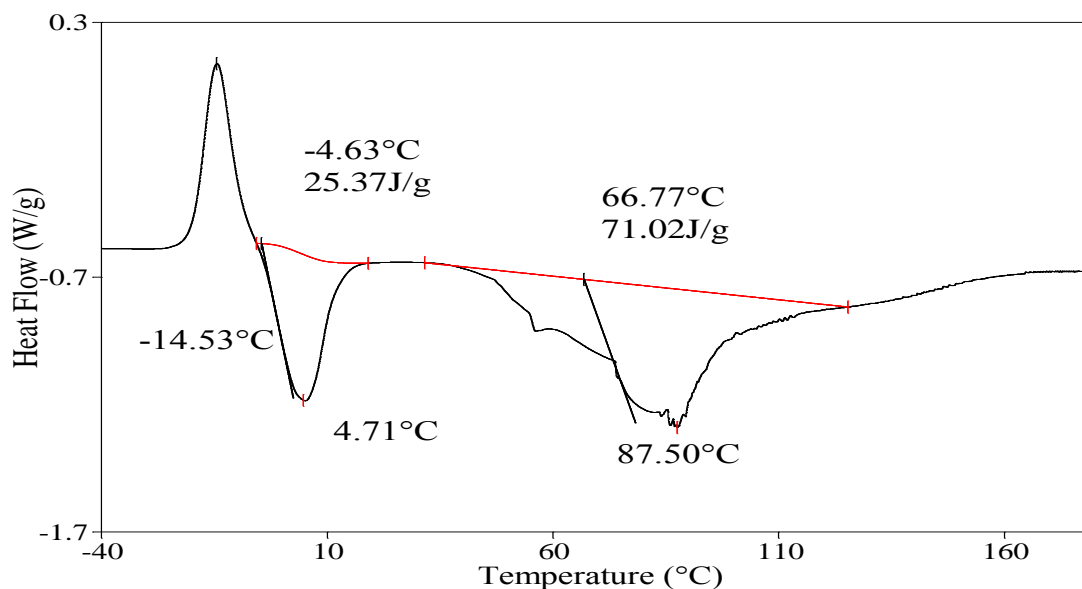


Figure 3.12 DSC results for film prepared from PM, PEG 600 and water.

The most important outcome from the DSC thermogram is the absence of PM melting transition which is evidence of conversion (Figure 3.12). The comparison between DSC results in Figure 3.9, Figure 3.10 and Figure 3.11 demonstrate that the conversion of PM was not due to addition of CAR 911 and P407 or applying heat ($40\text{-}50^{\circ}\text{C}$) during the gel formation process. They also however, suggest amorphous formation due to the presence of PEG 600. In summary, DSC results of physical mixtures showed that PEG 600 and P407 interacted during heating. These phenomena have a direct effect on melting point transitions of both PEG 600 and P407 as well as formation of the new entity. Additional results were thermal events following the addition of each individual polymer. The observations showed that crystalline PM was converted to amorphous form due to addition of PEG 600 and remained stable owing to prevention of recrystallization. Furthermore, the later results confirmed that heat which was applied during the gel formation ($40\text{-}50^{\circ}\text{C}$) and film formation (oven 60°C) was not the cause of crystalline to amorphous conversion. This observation was compatible to previous studies by Bely and co-workers (2010) and Chakravarty and co-workers (2011).

Chapter 4 : Development and characterisation of films

4.1 Film development

4.1.1 Gel formulation

Eudragit L100 did not dissolve in the aqueous system and did not produce a gel except with high percentage of ethanol as a co-solvent. This was deemed undesirable therefore this polymer was not used for further film development. In addition, stirring the system on a hot plate with a magnetic stirrer was time consuming and resulted in excessive loss of water by the time gel was formed. As a result, a motorized overhead homogenizer was employed for subsequent gel preparation. In addition, because P407 is a surfactant, its natural physico-chemical properties resulted in the generation of thick foam during the overhead stirring of the hydrated gels. This resulted in hydrated gels with lots of entrapped air bubbles (Figure 4.1) which were not easily released and affected the final appearance of the film. Such entrapped air bubbles can consequently affect other properties of the film such as tensile testing and drug release profiles. To reduce the amount of generated air bubbles and ease of their removal, two different approaches were attempted:

- 1) heating the polymer at very high temperatures (70-80°C).
- 2) stirring very slowly.

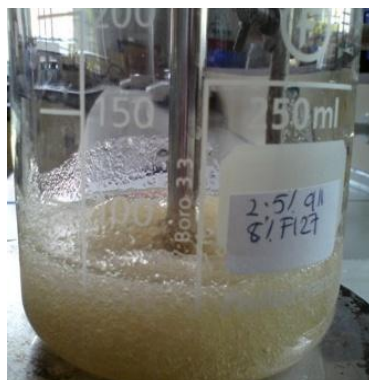


Figure 4.1 The physical appearance of gels containing high levels of P407 showing thick and foamy characteristic.

The time required for complete dispersion, hydration and subsequent dissolution of different polymers was different as most of the polymers are high molecular weight components with low ability to readily disperse in water. This was overcome in two ways; increasing the temperature of the water during dispersion caused an increase in hydration rate of the polymer and subsequent dissolution. By prolonging the swelling time of CAR in water from a few minutes to a 24 hour period, more complete hydration was achieved which allowed reduction in hydration temperature. This approach has both advantages and disadvantages: lowering the jellification temperature from 70-80°C to 40-50°C was deemed advantageous for possible future film formulation with thermolabile drugs such as proteins or peptides. However, this method is very time consuming as the hydration and swelling time is increased and requires formulation to be planned in advance to allow the 24 hour hydration time. Another observation from the slow homogenisation approach was that the upper layer of the gel solidified quickly and thus the gel becomes non-uniform which resulted in films with non-uniform thickness. Therefore, the most effective and optimum concentration of P407 to avoid excess bubble formation was $\leq 4\%$ (w/w).

Interestingly, the maximum percentages of the two insoluble drugs that could be loaded in the gels prepared by dissolution of drugs in deionized water were 0.4% for IND and 0.5% for IBU while the results from the films produced by dissolving drugs in ethanol showed a maximum drug loading of 0.6% (w/w) and 0.8% (w/w) for IND and IBU respectively. Therefore, it is confirmed that the drug loading capacity was increased by employing ethanol as a co-solvent and helped disperse the drug evenly within the gel.

4.1.2 Drying time

After several other experiments to investigate the appropriate time for various films to be dried in the oven, there were no significant differences in weight after 24 hours. It was decided to retain gels in the oven for 24 hours maximum for film formation. Noticeably, the drying process of unplasticized films took a shorter time (about 12 hours) whilst plasticized films required the maximum 24 hours for complete drying. This is because both glycerol and PEG used as plasticizer can retain water molecules which therefore slows down the rate of water removal.

4.1.3 Visual evaluation of initial gels and resulting films

The gels before solvent casting and the resulting films were visually evaluated and the results are summarised in Table 4.1. Evaluation of films was based on criteria such as:

- ❖ Transparency: films must be transparent without any entrapped air bubbles
- ❖ Plasticity: the film should not be brittle and fragile as it will affect physical and mechanical stability during handling
- ❖ Thickness: ideal films must have optimum thickness (less than 0.4 mm) as this impact on patient convenience when applied to the buccal mucosa. In addition, it has an effect on the drug release rate as it determines the thickness of the gel formed after hydration and therefore the diffusion distance of drug during release studies (Miller-Chou and Koenig, 2003). See Figure 4.2-Figure 4.5.

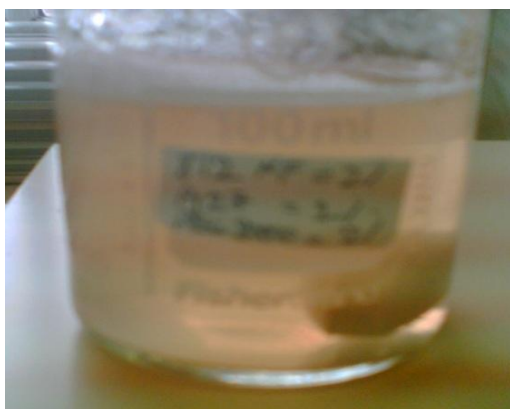


Figure 4.2 Clear, transparent gel (2% CAR 812 + 2% P407+2% PEG 2000).



Figure 4.3 Clear, transparent, well plasticised Film (1.5% CAR 911+2% P407+ 4.5% PEG 600).



Figure 4.4 Non transparent and brittle film (1.5% CAR 379+2% P407+3% PEG 6000).



Figure 4.5 Transparent, brittle un plasticised film (1.5% CAR 911).

4.1.4 Evaluation of drug loaded films

The preliminary evaluation of the physical appearance and characteristics of different films formulated, with different ratios of two grades of CAR (911 & 812), P407 and model drugs in the presence of two different plasticizers (glycerol & PEG) showed slightly different observations. The results demonstrated the need for modifications in the amounts and type of formulation components as well as the preparation method to achieve optimum characteristics. This implied further optimisation of the film formulation to account for the properties of the model drugs (PM which is a hydrophilic molecule and IBU and IND which are less hydrophilic). Dispersing the latter two model drugs within the gel required a co-solvent for achieving a suitable film due to their hydrophobic nature and poor solubility in aqueous media compared with PM. Addition of the model drugs also had effects on the physical and mechanical characteristics of the resulting films which were subsequently investigated using suitable characterisation techniques.

4.1.5 Poloxamer and carrageenan ratios

When the amount of P407 was increased to 8% w/w combined with 3% w/w CAR, the resulting film demonstrated ideal physical properties. However, these films were undesirably thick (0.7- 0.8 mm) and also exhibited excess air bubble due to incorporation of P407 at a concentration > 4% w/w as previously mentioned. Therefore the concentrations of both polymers were reduced to produce thinner films within reasonable formulation processing time. Films containing of 2.5% w/w CAR (812 & 911) and 8% w/w P407 showed sufficient physical stability but the foam generated during high speed stirring, as a consequence of the high ratio of P407, was a serious limitation.

Table 4.1 Physical characteristics of gels and films formulated with carrageenan (CAR), poloxamer 407 (P407) and different grades of PEG.

P407 (% w/w)	CAR (% w/w)	PEG (%w/w)	Gel characteristic	Film characteristic
2	2 (812)	-----	Transparent/ no bubbles/ easy to pour	Transparent/ very brittle
2	2 (812)	2 PEG 2000	Transparent/ no bubbles/ easy to pour	Transparent/ very brittle
3	1.5 (812,911,379)	4.5 PEG 600	Transparent/ no bubbles/ easy to pour	Transparent/ good film
5	1.5 (812,911)	4.5 PEG 600	Transparent/ no bubbles/ easy to pour	Transparent/ good film
6	1.5 (812,911)	4.5 PEG 600	Transparent/ no bubbles/ easy to pour	Transparent/ good film
7	1.5 (812,911)	4.5 PEG 600	Transparent/ no bubbles/ easy to pour	Transparent/ thick film
2	2 (379)	4.5 PEG 20000	Transparent/ no air bubbles/ easy to pour	Transparent/ very brittle
4	-----	-----	No gel structure	NA
2	2 (379)	-----	Transparent/ no air bubbles/ easy to pour	Not transparent
2	2 (911, 812)	3 PEG 2000	Agar structure/ transparent	Very brittle
3	1.5 (812, 911)	-----	Agar structure/ transparent	Brittle
3	1.5 (812, 911)	-----	Easy to pour/transparent gel	Brittle
2	1.5 (911)	-----	Easy to pour/transparent gel	Brittle
2	1.5 (379)	3 PEG20,000	Easy to pour/transparent gel	Very brittle/not transparent
8	4	5 PEG 600	Foamy gel/ high viscosity	Brittle/ thick

However, such high percentage of P407 allowed the incorporation of higher amounts of drug in the final films due to the surface active properties of P407 which helps drug molecules to be readily dispersed within the formulation.

As a compromise, the most appropriate polymer concentrations for optimum film formulation were 2.5% w/w CAR 911 and 4% w/w P407. In the case of CAR 812 based films, reduction in the concentration of P407 from 8% to 4% (w/w) produced films with “non-ideal” physical properties including non-uniform texture, non-transparent, patchy appearance arising from individual components precipitating out and brittle to handle. Furthermore, addition of model drugs resulted in increased gel viscosity and produced brittle and opaque films (Figure 4.6).

As a result, CAR 812 was not employed for further film development (Figure 4.6). CAR 379 produced non transparent and very brittle films (Figure 4.4) which are not desirable, though the initial gel showed acceptable properties.

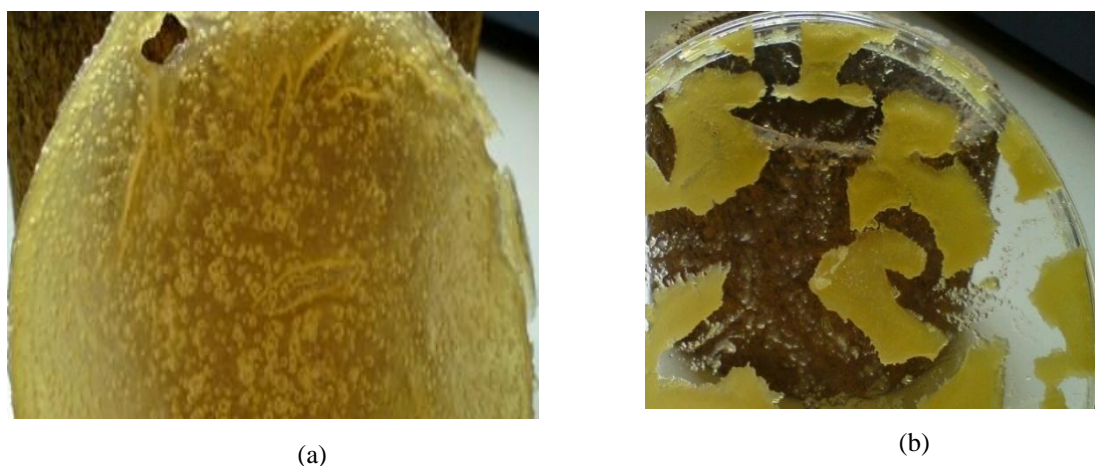


Figure 4.6 Films formulated with CAR 812 and IBU with (a) PEG and (b) GLY

4.1.6 Films plasticised with GLY or PEG

During the initial investigations, film formulation was carried out with and without plasticiser. Unplasticised films showed some plasticity but this was not flexible enough to satisfy the criteria outlined in section 4.1.3. Although use of GLY as plasticiser in blank films showed acceptable physical characteristics, employing GLY as a plasticizer had a detrimental effect on the physical properties of films containing a model active drug (Figure 4.7). The major limitation was that glycerol caused most of the incorporated drug to precipitate out and accumulate on the film surface resulting in an opaque and non-homogeneous film.

Optimization of various component ratios and plasticising effect of different grades of PEG was a critical step that required extensive investigation as summarised in Table 4.2 and Table 4.3. This effect might be associated with the physical characteristic of the PEG 20,000. On the other hand, the flakes of PEG 20000 dispersed in the system easily and produced a very transparent gel but not able to reduce the glass transition and thereby improve plasticity, resulting in much more brittle films. The results confirmed that the optimum plasticiser was PEG 600, and was therefore the plasticiser of choice for all subsequent films formulated. Films containing PEG 600 exhibited better physical characteristics with and without drug incorporation. Films plasticized with PEG 600 were clear, transparent, and possessed appropriate flexibility (Figure 4.8). The plasticizer in the system functions by providing increased free volume between the polymeric chains which allows them to slide together and subsequently produces appropriate flexibility and tensile strength. The optimum level of PEG 600 was evaluated by texture analysis and the results used to select the most flexible films that were easy to handle without breaking or sticking (Riggleman, *et al.*, 2007).

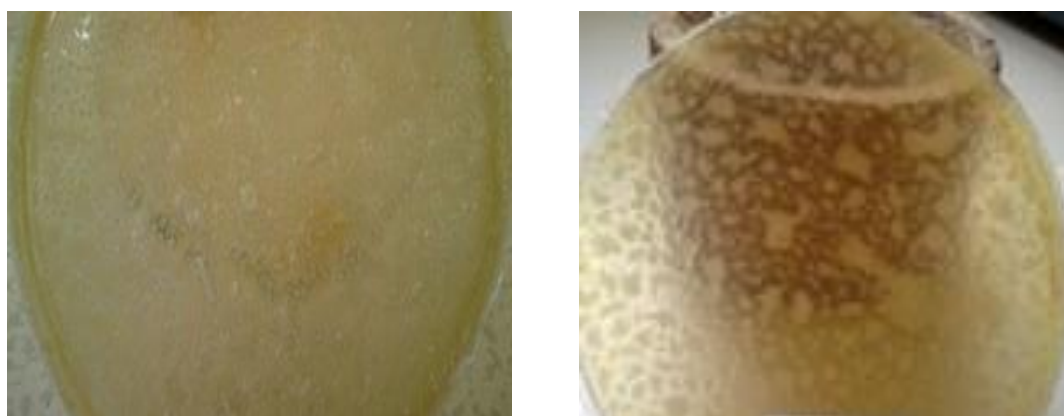


Figure 4.7 Films containing glycerol with loaded drug.

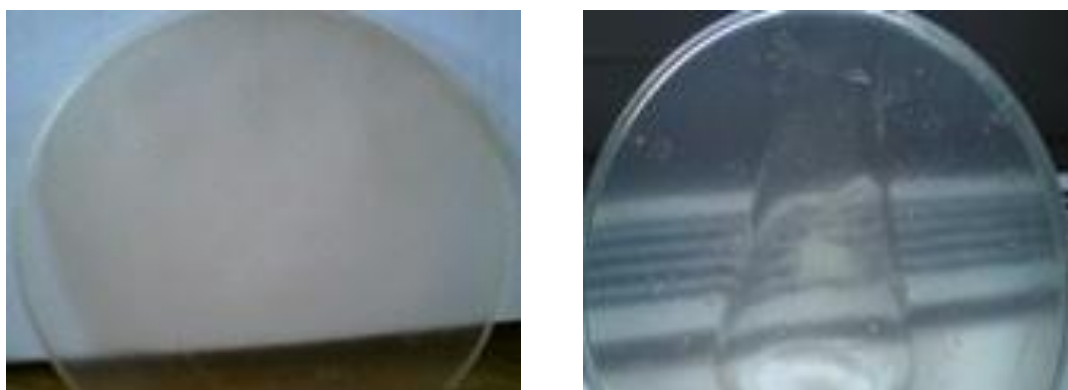


Figure 4.8 Films containing PEG with loaded drug.

Table 4.2 Characteristic of films, gels and films with three CAR grades, P407 and various grades of PEG.

P407 (% w/w)	CAR (% w/w)	PEG (% w/w)	Gel characteristic	Film characteristic
7.0	2.0 (812,911)	5.5 PEG 600	Transparent/no bubbles/easy to pour	Thick/transparent/flexible
8.0	3.0 (911,812)	5.5 PEG 600	Transparent/no bubbles/easy to pour	Thick/transparent/flexible
10.0	4.0 (812,911)	5.5 PEG 600	Transparent/no bubbles/easy to pour	Thick/transparent/brittle
2.0	2.0 (911)	5.0 PEG 20000	Transparent/no bubbles/easy to pour	Thick/transparent/very brittle
2.0	1.5 (812,911,379)	3.0 PEG 6000	Transparent/no bubbles/easy to pour	Transparent/very brittle
2.0	1.5 (812,911,379)	4.5 PEG 600	Transparent/no bubbles/easy to pour	Transparent/good elasticity
2.0	1.5 (812, 911,379)	4.5 PEG 2000	Transparent/no bubbles/easy to pour	Transparent/very brittle
2.0	1.5 (812, 911)	4.5 PEG 20000	Transparent/no bubbles/easy to pour	Transparent/very brittle
2.0	1.5 (812,911,379)	4.5 PEG 6000	Transparent/no bubbles/easy to pour	Transparent/ very brittle
2.0	1.5 (812,911,379)	-----	Transparent/no bubbles/easy to pour	Transparent/ brittle
4.0	2.5 (911)	3.5 PEG 600	Transparent/easy to pour	Very brittle
4.0	2.5 (911)	4.5 PEG 600	Transparent easy to pour	Very brittle
4.0	2.5 (911)	5.5 PEG 600	Transparent/ easy to pour	Flexible
4.0	2.5 (911)	6.0 PEG 600	Transparent/easy to pour	Rigid

4.1.7 Drug loading results

Based on the observations, dissolving the IBU and IND in ethanol increased the amount of incorporated drug from 0.5 to 0.8% w/w for IBU and 0.4- 0.6% w/w for IND within the initial gel. Watkinson and co-workers (2009) have also shown that the pka of IBU increased from 4.44 to 5.68 due to addition of ethanol hence the IBU solubility was enhanced 5,500-fold relative to its aqueous solubility. 1.6% (w/w) PM was easily dissolved in aqueous media hence, addition of ethanol as a co-solvent to dissolve drug was not necessary. The drug loading capacities of optimised films containing CAR 911: P407: PEG 600; as a function of total dry weight of film are summarised below:

- Indomethacin (IND) = 4.14 %
- Ibuprofen (IBU) = 5.79 %
- Paracetamol (PM) = 11.34

4.2 Characterisation of physical and mechanical properties of films

4.2.1 Texture analysis

Texture analysis was used to measure tensile properties; tensile strength (brittleness of films), elastic modulus (rigidity) and elongation (flexibility and elasticity). The specimens' thickness and width were measured and considered while calculating the stress and strain values. The elastic modulus was estimated from the initial linear portion of the stress-strain curve whilst tensile strength was calculated by dividing force at break by the initial cross-sectional area of the films specimen (Dixit & Puthli, 2009). Figure 4.9 shows that the elastic modulus decreased gradually with increasing PEG 600 concentration for films containing no drug. As Morales, *et al.*,(2011) stated, soft and weak polymers have low tensile strength, low elastic modulus (Young's modulus) and low elongation at break. In contrast a soft and strong polymer displays a reasonable tensile strength, low elastic modulus and a high elongation at break.

According to the results the concentration of 5.5% w/w PEG 600 in gel (corresponding to a CAR 911/PEG 600 ratio of 5:11) resulted in the elastic modulus reaching the minimum value while the percent elongation remained at the maximum.

Further increase in the PEG 600 concentration to 6.5% (w/w) resulted in a significant decrease in the percentage elongation and a corresponding increase in the elastic modulus.

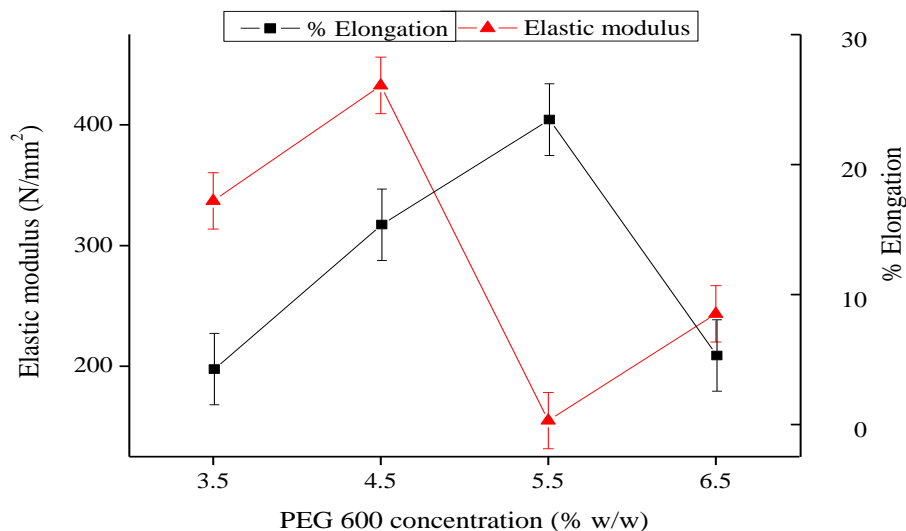


Figure 4.9 Elastic modulus and % elongation profile for pure films formulated with different concentration of PEG 600 {mean \pm s.d, (n=3)}.

However, different observations were made when drug was added to the optimized film. Figure 4.10 and Figure 4.11 show the tensile results for drug (IND, IBU and PM) loaded films. Following the addition of the model drugs, the elastic modulus was increased and required a change in PEG 600 content to obtain films with desirable tensile properties. The results showed that the optimum concentration of PEG 600 required increase to 6.5% w/w in the presence of the maximum 0.6% w/w IND or 0.8% w/w IBU to achieve desirable film flexibility matching that of the non-drug loaded films. In the case of PM, the maximum 1.6% loading required an increase in PEG 600 concentration to 6% w/w to match the flexibility of the non-drug loaded films. As noted above, such increase resulted in a sharp increase in percent elongation and corresponding decrease in elastic modulus for the non-drug loaded films which is an interesting observation.

These observations might be the consequence of the differences in molecular weight and log P values for IND (mw=357.78), IBU (mw=206.28) and PM (mw=151.16). The impact of the drug could relate to reduction in free volume between the polymeric chains and therefore, decrease in elongation and increase in elastic modulus.

To provide appropriate flexibility more plasticizer was required for the drug loaded films to maintain the required free volume that allows optimum flexibility (Zelkó, et al., 2002).

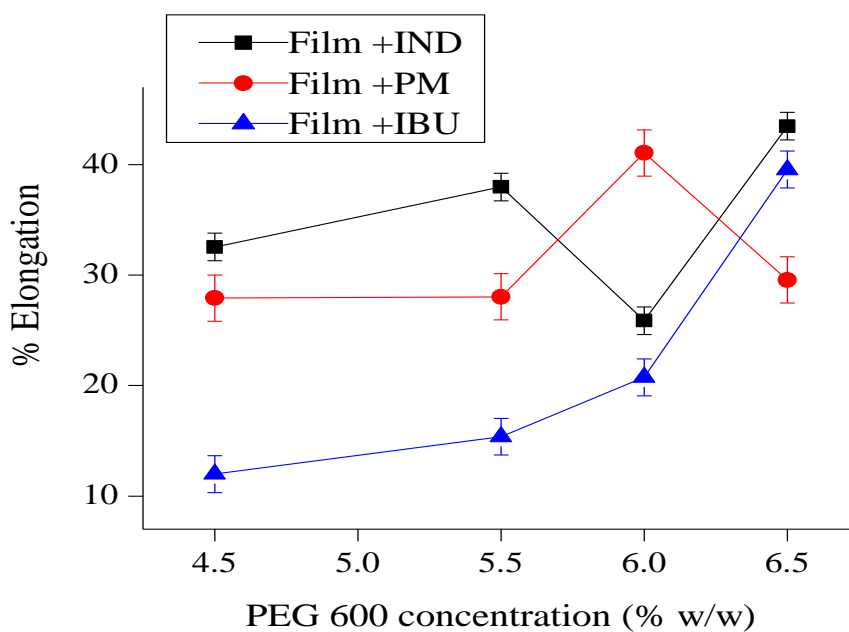


Figure 4.10 % Elongation profile for films formulated with model drugs {mean \pm s.d,(n=3)}.

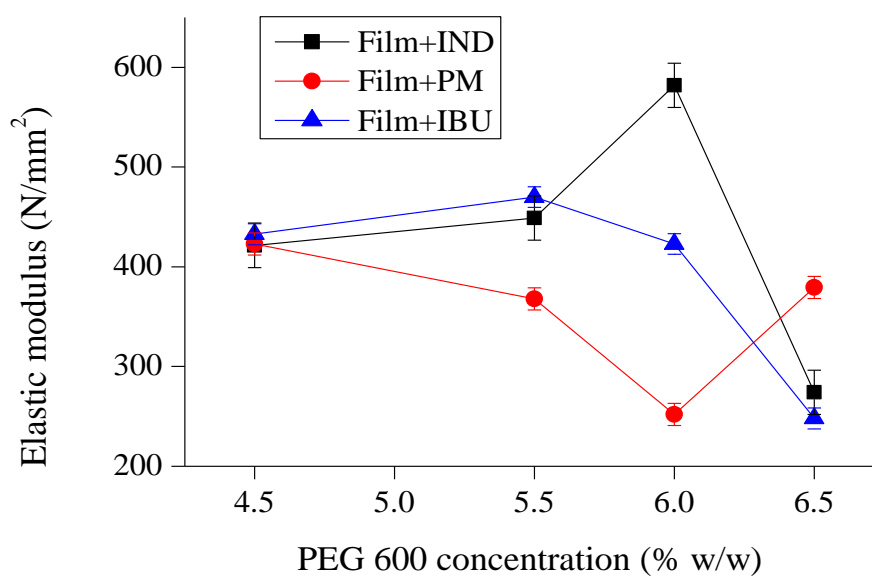


Figure 4.11 Elastic modulus profile for films formulated with different model drugs {mean \pm s.d,(n=3)}.

The tensile strength, elongation and elastic modulus values are relevant as they indicate the strength of the film under stress due to stretching and have a direct effect on patient's acceptance and clinical performance of the final dosage form. Flexible films provide better patient compliance as they are less likely to cause contact irritation whilst an excessively elastic film can cause problems with handling such as folding and stickiness (Boateng, *et al.*, 2009a).

4.2.2 HSM results

As the system contained several compounds with different melting, degradation or glass transition temperatures, the observed phase transitions were not clearly distinguishable. Therefore HSM results mainly specified the degradation point which helped in developing suitable methods for TGA and DSC such as the maximum temperature at which they were heated to.

4.2.3 TGA results (water content)

Polymers contain some water molecules bonded to the monomer parts and impact directly on glass transition temperature and other physico-chemical characteristics such as elastic modulus. Therefore evaluation and calculation of the water content in the pure polymers as well as the films was essential. The results are summarised in Table 4.3. The results shown in Table 4.3 demonstrate that different films (either blank or containing model drugs) have similar water content. Also their degradation points decreased in comparison to the original compounds and this shows the effect of formulation process in changing the physico-chemical properties of the starting materials due to interactions between the various components (Stephenson, *et al.*, 2001). As shown in Table 4.4 use of GLY as plasticiser caused an increase in amount of residual water in the films and it may account for relatively less stable films produced using glycerol. This is because glycerol is a known moisturizing agent and has a high affinity for water. Furthermore, films containing IBU showed higher amount of water compared to the other drugs. In addition, the grade of CAR should be considered as an important factor since CAR 812 showed higher capacity to retain water within the film.

Table 4.3 Water content in starting materials and optimum films prepared from gels plasticised with PEG 600 containing optimum amounts of the model drugs (mean \pm s.d, n=3).

Materials used and their concentrations (% w/w)	% H ₂ O content	Degradation temperature (°C)
2.5% CAR 911 + 4% P407 + 5.5% PEG 600	5.6 \pm 0.1	190
2.5% CAR 911 + 4% P407 + 6.5% PEG 600 + 0.6% IND	4.8 \pm 0.2	190
2.5% CAR 911 + 4% P407 + 6.5% PEG 600 + 0.8% IBU	5.1 \pm 0.03	190
2.5% CAR 911 + 4 % P407 + 6% PEG 600 + 1.6% PM	5.0 \pm 0.1	190
CAR 911 powder	13.6 \pm 0.1	220
P407 powder	0.2 \pm 0.01	370
PEG 600	1.1 \pm 0.3	360

Table 4.4 Water content of films formulated with gels containing carrageenan {(CAR) 911 or 812}, poloxamer 407 (P407) and plasticized with glycerol (GLY) or PEG 600 mean \pm s.d, n=3.

CAR (% w/w)	P407 (% w/w)	Plasticizer (% w/w)	IBU (% w/w)	% H ₂ O content
2.5 (812)	8.0	4.5 GLY	-----	16.5 \pm 0.8
2.5 (911)	8.0	4.5 GLY	-----	6.9 \pm 0.4
2.5 (812)	8.0	4.5GLY	0.9	19.9 \pm 1.0
2.5 (911)	8.0	4.5 GLY	0.9	23.5 \pm 1.2
2.5 (812)	8.0	4.5 PEG 600	-----	10.3 \pm 0.6
2.5 (911)	8.0	4.5 PEG 600	-----	2.2 \pm 0.3
2.5 (812)	8.0	4.5 GLY	0.6	17.3 \pm 0.7
2.5 (911)	8.0	4.5 GLY	0.6	13.9 \pm 0.8
2.5 (812)	8.0	5.5 PEG 600	0.9	12.2 \pm 0.8
2.5 (911)	8.0	5.5 PEG 600	0.9	3.8 \pm 0.2
2.5 (812)	8.0	5.5 PEG 600	0.6	9.9 \pm 0.5
2.5 (911)	8.0	5.5 PEG 600	0.6	11.0 \pm 0.4

TGA results for films stored over a six month period showed a decrease in water content (Table 4.5) which could be attributed to the conversion of free water to bound water within the polymeric matrix after six month of storage.

Table 4.5 Water content in films prepared from gels with various concentrations (% w/w) of CAR, P407, PEG 600 and optimum model drugs after six month storage (mean \pm s.d,(n=3)).

Composition (w/w) of film specimen	% H ₂ O content	Degradation point (°C)
2.5% CAR 911 + 4% P407 + 6.5% PEG 600 + 0.6% IND	1.5 \pm 0.2	160
2.5% CAR 911+ 4% P407+ 6.5% PEG 600 + 0.8% IBU	1.0 \pm 0.3	160
2.5% CAR 911 + 4% P407 + 6% PEG 600 + 1.6% PM	1.0 \pm 0.1	160

4.2.4 DSC results (melting point, glass transition)

DSC was used to characterize thermodynamic behaviour of CAR 911, P407, PEG 600 and three model drugs (IND, IBU, PM) within the films. However, to be able to interpret the results obtained from DSC analysis of the drug loaded films, the thermodynamic behaviour of pure drugs should be investigated (Barreiro-Iglesias, *et al.*, 2002). The results showed the sharp melting point of crystalline form of IBU at 77.7°C (Figure 4.12a). After sharp cooling all the crystals were changed to amorphous form which was stable during the second heating cycle (Figure 4.12b).

Further DSC investigation proved that IBU in the film was in amorphous form. Comparison of the results to that of Figure 4.12 and Figure 4.13 a& b shows that during the the first heating cycle, glass transition of IBU appeared at -59.5°C and the absence of the sharp melt peak expected for crystalline IBU between 70-80°C. Instead, three sharp peaks were detected at -11.0°C, 22.7°C and 34.1°C corresponding to PEG 600, mixture of PEG 600 and P407 and P407. This could be a eutectic mixture of PEG 600 and P407, however; additional experiments were conducted to identify the mixture (Newa, *et al.*, 2008).

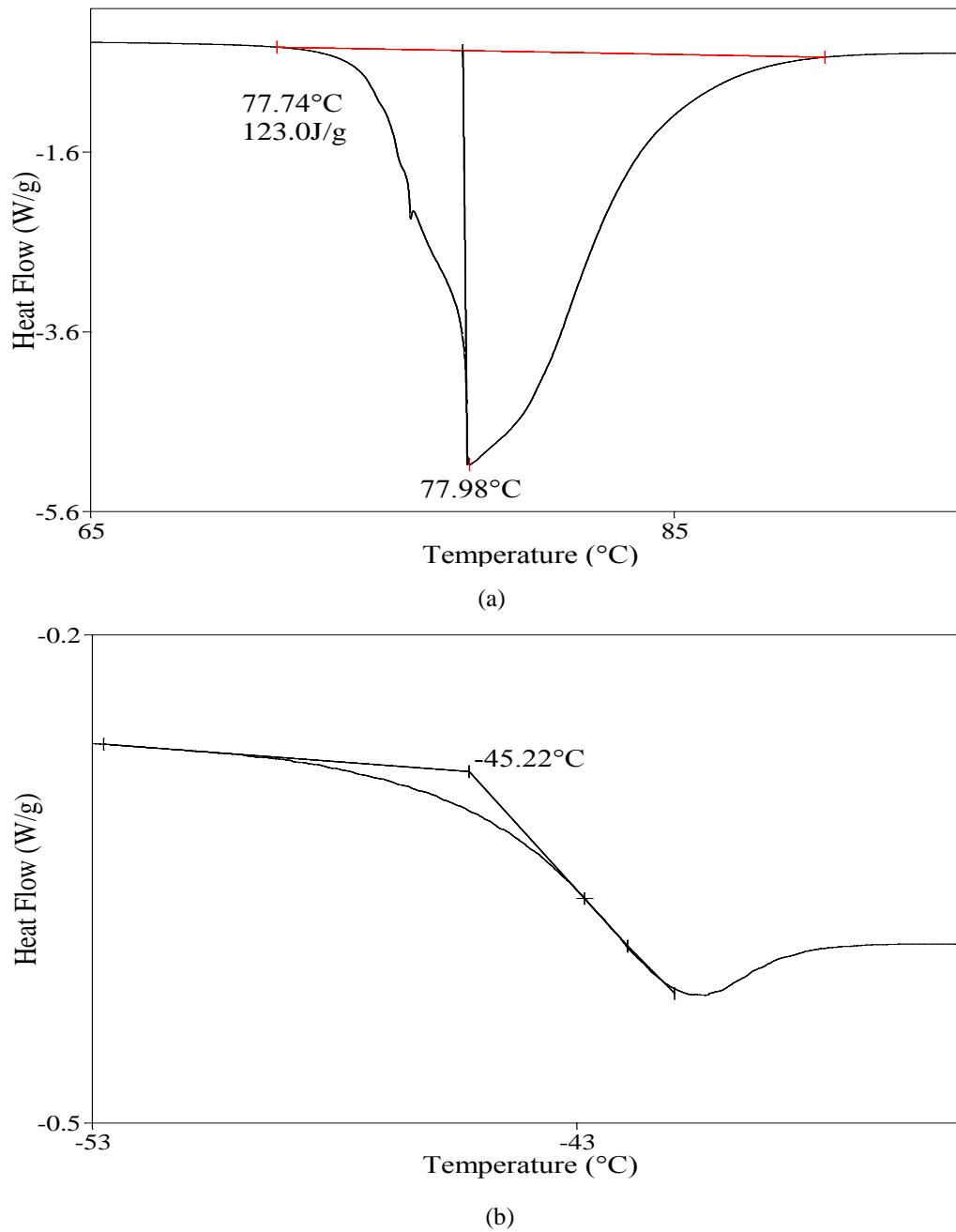


Figure 4.12 DSC results showing (a) melting point and (b) glass transition of pure IBU.

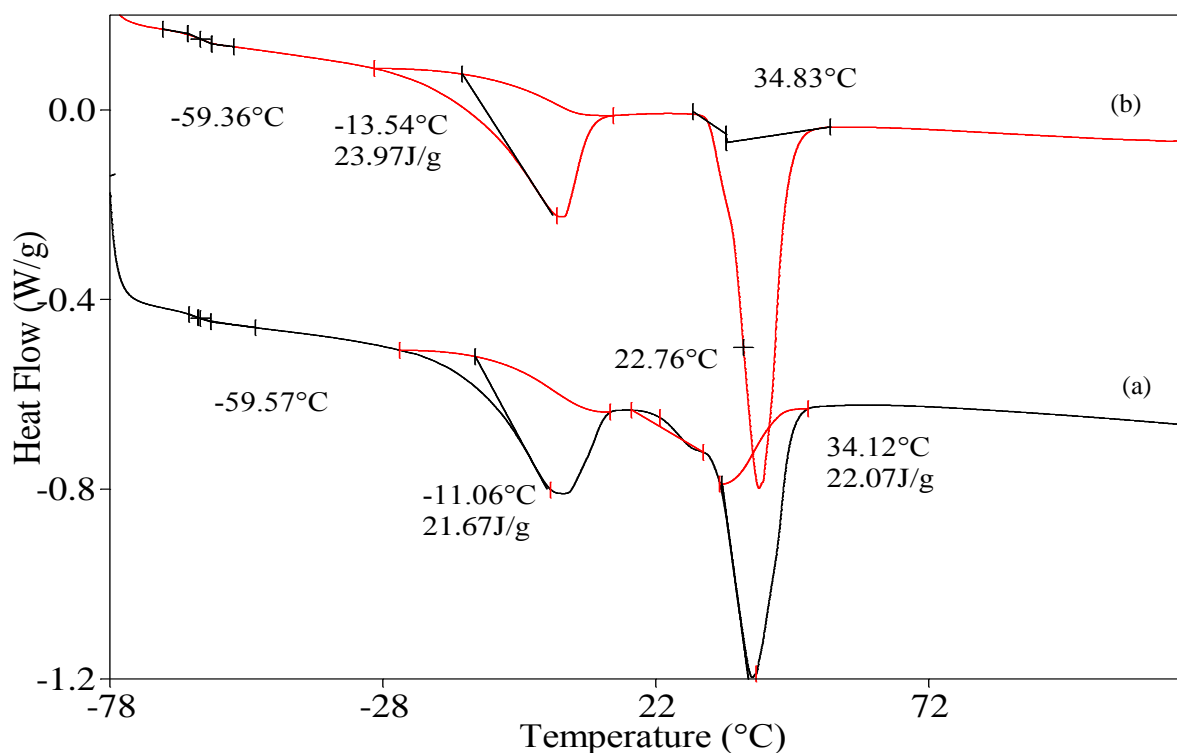
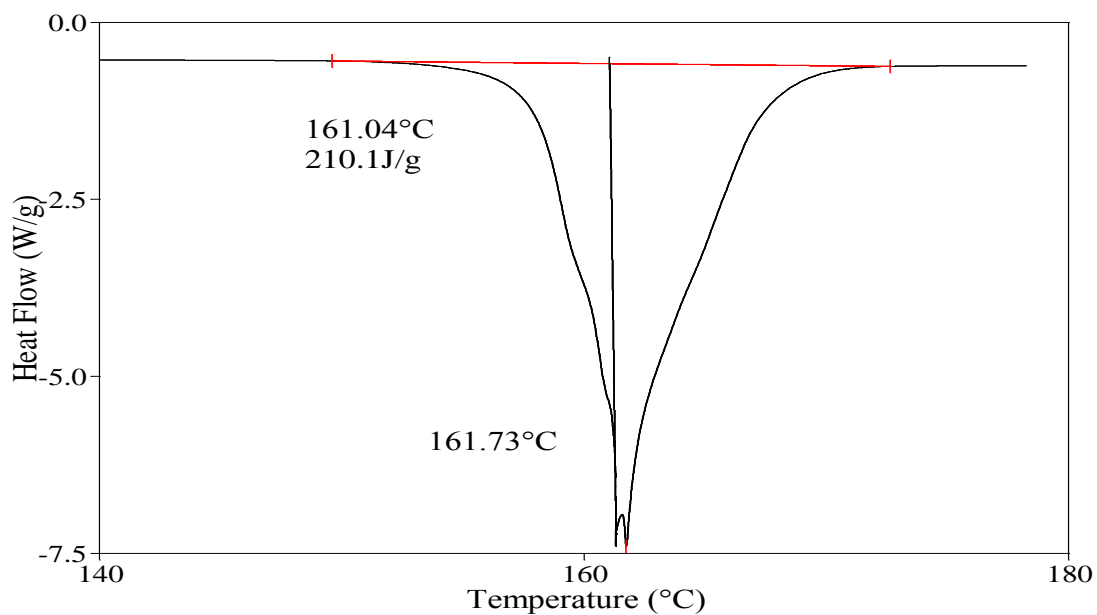


Figure 4.13 DSC results of (a) fresh film prepared from gels comprising 2.5% CAR 911+ 4% P407+ 6.5% PEG 600 and 0.8% IBU and (b) films containing IBU after 6 months storage.

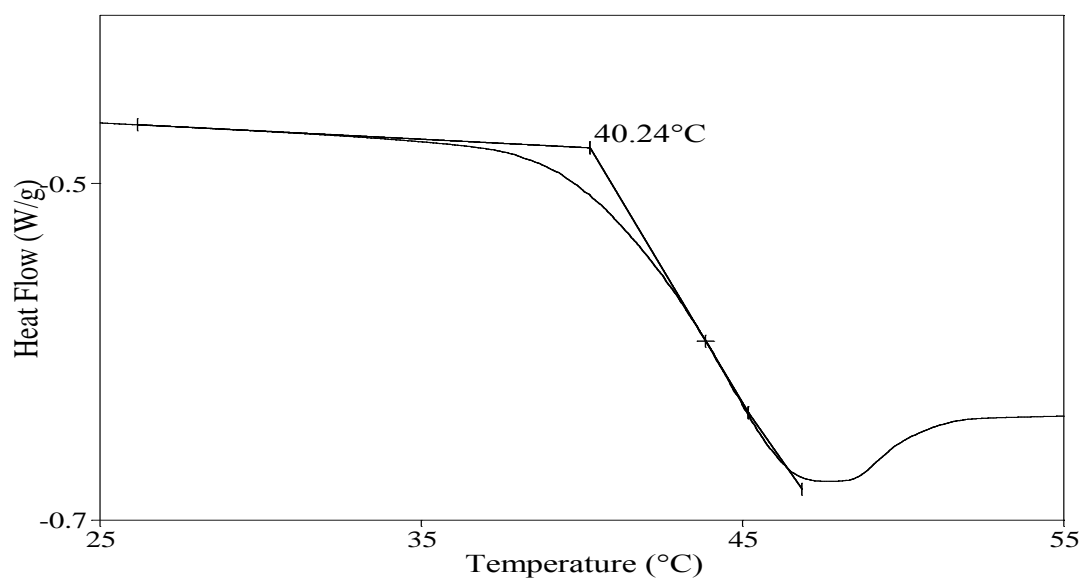
The results confirmed that the incorporated drugs were stable in the amorphous form within the film matrix. However, following storage, the films lost some of the residual water originally present which may account for observed changes in the DSC profile relating to PEG 600 and P407 phase transitions. This is illustrated by a comparison between the thermograms belonging to freshly prepared films and films stored for six months which indicate that water can have an effect on the physico-chemical characteristics of these two polymers.

Analysis of the data in Figure 4.13b reveals that the transition peak corresponding to the mixture of PEG 600 and P407 disappeared following the reduction of residual water content in the films containing IBU. The foregoing conclusion is evidenced by detection of only two peaks in Figure 4.13b with onset of melting at -13.5°C and 34.8°C corresponding to PEG 600 and P407, respectively. The proposed explanation is that the presence of water within the system increases the opportunity for interaction between PEG 600 and P407 which was decreased during storage as a result of water loss.

The consequence was the disappearance of the peak corresponding to the mixture formed from interaction between PEG 600 and P407. Similar results were observed for PM and IND loaded films after six months storage time and the fact that the amorphous forms were preserved during the storage period.



(a)



(b)

Figure 4.14 DSC results of pure IND (a) melting point and (b) glass transition.

For pure IND the results from the first heating stage showed the sharp melting point of crystalline form at 161.0°C. After fast cooling, all the crystals converted to a stable amorphous form and during the second heating cycle its glass transition was detected at 40.2°C (Figure 4.14 a & b). The DSC plot for films containing IND confirmed that the amorphous form of the drug was present in the film. Heat flow plots showed the glass transition at 23.4°C and two melting transitions belonging to PEG 600 and P407 alone (Figure 4.15). The reason for the disappearance of the melt transition corresponding to PEG 600/P407 mixture could be due to the slightly lower water content in IND loaded films compared to films containing IBU (Table 4.3). This resulted in the melting peak of the mixture being masked by the P407 melting transition.

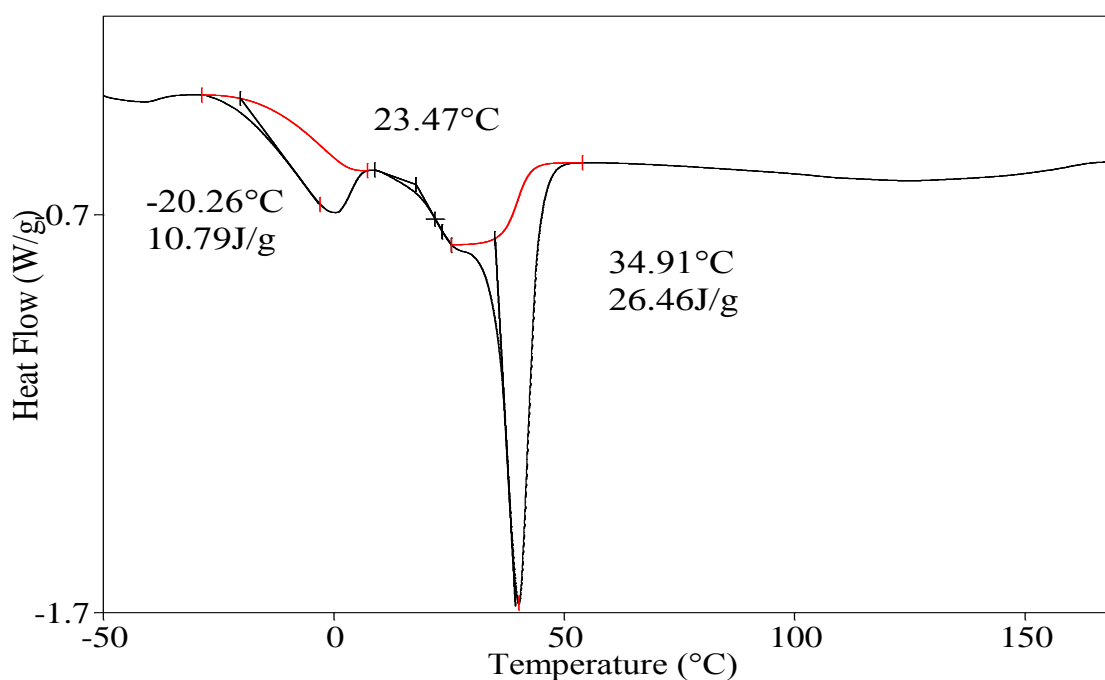


Figure 4.15 DSC results of film comprising 2.5% CAR 911+ 4% P407+ 6.5% PEG 600 and 0.6% IND within the initial gel.

Similarly, PM showed a sharp melting peak at 168.6°C in the first heating cycle. During the sharp cooling, the crystalline form was changed to the amorphous form (Qi, *et al.*, 2008). However, this amorphous form was unstable and recrystallized at 80.5°C. For PM, the T_g was detected at 21.8°C and a sharp melting peak confirming the recrystallization process (Figure 4.16).

This result is comparable with the thermogram for the film with glass transition at 23.1°C while the expected melting peaks of PM around 157°C (orthorhombic polymorph) or 170°C (monoclinic polymorph) were absent and confirms that the drug within the film was in the amorphous form (Figure 4.17).

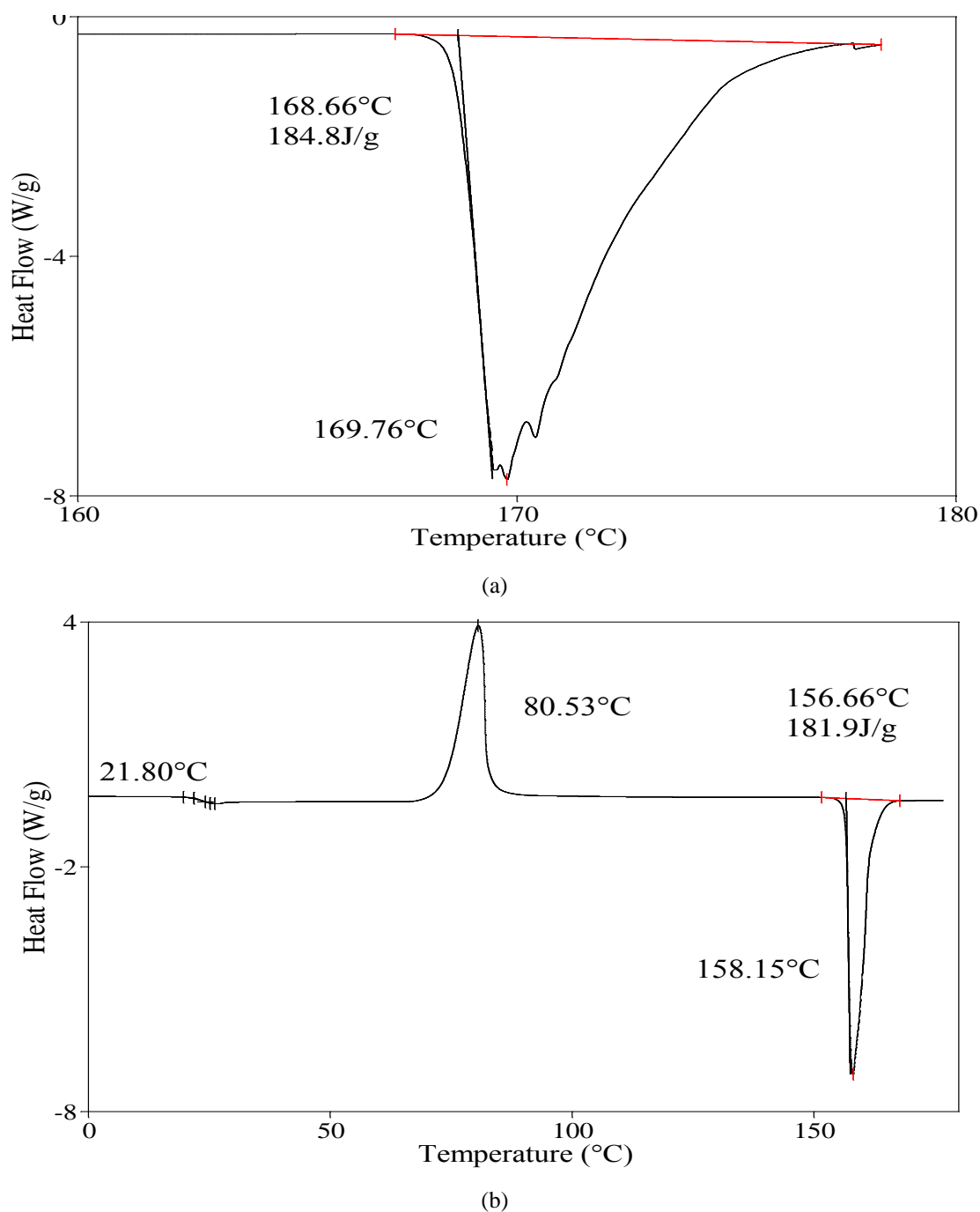


Figure 4.16 DSC results showing a) melting point and b) glass transition of pure PM.

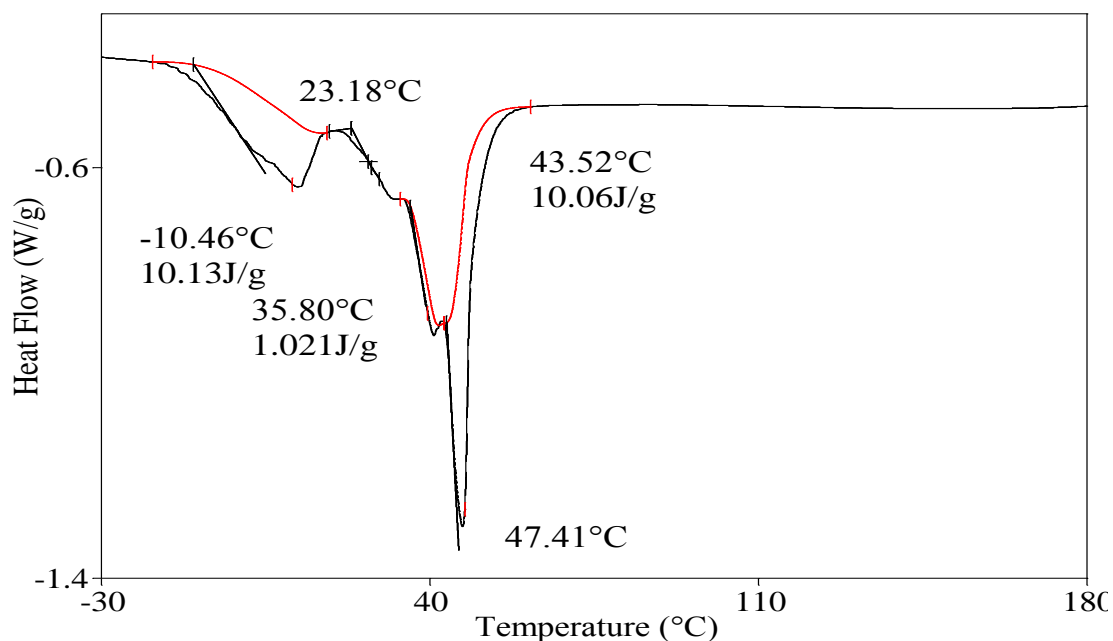


Figure 4.17 DSC results of film prepared from gels containing 2.5% CAR+ 4% P407+ 6% PEG 600 and 1.6% PM.

Though amorphous forms are known to be more soluble, they do present stability challenges owing to their tendency to convert back to the crystalline form (Tusi, 2004; Hancock & Parks, 2000). To investigate the stability of model drugs within the films, further DSC experiments were conducted to determine whether it remained in an amorphous form or was converted back to the crystalline form during storage.

4.2.5 SEM results

SEM was conducted to determine the topographic view of the films' surface and how this could affect dissolution profiles and stability. The microscopic appearance of the film surface showed continuous film formation which was also uniform with no obvious porous region.

This continuous sheet of film was maintained after incorporation of drug although drug loaded films appeared slightly more brittle on the surface (Figure 4.18- Figure 4.21). This is important because the rates of hydration, swelling and eventual drug dissolution are

dependent on the surface integrity of the film structure as it affects the initial rate of water ingress (Boateng, *et al.*, 2010).

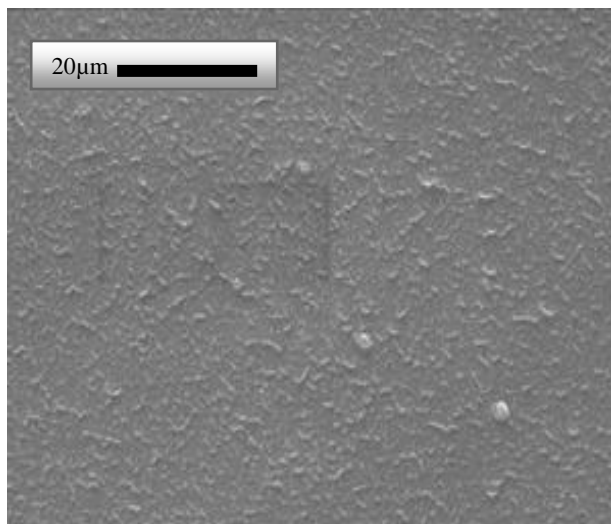


Figure 4.18 Film prepared from gel comprising 2.5% CAR 911+4% P407 +6% PEG 600.

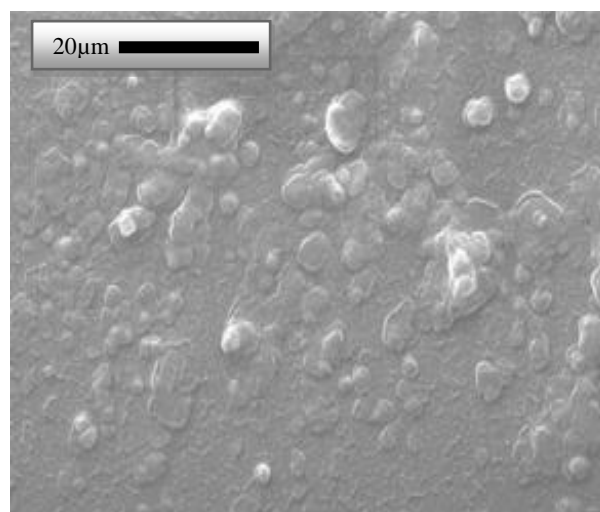


Figure 4.19 Film prepared from gel comprising 2.5%CAR 911+ 4% P407 +6.5% PEG 600+0.8% IBU.

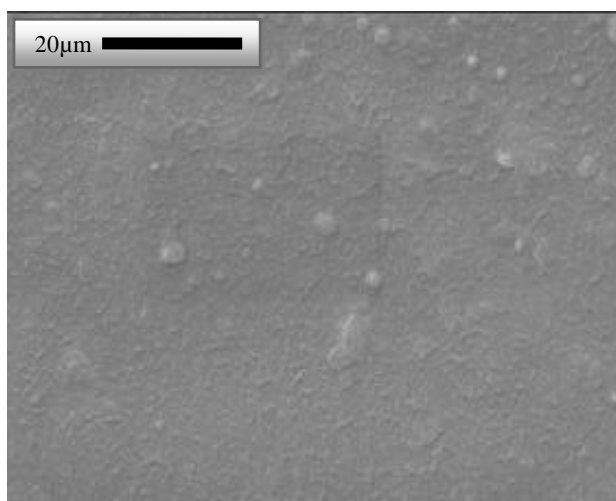


Figure 4.20 Film prepared from gel comprising 2.5% CAR 911+ 4% P407 + 6.5% PEG 600+ 0.6% IND.

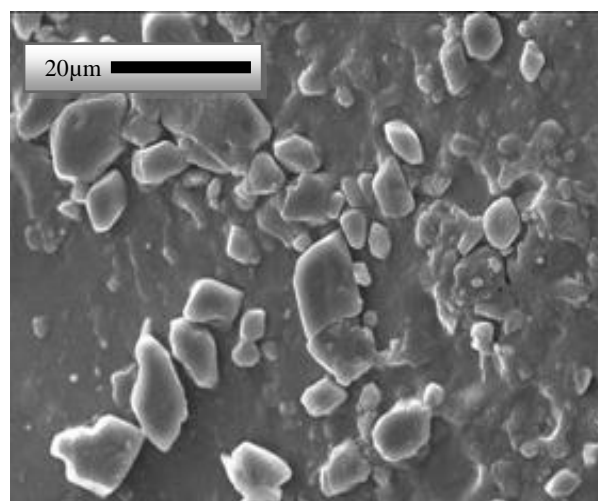


Figure 4.21 Film prepared from gel comprising 2.5% CAR 911+ 4% P407 + 5.5% PEG 600+ 1.6 % PM

Obviously drug release from the surface will be very fast during the initial stage of dissolution. However, drug which is completely dispersed within the polymer matrix will be affected by swelling, erosion and diffusion and this is expected to be the determining factor controlling drug release.

Figure 4.22 to Figure 4.24 illustrate the surface morphology of the films with higher ratios of CAR 911 and P407, showing similar results as films with lower concentration of these polymers. The figures also showed that variation of the P407 percentage didn't have any impact of the surface properties of the film.

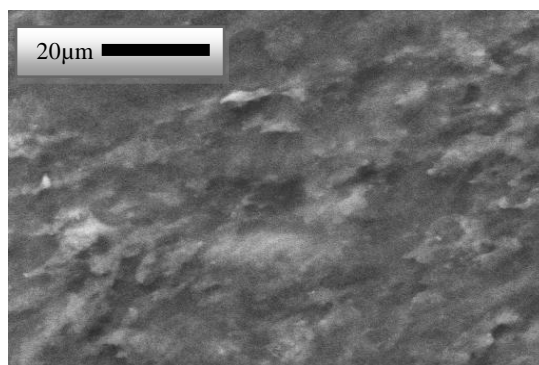


Figure 4.22 Morphology of the film prepared from prepared from gel comprising 2.5% CAR 911+ 8% P407 + 5.5% PEG 600.

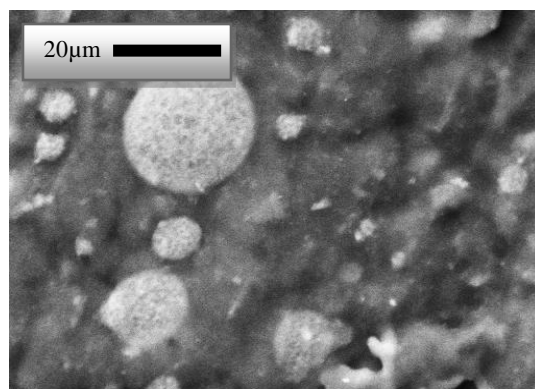


Figure 4.23 Surface morphology of the film prepared from gel comprising 2.5% CAR 911 + 8% P407 + 6.5% PEG 600 + 0.7% IBU.

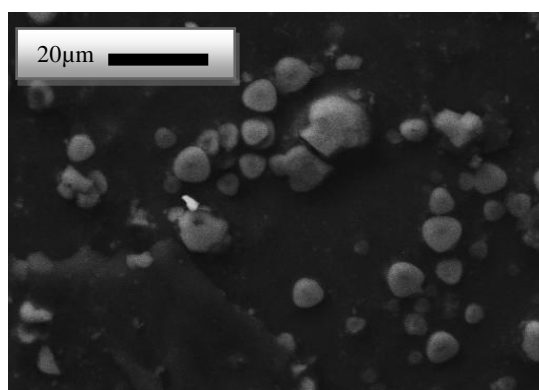


Figure 4.24 Surface morphology of film prepared from gel comprising 2.5% CAR 911 + 8% P407 +5% PEG + 0.7% IBU.

4.2.6 XRPD results

To investigate the crystalline/amorphous characteristics of all initial compounds and films XRPD experiments were conducted. Amorphous compounds showed very broad peaks which were distinguishable in comparison to the sharp peaks belonging to the crystalline form. XRPD also provided information about the crystalline-amorphous ratios for the various starting materials and for the formulated films.

In the case of CAR 911 powder, the results showed some peaks which indicated a small level of crystallinity but significantly amorphous which was reproducible before and after grinding (crystalline/amorphous: 4/96%). Also XRPD analysis for P407 showed that the crystalline amorphous ratio was 50/50.

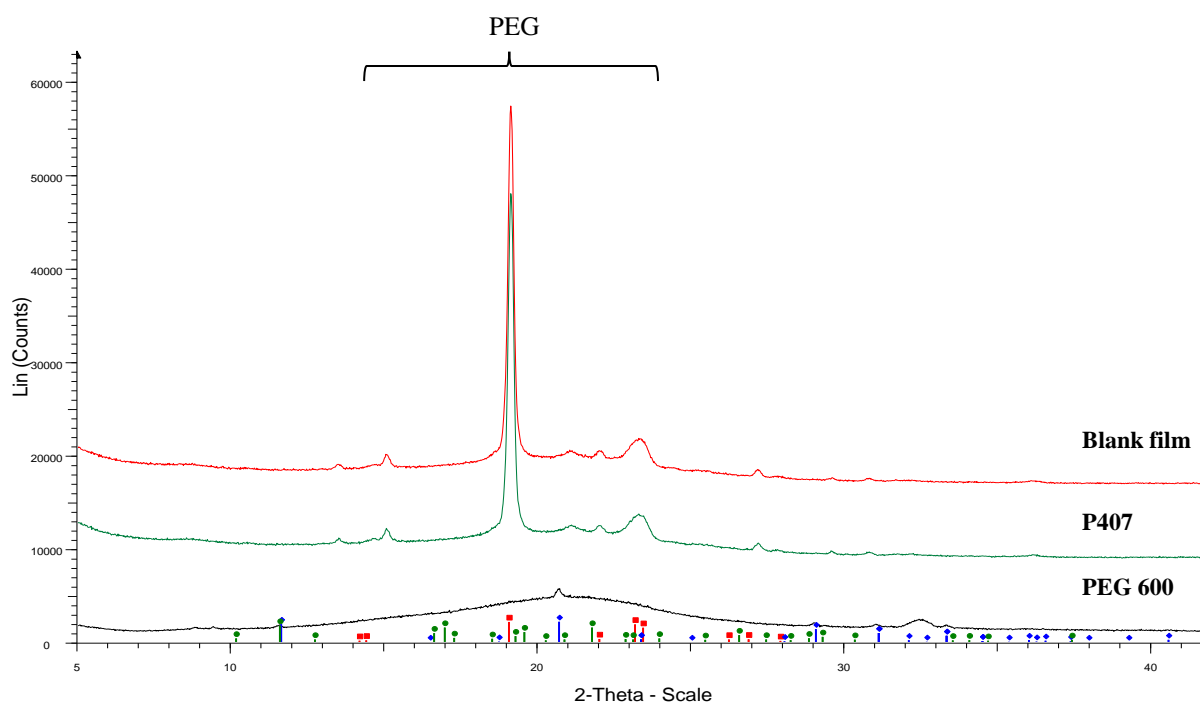


Figure 4.25 XRPD diffractogram of PEG 600, P407, films containing CAR 911 + P407 and PEG 600 without drug.

To check the crystalline-amorphous ratios and confirm the physical form of the various components within the films, further XRPD analyses were performed. Figure 4.25 shows the XRPD spectra of the non-drug loaded films. The results demonstrated that there are various crystalline forms present in the film belonging to PEG 600.

P407 is a block co-polymer comprising 56 units of a polypropylene oxide core (21%) and two polyethylene glycol tails (79%) with 101 units hence, the detected PEG crystalline peaks in crystallography results associated with P407.

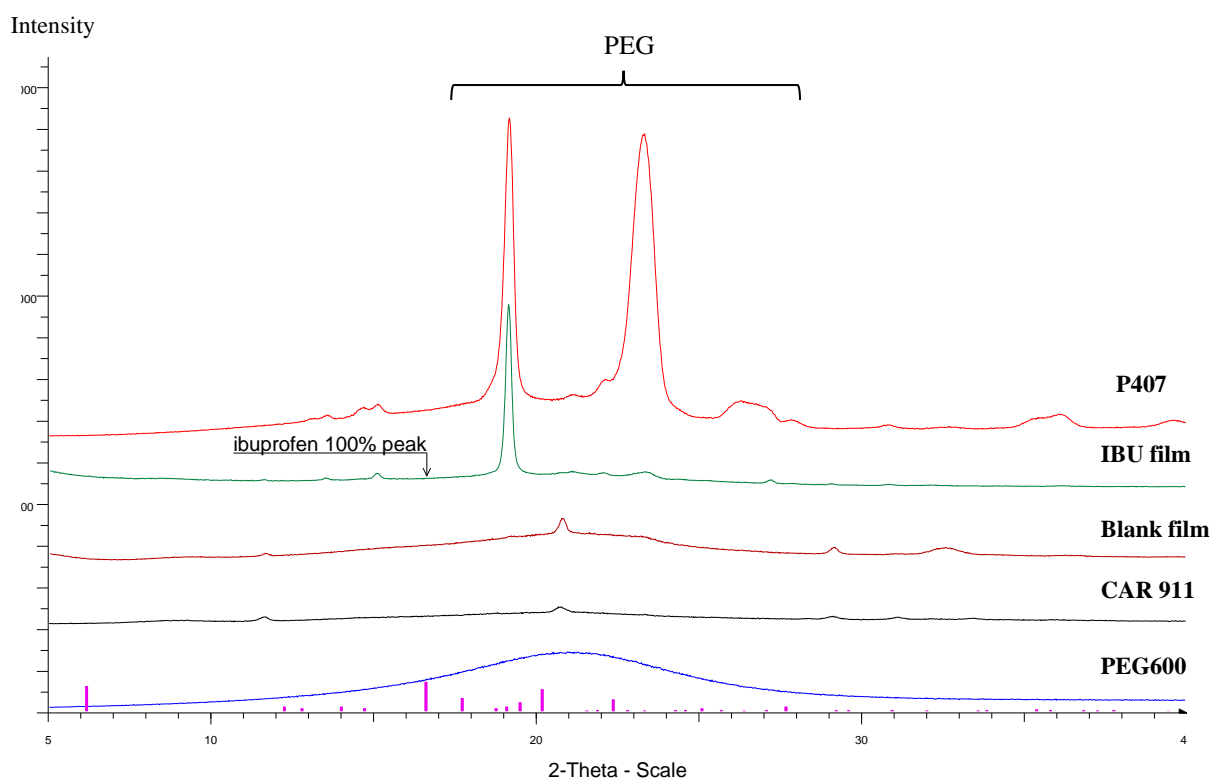


Figure 4.26 XRPD diffractograms of CAR 911, P407, PEG 600, blank and IBU loaded film.

The XRPD results also confirmed the absence of crystalline IBU form in the film matrix (Figure 4.26). As CAR is available in amorphous form the background spectrum was subtracted from original curve (top spectrum) and the absence of the main peak for IBU expected at about 16.2, 2θ confirms the amorphous form of IBU in the film. Similar results showed the presence of amorphous PM (Figure 4.27) incorporated in the film matrix and the same result was achieved for IND loaded films (Figure 4.28). According to the calculations from area under the curve the ratio of crystalline to amorphous are as below:

Non drug loaded film crystalline: amorphous = 5:95

0.8 % w/w IBU and 1.6 % w/w PM loaded films crystalline: amorphous = 4:96 which shows that addition of the drug induce the crystallization of PEG.

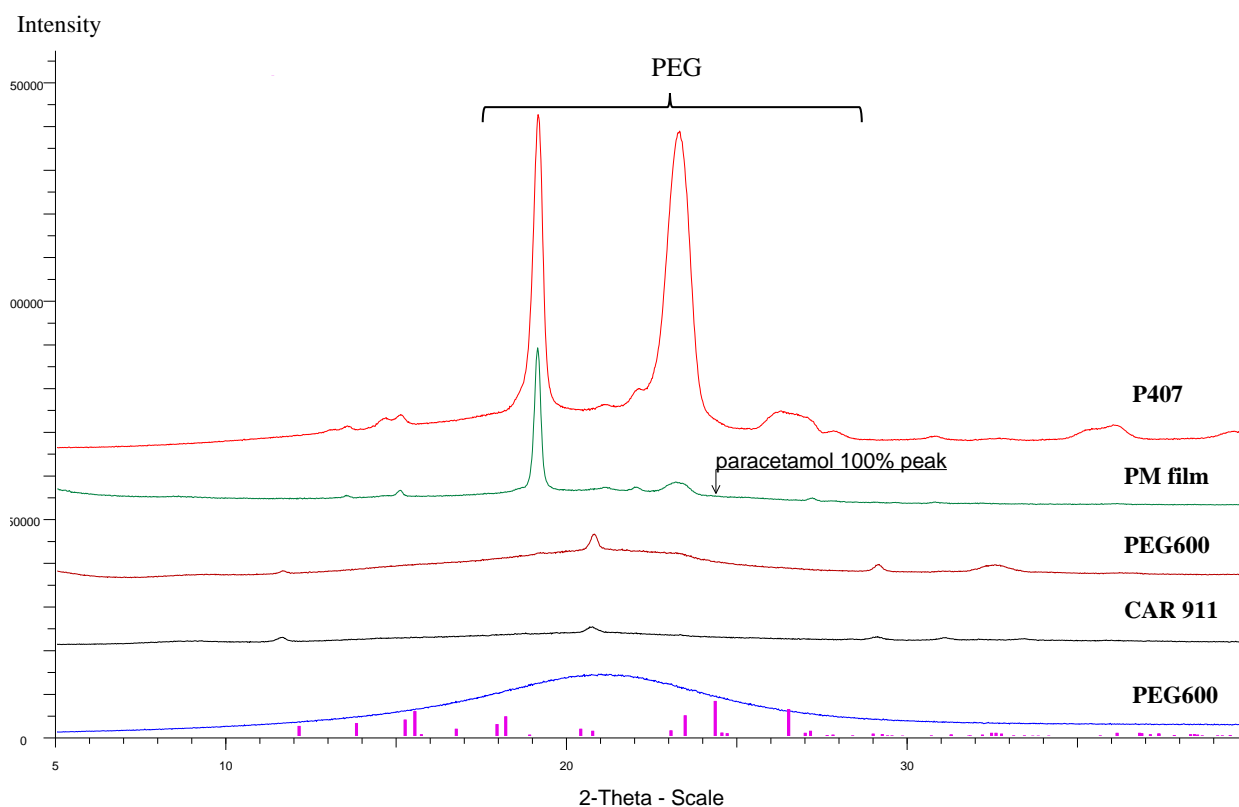


Figure 4.27 XRPD spectrum of XRPS diffractogram of CAR 911, P407, PEG 600, blank and PM loaded films.

Among the many experimental techniques available for the identification of solid forms, (including polymorphs, solvates, salts, co-crystals and amorphous), XRPD is generally accepted as a gold standard. XRPD has applications throughout the formulation development process, usually in combination with other experimental techniques such thermal analysis techniques. The efficacy of XRPD is evident when one considers the direct relationship between the measured XRPD pattern and the molecular structure of the drug incorporated in films or wafer as it also provided information about the structure of the excipient material, whether it exhibits long-range order as in crystalline materials, or short-range order as in glassy or amorphous materials. This information is unique to individual structure (crystalline or amorphous) (Ivanisevic, *et al.*, 2010).

XRPD can also be employed to monitor re-crystallization of amorphous materials. A classic application of this technique would be to characterize the extent of crystallinity during storage over the intended shelf life of the drug product to ensure safety and efficacy (Ivanisevic, *et al.*, 2010). This is relevant for the stability of the two formulations of interest in this project, where all the model drugs initially added in crystalline forms, were converted to the amorphous form during film formation and freeze-drying.

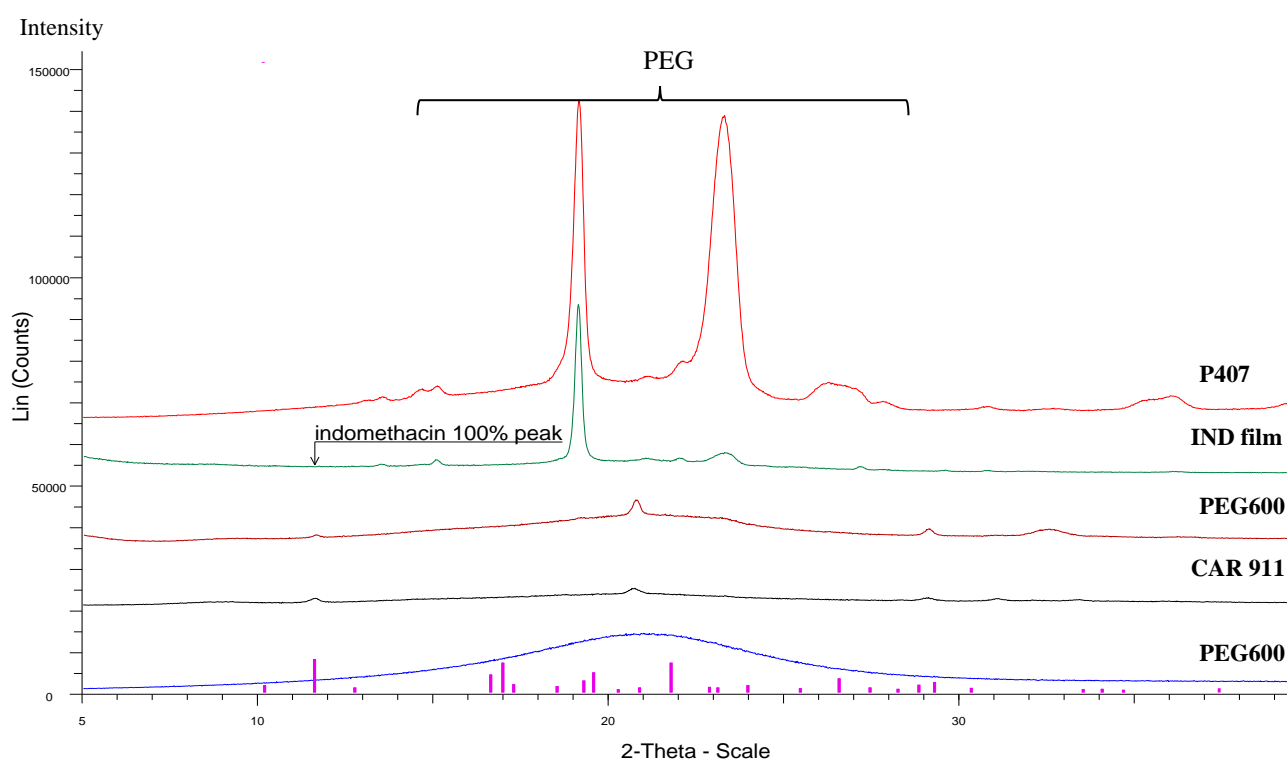


Figure 4.28 XRPD diffractogram of CAR 911, P407, PEG 600, blank and IND loaded films.

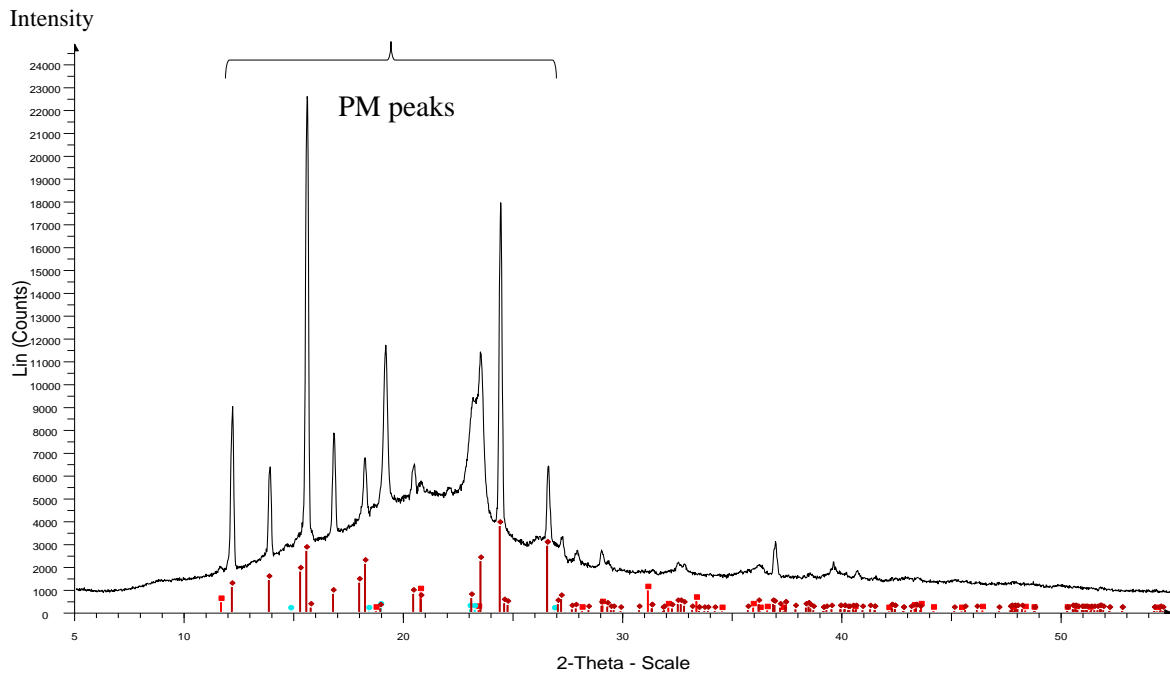


Figure 4.29 XRPD diffractogram of films containing excess amounts of PM.

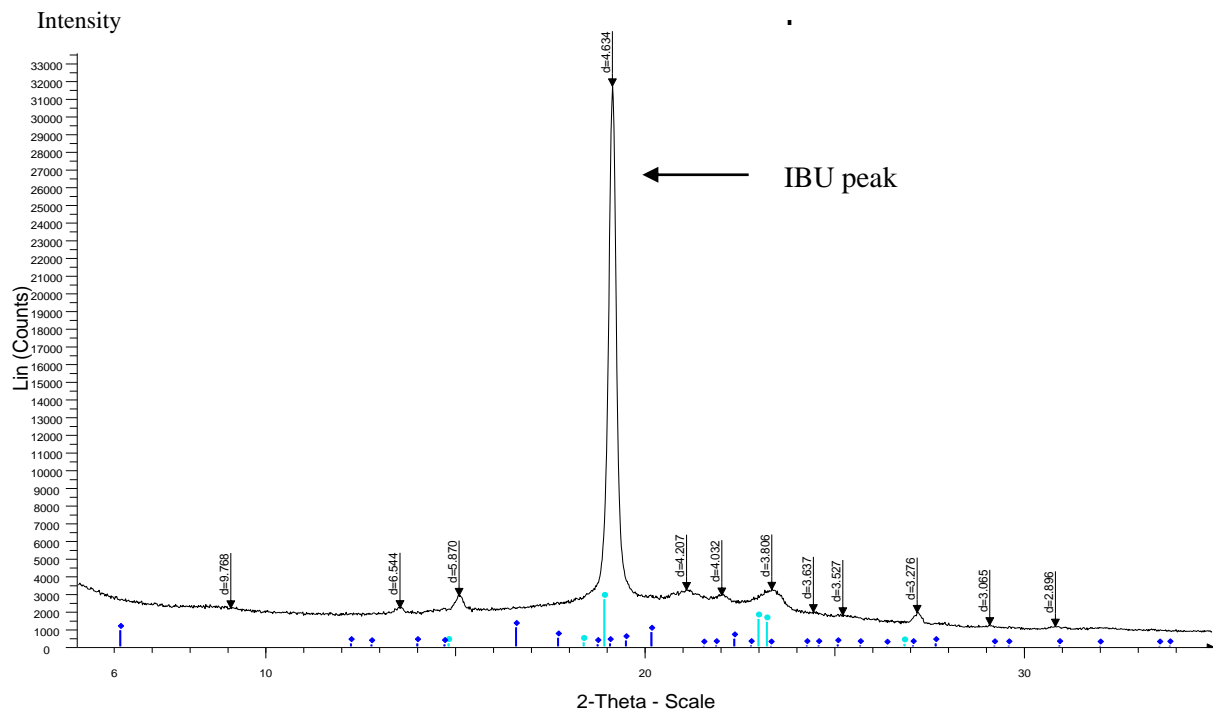


Figure 4.30 XRPD diffractogram of films containing excess amount of IBU.

XRPD analysis of films containing excess amounts of model drugs was performed and compared with previously discussed films containing only amorphous drug. The results showed that excess amount of drug recrystallized out of the film matrix. Consequently the

XRPD results showed significant differences with sharp peaks belonging to the re-crystallized model drugs for PM (Figure 4.29), IBU (Figure 4.30) or IND (Figure 4.31). As the thermodynamic energy of amorphous is significantly higher than crystalline form, they are more soluble hence, are expected to be released more rapidly when applied in-vivo. However it is important to be maintained in amorphous form since higher energy level in amorphous form may cause it to revert back to the crystalline form. Therefore, further XRPD studies were conducted to confirm the DSC results of films stored for 6 months at room temperature. As it was shown in DSC thermograms, film matrix maintained all three model drugs in amorphous form after storage period (the reproducible XRPD spectra can be found in the appendix and confirmed the film matrix's ability to retain model drugs in a stable amorphous form over six months (Figure 4.32, Figure 4.33 and Figure 4.34).

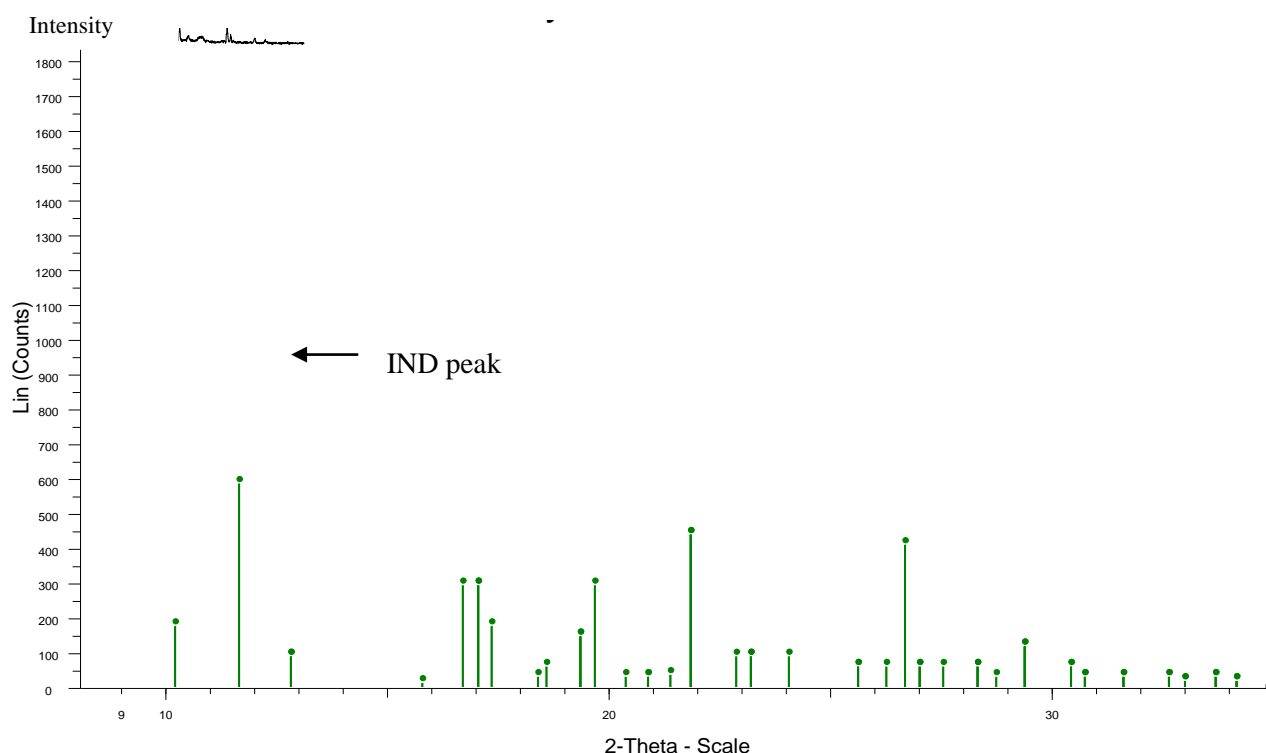


Figure 4.31 XRPD diffractogram of films containing excess amount of IND.

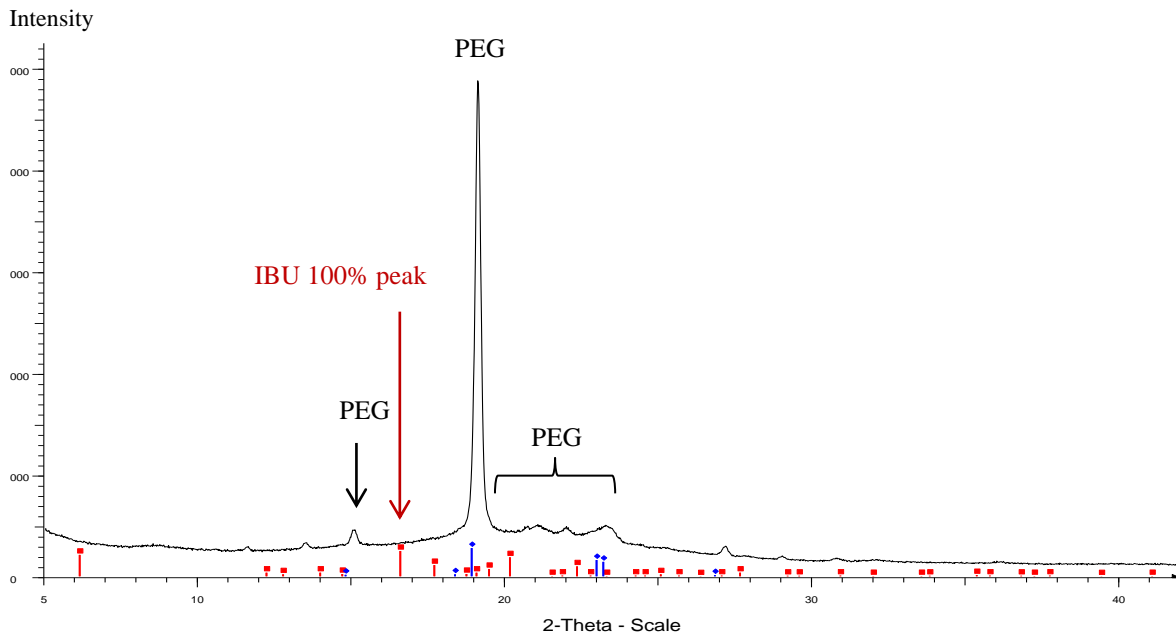


Figure 4.32 XRPD diffractogram for IBU loaded films stored for 6 months.

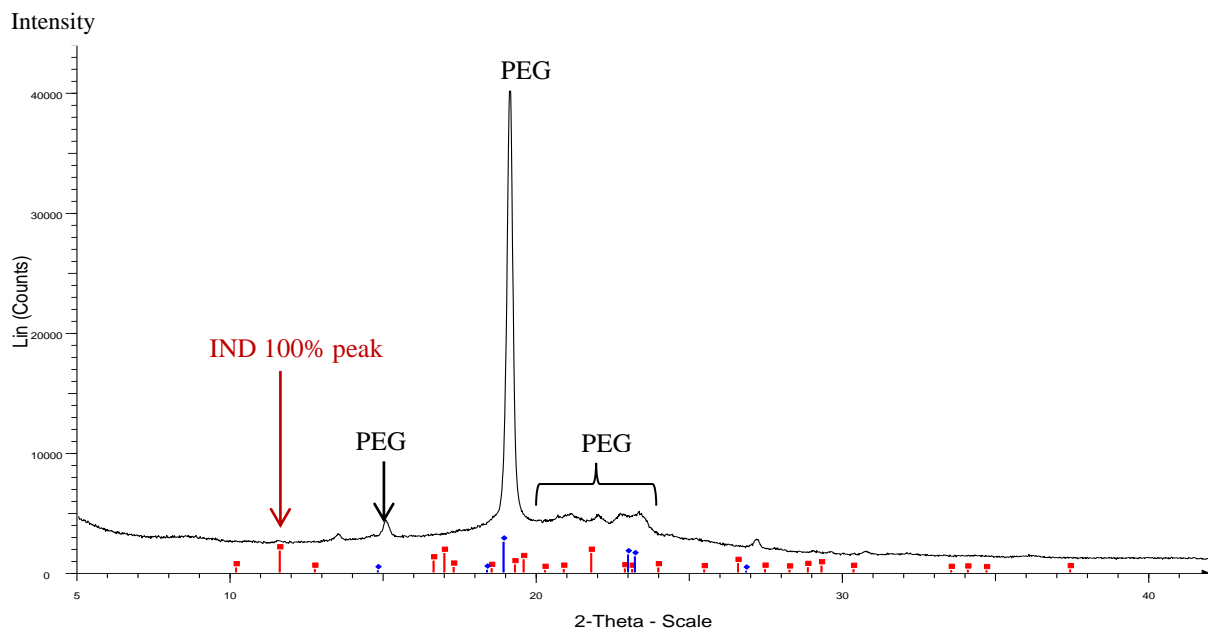


Figure 4.33 XRPD diffractogram for IND loaded films stored for 6 months.

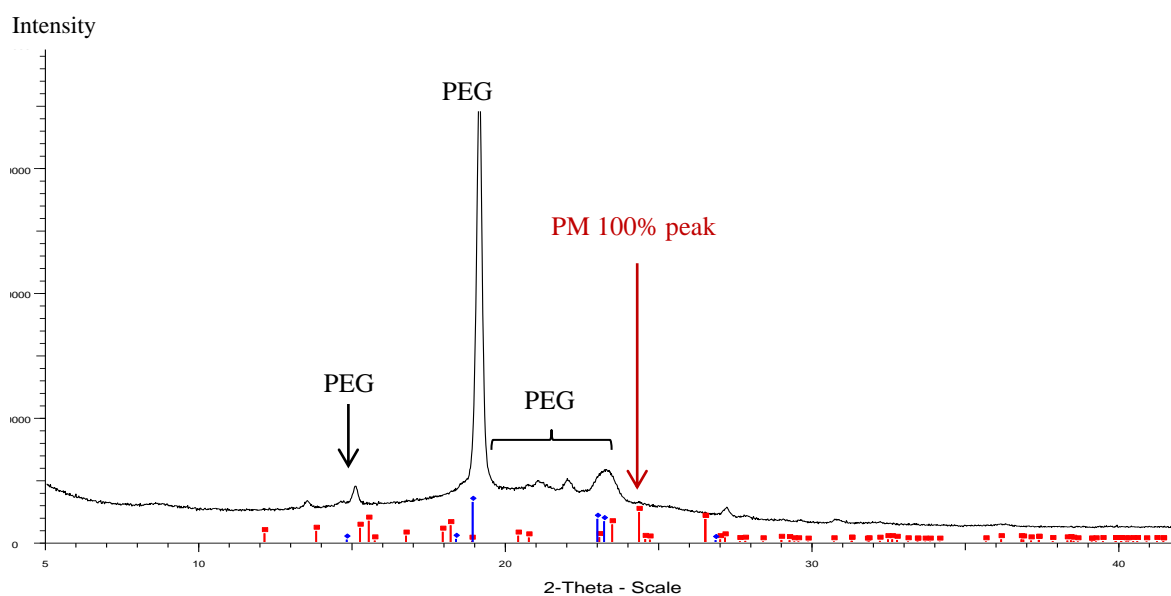


Figure 4.34 XRPD diffractogram for PM loaded films stored for 6 months.

4.2.7 Stability studies

HPLC results showed that the actual assayed concentration of IND, IBU and PM in the film sample remained relatively unchanged (>96%) after twelve month storage at room temperature and 45% RH (Figure 4.35).

The pure crystalline IBU, IND and PM used as control also remained stable over 12 months. Though this is highly desirable, longer term stability of model drugs within the films will need to be studied under accelerated conditions of higher temperature and relative humidity. Farmer and co-workers (2002) demonstrated that the degradation of IBU in bulk-drug samples ranged between 2.9 and 11.4% following storage at the higher temperature of 80°C. IBU degradation under high temperature conditions is likely given the alcohol functions present which could result in possible ester formation between PEG 600 and IBU. Cory, *et al.*, (2010) have shown previously that PEG enhances the degradation of IBU in tablets under accelerated conditions of 70°C and 75% RH and such studies will be required to confirm this in the films.

These results show the ability of CAR 911, P407 and PEG 600 based films to maintain the chemical stability of IBU, IND and PM. However, the stability studies over a longer period of time will need to be conducted.

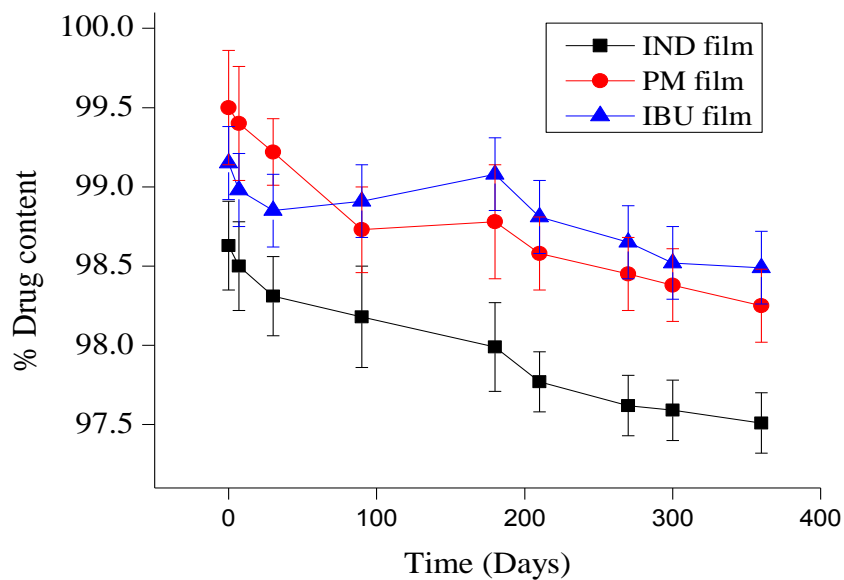


Figure 4.35 Plot showing the percentage of drug remaining within the films during storage at room temperature up to twelve months {mean \pm s.d. (n=3)}.

Chapter 5 : Lyophilized wafer development and characterisation

5.1 Formulation development

5.1.1 Gel formation

The initial studies during wafer formulation development involved the optimisation of gel formation, although the content of the starting materials and their characterisation were similar to the solvent cast films. This similarity allowed for a valid comparison of relevant characteristics such as dissolution, drug loading capacity, stability, hydration and tensile strength. However, due to the obvious differences between the freeze-dried wafers and solvent cast films, some of the physical evaluation and characterisation such as transparency and tensile elongation were not applicable to the wafers.

This exception allowed the formulation development of wafers with or without plasticizer as well as varying the amounts of CAR 911 to enable the formulation of optimised wafer suited for potential buccal drug delivery application.

5.1.2 DSC application to develop the freeze drying cycle

Establishing a suitable thermal profile for any gel for freeze drying was fundamental and helped to develop an optimized lyophilization cycle. Each individual formulation component (either active or excipients) demonstrated unique thermal properties within the formulation and it was critical to characterize each component separately as well as within the formulation. There are three critical parameters which need to be determined; eutectic temperature (T_{eu}), glass-transition temperature (T_g) and collapse temperature (T_c). T_{eu} defines the crystalline systems detectable by DSC and exceeding that during primary drying causes the compound to melt during processing. Generally, eutectic or glass-transition temperatures determine the maximum temperature that the formulated product can resist during primary drying without the loss of structure (Schwegman, 2009). Each formulation has a definitive collapse temperature, beyond the T_c point formulation might be unusable and experience processing defects.

Retaining the temperature below the critical limits before freezing or before the frozen water is removed is vital or the sample can be ruined during the process. Therefore, determination of the critical temperatures of a formulation before lyophilization is essential (McGinn, 2009).

In addition, following any of alteration either active ingredient or excipients or changing their constituent ratios, supportive DSC investigation was required to detect the critical points.

The eutectic point (T_{eu}) was observed at 12.8°C (Figure 5.1) for the initial gels with or without addition of model drugs.

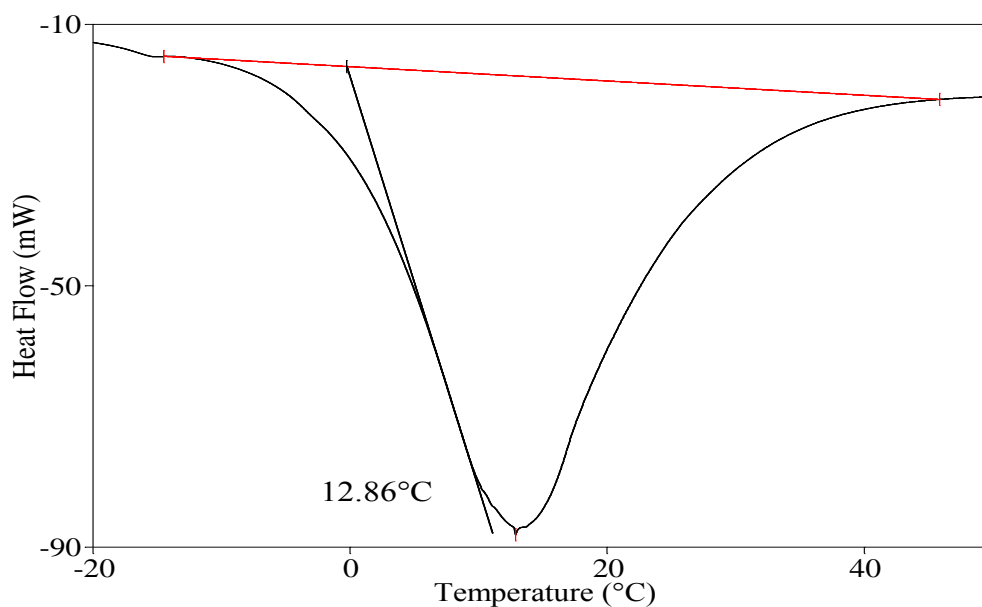


Figure 5.1 DSC results of the gel formulated with 2% w/w CAR 911 + 4% w/w P407 +4.4% w/w PEG 600.

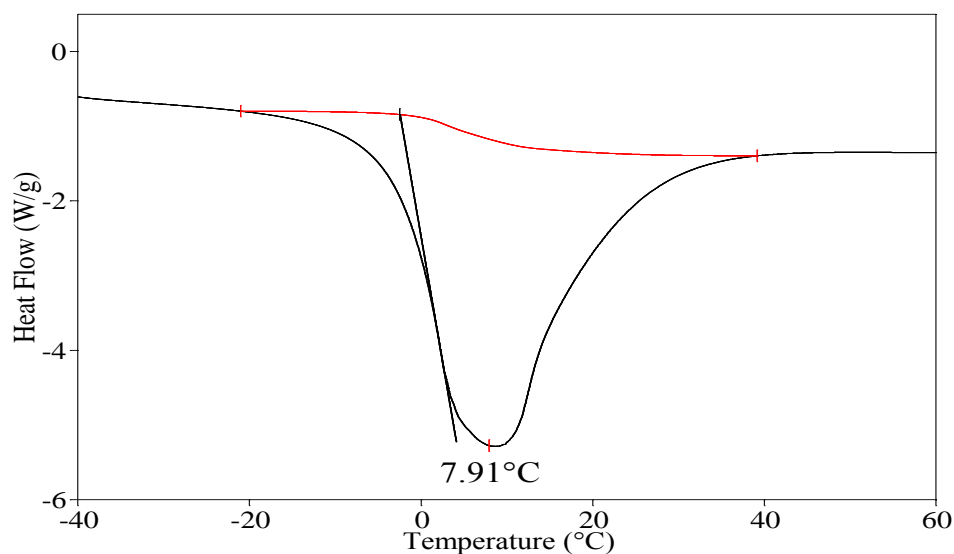


Figure 5.2 DSC results of the gel formulated with 2% w/w CAR 911 + 4% w/w P407 + 4.4% w/w PEG 600 + 0.6% w/w IBU .

Similar DSC results were obtained for IBU, IND and PM loaded wafers. Figure 5.2, Figure 5.3 and Figure 5.4 confirmed that the T_{eu} for all of formulations were close and increasing the temperature up to 0°C during the primary drying was feasible for producing ideal wafers. As a result, it was not deemed necessary to change the freeze drying cycle between blank and each drug loaded wafer.

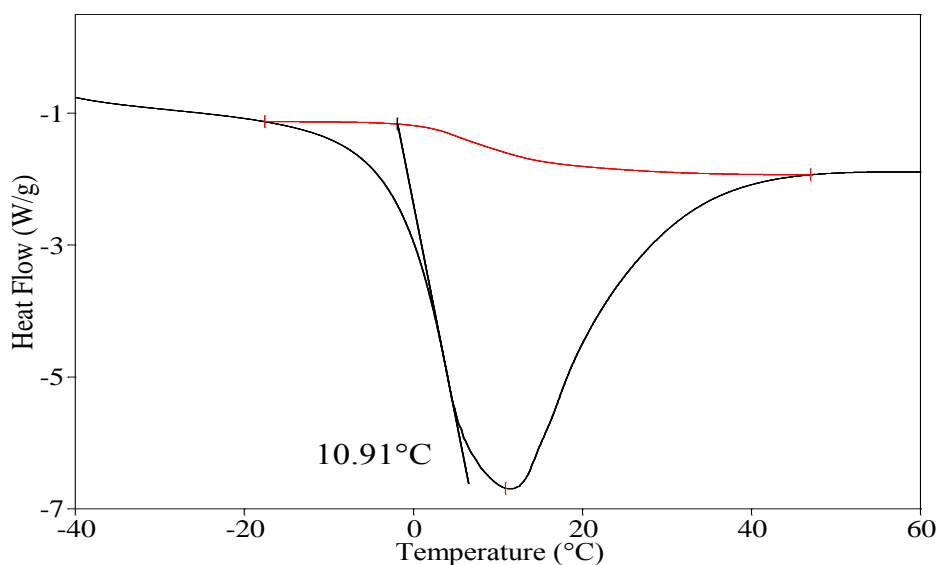


Figure 5.3 DSC results of the gel formulated with 2% w/w CAR 911 + 4% w/w P407 + 4.4% w/w PEG 600 + 1.8% w/w PM.

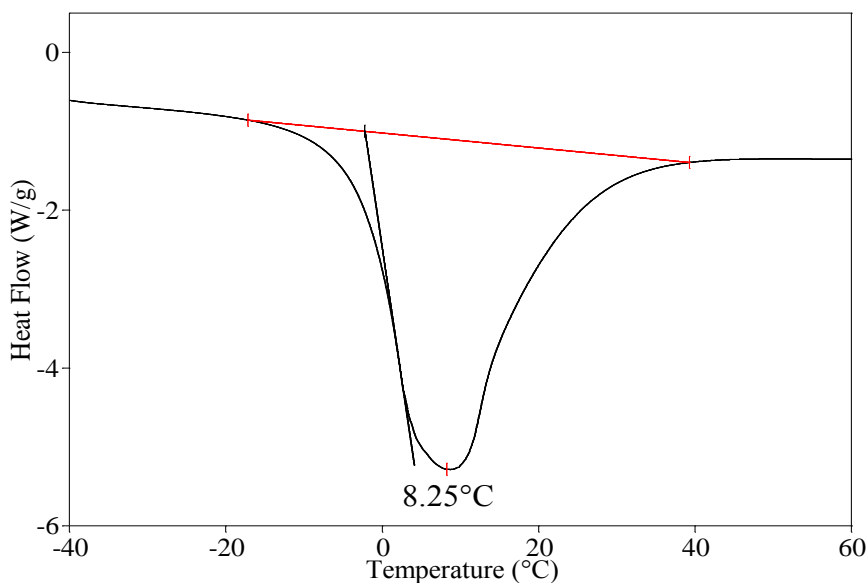


Figure 5.4 DSC results of the gel formulated with 2% w/w CAR 911 + 4% w/w P407 + 4.4% w/w PEG 600 + 0.6% w/w IND.

5.1.3 Freeze-drying process

Following the gel preparation they were dispensed into suitable containers. The ideal container must be stable during the freeze drying process and result in the gel setting with uniform thickness and surface area to allow rapid removal of water during sublimation. The resulting wafer should also be easily recovered from the container without sticking to it which could cause loss of material. Therefore, gels were poured into six-well polystyrene plates with diameter 0.354 mm and filled to a height of 1mm.

Freeze drying cycles:

(i) Freezing or freeze-annealing:

The freezing cycle was performed initially as simple freezing which was conducted by freezing the gel up to -55°C and kept for 96 hours with primary drying step following immediately after freezing. The resultant wafers were not adequately dried with several traces of trapped ice visibly present on the surface (Figure 5.5). Therefore, an annealing step was added to the cycle to produce bigger ice crystals to allow the sublimation to proceed more efficiently.

Two different annealing steps were attempted. The step which was performed by cooling the gel initially to -35°C following a temperature rise to -10°C resulted in wafers with unacceptable physical characteristics due to melt back which caused a collapse in the wafer's structure (Figure 5.6).

However, gels which were cooled down to -55°C and annealed by increasing the temperature to -35°C and cooling back to -55°C produced wafers with an acceptable texture and physical properties i.e. flexibility, porous texture, without any trace of ice crystals (Figure 5.7). Noticeably, the pressure condition was critical during the whole freeze-drying process and was maintained at 200 mTorr during the freezing and 50 mTorr during the drying stages as the pressure of environment should be higher than the pressure in the frozen gel. This results in sublimation of the ice crystals from the surface of the frozen gel.

(ii) Primary drying

The primary drying process was conducted by gradual temperature elevation from -10°C to 0°C which is at least 5°C less than the T_{eu} (determined from the preliminary DSC studies) while the appropriate pressure condition was applied which resulted in significant reduction in water content.

(iii) Secondary drying

During secondary drying desorption occurred and the last traces of water vapour were removed. This stage of freeze drying provided heat to maintain the wafers at ambient temperature and produce wafers with desirable texture and stability during storage. Overall, the optimised freeze-drying cycle incorporating the annealing step totalled 42 hours and produced wafers with a balance between flexibility and residual water content.

The results from the optimised freeze-dried process ascertained the necessity to establish an ideal combination of shelf temperature and system vacuum level during each process stage (freezing, primary and secondary drying). This culminates in the appropriate vapour pressure for ice sublimation and ideal sample temperature.

During each step, the sample temperature was monitored by thermocouples while shelf temperature was increased to achieve the target sample temperature. If the gel has high resistance to vapour flow in the dried section of the cake, the shelf temperature should be elevated towards the end of primary drying to maintain the wafer temperature at target point and prevent it from collapsing (www.biopharma.co.uk- date accessed 20/06/2011).

5.1.4 Results after freeze-drying

Following freeze-drying the water content should be typically between 0.5% and 3%. Subsequently, the optimised wafers were selected with the aid of visual observations and analytical techniques such as SEM, compression profile and mucoadhesivity (www.biopharma.co.uk- date accessed 20/06/2011).

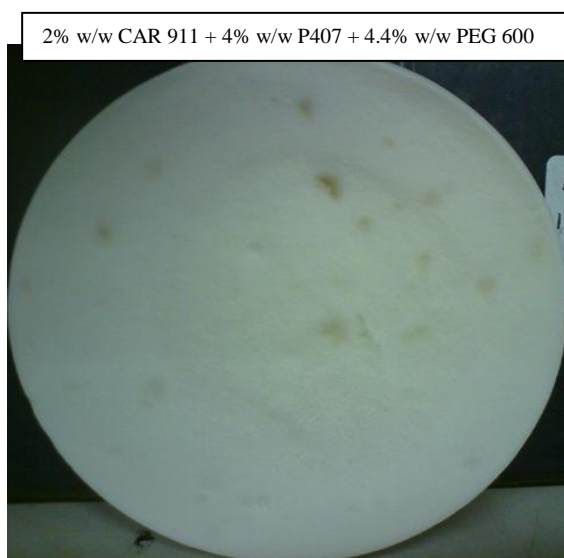


Figure 5.5 Wafer prepared without annealing.



Figure 5.6 Wafer prepared by non-appropriate annealing cycle.

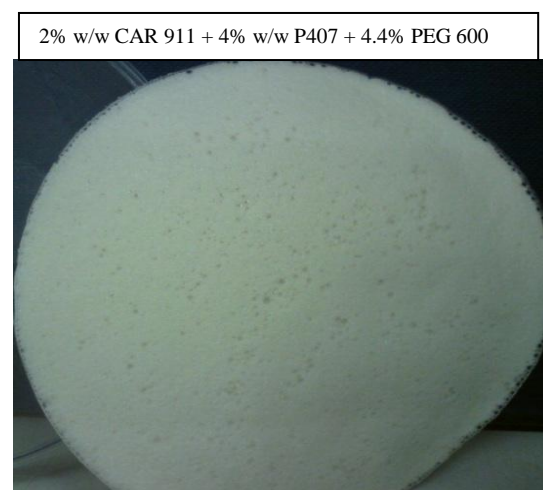


Figure 5.7 Wafer prepared by the appropriate annealing method.

5.1.5 Visual evaluation of wafers

The preliminary observations were performed and the results obtained are summarized in Table 5.1 however, this was the first stage and further investigations were required. Evaluation of wafers was based on criteria such as:

- ❖ Softness: wafers must be soft and easy to apply on the mucosal tissues.
- ❖ Plasticity: the wafer should not be brittle and fragile as it will affect physical and mechanical stability during handling as well as potential contact irritation during application.

- ❖ **Thickness:** Ideal wafer must have optimum thickness (less than 2cm pre-hydration) otherwise it might not be convenient for patient to apply in buccal mucosal area. This will provide the stability to be placed at buccal surfaces and prolong the residence time. Thick wafers present the possibility of inconvenience from teeth movement and dislodging by tongue movement. In addition, thickness affects the drug release rate since wafer forms gel following hydration and drug diffusion distance has significant effect on drug release profile.

Table 5.1 Characteristic of wafers prepared using different (% w/w) concentrations of PEG 600, CAR 911 and 4% w/w P407.

CAR 911% (w/w)	P407% (w/w)	PEG 600% (w/w)	Wafer characteristics
5.0	4	0	Rough & brittle
2.0	4	0	Rough & brittle
2.5	4	0	Rough & brittle
1.5	4	3.3	Soft, flexible
2.0	4	4.4	Soft, flexible
2.5	4	5.5	Soft, flexible
1.5	4	5.5	Soft, flexible
2.0	4	5.5	Soft, flexible
2.5	4	5.5	Soft, flexible

Formulating wafers with varying amounts of PEG 600 and CAR 911 with or without annealing and evaluating according to the above criteria was conducted. Afterward, additional texture analysis studies were performed to determine the physical properties and select the optimum wafers with appropriate flexibility. Results from the wafers produced with non-annealing cycle didn't demonstrate acceptable parameters during the initial observations due to excessive brittleness which was confirmed by the texture analysis results as well (Figure 5.5 and Figure 5.10).

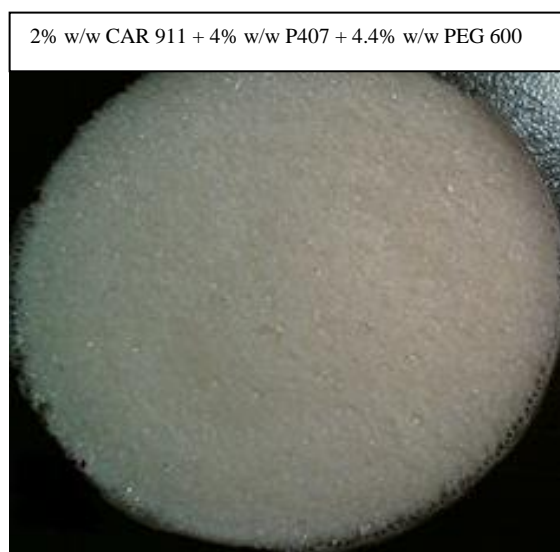


Figure 5.8 Optimized wafer produced with appropriate contents of CAR 911, P407, PEG 600 with annealing method.

5.2 Wafer characterisation

5.2.1 Texture analysis results

Following the development of different wafers by annealing and non-annealing process, texture analysis studies were performed. All wafers were compressed to the depth of 2 mm and the work of compression and peak force at maximum depth of compression were measured. There were two sets of experiments performed to determine the optimum amounts of each starting material used to formulate the wafers.

The preliminary evaluation involved texture analysis of wafers containing different amounts of CAR 911 with or without PEG 600 to determine effect on mechanical strength. The second evaluation involved the effect of the annealing process on textural (mechanical) characteristics of the wafers. Results in Figure 5.9 show that wafers formulated without PEG 600 were very rigid with very high work of compression and peak compression force values. In addition, according to Figure 5.10 the non-annealed wafers didn't compress appropriately upon application of force due to non-porous texture.

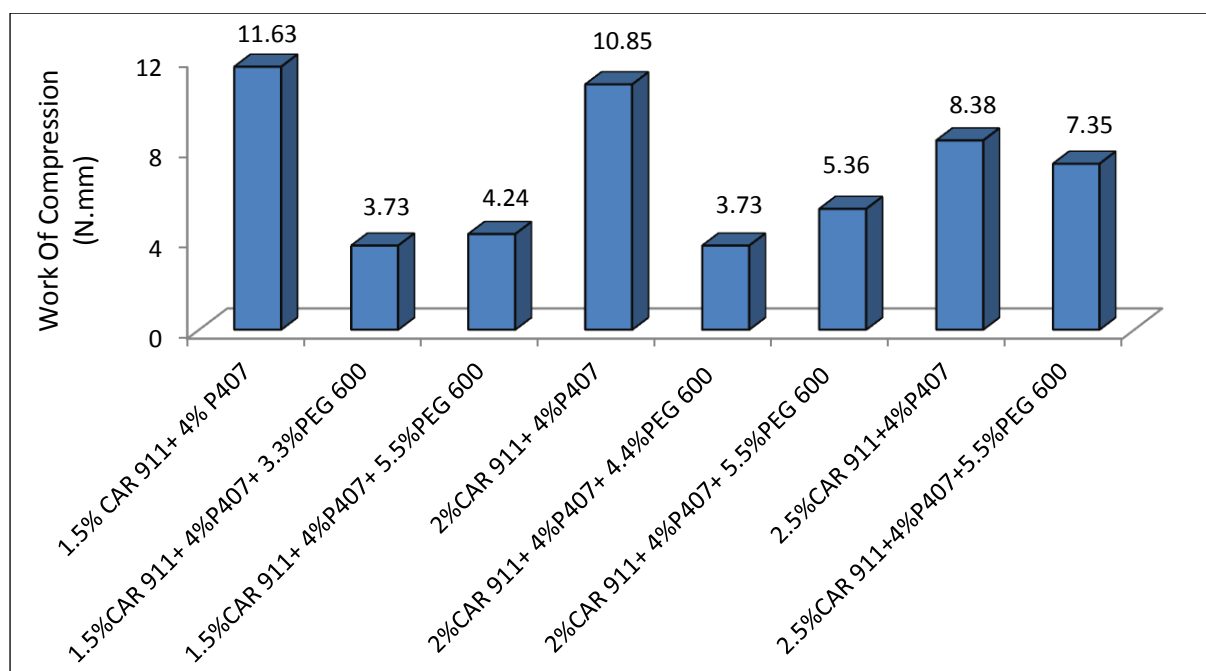


Figure 5.9 Compression profiles for wafers formulated with various amounts of initial compounds {mean \pm s.d. (n=3)} .

Therefore, addition of PEG 600 and developing wafers by freeze-drying with an annealing step significantly impacted upon the mechanical strength of the wafers. The investigations showed that wafers containing 2% w/w CAR 911, 4% w/w P407 and 4.4% w/w PEG 600 exhibited the most optimum mechanical strength (Figure 5.9) while the other wafers were very brittle and rigid. Although wafers prepared with 1.5% w/w CAR 911, 4% w/w P407 and 3.3% w/w PEG 600 showed similar compression profiles, the comparison of other properties such as hydration, mucoadhesion and water content confirmed that the wafers containing 2% w/w CAR 911 and 4.4% PEG 600 as the most appropriate choice.

Figure 5.10 show that addition of IBU increased the wafers' work of compression (De Brabander, 2002) while adding PM decreased this value to approximately half that of IBU loaded wafers, and also lower than the blank wafer. The similar decrease in work of compression was observed when IND was used. These results combined with SEM observations showing that addition of PM and IND decreased mechanical strength owing possibly to formation of polymeric matrix with lower porosity. To evaluate whether

increasing the concentration of PEG 600 (4.4%, 5% and 5.5% w/w) improved the compressibility a new set of experiments were conducted. According to the results shown in Table 5.2 addition of PEG 600 did not have a significant effect on compression profiles of the wafers loaded with IND or PM. Consequently, 4.4% (w/w) of PEG 600 was selected to formulate drug loaded wafers.

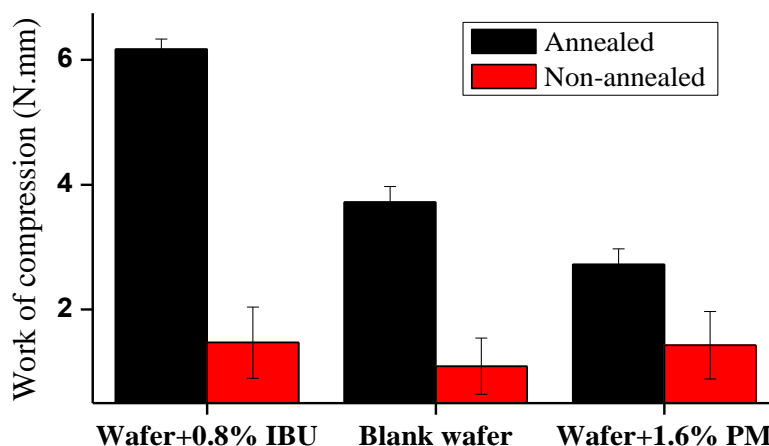


Figure 5.10 Work of compression of wafer produced using 2% CAR w/w 911, 4% w/w P407 + 4.4% w/w PEG 600 {mean \pm s.d. (n=3)}.

Table 5.2 Work of compression (WOC) and peak compression force (CF) of the wafer's produced from (% w/w) concentration of CAR 911, P407 and various concentrations (w/w) of drugs {mean \pm s.d. (n=3)}.

Wafer composition	WOC (N.mm)	CF (N)
2% CAR 911 + 4% P407+ 4.4% PEG 600 + 0.6% IND	3.6 \pm 0.2	3.6 \pm 0.3
2% CAR 911+ 4% P407+ 5% PEG 600 + 0.6% IND	2.1 \pm 0.4	2.3 \pm 0.6
2% CAR 911+ 4% P407+ 5.5% PEG 600 + 0.6% IND	2.5 \pm 0.3	2.0 \pm 0.3
2% CAR 911+ 4% P407+ 4.4% PEG 600 + 1.8% PM	3.4 \pm 0.3	4.5 \pm 0.2
2% CAR 911+ 4% P407 + 5% PEG 600 + 1.8% PM	3.5 \pm 0.5	3.4 \pm 0.3
2% CAR 911+ 4% P407 + 5.5% PEG 600 + 1.8% PM	2.9 \pm 0.2	3.1 \pm 0.2

Further, the compression profiles of the wafers in the presence of 4.4% PEG 600 and containing IBU showed improvement in mechanical strength. Loading IND and PM into the wafers decreased the work of compression and higher levels of PEG 600 also did not present acceptable compression profile therefore PEG 600 at 4.4% w/w within the gel for all pure and drug loaded wafers was the concentration of choice.

Table 5.3 Work of compression (WOC) and compression force (CF) of the wafers produced from (% w/w) concentration of CAR 911, P407 and various amount of drugs {mean \pm s.d. (n=3)}.

Wafer composition	WOC (N.mm)	CF (N)
2% CAR 911 + 4% P407+ 4.4% PEG 600 + 0.6% IND	3.6 \pm 0.4	3.6 \pm 0.3
2% CAR 911 + 4% P407+ 4.4% PEG 600 + 0.6% IBU	6.5 \pm 0.2	6.6 \pm 0.4
2% CAR 911 + 4% P407+ 4.4% PEG 600 + 0.8% IBU	6.7 \pm 0.4	6.8 \pm 0.2
2% CAR 911 + 4% P407+ 4.4% PEG 600 + 1.8% PM	3.4 \pm 0.3	4.5 \pm 0.2

Therefore, it was concluded that the wafer with most appropriate mechanical strength was produced following the addition of 0.8% w/w IBU, 0.6% w/w IND or 1.8% w/w PM to the gel comprising 2% w/w CAR 911, 4% w/w P407 and 4.4% w/w PEG 600. The percent drug loading as a function of the total dry weight of the wafers are summarised below.

- Indomethacin (IND) = 5.45 %
- Ibuprofen (IBU) = 7.14 %
- Paracetamol (PM) = 14.40

When compared with the corresponding films, it can be seen that the porous wafers exhibited higher drug loading capacities compared to the dense films. This was attributed to the differences in physical structure of the two formulations with the wafers maintaining the original volume of the initial gel due to the freezing stage with drug uniformly distributed

while the films were formed after collapse of the initial gel during drying, hence excess drug crystallise onto the surface which was undesirable (Boateng *et al.*, 2010).

5.2.2 TGA results (water content)

The residual water within the wafers produced either by annealing or non-annealing process was determined by TGA. The water content of each individual wafer analysed by TGA is summarised in Table 5.4 and Table 5.5.

The water content was considerably higher in non-annealed wafers which consequently could have an undesirable effect on the stability of incorporated drugs. There is a potential risk that residual water may act as seeds to initiate and accelerate the crystallization of amorphous drug during storage. Water is a very effective plasticizer which significantly depresses the T_g of the amorphous drug and excipients by increasing molecular mobility which results in instability (Passerini and Craig, 2001). Therefore, it has been confirmed again that annealing is a desirable process to develop and produce wafers with appropriate stability due to lower residual water content.

Furthermore, the results show that increasing the CAR 911 content resulted in an increase in water content and similar trends were observed following the addition of PEG 600 to the formulation. However, the presence of PEG 600 was essential to achieve desirable flexibility in the wafers.

Wafers prepared from 2% w/w CAR 911, 4% w/w P407 and 4.4% w/w PEG 600 retained the lowest amount of water and provides a greater likelihood of maintaining drug stability over a longer period and was therefore the formulation of choice for drug loading. The water content of drug (IND, IBU and PM) loaded wafers were measured in two different time periods: immediately after completion of the freeze-drying cycle and then after one month storage in a desiccator at room temperature and relative humidity of 10%.

Table 5.4 % Water content for wafers produced from concentrations (% w/w) of CAR 911, P407 and PEG 600 by annealing and non-annealing process {mean \pm s.d, (n=3)}.

Freeze-dried wafer	Annealed	Non-annealed
1.5% CAR 911 +4% P407+ 5.5% PEG600	2.1 \pm 1.2	5.3 \pm 1.3
1.5% CAR 911 + 4% P407	0.7 \pm 0.0	4.7 \pm 0.6
1.5% CAR 911 +4% P407+ 3.3% PEG 600	2.2 \pm 1.0	4.3 \pm 0.8
2% CAR 911 + 4% P407	1.5 \pm 1.4	4.7 \pm 1.2
2% CAR 911 + 4% P407+ 4.4% PEG 600	1.2 \pm 0.5	5.3 \pm 0.5
2% CAR 911+ 4% P407 + 5.5% PEG 600	2.5 \pm 1.0	5.4 \pm 0.5
2.5% CAR 911 + 4% P407	1.4 \pm 0.0	4.5 \pm 0.3
2.5% CAR 911 + 4% P407 + 5.5% PEG 600	1.8 \pm 0.1	5.8 \pm 0.3

TGA results for the wafers before and after loading IND, IBU or PM are presented in Table 5.5. The results demonstrate that addition of model drugs has significant effect on residual water content in the wafer. All model drugs (IND, IBU and PM) are dispersed in the hydrogel (CAR 911) matrix through possible interaction by hydrogen bonding. Therefore, hydroxyl groups of the polymer are occupied by model drug molecules and less water would be retained within the polymeric matrix. This effect on the results of the water content is summarized in Table 5.5.

Table 5.5 Water content in the wafers formulated with different concentrations (% w/w) of the various drugs and initial compound either immediately (IM) after freeze-drying or after one month of storage {mean \pm s.d (n=3)}.

Freeze-dried wafer	%H ₂ O content	% H ₂ O content
	(IM)	(1 month storage)
2% CAR 911+ 4% P407+ 4.4 % PEG 600	1.5 \pm 0.1	1.5 \pm 0.3
2% CAR 911+ 4% P407 4.4 % PEG 600 + 1.8% PM	0.9 \pm 0.0	1.9 \pm 0.1
2% CAR 911 + 4% P407 +4.4 % PEG 600 + 0.8% IBU	1.1 \pm 0.2	1.4 \pm 0.3
2% CAR 911 + 4% P407+4.4 % PEG 600 + 0.6% IND	0.8 \pm 0.2	1.2 \pm 0.1

According to the results the amount of residual water was reduced considerably due to addition of IND and PM while IBU loaded wafers showed higher water content. Wu and McGinity (2001) have shown that T_g of the polymers would be decreased due to the presence of IBU within the polymeric wafer though their study was based on solid dispersion of IBU in polymeric matrix. This effect might be a consequence of retaining more water in the wafer matrix which has been confirmed by the TGA results and previous texture analysis data.

5.2.3 DSC results

The thermodynamic characteristics of CAR 911, P407, PEG 600 and various model drugs (IND, IBU, PM) were conducted. The DSC results for the blank and drug loaded wafers demonstrated that all the model drugs were in amorphous form as was observed for the films. Figure 5.11 shows the DSC results for the blank wafer showing the sharp melting point of PEG 600, P407 and the mixture of PEG 600/P407 at about -4.4, 24.5 and 38.5°C respectively.

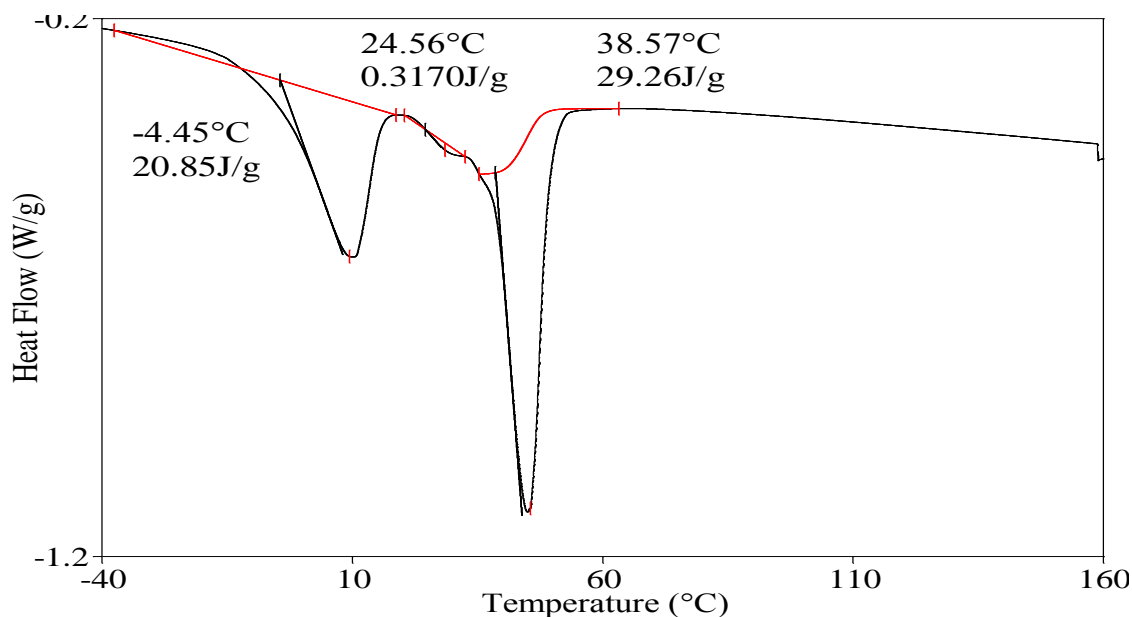


Figure 5.11 DSC results of wafer comprising 2% w/w CAR 911 + 4% w/w P407 + 4.4% w/w PEG 600.

An extensive DSC investigation and comparison between Figure 4.12(a & b) with Figure 5.12 proved that IBU in the wafer was in amorphous form. Reference to Figure 4.12 (a & b) DSC analysis of pure IBU showed that during the first heating cycle a sharp melting transition was detected at 77.7°C and following the sharp cooling glass transition of the amorphous was detected at -45.2°C though this transition was shifted to -59.0°C within the wafer. Figure 5.12a also showed three sharp peaks (-2.4°C, 31.4°C and 39.6°C) corresponding to PEG 600, P407 and the mixture of these two polymers respectively and the lack of IBU melting transition.

Figure 5.12b shows the DSC thermogram of IBU loaded wafer after six months storage. These reproducible results compared with the freshly prepare wafer's (Figure 5.12a) thermogram confirmed that the drug was maintained in amorphous form after six month storage in room temperature and 45% RH.

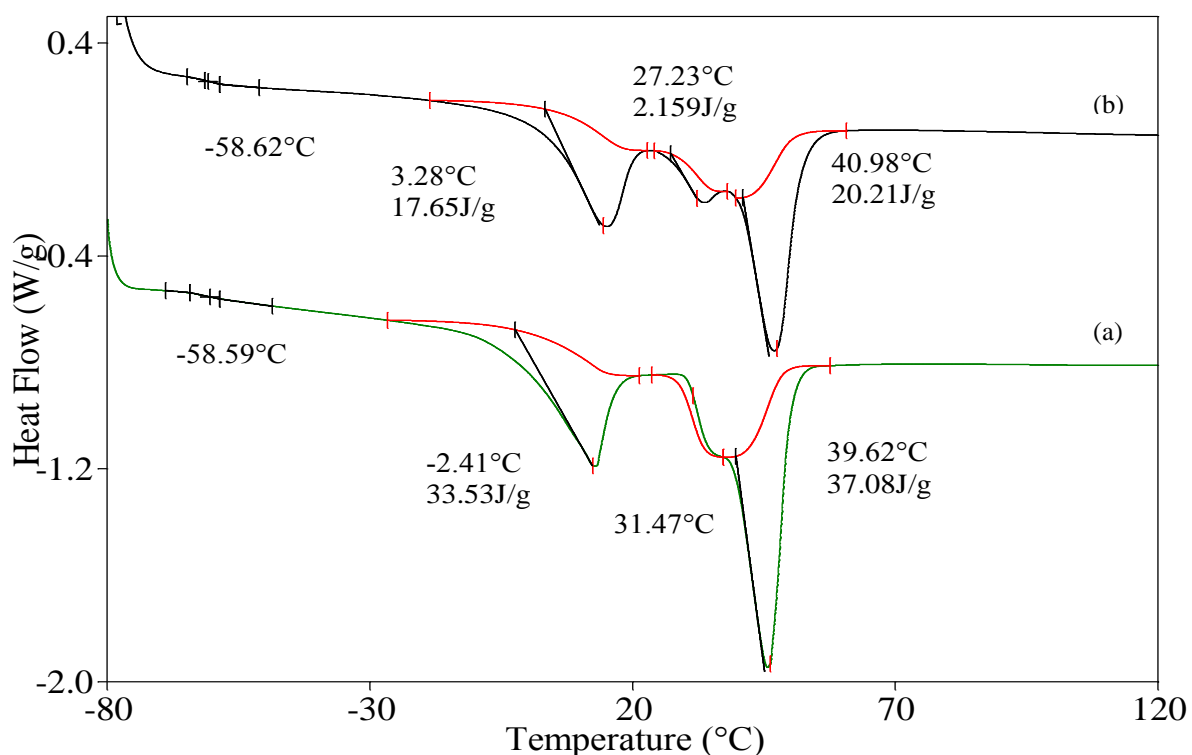


Figure 5.12 DSC results for (a) fresh wafer prepared from gels containing of 2% w/w CAR+ 4% w/w P407+ 4.4% w/w PEG 600 and 0.8% w/w IBU in the initial gel and (b) wafer prepared from gel containing 0.8% w/w IBU after six month's storage.

Comparable results were observed with the thermograms of pure IND and within the wafers. From Figure 4.14a & b DSC thermogram of pure crystalline IND demonstrates melting transition at 161.0°C and glass transition after quench cooling at 40.2°C. Additional studies were performed to investigate the stability of amorphous model drugs (whether recrystallization to the crystalline could occur). DSC results for IND loaded wafers showed three sharp peaks at 8.2°C, 44.2°C and 32.6°C corresponding to PEG 600, P407 and mixture of the two polymers (Figure 5.13).

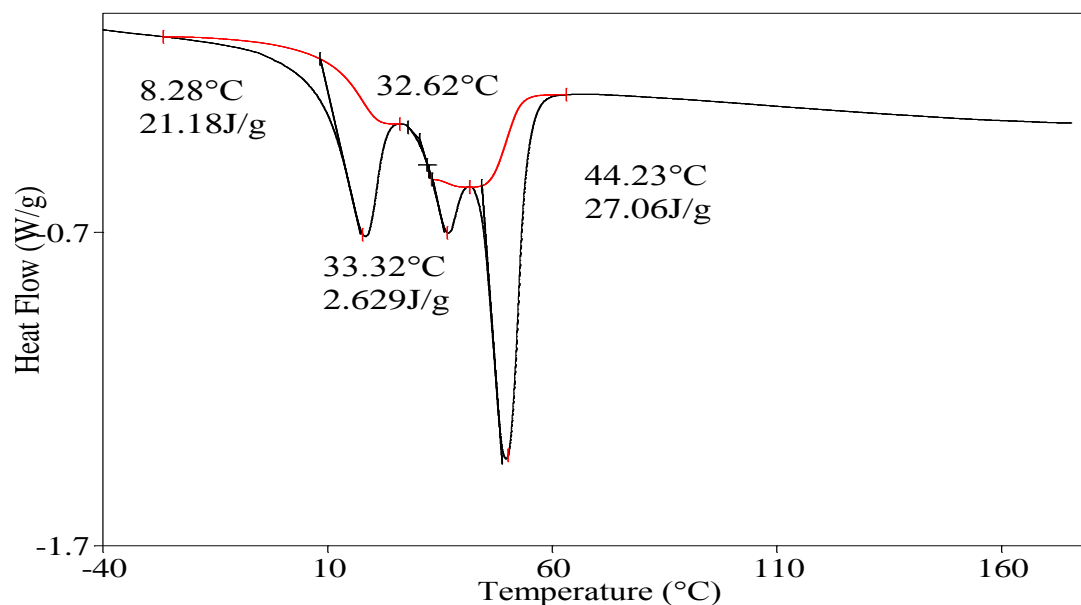


Figure 5.13 DSC results for wafer comprising 2.5% w/w CAR 911+ 4% w/w P407 + 4.4% w/w PEG and 0.6% w/w IND in the initial gel.

Similarly, pure PM showed a sharp melting peak at 169.0°C in the first heating cycle. During the sharp cooling, the crystalline drug was changed to amorphous form (Qi, et al., 2008). However, amorphous form is unstable and recrystallized at 80°C. The PM, T_g was detected at 21.8°C and a sharp melting peak confirmed the recrystallization process (Figure 4.16). This result was compared with thermogram of the PM loaded wafer and showed a stable amorphous form of PM in the wafer with glass transition at 21.7°C with the absence of the expected melt peaks 157°C (orthorhombic polymorph) and 169°C (monoclinic) confirmed the existence of amorphous form of the drug in the wafer (Figure 5.14). The most interesting results is the absence of the melting transition of mixture of PEG 600/P407 in PM loaded wafers.

As mentioned before, the presence of water in the system has a significant effect on interaction between PEG 600 and P407. As the PM molecules compete with water molecule to interact with CAR 911 through hydrogen bonds; this is possible given the higher amounts of PM within the polymeric matrix is compared with IBU and IND loaded wafers where the lower water content limited the interaction of PEG 600 and P407. Reproducible results similar to that observed for IBU loaded wafer (fresh and after six months storage) were also obtained for IND and PM loaded wafers.

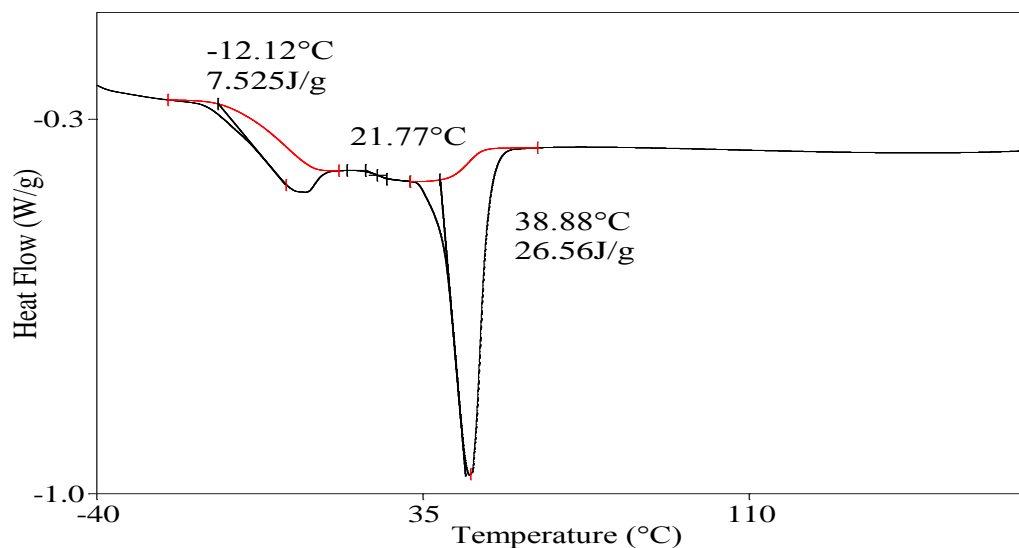


Figure 5.14 DSC results for wafer containing 2.5% w/w CAR 911+ 4% w/w P407+ 4.4% w/w PEG 600 and 1.8% w/w PM in initial gel.

5.2.4 SEM results

Scanning electron microscopy was performed to evaluate the morphology of freeze-dried wafer at the microscopic level. The topographic image of all of the wafers with various compositions of CAR 911, P407 with or without the presence of the PEG 600 showed a porous texture. Interestingly, the relative size of the pores relatively depends on the content of the CAR 911 while their uniformity of pore distribution correlated with the presence of PEG 600. According to the SEM results for the non-drug-loaded wafer (Figure 5.15- Figure 5.20) increasing the ratio of CAR 911 caused an increase in the size of the pores. Larger pore and free spaces can be occupied by higher amounts of drugs and water and consequently affect the release of drugs during dissolution studies.

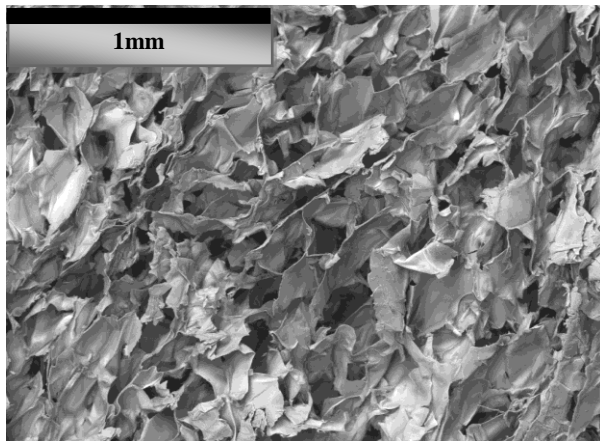


Figure 5.15 Wafer comprising 1.5% w/w CAR 911+ 4% w/w P407.

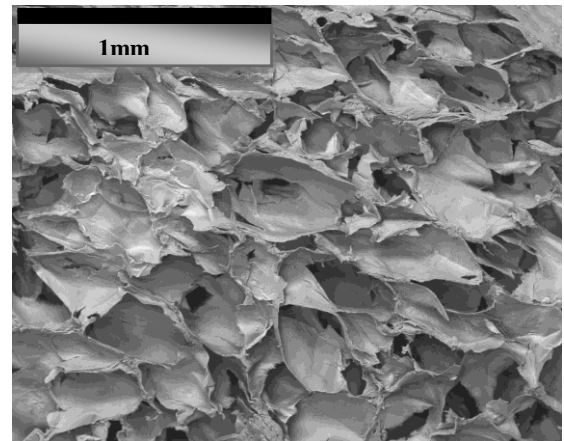


Figure 5.16 Wafer comprising 1.5% w/w CAR 911 +4% w/w P407 +3.3% w/w PEG 600.

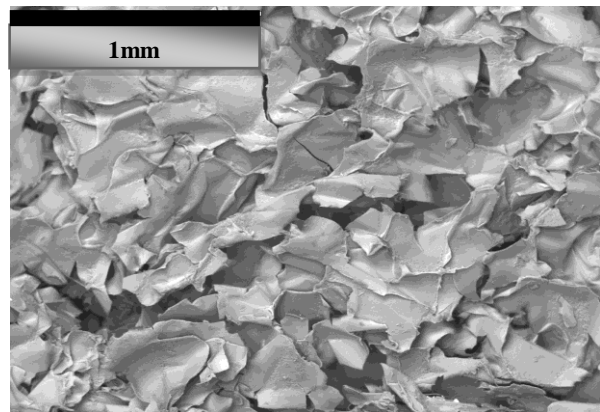


Figure 5.17 SEM of wafer comprising 2% w/w CAR 911+ 4% w/w P407.

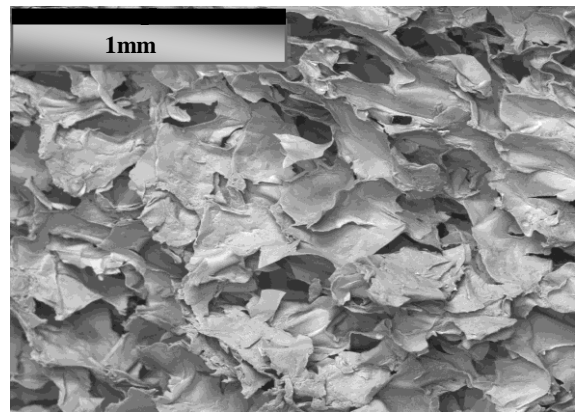


Figure 5.18 SEM of wafer comprising 2% w/w CAR 911+ 4% w/w P407+4.4% w/w PEG 600.

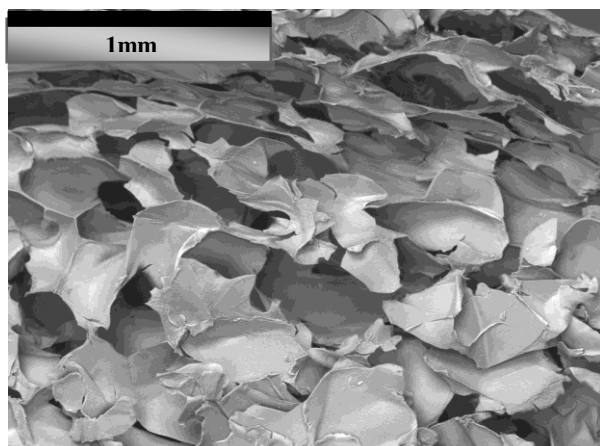


Figure 5.19 SEM of wafer comprising 2.5% CAR 911 + 4% P407.

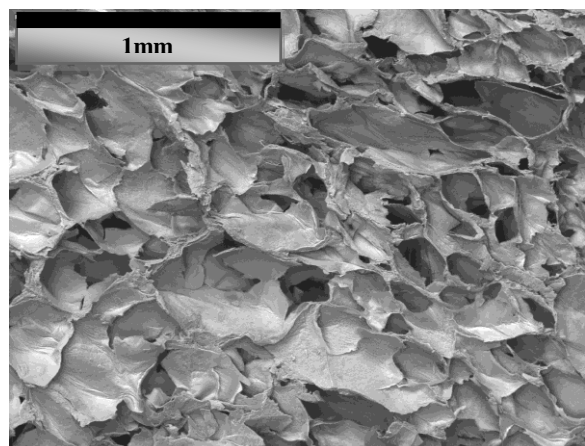


Figure 5.20 SEM of wafer comprising 2.5 % CAR 911+ 4% P407 +5.5% PEG 600.

This could be attributed to the increase in water ingress expected for wafers having larger pore. However, this is also dependent on the amounts of PEG 600 present as wafers with higher amounts of the hydrogel CAR 911 are expected to swell more slowly.

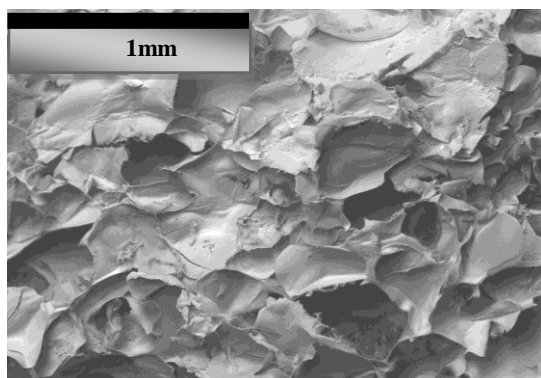


Figure 5.21 Wafer comprising 2 % CAR w/w 911 + 4% w/w P407 +4.4% w/w PEG 600.

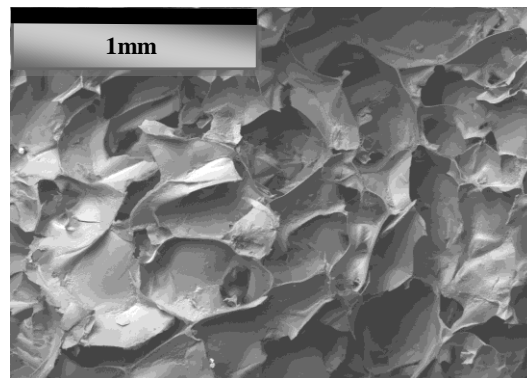


Figure 5.23 Wafers comprising 2% w/w CAR 911 +4% w/w P407+4.4% w/w PEG600+ 0.6% w/w IND.

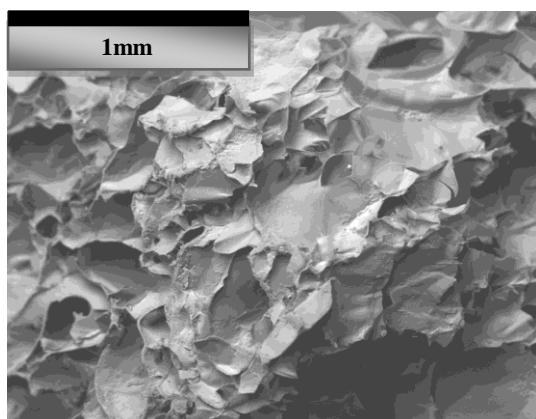


Figure 5.22 Wafer comprising 2% w/w CAR 911+ 4% w/w P407 + 4.4% w/w PEG 600+ 0.8% w/w IBU.

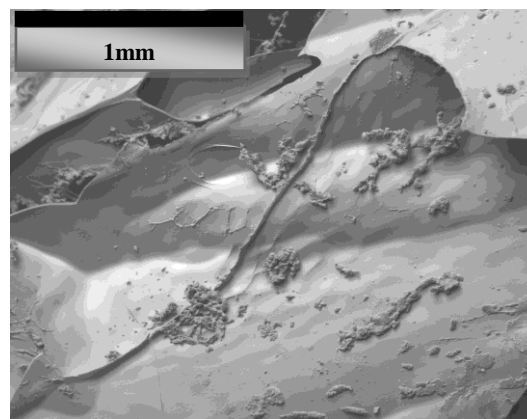


Figure 5.24 Wafer comprising 2% w/w CAR 911+ 4% w/w P407 407+4.4% PEG 600+ 1.8% w/w PM.

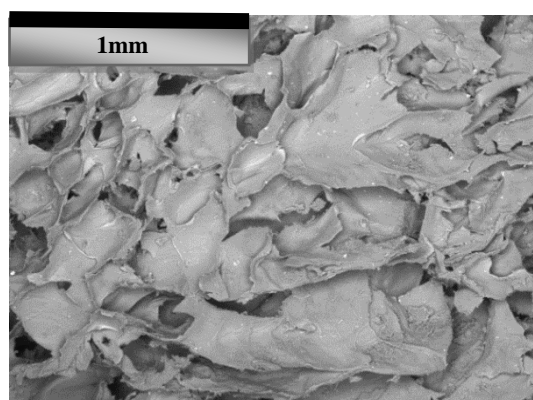


Figure 5.25 2% Wafers comprising 2% CAR w/w 911 + 4% w/w P 407+ 4.4% w/w PEG 600+ 0.6% w/w PM.

Figure 5.21-Figure 5.25 show the SEM images of drug loaded wafers showing differences between the surface topography of wafers formulated with various model drugs. The PM loaded wafer showed the least porosity as the surface texture appeared to be leafy while IND loaded wafer shows a more porous texture with uniform pore sizes. Comparison of the SEM images of wafers loaded with 0.6% w/w and 1.8% w/w PM showed that the leafy surface structure described above is due to higher amounts of PM incorporated in the wafer's matrix. The wafers containing lower amounts of PM (Figure 5.25) showed a more porous structure compared to the leafy texture of wafers containing 1.8% w/w PM.

5.2.5 XRPD results

XRPD studies provided supplementary data which confirmed the results obtained from DSC analysis and determined the physical form (polymorphic or amorphous) of incorporated drugs within the wafer matrices. Figure 5.26 shows the diffractogram of blank wafer's which shows the presence of PEG crystals belonging to P407 within the wafer matrix.

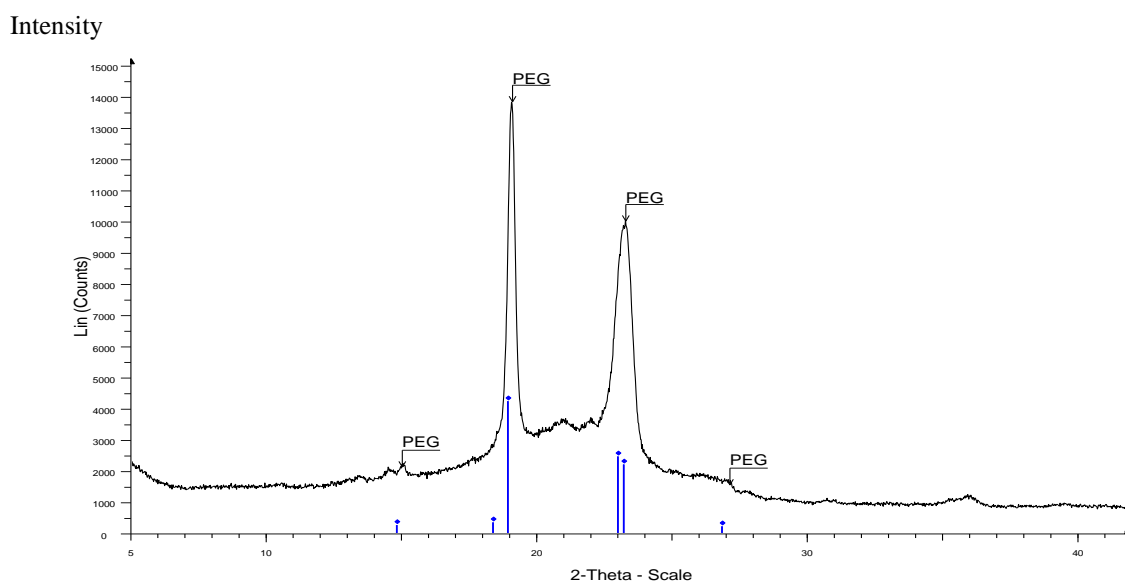


Figure 5.26 XRPD diffractograms for pure wafer comprising 2% w/w CAR 911 + 4% w/w P407+ 4.4% w/w PEG 600.

Similar XRPD results were obtained for drug loaded wafers as was observed for the solvent cast films. The absence of the peak which should be detected in a certain area for each model drug (IBU, IND, PM) confirmed the DSC thermogram results.

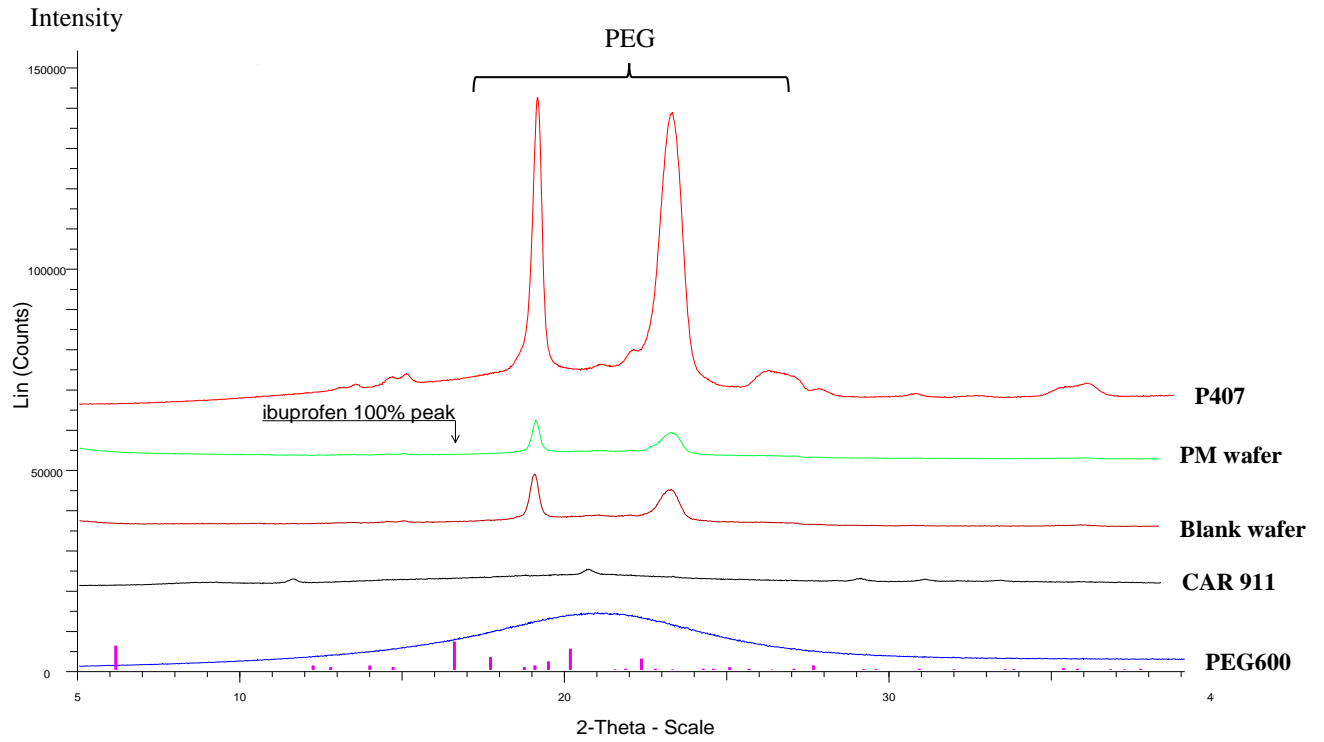


Figure 5.27 XRPD diffractograms for CAR911, P407,PEG600, blank and IBU loaded wafer.

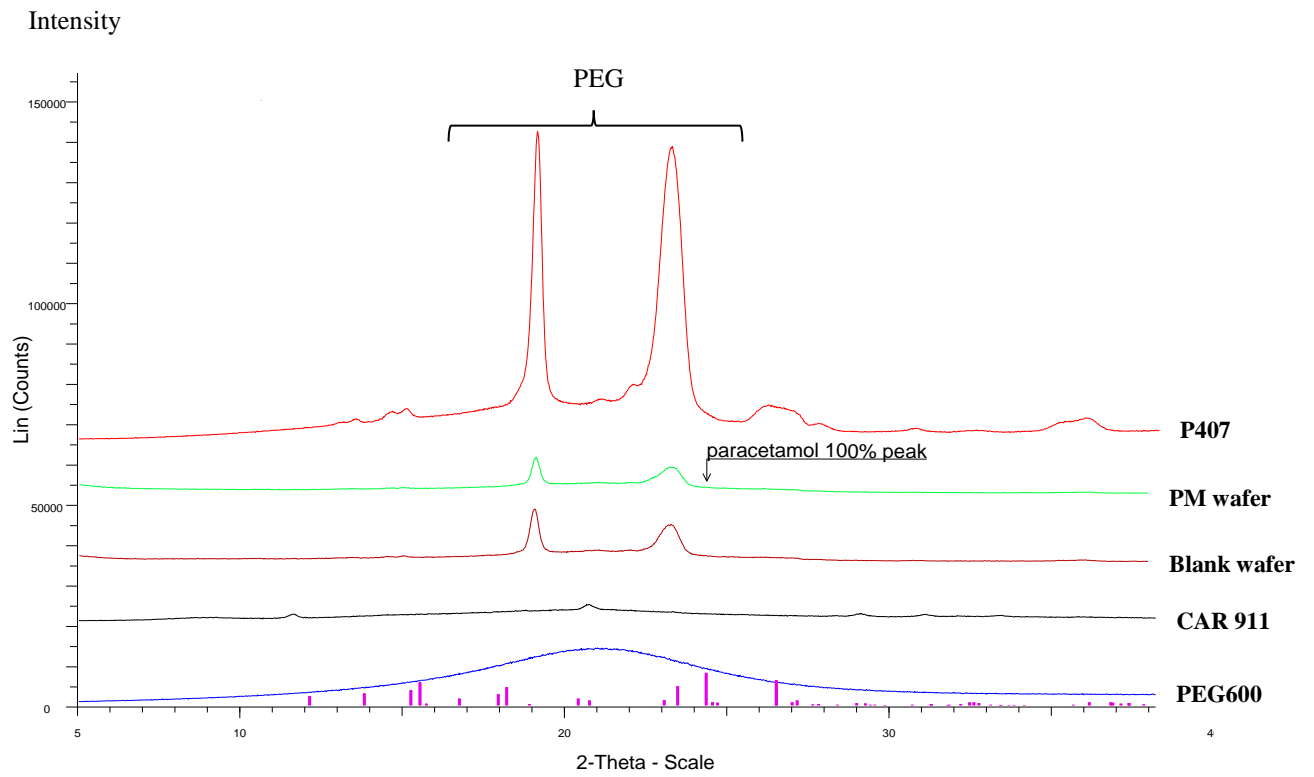


Figure 5.28 XRPD diffractogram of CAR911, P407,PEG600, blank and PM loaded wafer.

Figure 5.27 clearly shows the absence of IBU's crystalline peak expected to be detected at 16.7 (2θ). The results for PM (Figure 5.28) and IND (Figure 5.29) loaded wafers showed the same trend as in IBU diffractogram. It was evidenced by absence of the main crystalline peak expected at about 24.5 and 11.7 (2θ) for PM and IND respectively. The implication of these results is the discovery of similar effect of wafer matrix on the drug molecules. These observations confirm the matrix capability to transform crystalline drugs to the amorphous form and maintaining the amorphous state by preventing recrystallization.

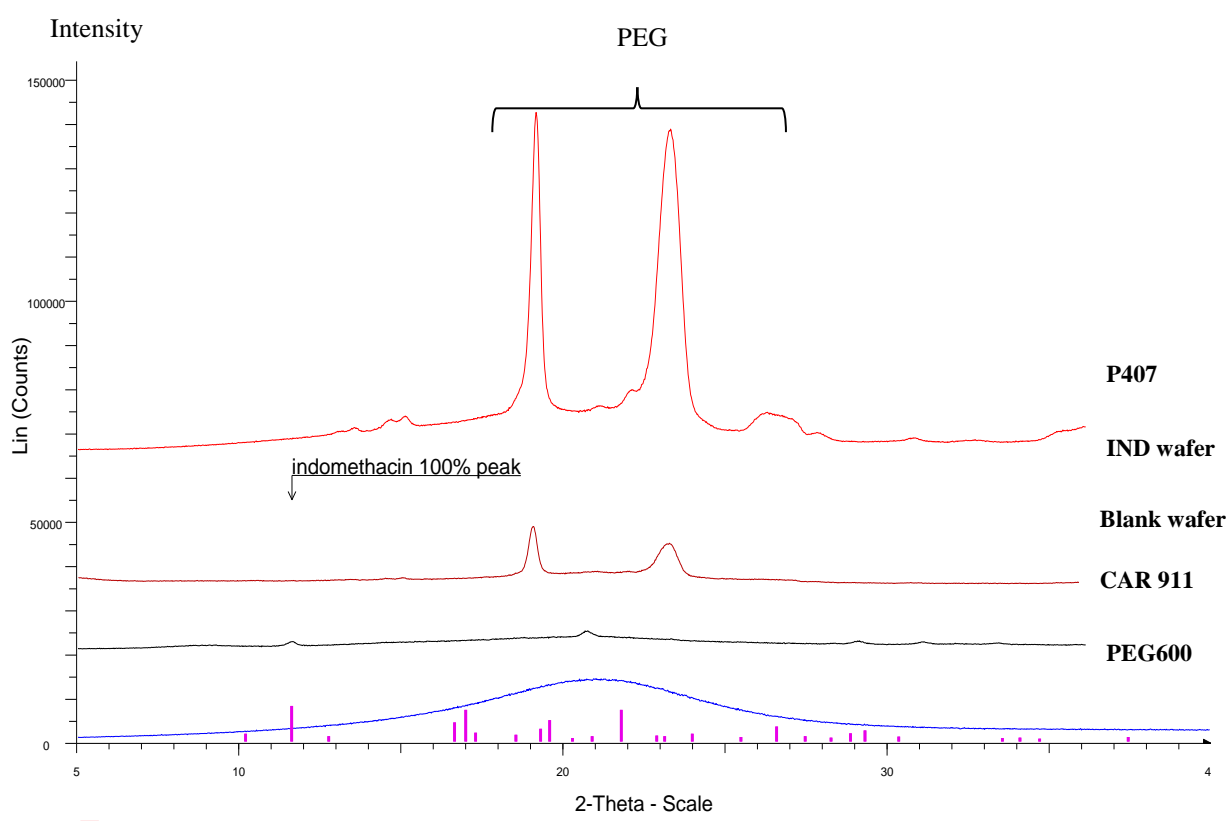


Figure 5.29 XRPD diffractogram of CAR911, P407, PEG600, blank and PM loaded wafers.

Additional studies were conducted to confirm the stability of amorphous drug within the system following the six months storage at room temperature. The reproducible results established that matrix had ability to maintain the drug molecules in the form of amorphous up to six months (Figure 5.30, Figure 5.31 and Figure 5.32).

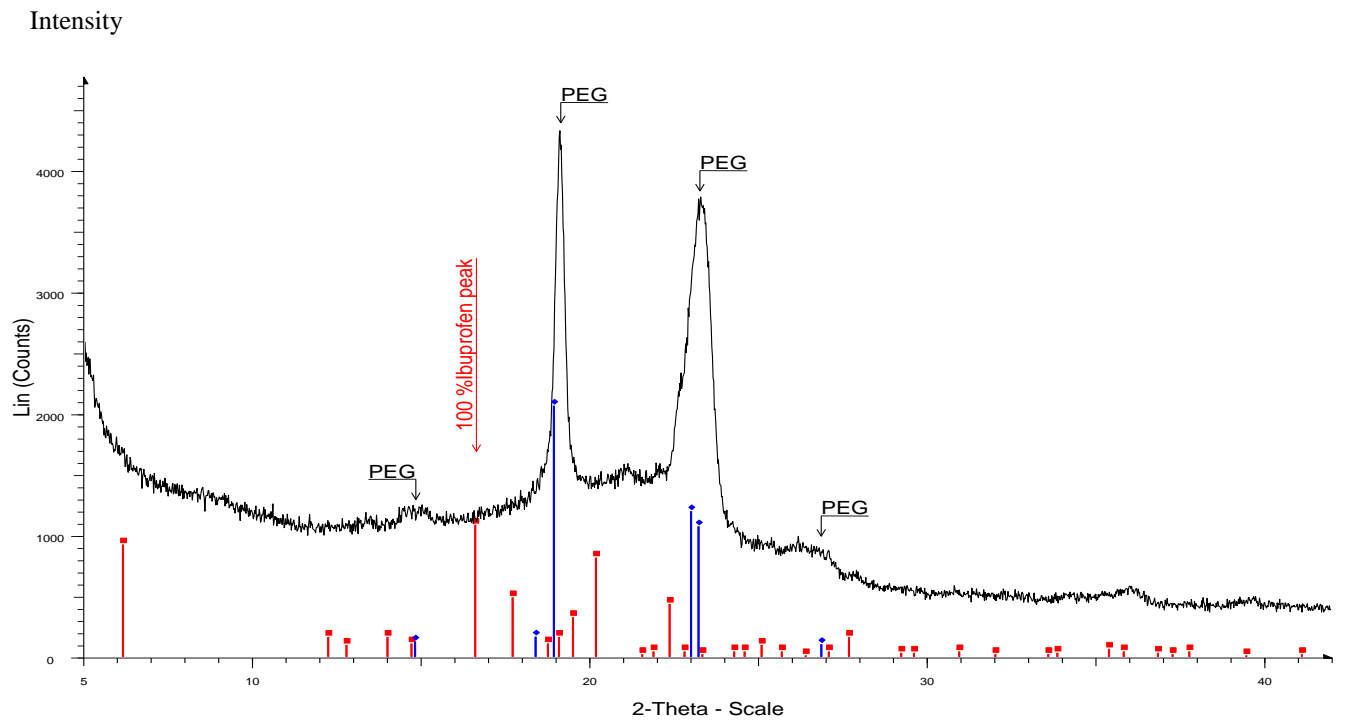


Figure 5.30 XRPD diffractogram for IBU loaded films stored for 6 months.

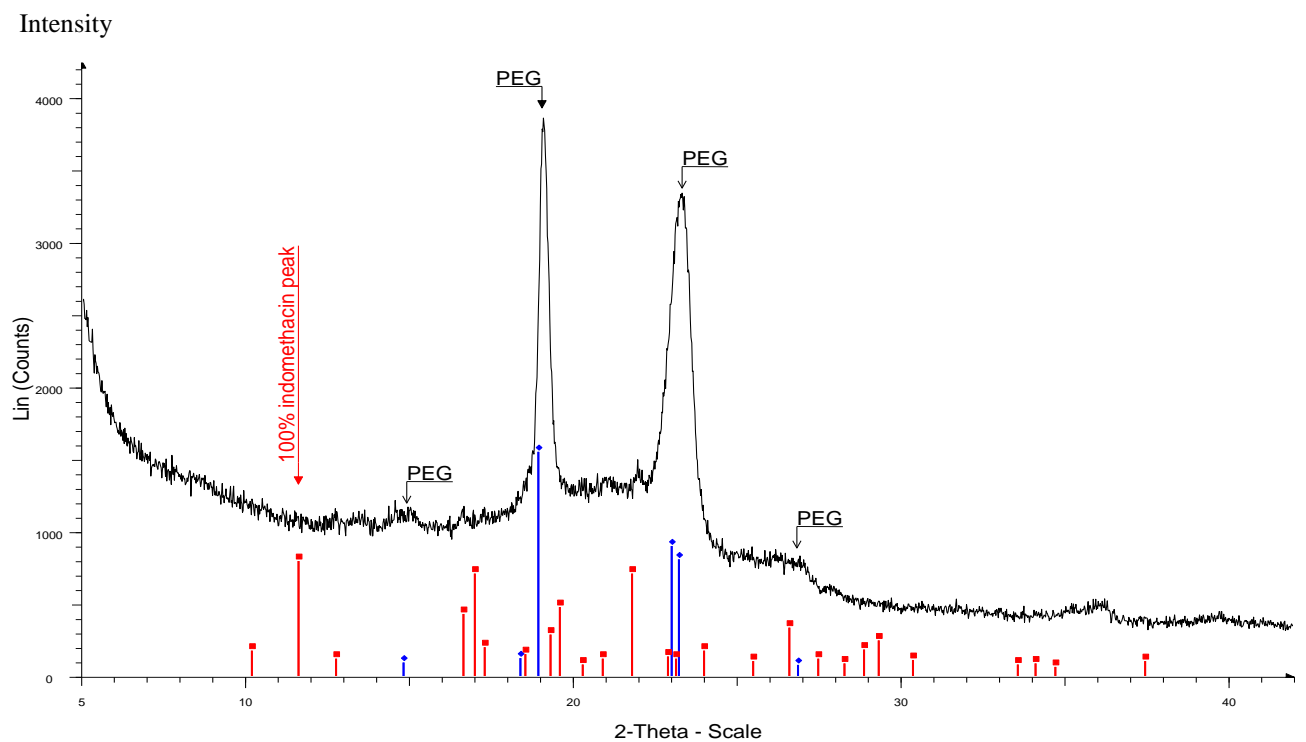


Figure 5.31 XRPD diffractogram for IND loaded films stored for 6 months.

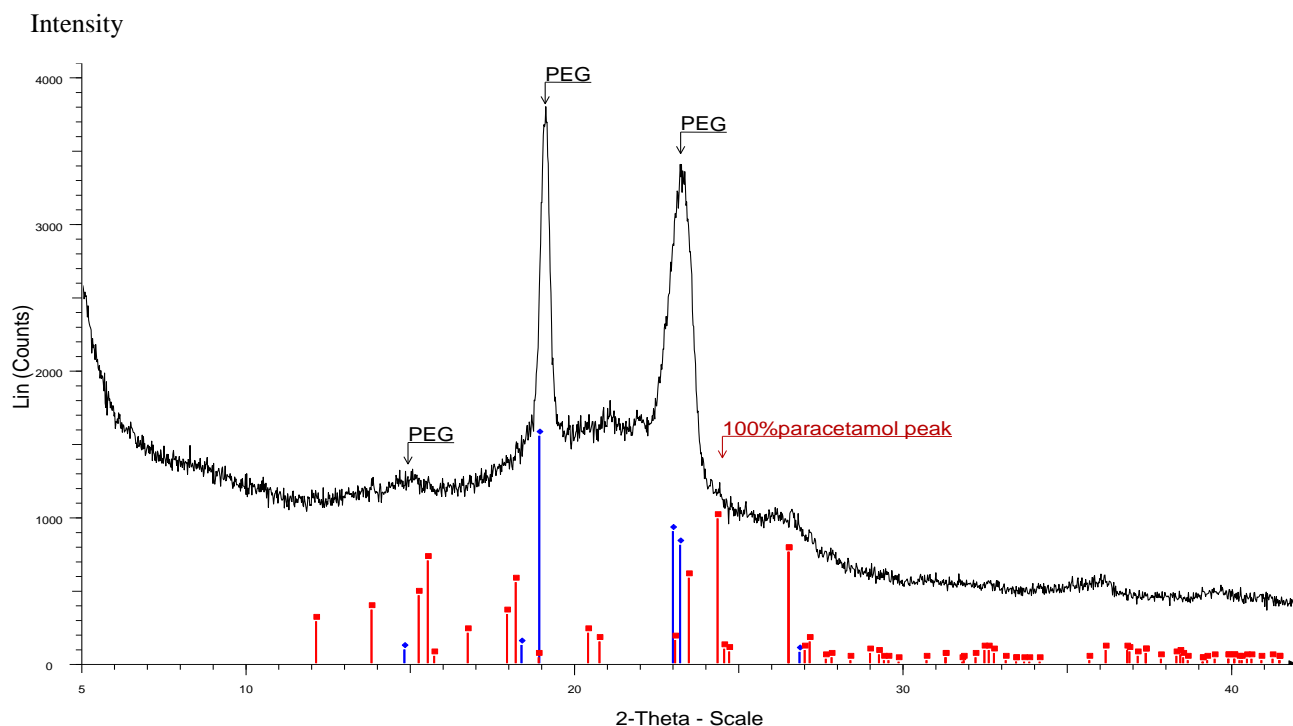


Figure 5.32 XRPD diffractogram for PM loaded films stored for 6 months.

As noted earlier, XRPD is an efficient technique to check the stability of amorphous drugs within the formulations. Such stability studies are especially essential because, apart from the possibility of re-crystallization, the amorphous materials are also more hygroscopic and often less chemically stable than the corresponding crystalline forms. This property is very critical especially for freeze-dried wafer's formulation where the residual water can deteriorate the stability of the drug delivery system. Furthermore, the technique has also been employed to establish that the formulation tested in pre-clinical studies maintain its amorphous character and no detectable crystalline character (Sarsfield, *et al.*, 2006).

5.2.6 Stability studies

HPLC results showed that the actual concentration of IND, IBU and PM within the wafers' sample remained relatively unchanged (> 98%) after six month storage at room temperature and 45% RH (Figure 5.33). The actual drug content was measured quantitatively with HPLC. Unlike the films, these studies were only conducted over six months because of time

constraints. The pure crystalline IBU, IND and PM used as control also remained stable over 6 months.

Although the stability studies were conducted up to six months period longer term stability test for model drugs within the wafer would be more desirable to ascertain how the drugs behave under accelerated conditions with higher temperature and relative humidity. The overall results from HPLC analysis, DSC thermograms and XRPD crystallographic pattern illustrate the ability of CAR 911, P407 and PEG 600 based wafers to preserve the stability of amorphous IBU, IND and PM though the stability inspection during longer period of time would be advantageous.

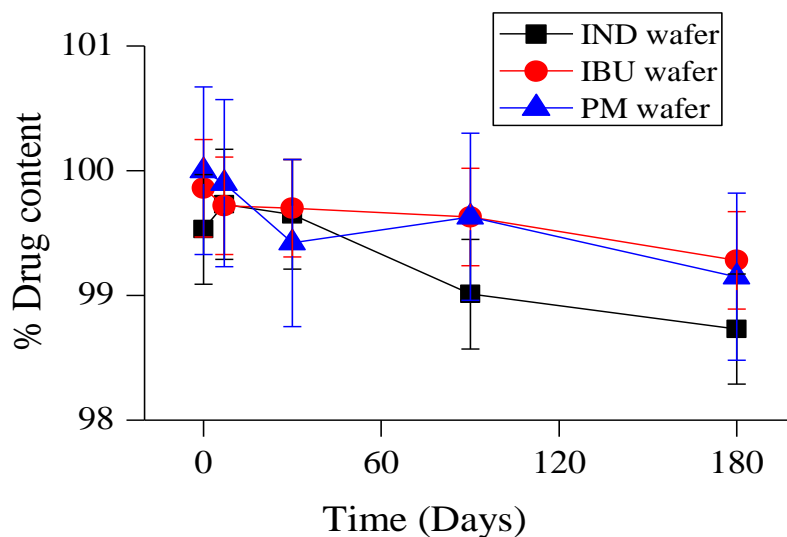


Figure 5.33 Percent drug content within the wafers during storage of up to six months {mean \pm s.d, n=3}.

Chapter 6 : Comparison of hydration, dissolution and mucoadhesive properties of solvent cast films and freeze-dried wafers

Subsequent to the development of two proposed buccal dosage forms (film and wafers) a comprehensive comparison was conducted to evaluate their functional properties which are drug dissolution and release profiles. However, since drug dissolution and release properties were directly affected by hydration and swelling, further experiments were required to determine the hydration and swelling behaviour. In addition, *in-vitro* mucoadhesion studies were necessary to evaluate the potential performance of dosage forms within the buccal mucosal membrane.

6.1 Hydration\swelling profiles

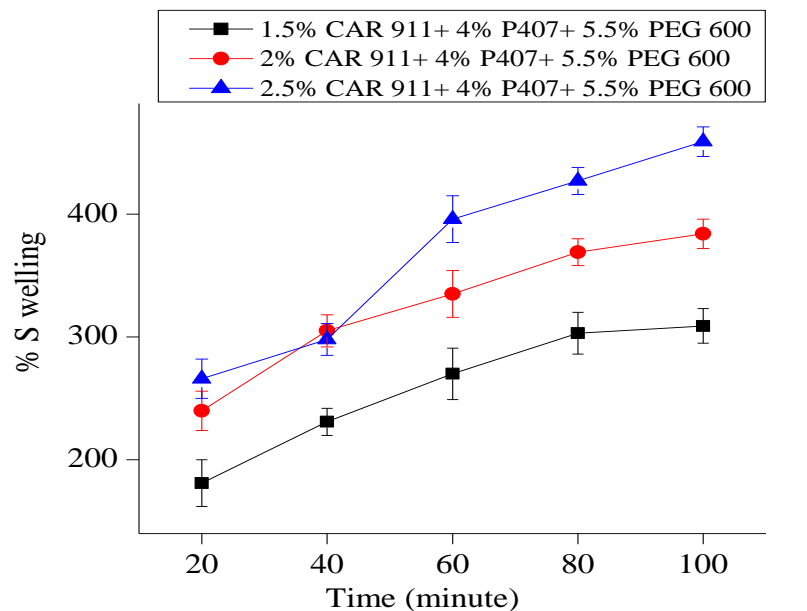
The preliminary studies were specifically focused on investigating the effect of pH on swelling as well as the maximum time requirement for films or wafers to be completely hydrated. Therefore, hydration and swelling experiments were conducted in two different media as:

- 1) saline solution (0.9 mg/mL NaCl) at pH= 5.6
- 2) phosphate buffer solution (prepared with 0.1 M of KH_2PO_4 and NaOH) at pH=6.2 to mimic the saliva pH

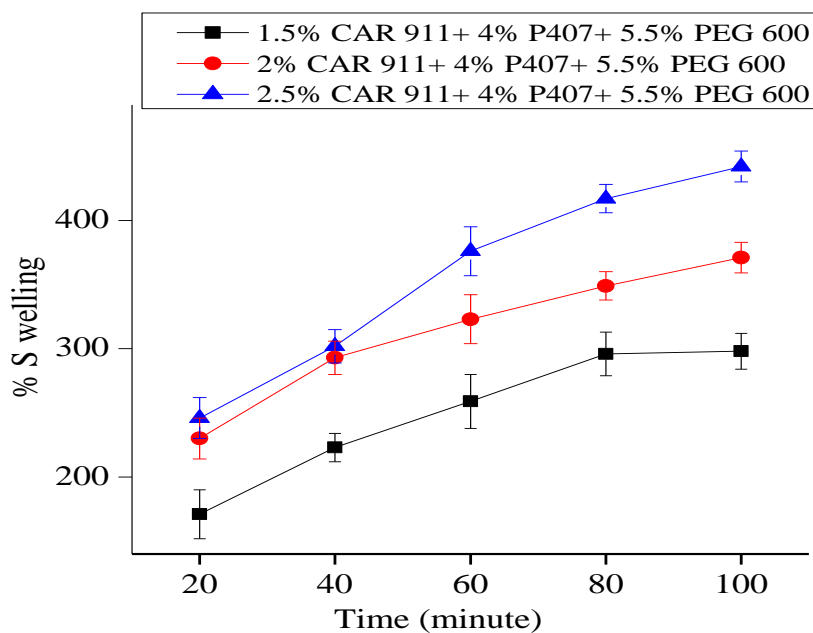
6.1.1 Films hydration and swelling

In both media, maximum hydration for films occurred within 100 minutes although the percentage swelling was fairly constant after 80 minutes. According to Figure 6.1 (a & b) different pH conditions did not have a significant effect on hydration and swelling profiles. However, these figures also show that the percentage content of CAR 911 had significant effect on hydration properties of the films. They highlighted that the percentage swelling for films containing 2.5% w/w CAR 911 was increased to almost 200% in comparison to films formulated with 1.5% w/w CAR 911. This effect is associated with the increase in hydroxyl

groups which provide more hydrogen bonding sites for water molecules and therefore increases the swelling capacity.



(a)

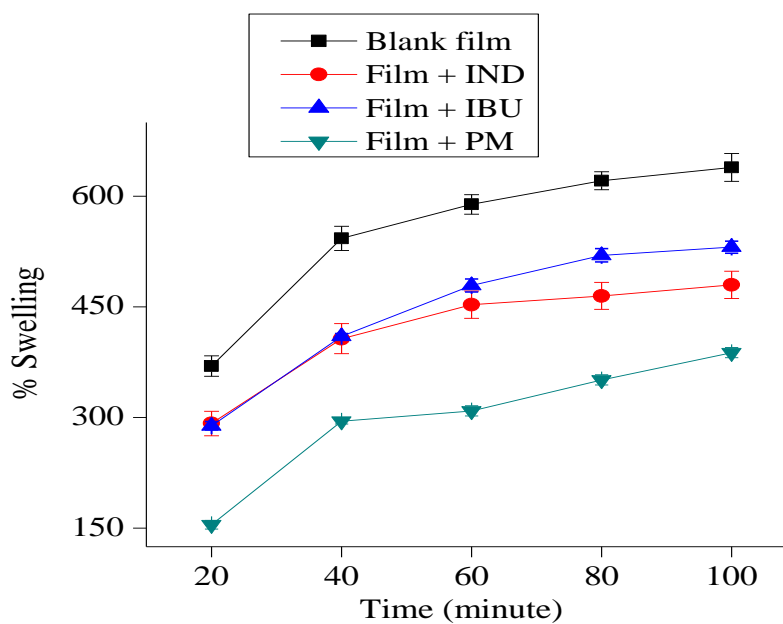


(b)

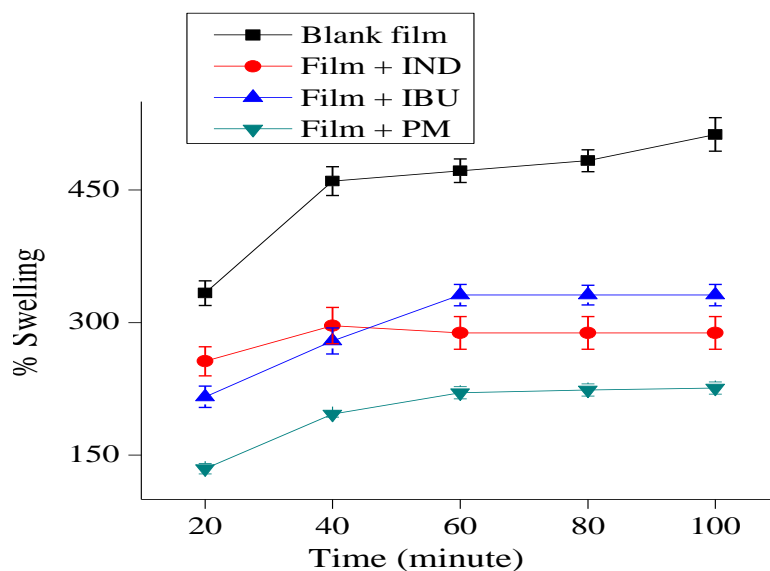
Figure 6.1 Hydration profile showing the % swelling for the films containing various concentration of CAR 911, 4% w/w P407 and PEG 600 in (a) saline solution and (b) phosphate buffer {mean \pm s.d, n=3}.

Comparison of the swelling profiles of the blank films (Figure 6.1) to those of drug loaded films showed that the maximum increase in percentage swelling for both sets of films occurred within 100 minutes. For example blank and IND loaded films showed increase in weight of about 600% and 500%, respectively of the initial weight in 60 minutes. The percentage swelling then increased more gradually to 650% and 520%, respectively for blank and IND loaded films at time 100 minutes. IBU loaded films also showed a similar swelling trend attaining 520% swelling in 80 minutes and a more gradual increase to 550% in 100 minutes. In the case of PM loaded films, there was no sharp initial increase but a more gradual and continuous increase to 400% in 100 minutes. Although the films containing IBU and IND with higher Log P they absorbed more water in comparison to the films containing PM with lower Log P (more hydrophilic) which were expected to hydrate more. These results can be attributed to the availability of more hydrogen and OH group in CAR 911 to bind with water while in PM film higher amounts of drug within the polymeric matrix retained less hydrogen bonding sites. This explanation is applicable in blank film with higher hydrogen bonding sites.

The overall results indicate that blank films showed a higher propensity to hydrate and swell more easily compared to the films containing the three model drugs. A similar swelling profile was observed for films formulated with or without model drugs in buffer solution (pH=6.2). However the overall swelling capacity in the buffer was lower than in the acidic medium (pH=5.6). This might be attributed to the presence of more hydrogen ions in the acidic medium which results in more hydrogen bonds with CAR and thereby enhanced the hydration capacity. The maximum % swelling for blank film in pH=6.2 was about 460% of initial weight within 40 minutes, ultimately reached 500% after 100 minutes. For IND loaded films the maximum swelling reached about 300% of initial weight and remained constant up to 100 minutes. The IBU film swelled to maximum capacity within 60 minutes and remained at about 340% afterward up to 100 minutes. PM film showed a gradual swelling within 60 minutes and reached 230% of the initial weight.



(a)

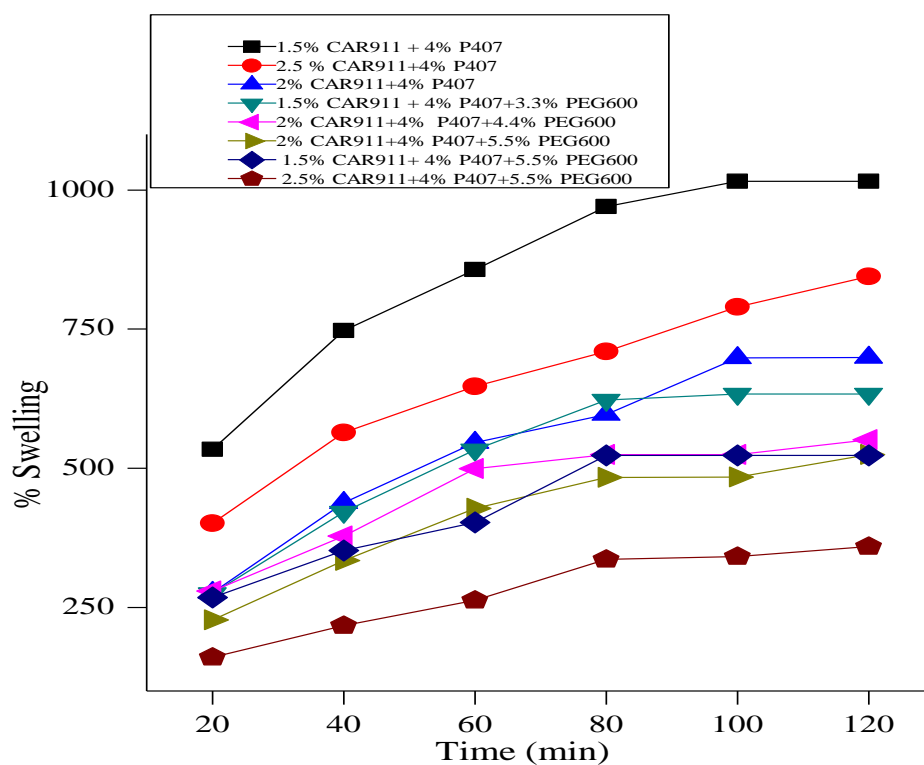


(b)

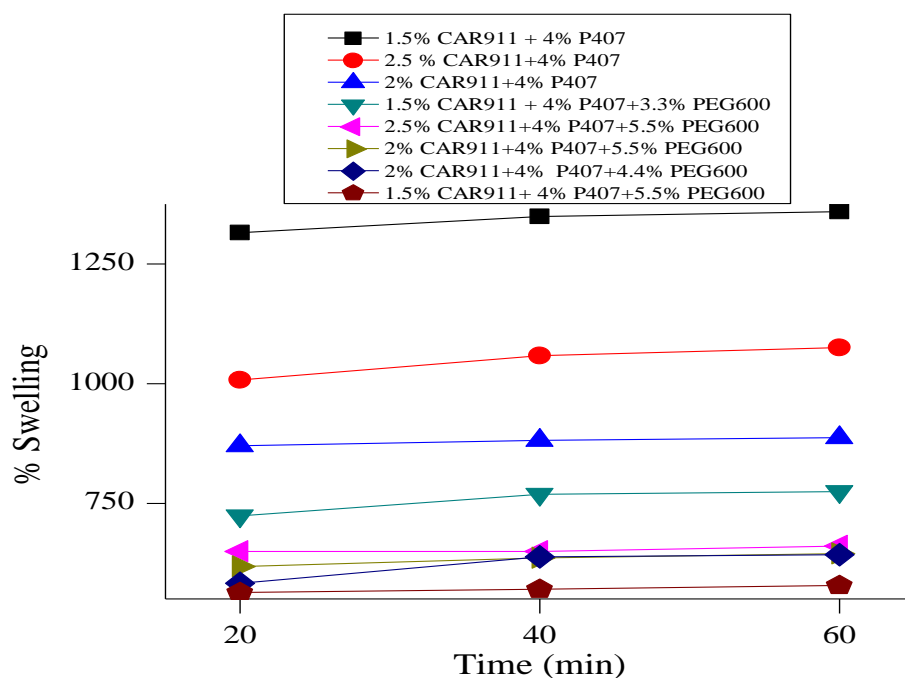
Figure 6.2 Hydration profile showing the % swelling for the film formulated with 2.5% w/w CAR 911 with or without model drugs (IBU, IND or PM) in (a) saline solution and (b) phosphate buffer {mean \pm s.d, n=3}.

6.1.2 Wafer hydration and swelling

The overall observation of blank and drug loaded wafers (Figure 6.3 and Figure 6.4) in two different media at various pH values demonstrated the effect of pH on the swelling capacity, unlike the films.



(a)

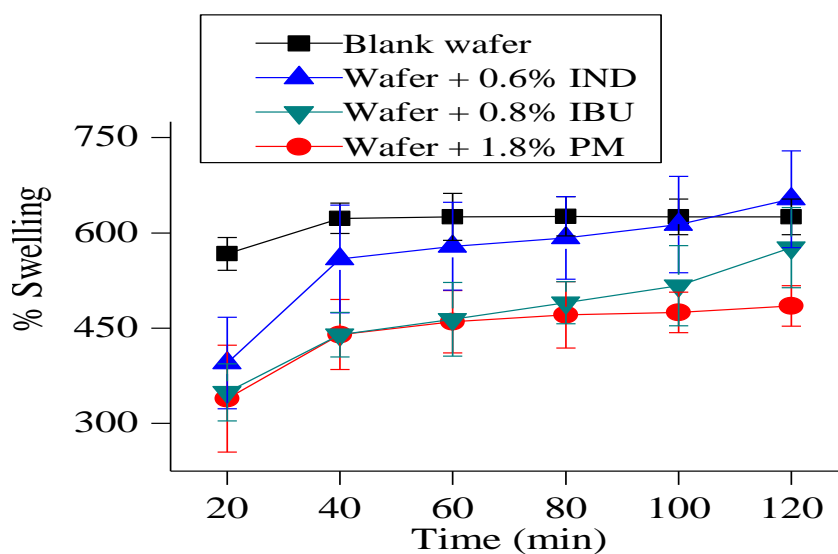


(b)

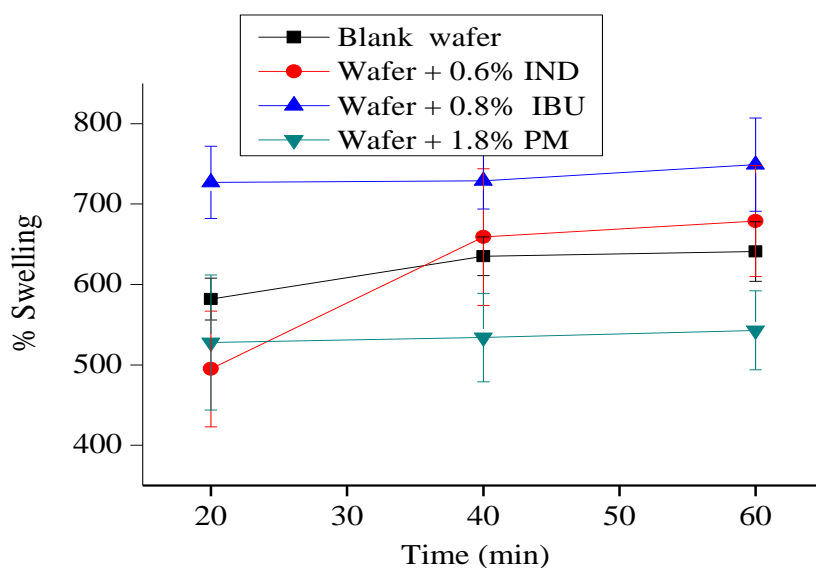
Figure 6.3 Degree of wafer swelling formulated with various ratios of carrageenan 911 (CAR), poloxamer (P407) and PEG 600 in (a) saline solution (pH= 5.6) and (b) phosphate buffer solution (pH= 6.2) {mean \pm s.d (n=3)}.

The results showed that the maximum swelling for wafers in slightly acidic pH (saline solution) occurred within a longer time period (120 minutes) and the overall swelling capacity is lower in comparison to wafers immersed in buffer media. Wafers placed in salt condition (buffer solution at pH=6.2) showed a maximum swelling capacity in 60 minutes that was 300% higher than in saline solution. The observations proved the stimulation effect of the higher pH on swelling ability.

Figure 6.3 also showed that the wafers formulated with lower amounts CAR 911 and without PEG 600 showed the highest percentage swelling and this trend was steady during the whole experiment time. The effect is more related to the ratio of CAR 911 with its dominant effect on hydration profile. According to the SEM results (Figure 5.15 to Figure 5.20) increasing the CAR 911 ratio resulted in wafers with smaller pores. Therefore, smaller pores have less capacity for water ingress as well as to be occupied by water molecules and therefore hydrated to a lesser extent. The highest swelling capacity of approximately 1000% and 1300% in saline and buffer solution respectively was exhibited by wafers comprising 1.5% w/w CAR 911 and 4% w/w P407. As noted earlier, addition of PEG 600 however, decreased the swelling percentage significantly. This is shown in Figure 6.3 by wafers comprising CAR 911 at 2.5% w/w and 5.5% PEG 600 had a lower swelling propensity.



(a)



(b)

Figure 6.4 Swelling profile for wafers formulated with various amounts of model drugs placed in (a) saline solution (pH=5.6) and (b) phosphate buffer solution (pH=6.2) {mean \pm s.d, n=3}.

Figure 6.4 shows the swelling profiles of optimised wafers formulated with gels containing 2% w/w CAR 911, 4% w/w P407 and 4.4% w/w PEG 600 containing the different model drugs (IBU, PM and IND) in two pH conditions.

The overall trend shows higher and faster swelling capacity in the buffer solution (pH=6.2) within 40 minutes compared to saline solution where complete and maximum swelling was attained in 120 minutes.

The blank and PM loaded wafers in both saline and buffer solutions hydrated relatively rapidly. These formulations attained maximum swelling of 620 and 450% respectively after 40 minutes after which the weight changes remained constant. The implication of this phenomenon can be related to the more extensive porosity in blank wafer and the alkaline nature of PM which will be more miscible with water. IND and IBU loaded wafers on the other hand showed slightly different swelling behaviour which continued for 120 minutes (580% and 620% respectively) in the saline solution, as the steepest weight changes occurred within the first 40 minutes due to slightly acidic nature of both model drugs. The hydration and swelling tendency for IBU loaded wafer in the buffer solution was higher than IND loaded wafer whilst the opposite was true in saline solution. This is correlated to the molecular structure of IND (Figure 6.6a) with three potential sites to form hydrogen bonds in acidic condition whilst IBU (Figure 6.6b) has two potential sites and the number of hydrogen bonds are less in acidic condition which directly affect the solubility.

Figure 6.5 confirms that the swelling capacity of IND and IBU loaded matrices (films and wafers) in both media was considerably higher in comparison to PM, owing to the presence of more hydrogen bonding sites.

The differences in swelling behaviour between films and wafer can be listed as:

1. the general trend of swelling in either blank or drug loaded wafers is about three times higher compared with films due to significantly porous texture (Figure 6.5).
2. the film swelling occurred within 100 minute in contrast to sharp swelling behaviour in wafers which was within 20 minutes.
3. increasing the ratio of CAR 911 within the blank film formulation increased the swelling affinity in contrast to blank wafers.
4. pH has a considerable effect on wafer's swelling profile whilst it did not have significant effect on film's swelling profile.

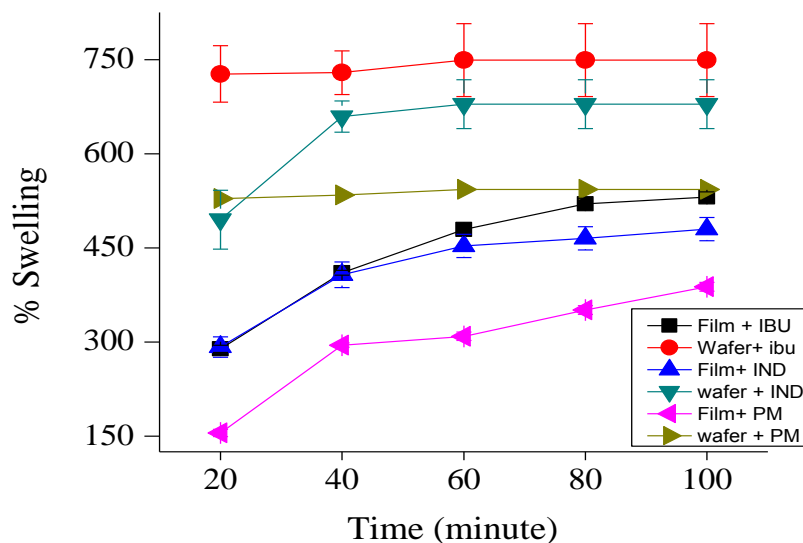
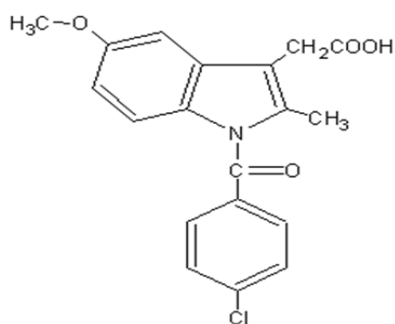


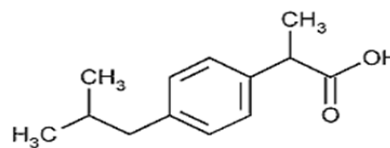
Figure 6.5 Comparison of the swelling profile of optimized drug loaded films and wafers.

6.2 Drug dissolution profile

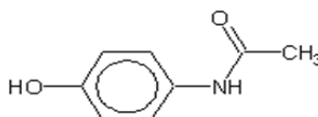
Before investigating the dissolution of films and wafers the physico-chemical characteristics of model drugs were considered. According to the literature IND (Figure 6.6a) has a pKa of 4.5 which is stable in neutral or slightly acidic media while decomposing in strong alkali.



Indomethacin



Ibuprofen



Paracetamol

Figure 6.6 IND, IBU and PM chemical structures.

PM (Figure 6.6c) is a weak basic drug with pKa 9.5 and is stable in alkali condition whilst IBU (Figure 6.6b) is a relatively weak acidic with the pKa about 4.4 also its solubility in water or at acid pH is very low. Scientifically a lower proportion of drug with higher Log P dissolve in aqueous media hence, it is expected for IND and IBU loaded films and wafers to have slower dissolution rate in comparison to PM loaded formulations.

6.2.1 Film drug dissolution profiles

Figure 6.7, Figure 6.8 and Figure 6.9 compare the dissolution profiles for IBU, IND and PM respectively in pure form (control) and within the films using the two different dissolution media (saline and buffer solution to determine the effect of pH). The most interesting finding was that the cumulative percentage release of pure model drug which was considerably lower in comparison to that present in the film matrices. This effect was observed for all three model drugs.

Pure IBU initially dissolved relatively quickly possibly due to the immediate contact with the dissolution medium but reached a plateau in 10 minutes. In contrast, IBU was initially released from the film matrix more quickly but showed sustained release profiles overall, reaching release of 65% and 58% in 120 minutes for buffer and deionised water, respectively. The dissolution profiles and gradient derived from the initial linear portion of the drug release vs. time curves confirmed the effect of pH on drug release rate from the film matrix. These results showed that the rate of drug release was faster in the simulated saliva pH environment compared with the acidic pH condition (deionized water). In addition, the maximum drug release in buffer solution was about 8% higher than in acidic pH (corresponding to stomach dissolution media). This presents a potential advantage of buccal delivery over the traditional oral route. This is an interesting finding for films intended for buccal mucosa applications. However, this needs further investigations as the difference observed could relate to ionisation suppression of the acidic IBU at the lower pH of deionised water. These results indicate that IBU was present in the films in the amorphous form as compared to the pure crystalline form used as a control. Pure PM dissolved rapidly, within 5 min, before reaching a plateau in the percentage released.

The pure crystalline IND also dissolved relatively quickly initially and reached a plateau in the percentage released after 10 min in buffer solution. However, PM was released from the film matrix more slowly initially but showed higher cumulative release profiles (compared to pure crystalline drug) reaching about 40% in 25 minutes and ultimately 45% after 40 minutes in buffer. The ultimate drug release of PM from the film in buffer solution was about 25-30% less than IBU or IND loaded films which are related to the swelling index and low hydration capacity of PM loaded films.

Similar trends were observed for IND loaded films though the release was slightly faster and the maximum release (57%) occurred within 40 minutes. Interestingly, drug loaded films demonstrated lower % release in deionized water than in buffer, which shows the effect of pH on drug release kinetics from the films. The faster release rate in buffer solution (mimicking pH of saliva) compared with acidic pH confirmed that the film was a viable matrix to deliver drugs via the buccal cavity rapidly. The maximum drug release from the IND loaded film in buffer solution was about 8-10% less than IBU loaded film; this can be correlated to the effect of pH on solubility of IBU.

It is also interesting to note that the release profiles for PM and IND from the films were generally similar, even though the pure crystalline forms of the two drugs have significant differences in solubility. This seems to confirm the point that all three drugs were present in the films in the amorphous form as compared to the pure crystalline forms used as control.

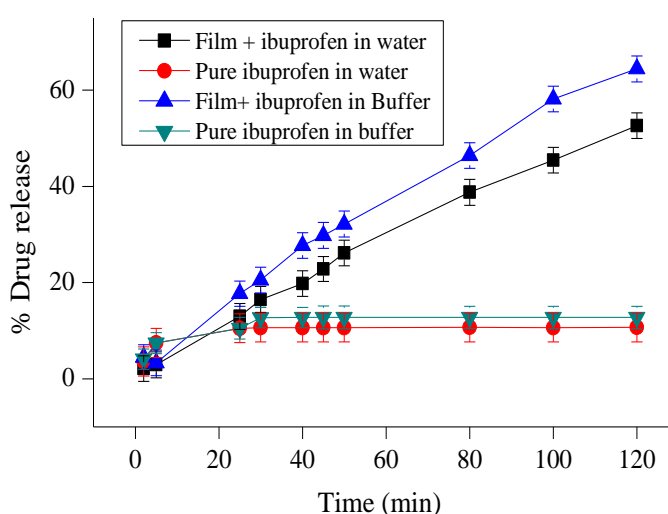


Figure 6.7 Dissolution profile showing the drug release from the film containing IBU {mean \pm s.d.(n=3)}.

Conventionally, the amorphous form of a drug displaying higher water solubility is expected to have higher rates of dissolution according to the Noyes-Whitney equation and therefore may account for the higher than expected rates of release by diffusion and eventual erosion of the polymer matrix when compared with the pure crystalline drug. The IBU release from the CAR 911 matrices is also medium-dependent due to the anionic nature of the polymer. As the pH increased, swelling index of the polymeric matrix increased and formed a gel layer which sustains the drug release. Due to the very rapid wicking, or water uptake, between the polymeric matrix and the resultant gelation, the surface pores are sealed preventing further rapid drug release (Boyapally, *et al.*, 2010).

The kinetics of IBU release from the films were evaluated by determining the best fit of the dissolution data (percentage release vs time) to the Higuchi, Korsmeyer–Peppas, zero order, first order and Hixson-Crowell equations by determining the R^2 values. According to Table 6.1 the drug release was proportional to time (or log of time in the case of IND). When percentage of cumulative drug released versus time was plotted in accordance with first-order and zero-order, Higuchi and Korsmeyer- Peppas equations, the determined R^2 values for the films' polymeric matrix were.

Verelas, *et al.*, (1995) proposed that in many cases zero order kinetics can be applied to describe the drug release from several types of modified release pharmaceutical dosage forms such as polymeric matrices. When drug release rate is proportional to the remaining concentration of drug in the dosage form, dissolution can be described by first order release kinetics, predominantly for water soluble model drugs. The best fit for various models investigated for IBU and IND loaded films ranked in the order of Hixson– Crowell > first order. As shown in Table 6.1, the coefficients (R^2) have similar values in more than one kinetic model of the same formulation. Thus, the selection of the adequate model was based on comparisons of higher determination coefficient, smaller standard error of model parameters and smaller residual mean square. On the basis of these comparisons the first order model was found to describe PM loaded film formulation (Yuksel, *et al.*, 2000; Boateng *et al.*, 2009b; Ritger and Peppas, 1987).

This shows that there is a change in surface area, diameter of the dissolved film specimens and the change in diffusion path length during the dissolution process following the cube root law. Further, the n values from the Peppas equation were considered. The Peppas equation ($Q=kt^n$) is generally used to analyse the release of pharmaceutical polymeric dosage forms when the release mechanism is not well known (anomalous transport release). It is also useful when more than one type of release phenomenon could be involved, for example, swelling and erosion of polymer.

The equation becomes more realistic in two main cases; pure diffusion controlled drug release, $n=0.5$ and swelling controlled drug release, $n=1$ (Case II transport). Other values of n indicate anomalous transport kinetics i.e. a combined mechanism of pure diffusion and swelling and the magnitude of n can be used as an indication of the type of transport mechanism for the drug. A value of $n \leq 0.45$ corresponds to Fickian diffusion release (case I diffusional), ($0.45 < n \leq 0.89$) to an anomalous (non-Fickian diffusion) transport i.e. a gel erosion release mechanism, $n=0.89$ to a zero-order (case II) release kinetics, and $n > 0.89$ to a super case II transport. In the current study, the value of n was found to be greater than one for all the three drugs indicating super case II transport (Siepmann & Peppas, 2001) for drug release from the CAR based films. In this type of drug release kinetics the dominant mechanism for drug transport is due to polymer relaxation as the gel swells and are known as swelling-controlled release systems (Siepmann & Peppas, 2001). According to the above classification IBU and IND loaded films demonstrate an anomalous transport model whereas the drug release model for the film polymeric matrix, loaded with PM observed as case I diffusional.

The law of mass action proposed that, the velocity of a chemical reaction is proportional to the concentrations of drug. The change in concentration (dC) over a time interval (dT) is the velocity of the swelling (dC/dT) which is proportional to concentration. However, the velocity declines with time and decreases the drug content within the polymeric matrix and the concentration plot against time would yield a curve of gradually declining slope.

Table 6.1 Fitting of dissolution data of the three model drugs to various kinetic models for drug release from films.

Dissolution models		IND film	IBU film	PM film
Zero order	k^0 (%hr ⁻¹)	1.145	0.374	0.375
	R ²	0.988	0.991	0.998
	RSM	85.93701	112.2964	85.9370
First order	k_1 (h ⁻¹)	$7.2 \times 10^{-3} \times 6.3773E-005$	$8.0 \times 10^{-3} \pm 6.9377E-005$	0.0084 ± 0.0012
	R ²	0.9988	0.9989	0.00
	RSM	0.8877	0.9337	247.1522
Higuchi	k_H (% hr ^{-1/2})	4.5683 ± 0.1910	4.9269 ± 0.2018	5.1909 ± 0.3267
	R ²	0.9493	0.9510	05305
		35.5760	39.7184	104.0539
Hixson–Crowell	k_{HC} (%h ^{-1/3})	$2.2 \times 10^{-3} \pm 1.8684E-005$	$2.4 \times 10^{-3} \pm 1.4722E-005$	$2.4 \times 10^{-3} \pm 0.0003$
	R ²	0.9986	0.9993	0.9777
	RSM	0.9881	0.5620	276.9067
Peppas	k_p (hr ⁻ⁿ)	1.1269 ± 0.0925	1.2372 ± 0.0811	17.7272 ± 2.2737
	R ²	0.9979	0.9986	0.9134
	n	0.8323 ± 0.0188	0.8281 ± 0.0150	0.2004 ± 0.0328
	RSM	1.6081	1.2015	25.1892

RSM: residual mean square; n: dissolution exponent.

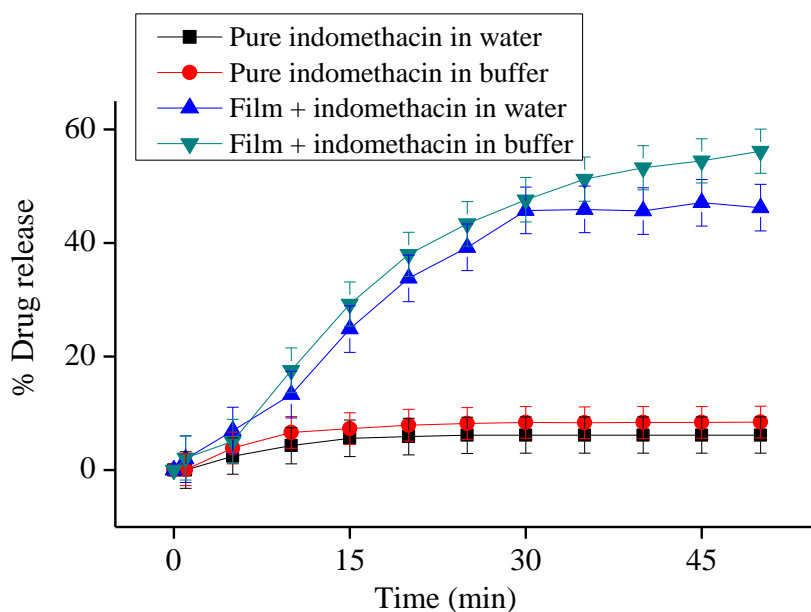


Figure 6.8 Drug dissolution profiles from the IND loaded films {mean \pm s.d (n=3)}.

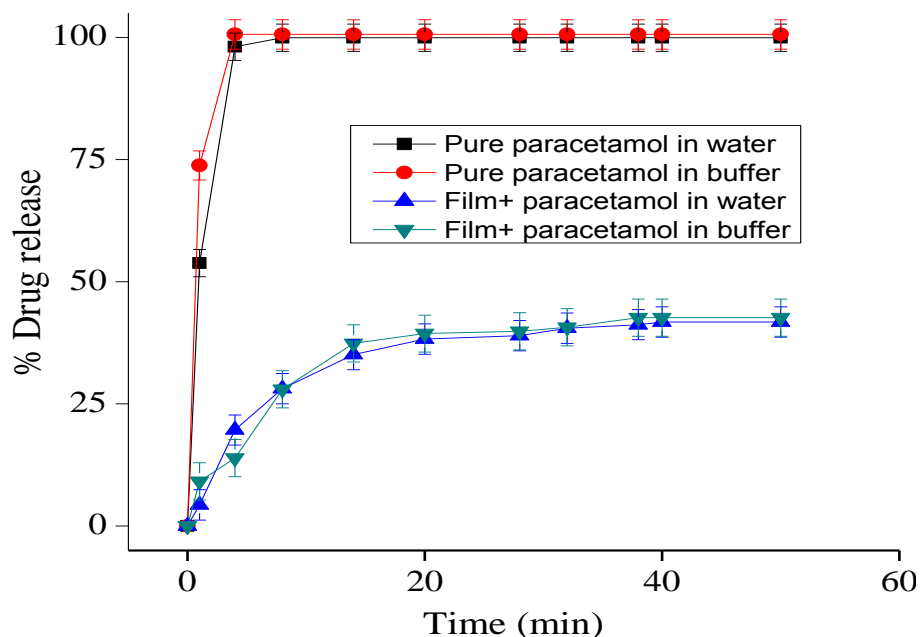


Figure 6.9 Drug dissolution profiles for the PM loaded films {mean \pm s.d } (n=3)}.

6.2.2 Wafer drug dissolution profiles

Figure 6.10 to Figure 6.12 compare the dissolution profiles for IBU, IND and PM, respectively in pure form (control) and within the wafer using the two different dissolution media (deionised water and buffer to determine the effect of pH). Interestingly the effect of pH= 6.2 for IBU and IND loaded wafers on release profile were quite obvious which could be attributed to their acidic nature. For PM loaded wafer the change of the pH from 5.6 to 6.2 did not have any obvious effect on the dissolution behaviour probably because PM is basic in nature and in both of these conditions it was existed in ionised form and therefore showed similar dissolution profiles.

PM was released from the wafers relatively quickly initially before reaching a plateau in 15 minutes, whilst IND and IBU showed sustained release behaviour with a gradual release from the matrix up to 110 and 100 and minutes respectively. The maximum cumulative percentage release of IBU from the wafer was about 75% and 69% for IND. The release of PM from the wafer matrix reached to just about 40% which is significantly lower than the other two model drug with are hydrophobic in nature.

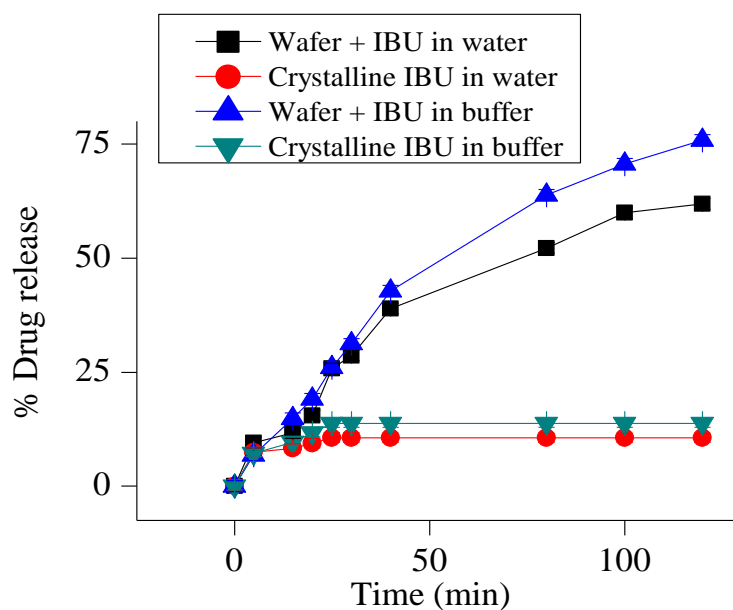


Figure 6.10 Drug dissolution profile for wafers formulated with IBU {mean \pm s.d. (n=3)}.

Table 6.2 Fitting of dissolution data of the three model drugs to various kinetic models for drug release from wafers.

Dissolution models		IND wafer	IBU wafer	PM wafer
Zero order	k_0 (%hr ⁻¹)	0.453	0.951	1.255
	R ²	0.924	0.955	0.883
	RSM	206.3896	159.2146	101.5934
First order	k_1 (h ⁻¹)	$1.2 \times 10^{-3} \pm 0,0002$	$1.29 \times 10^{-2} \pm 0,0002$	$8.4 \times 10^{-3} \pm 0,0015$
	R ²	0.9957	0.9969	0.00
	RSM	5.5408	4.0450	409.7825
Higuchi	k_H (% hr ^{-1/2})	$6.4306 \pm 0,2226$	$6.7194 \pm 0,2027$	5.4055 ± 0.4663
	R ²	0.9618	0.9693	0.00
	RSM	48.3261	40.0501	212.0020
Hixson–Crowell	k_{HC} (%h ^{-1/3})	$3.5 \times 10^{-3} \pm 8.684E-005$	$3.7 \times 10^{-3} \pm 8.0534E-005$	$2.5 \times 10^{-3} \pm 4 \times 10^{-4}$
	R ²	0.9915	0.9925	0.00
	RSM	10.8981	9.8788	444.4980
Peppas	k_P (hr ⁻ⁿ)	$2.7095 \pm 0,4699$	3.1281 ± 0.4519	$31.5917 \pm 1,6707$
	R ²	0.9867	0.9898	0.9569
	n	$0.7063 \pm 0,0401$	0.6826 ± 0.0335	$6.48 \times 10^{-2} \pm 0.0143$
	RSM	17.8553	14.1677	7.6352

RSM: residual mean square; n: dissolution exponent.

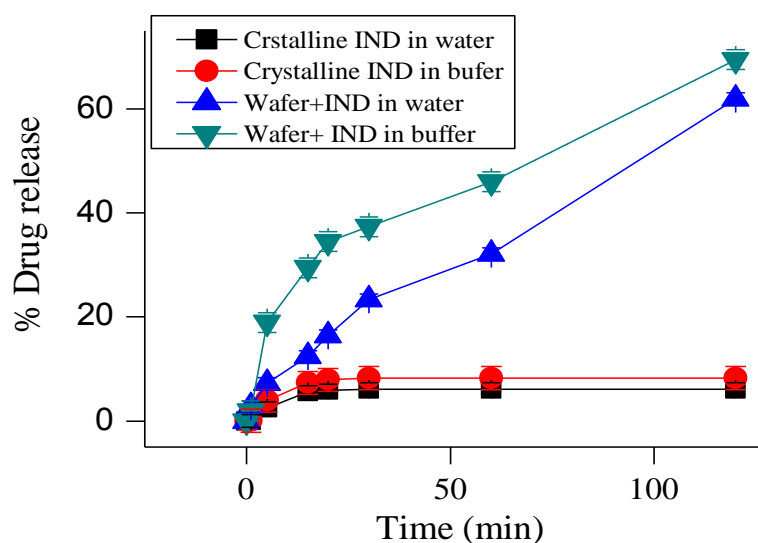


Figure 6.11 Drug dissolution profiles for wafers formulated with IND {mean \pm s.d (n=3)}.

The faster release rate in buffer solution (mimicking saliva) compared with acidic pH as well as higher maximum release for IND (approximately 10% higher) and PM (about 5% higher) in buffer solution showed that wafers are a desirable matrix for drug delivery via the buccal mucosa.

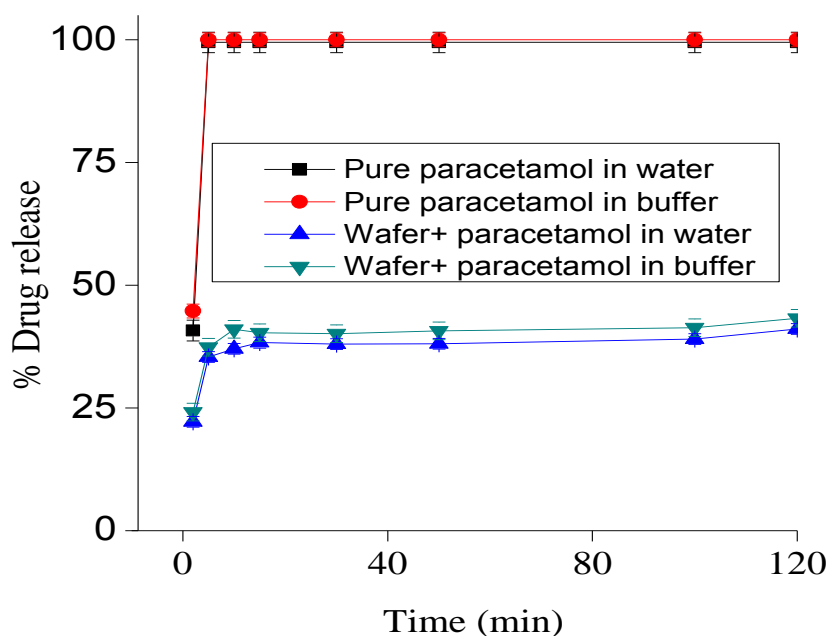


Figure 6.12 Drug dissolution profiles for wafers formulated with PM {mean \pm s.d (n=3)}.

As was the case for the films, the presence of the model drugs in amorphous form within the wafers was confirmed, evidenced by the faster dissolution rates from the wafers compared to the pure crystalline drugs used as controls. According to the data in Table 6.2 the R^2 values show that the kinetic model that best fit the release data was Korsmeyer-Peppas which involved a combination of diffusion in the first step followed by erosion of the polymeric matrix. The n value of drug release kinetics were calculated and compared with the literature (Balji & Peppas, 1996). According to literature $n \leq 0.45$ corresponds to Fickian diffusion release (case I diffusional), and $n > 0.89$ follows the super case II transport. Since, IBU and IND loaded wafers showed $0.45 > n > 0.89$, the drug release from the polymeric matrix was based on anomalous transport which means that diffusion and erosion played the key role in drug release behaviour.

This value for PM loaded wafer however, showed the value of $n < 0.45$ corresponding to Fickian diffusion release (case I diffusional). In this category of drug release kinetic, the dominant mechanism for drug transport is due to diffusion through the pores of polymer and the polymer chains relax and disperse in the media erosion occur which is known as erosion-controlled release systems (Siepmann & Peppas, 2001). This type of drug release system also can be used for sustained release purposes.

To compare the dissolution release profile from film and wafer matrices f_2 similarity values were calculated. As Table 6.3 demonstrates, the f_2 values are far less than 50 which indicate that the rate of drug dissolution from the polymeric matrices of film and wafer dosage forms are significantly different.

Table 6.3 Comparison of the f_2 values (at 60 min) of drug release from films and wafers.

Model drug loaded within the matrices	Film f_2 value	Wafer f_2 value
IND (t₆₀)	14.45	13.22
IBU (t₆₀)	14.38	13.06
PM (t₆₀)	14.39	15.04

This observed difference correlated very well with results obtained from swelling studies which showed significantly higher rates of swelling for wafers. This can be attributed to the differences in the microstructures between the porous wafers and dense continuous films (Boateng, *et al.*, 2010).

6.3 *In-vitro* mucoadhesivity

In vitro mucoadhesion tests were performed to predict the stickiness and affinity of the films and wafers to adhere to buccal mucosal surfaces. According to the chemical structure of mucin the feasibility of hydrogen bonds formation between mucin and CAR 911 results in mucoadhesion. In addition, the possibility of the formation of dative covalent bond between the sulphate group in CAR 911 and NH_2 group in mucin might result in stronger mucoadhesion force. Ruiz and Ghaly (2006) have also confirmed the ability of CAR film to adhere to agar gel surface. In addition to hydrogen bonds mucoadhesion can be generated due to van der Waals bonds or entanglement between polymeric matrix and agar (Smart, 2005). Also pH at the mucoadhesive interface affects the adhesion of mucoadhesives owing to generation of ionizable groups.

As CAR 911 is a polyanion and the local pH=6.2 is above the $\text{pK}=6.1$, it will be mostly ionized and result in enhanced mucoadhesion. Shaikh and co-workers (2011) stated that “the maximum mucoadhesive strength of polyanion is observed around pH 4–5 however, it decreases gradually above the pH of 6”. The application of CAR 911 based buccal dosage form in media with pH=6.2 is not expected to have a negative impact on mucoadhesion force since the pH is not considerably higher than 6. During the mucoadhesivity studies work of adhesion which is the work required to overcome the attractive forces between the surface of the film or wafer and the surface of the agar was measured.

The stickiness factor identified as maximum force (N) required for detaching the film or wafer from the surface of the agar. Also cohesiveness is defined the distance (mm) film or wafer travels to detach from the agar surface. All of these factors are correlated with the mucoadhesion characteristics and the strength of the bonds formed between the polymeric matrix and agar during the contact time (Bansal *et al.*, 2009).

6.3.1 Film mucoadhesion

Boyapally, *et al.*, (2010) reported that the highest work of adhesion and detachment force would be dependent on the formation of hydrogen bonds between the functional (hydroxyl) groups of the CAR 911 and the agar substrate. Physical entanglement is also associated with the highest detachment forces due to chain inter-locking induced following the inter-diffusion of the polymer chains into the agar glycoproteins. In addition, to obtain the highest work of adhesion and mucoadhesion force, the polymeric matrix should be in the non-ionized form. CAR 911 with $pK_a=6.2$ at the pH corresponding saliva (6.2-6.8) is not ionized which induces the mucoadhesion force.

Results for the film have been summarized in Table 6.4. Interestingly the results demonstrated that addition of drugs decreased the mucoadhesive strength of the film which could be due to a decrease in the hydrogen bonds between film matrix and agar. Incorporating the hydrophobic drugs suppressed the films' work of adhesion slightly from 0.47 N.mm in blank film to 0.34 and 0.32 N.mm in IND and IBU loaded films respectively. However the statistical results derived from one-way Anova tests showed that the effect of hydrophobic drugs on the strength of mucoadhesion (stickiness) compared with the blank film was not significant ($P=0.638$ for IND loaded film and $P=0.124$ for IBU loaded film). High swelling index in IND and IBU films promotes rapid interaction with the agar, due to the large adhesive surface, leading to effective adhesion. Hydrogen bonding (secondary bonds) is the main mechanism for enhanced adhesion of CAR 911 matrices due to the large number of hydroxyl groups, which enhance hydrogen bond formation. This can be attributed to the more acidic nature of IBU and IND which provide more hydrogen bond sites for CAR 911 following the decrease in the pH of the medium. Consequently the observed strength in IBU and IND films behaviour is probably due to chain interpenetration followed by the formation of secondary mucoadhesion bonds with the agar. As the polymer chains undergo rapid swelling, the interpenetration into the interfacial region occurs, whereas the extent of the adhesion in PM films is only superficial (Duchen, *et al.*, 1988; Nair, *et al.*, 1996). PM (hydrophilic model drug) loaded film showed a significantly lower work of adhesion and stickiness compared with the blank film ($P=0.006$).

The significant suppression in stickiness for PM loaded films is probably due to the higher swelling index which results in a slippery mucilage that loses mucoadhesion contact. However it might be due to the basic nature of the PM which increases the pH of the agar surface and consequently increase the CAR 911 ionized proportion thereby suppressing the mucoadhesion ability.

In addition the higher percentage of model drug (PM) could have played a critical role in the reduction of mucoadhesion since the hydrogen bond between CAR 911 and mucoadhesive surface are displaced by new hydrogen bonds between the CAR 911 and PM. Sheikh and co-workers (2011) also observed that the ratio of drug/polymers influence the mucoadhesion properties.

Table 6.4 Mucoadhesivity results for films formulated with different model drugs in gels containing 2.5% w/w of CAR 911, 4% w/w P407 with the appropriate content of PEG 600 for each sample (mean \pm s.d. n= 3).

Film sample	Work of Adhesion (N.mm)	Stickiness (N)	Cohesiveness (mm)
Blank film	0.47 \pm 0.06	1.18 \pm 0.21	0.65 \pm 0.18
Film + 0.6% w/w IND	0.34 \pm 0.04	0.98 \pm 0.24	0.57 \pm 0.14
Film + 0.8% w/w IBU	0.32 \pm 0.01	0.84 \pm 0.23	0.62 \pm 0.25
Film + 1.6% w/w PM	0.14 \pm 0.03	0.36 \pm 0.12	0.58 \pm 0.11

6.3.2 Wafer mucoadhesion

Following the attachment of wafers on the agar surface mucoadhesivity bonds between CAR 911 and agar are formed. This could be as a consequence of water absorption from the agar and formation of hydrogen and dative covalent bonds as previously noted.

Table 6.5 Mucoadhesivity profile for wafers formulated with gels comprising CAR 911, P407 and various ratios of PEG 600 (mean \pm s.d, n= 3).

Sample wafer on agar	WOA (N.mm)	Stickiness (N)	Cohesiveness (mm)
1.5% CAR 911 + 4% P407	0.36 \pm 0.11	0.99 \pm 0.35	0.36 \pm 0.15
1.5% CAR 911 + 4% P407 + 3.3% PEG	0.33 \pm 0.17	0.78 \pm 0.29	0.67 \pm 0.23
1.5% CAR + 4% P407 + 5.5% PEG	0.31 \pm 0.14	0.95 \pm 0.19	1.10 \pm 0.31
2% CAR 911+ 4% P407	0.39 \pm 0.08	1.08 \pm 0.21	0.34 \pm 0.11
2% CAR 911 + 4% P407 + 4.4% PEG	0.47 \pm 0.29	1.77 \pm 0.23	0.41 \pm 0.27
2% CAR 911+ 4% P407 + 5.5% PEG	0.31 \pm 0.18	0.79 \pm 0.11	0.42 \pm 0.09
2.5% CAR 911 + 4% P407	0.43 \pm 0.40	0.81 \pm 0.35	0.69 \pm 0.13
2.5% CAR 911 + 4% P407+ 5.5% PEG	0.31 \pm 0.14	1.29 \pm 0.09	0.42 \pm 0.21

According to Table 6.5 which is the work of mucoadhesivity and maximum force that was applied to detach the wafers from the surface (stickiness) of the agar was positively affected by PEG 600. Results showed that maximum mucoadhesivity is observed for the wafer comprising 2% w/w of CAR 911 and 4% w/w P407 in the presence of 4.4% PEG 600 which previously showed appropriate flexibility to administer in mucosal area or remain stable during handling. The mucoadhesion and swelling index should be correlated since too much moisture and high degree of swelling produce slippery mucilage which can be easily removed from the mucosal surfaces. The content of the PEG 600 as a plasticizer is correlated to the amount of water within the polymeric matrix.

In the presence of higher amounts of PEG 600, the quantity of water increased that result in the drug precipitation and a slight decrease in the adhesive performance (Shaikh, *et al.*, 2011). Therefore, the amount of the PEG 600 in the system should be kept at the lowest optimum level. The overall observations indicated that the most effective mucoadhesion profile would be obtained at certain polymer combinations and optimum ratio of CAR 911 to PEG 600.

Table 6.6 Mucoadhesivity profile for wafers formulated with gels containing CAR 911, P407 and various ratios of PEG 600 (n= 3).

Wafer sample	Work of Adhesion (N.mm)	Stickiness (N)	Cohesiveness (mm)
Blank wafer	0.63 ± 0.06	1.77 ± 0.24	0.41 ± 0.08
Wafer + 0.6% w/w IND	0.38 ± 0.04	1.29 ± 0.19	0.34 ± 0.03
Wafer + 0.8% w/w IBU	0.43 ± 0.01	1.36 ± 0.31	0.39 ± 0.11
Wafer + 1.8% w/w PM	0.78 ± 0.14	1.85 ± 0.27	0.60 ± 0.15

The mucoadhesion results for the drug loaded wafers indicated that incorporating the hydrophobic drugs (IBU and IND) in the wafers' matrix resulted in a slight decrease in mucoadhesion affinity compared with blank wafer though it was not significant according to statistical results obtained from one-way Anova (P=0.0532).

Interestingly, addition of PM which is a hydrophilic drug had a positive effect on the work of adhesion, stickiness and cohesiveness values. The swelling index of the PM loaded wafer confirmed the lower swelling affinity in comparison to blank wafer or IBU and IND loaded wafers which helped the wafer to stabilize on the agar surface. This could be attributed to the swelling extent and prevention of slippery mucilage on the agar surface which decreases the mucoadhesion force. However, it could also be due to additional secondary forces such as van der Waals between wafers' matrix and agar surface in addition to hydrogen and dative covalent bonds and mechanical entanglement.

The overall mucoadhesion results from the blank and drug loaded wafers confirm that porosity plays the most critical role due to affinity to absorb water and produce hydrogen bonds required for mucoadhesivity attraction.

The P value (0.0328) confirmed the significant difference between blank film and wafer mucoadhesion force (stickiness) while hydrophobic drug loaded films and wafers did not follow the same trend and were not significantly different in mucoadhesivity index (P=0.1543). A significant difference between PM loaded wafers and films was observed in their mucoadhesion behaviour (P=0.0009).

In contrast to PM loaded films which might produce slippery mucilage between the film and agar interface, corresponding wafer is able to absorb more water and retain it resulting in less water present on the agar surface and therefore higher force of detachment. This phenomenon could be due to the non-porous nature of the film surface which does not allow water to penetrate the matrix to the same extent as the more porous wafers (Madsen, *et al.*, 1998., Roy, *et al.*, 2009).

The comparison between films and wafers mucoadhesivity results demonstrated the overall effect of porosity on mucoadhesion affinity. This is directly attributed to their ability to absorb water and generate hydrogen bonds. To summarize, wafers are better mucoadhesive dosage forms with acceptable mucoadhesion force which expected to remain in the buccal area for longer period of time compared to films (Sudhakar *et al.*, 2006).

Chapter 7 : Conclusions & future work

7.1 Conclusions

The main advantage of solvent cast films and freeze-dried wafers as potential novel buccal mucosal drug delivery systems is that they contain lower drug loadings to achieve the desirable therapeutic effect compared with traditional systemic therapies such as tablets and capsules. Furthermore, these formulations would be potentially highly acceptable and comfortable subject to non-irritant nature and might be preferred over adhesive tablet in terms of flexibility. They also present the possibility to better protect the mucosa in the case of mouth ulcers or inflamed surfaces in comparison to mucoadhesive buccal tablets which have less flexibility. Both films and wafers possess relatively high mucoadhesive force and therefore less chance of involuntary dislodging by the tongue and therefore expected to allow better retention in the buccal region compared with sublingual dosage form.

The overall outcome from this study was the formulation design, development and optimization of stable solvent cast films and freeze-dried wafers as potential platforms for buccal drug delivery. Optimised films with ideal flexibility and toughness were obtained from the polymeric gel comprising 2.5% w/w CAR 911 in combination with 4% w/w P407. Maximum drug loading of 0.8% w/w IBU and 0.6% w/w IND was achieved with 6.5% w/w PEG 600. However, the content of PEG 600 required for loading a maximum 1.6% w/w of the more water soluble PM was 6% w/w. Similarly, optimized wafers were developed from gels comprising 2% w/w CAR 911, 4% w/w P 407 and 4.4% w/w PEG 600 with maximum drug loadings of 0.8% w/w IBU, 0.6% w/w IND and 1.8% w/w PM. These percentages correspond to 4.41%, 5.79% and 11.34% of the total dry weight of films for IND, IBU and PM, respectively as well as 5.45%, 7.14% and 14.40%, respectively of total wafer dry weight. The optimum formulation was the one with an ideal balance between flexibility, swelling capacity and mucoadhesivity which is expected to enable longer contact time and patient convenience during handling and application.

Thermal analysis showed that an interaction occurred between PEG 600 and P407 within the films. However, the extent of such interactions was dependent on the ratio of the two components within the film.

The interaction occurred due to the formation of inter-chain hydrogen bonding between PEG 600 and P407. The key finding of this study lies in the fact that model drugs (IND, IBU and PM), originally added as crystalline polymorphs, were converted into a stable amorphous form during film formation and freeze-drying and this has an impact on the drug release profiles from the film and wafer matrix in dissolution medium simulating the pH of saliva at 37°C.

Interestingly the most significant observation during hydration and swelling studies was the higher ability of wafers to swell in the buffer solution compared with films with significant differences in the drug release characteristics between the two formulation types.

By fitting of dissolution data to Korsmeyer-Peppas equation, the results showed that the drugs were released from the film matrix following diffusion and swelling with the kinetics of release following super case II transport. This indicated that drug solubility and mass transfer (diffusion) phenomena were involved in drug release as a consequence of zero order kinetics where the plasma concentration of a drug within the polymeric matrix decreases at a constant rate. For IBU and IND loaded wafers $n > 0.89$ corresponding to the super case II transport drug released from the polymeric matrix showed that drug release occurred due to diffusion and erosion. However, this value for PM loaded wafer showed $n \leq 0.45$ corresponding to Fickian diffusion release (case I diffusional).

The p value for drug release rate comparison between films and wafers confirmed that the drug release rate from the wafer's matrix was significantly higher than film's matrix owing to the differences in porosity. In addition, the results showed that drug release rates were faster at pH corresponding to that of saliva than at slightly acidic pH for deionised water which could be related to ionisation suppression of the slightly acidic IBU or IND at the lower pH of deionised water. This effect was not observed for PM loaded films and wafers and could be attributed to the weakly basic nature of the drug. The positive effect of pH on the drug release rate for dosage forms intended for buccal applications is considered favourable. However the dissolution profiles were more significantly affected by polymers' (CAR 911 and P407) content with increasing CAR content resulting in sustained drug release.

In addition, the drug loading capacity of hydrophilic drugs in wafer was about 20% higher than film and attributed to the differences in the physical nature of the two formulations; wafers being more porous with higher volume compared to the denser and thinner films.

In summary the differences between the physico-mechanical properties of the films and wafers will enable formulators to design appropriate buccal formulations to achieve the expected therapeutic effect.

7.2 Future work

Studies which would provide additional information with regards to the developed films and wafers could involve the following.

- Investigation of the effect of polymeric matrix on alternative drugs with different log P such as lipophilic drugs ({e.g. steroids, thyroid hormones or anti-fungal drugs}) which are required at lower doses than the model drugs used.
- Also additional *in-vivo* studies to determine bioadhesivity on *ex-vivo* tissues model surfaces.
- Investigation of the mechanism of drug incorporation into the PEG 600/P407 mixture. For example the possibility of formation of micelles or nanoparticle could be explored.
- Further supplementary studies should be performed to obtain *in-vivo* data for drug release and transport across buccal tissues and systemic drug bioavailability.

Chapter 8 : References

- Ahmad, Z., Stride, E. Edirisinghe, M. 2009. Novel preparation of transdermal drug-delivery patches and functional wound healing materials. *J Drug Target*, 17, 724-729.
- Alanazi, F.K., Abdel Rahman, A.A., Mahrous, G.M., Alsarra, I.A. 2007. Formulation and physicochemical characterization of buccoadhesive films containing ketorolac. *J Drug Deliv Sci*, 7 (3), 183-192.
- Alfadhel, M., Puapermpoonsiri, U., Ford, S.J., McInnes, F.J, van der Walle C.F. Lyophilized inserts for nasal administration harboring bacteriophage selective for *Staphylococcus aureus*: in vitro evaluation. *Int J Pharm*, 416(1), 280-287.
- Allen, T.M., Cullis, P.R. 2004. Drug delivery systems: Entering the mainstream. *Science*, 303, 1818-1822.
- American Society of Health-System Pharmacists.2008-2009. Best Practices for Hospital & Health-System Pharmacy Positions & Guidance Documents. Bethesda: American Society of Health-System Pharmacists (ASHP), p16-19
- Andrews, G. P., Jones, D. S., Abu Diak, O., Margetson, D. N., McAllister, M. S., 2009. Hot-melt extrusion: an emerging drug delivery technology. *Pharm Technol Eur*, 21, 27-32.
- Angell, C.A. 2008. Glass formation and glass transition in supercooled liquids, with insights from study of related phenomena in crystals. *J Non-Cryst Solids*, 354, 4703-4712.
- Angell, C.A. 1995. The old problems of glass and the glass transition, and the many new twists. *Proc Natl Acad Sci*, 92, 6675-6682.
- Angell, C.A., Moynihan C.T., Hemmati, M. 2000. Strong and super-strong liquids and an approach to the perfect glass state via phase transition. *J Non-Cryst Solids*, 274, 319-331.
- Anderson, N.S., Dolan, T.C.S., Reeds, D.A. 1973. Carrageenans .part VII. Polysaccharides from *Eucheuma-Spinosum* and *Eucheuma-Cottonii*- Covalent structure of Iota-carrageenan. *J Chem Soc Perkin Trans*, 1, 2173-2176.
- Ansel, H.C. and Popovich, N.G., 2004. Pharmaceutical Dosage Forms and Drug Delivery Systems, 5th Edition. Philadelphia, Pennsylvania, USA: Lea and Febiger; p152-158.
- Aronson, J.K. 2009. Routes of drug administration: uses and adverse effects: Part 2: sublingual, buccal, rectal, and some other routes. *Adverse Drug React Bulletin*, 254, 975-

- 978.
- Averineni, R.K., Sunderajan, S.G., Mutalik, S., Nayak, U., Shavi, G., Arumugam, K., Meka, S. R., Pandey, S. & Nayanabhirama, U. 2009. Development of mucoadhesive buccal films for the treatment of oral sub-mucous fibrosis: a preliminary study. *Pharmaceut Devel Tech*, 14, 199-207.
 - Balji, N., Peppas, N.S. 1996. Molecular analysis of drug delivery systems controlled by dissolution of the polymer carrier. *J Pharm Sci*, 89, 297-304.
 - Bansal, K., Rawat, M. K., Jain, A., Rajput, A., Chaturvedi T. P., Singh, S. 2009. Development of Satranidazole Mucoadhesive Gel for the Treatment of Periodontitis. *AAPS PharmSciTech*, 10 (3), 716-723.
 - Barichello, J.M., Morishita, M., Takayama, K. Nagai, T. 1999b. Absorption of insulin from Pluronic F-127 gels following subcutaneous administration in rats. *Int J Pharm*, 184, 189-198.
 - Barley, J. 2009. Basic principle of freeze drying. Product manager. SP Industries Inc. Unpublished.
 - Barreiro-Iglesias, R., Aavarez-Lorenzo, C., Concheiro, A. 2002. Thermal and FTIR characterization of films obtained from carbopol/surfactant aqueous solutions. *J Therm Anal Calorim*, 68, 479-488.
 - Biopharma Process Systems. Introduction to freeze drying. Available at: <<http://www.biopharma.co.uk/2010/11/29/introduction-to-freeze-drying/>>. [Accessed 29 July 2011].
 - Bley, H., Fussnegger, B., Bodmeier, R. 2010. Characterization and stability of solid dispersions based on PEG/polymer blends. *Int J Pharm*, 390(2), 165-173.
 - Boateng, J.S., Auffret, A.D., Humphrey, M. J., Matthews, K.H. Eccleston, G.M., Stevens H.N.E. .2002. The mechanical properties of solvent cast films. *AAPS Pharmsci*, 4(4), T3186.
 - Boateng JS, Auffret, AD, Humphrey MJ, Matthews KH, Stevens HNE., Eccleston GM. Mechanical and dissolution properties of freeze-dried and solvent cast films. *AAPS Pharmsci*, 2003, 5(4), s4101.
 - Boateng, J.S., Matthews, K.H., Stevens, H.N.E. Eccleston, G.M. 2008. Wound healing

- dressings and drug delivery systems: A review. *J Pharm Sci*, 97, 2892-2923.
- Boateng, J.S., Stevens, H.N., Eccleston, G.M., Auffret, A.D., Humphrey, M.J. Matthews, K.H. 2009. Development and mechanical characterization of solvent-cast polymeric films as potential drug delivery systems to mucosal surfaces. *Drug Dev Ind Pharm*, 35(8):986-996.
 - Boateng, J.S., Auffret, A.D., Matthews, K.H., Humphrey, M.J., Stevens, H.N. E., Eccleston, G.M. 2010. Characterisation of freeze-dried wafers and solvent evaporated films as potential drug delivery systems to mucosal surfaces. *Int J Pharm*, 389, 24-31.
 - Boyapally, H., Nukala, R. K., Bhujbal, P and Douroumis, D.2010. Controlled release from directly compressible theophylline buccal tablets. *Colloids Surfaces B*, 77, 227–233.
 - Breuer, E., Chorchade, M., Fischer, J., Golomb, G. 2009. Glossary of terms related to pharmaceuticals. *IUPAC Publication*, 81.
 - Bugay, D.E. 2001. Characterization of the solid-state: spectroscopic techniques. *Adv Drug Deliv Rev*, 48, 43-65.
 - Casolaro, M., Bottari, S., ITO, Y. 2006. Vinyl polymers based on L-histidine residues. Part 2. Swelling and electric behaviour of smart poly (ampholyte) hydrogels for biomedical applications. *Biomacromolecules*, 7, 1439-1448.
 - Chakravarty, P., Alexander, K.S., Riga, A.T., Chatterjee, K. 2011. Tolbutamide-PEG 8000 Solid Dispersions. University of Toledo: Amgen Inc Fund, p31-37
 - Chiellini, E., Sunamoto, J., Migliaresi, C., Ottenbrite, R. M., Cohn, D. 2001. *Biomedical Polymers and Polymer Therapeutics*. New York: Kluwar Academic/ Plenum Publishers, p 75-88.
 - Chieng, N., Rades, T Aaltonen, J. 2011. An overview of recent studies on the analysis of pharmaceutical polymorphs. *J Pharm Biomed Anal*, 55 (4), 618-644.
 - Chowdary, K.P.R and Srinivasa Rao, Y. 2003. Mucoadhesive Microcapsules of Glipizide: Characterization, In Vitro And In Vivo Evaluation. *Ind J Pharm Sci*, 65 (3), 279-284
 - Cilurzo, F., Cupone, I.E., Minghetti, P., Selmin, F., Montanari, L. 2008. Fast dissolving films made of maltodextrins. *Eur J Pharm Biopharm*, 70, 895-900.
 - Cosslett, V.E. 1986. Scanning electron-microscopy-physics of image-formation and microanalysis- Reimer, L. *Nature*, 323, 212-212.
 - Craig, D.Q.M. 1995. A review of thermal methods used for analysis of the crystal form,

- solution thermodynamics and glass-transition behaviour of polyethylene glycols. *Thermochim Acta*, 248, 189-203.
- De Brabander, C., Van Den Mooter, G., Vervaet, C., Remon. J.P.2002. Characterization of ibuprofen as a non-traditional plasticizer of ethyl cellulose. *J Pharm Sci*, 91 (7), 1675-1785.
 - De Moura, M.R., Aouada, F.A., Avena-Bustillos, R.J., Mchugh, T.H., Krochta, J.M. Mattoso, L.H.C. 2009. Improved barrier and mechanical properties of novel hydroxypropyl methylcellulose edible films with chitosan/tripolyphosphate nanoparticles. *J Food Process Eng*, 92, 448-453.
 - Degim, T., Eglen, B. Ocak, O. 2006. A sustained release dosage form of acyclovir for buccal application: An experimental study in dogs. *J Drug Target*, 14, 35-44.
 - Di Martino, P., Guyot-Hermann, A.M., Conflant, P., Drache, M., Guyot, J.C. 1996. A new pure PM for direct compression: The orthorhombic form. *Int J Pharm*, 128(1-2), 1-8.
 - Dirim, S.N., Ozden, H. O., Bayindirli, A., Esin, A. 2004. Modification of water vapour transfer rate of low density polyethylene films for food packaging. *J Food Eng*, 63, 9-13.
 - Dixit, R.P., Puthli, S.P. 2009. Oral strip technology: Overview and future potential. *J Control Release*, 139, 94-107.
 - Donhowe, I.G. & Fennema, O. 1993. The effects of solution composition and drying the effects of solution composition and drying temperature on crystallinity, permeability and mechanical-properties of methylcellulose films. *J Food Process and Preservation*, 17, 231-246.
 - Duchene, D., Touchard, F and Peppas, N.A.1988. Pharmaceutical and medical aspects of bioadhesive systems for drug administration. *Drug Dev Ind Pharm*. 14, 283–318.
 - Ediger, M. D., Angell, C. A., Nagel, S. R. 1996. Supercooled Liquids and Glasses. *J Phys Chem*, 100, 13200-13212.
 - Eliasson, L., Birkhed, D., Carlen, A. 2009. Feeling of dry mouth in relation to whole and minor gland saliva secretion rate. *Arch Oral Biol*, 54(3), 263-267.
 - El-Samaligy, M.S., Afifi, N.N., Mahmoud, E.A. 2006. Evaluation of hybrid liposomes-encapsulated silymarin regarding physical stability and in vivo performance. *Int J Pharm*, 319, 121-129.
 - Figueiras, A., Sarraguça, J. M. G., Carvalho, R.A., Pais, A and Veiga, F. J. B. Interaction

- of omeprazole with a methylated derivative of beta-cyclodextrin: phase solubility, NMR spectroscopy and molecular simulation. 2007. *Pharm Res*, 24(2):377-89.
- Gabriele, A., Spyropoulos, F., Norton, I. T. 2009. Kinetic study of fluid gel formation and viscoelastic response with kappa-carrageenan. *Food Hydrocolloids*, 23, 2054-2061.
 - Giannola L., De Caro, V., Giandalia. G., Siragusa, M.G., Campisi, G., Florena, A.M and Ciach, T. 2007. Diffusion of naltrexone across reconstituted human oral epithelium and histomorphological features. *Eur J Pharm Biopharm*, 65(2), 238-46.
 - Giron, D. 2001b. Investigations of polymorphism and pseudo-polymorphism in pharmaceuticals by combined thermoanalytical techniques. *J Therm Anal Calorim*, 64, 37-60.
 - Gong, C.Y., Shi, S., Dong, P. W., Zheng, X. L., Fu, S. Z., Guo, G., Yang, J. L., Wei, Y. Q., Qian, Z. Y. 2009. In vitro drug release behavior from a novel thermosensitive composite hydrogel based on Pluronic f127 and poly (ethylene-glycol)-poly (epsilon-caprolactone)-poly (ethylene-glycol) copolymer. *BMC Biotechnol*, 9, 8.
 - Gijpferich, A. 1996. Mechanisms of polymer degradation and erosion. *Biomaterials*, 17, 103-114.
 - Graeser, K.A., Patterson, J.E., Zeitler, J.A., Gordon, K.C., Rades, T. 2009. Correlating thermodynamic and kinetic parameters with amorphous stability. *Eur J Pharm Sci*, 37, 492-498.
 - Grant, Y., Matejtschuk, P., Dalby, P.A. 2009. Rapid optimization of protein freeze-drying formulations using ultra scale-down and factorial design of experiment in microplates. *Biotechnol Bioeng*, 104, 957-64.
 - Hamidi, M., Azadi, A., Rafiel, P. 2008. Hydrogel nanoparticles in drug delivery. *Adv Drug Deliv Rev*, 60, 1638-1649.
 - Hanke, L. 2010. *Handbook of Analytical Methods for Materials*, Plymouth: Materials Evaluation and Engineering, Inc. p34-45.
 - He, C., Kim, S.W., Lee, D. S. 2008. In situ gelling stimuli-sensitive block copolymer hydrogels for drug delivery. *J Control Release*, 127, 189-207.
 - Hearnden, V., Sankar, V., Hull, K., Jurase, D. V., Greenberg, M., Kerr, A. R., Lockhart, P. B Lauren., Patton, L., Porter, S and Thornhill, M. H. 2011. New developments and opportunities in oral mucosal drug delivery for local and systemic disease. *Adv Drug*

- Deliv Rev.* 153, 106–116.
- Hoare, T. R., Kohane, D.S. 2008. Hydrogels in drug delivery: Progress and challenges. *Polymer*, 49, 1993-2007.
 - Hoffman, A.S. 2002. Hydrogels for biomedical applications. *Adv Drug Deliv Rev*, 54, 3-12.
 - Hussein, G.A., Pitt, W.G. 2008. Micelles and nanoparticles for ultrasonic drug and gene delivery. *Adv Drug Deliv Rev*, 60, 1137-1152.
 - Ivanisevic, I., McClurg, R. B and Schields, P. J. 2010. *Uses of X-Ray Powder Diffraction in the Pharmaceutical Industry*, New York: John Wiley & Sons, Inc, p 38-45.
 - Jennings, V., Schafer-Korting, M., Gohla, S. 2000. Vitamin A-loaded solid lipid nanoparticles for topical use drug release properties. *J Control Release*, 66, 115-126.
 - Ji, J., Tay, F., Ilescu, C., Miao, J. 2006. Microfabricated Silicon Microneedle Array for Transdermal Drug Delivery, *J Physiol: Conference Series*, 34, 1127–1131.
 - Jones, D. 2004. *Pharmaceutical applications of polymers for drug delivery*, Shrewsbury: Smithers Rapra Publishing, p13-37
 - Joshi, M., Müller, R., 2009. Lipid nanoparticles for parenteral delivery of actives. *Eur J Pharm Biopharm*, 71(2), 161-172.
 - Kamada, K., Yoshimura, S., Murata, M., Murata, H., Nagai, H., Ushio, H., Terada, K. 2009. Characterization and monitoring of pseudo-polymorphs in manufacturing process by NIR. *Int J Pharm*, 368, 103-108.
 - Kasper, J.C., Friess, W. 2011. The freezing step in lyophilisation: Physico-chemical fundamentals, freezing methods and consequences on process performance and quality attributes of biopharmaceuticals, *Eur J Pharm Biopharm*, 78, 248–263.
 - Kauzmann, W. 1933. The Kauzmann paradox- A Thermodynamic quandary- a citation-classic commentary on the nature of the glassy state and the behaviour of liquids at low-temperatures. *CC/Eng Tech Appl Sci*, 8-8.
 - Kislalioglu, M.S., Khan, M.A., Blount, C., Goettsch, R.W., Bolton, S. 2006. Physical characterization and dissolution properties of IBU: Eudragit coprecipitates, *J Pharm Sci*, 80, 799-804.
 - Kiparissides, C., Kammona, O. 2008. Nanotechnology advances in controlled drug delivery systems. *Physica Status Solidi C–Curr Top Solid State Physics*, 5(12), 3828-

3833.

- Klang, S.H., Frucht-Pery, J., Hoffman, A., Benita, S. 1994. Physicochemical characterization and acute toxicity evaluation of a positively-charged submicron emulsion vehicle. *J Pharm Pharmacol*, 46(12), 986-93.
- Kydonieus, L. 2004. *Treatise on Controlled Drug Delivery*. New York: Marcel Dekker, p103-111.
- Laidler, K.J., Meiser, J.H., Sanctuary, B.C. 2003. *Physical Chemistry*, 4th edition, Boston: Houghton Mifflin Company, p25-278.
- Lee, J. W., Park, J. H., Robinson, J. R. 2000. Bioadhesive-based dosage forms: The next generation. *J Pharm Sci*, 89, 850-866.
- Li, S., Tiwari, A., Prabakaran, M., Arayal, S. 2010. *Smart Polymer Materials for Biomedical Applications*, Hauppauge: Nova Science Publishers, Inc, p79-112.
- Liekweg, A., Westfeld, M., Jaehde, U. 2004. From oncology pharmacy to pharmaceutical care: new contributions to multidisciplinary cancer care. *Support Care Cancer*, 12, 73-79.
- Lin, C and Metters, A.T. 2006. Hydrogels in controlled release formulations: Network design and mathematical modelling. *Adv Drug Deliv Rev*, 58(12-13), 1379-1408.
- Llabot, J. M., Manzo, R. H and allemande, A. 2002. Double-layered mucoadhesive tablets containing nystatin. *AAPS PharmSciTech*, 3(3), 47-52.
- Loth, H., Schreiner, T., Wolf, M., Schittkowski, K., Schafer, U. 2007. Fitting drug dissolution measurements of immediate release solid dosage forms by numerical solution of differential equations. *Academic Press*, 1-12.
- Maccaroni, E., Alberti, E., Malpezzi, L., Masciocchi, N., Pellegatta, C. 2008. Characterisation of pharmaceuticals by XRPD and thermal analysis: bupropion hydrochloride. *J Pharm Sci*, 97, 5229-5239.
- Madsena, F., Ebertha, K and Smartb, J. D. 1998. A rheological examination of the mucoadhesive/mucus interaction: the effect of mucoadhesive type and concentration. *J Control Release*, 50, 167-178.
- Malamataris, S and Avgerinos, A. 1990. Controlled release indomethacin microspheres prepared by using an emulsion solvent-diffusion technique. *Int J Pharm*, 62 (2-3), 105-111.
- Maniruzzaman, M., Boateng, J. S., Bonnefille, M., Aranyos, A., Mitchell, J.C.,

- Douroumis, D. 2011. Taste Masking of Paracetamol by Hot Melt Extrusion: an *in vitro* and *in vivo* evaluation. *Eur J Pharm Biopharm.* 80 (2), 433-42.
- Marsh, T.C., Boyd, D.C. 2008. CHED 30-Thermal analysis in the undergraduate chemistry laboratory: Thermogravimetric analysis and differential scanning calorimetry as an introduction to materials chemistry. *Abstracts of Papers of the American Chemical Society*, 236, 30-CHED.
 - Mathkar, S., Kumar, S., Bystol, A., Olawoore, K., Min, D., Markovich, R. & Rustum, A. 2009. The use of differential scanning calorimetry for the purity verification of pharmaceutical reference standards. *J Pharm Biomed Anal*, 49, 627-631.
 - Matthews, K.H., Stevens, H.N.E., Auffert, A.D., Humphrey, M.J., Eccleston, G.M. 2006. Gamma-irradiation of lyophilised wound healing wafers. *Int J Pharm*, 313, 78-86.
 - Matthews, K.H., Stevens, H.N.E., Auffret, A.D., Humphrey, M.J., Eccleston, G.M. 2008. Formulation, stability and thermal analysis of lyophilised wound healing wafers containing an insoluble MMP-3 inhibitor and a non-ionic surfactant. *Int J Pharm*, 356, 110-120.
 - McGinn, J. 2009. Freeze-dry microscopy improves pharmaceutical efficiency, cost and quality. Westmont, Illinois: The McCrone Group's College
 - Menczel, J.D., Prime, R.B. 2009. *Thermal analysis of polymers: fundamentals and applications*. New Jersey: John Wiley & sons Inc, p343-345.
 - Meng, Q.G., Zhou, J.K., Li, J.G. 2007. Correlation of superheated fragility and glass-forming ability in AlNiPr (Si,Cu) alloys. *Mater Chem Phys*, 102, 39-42.
 - Meng, F., Zhong, Z and Feijen, J. 2009. Stimuli-Responsive Polymersomes for Programmed Drug Delivery. *Biomacromolecules*, 10 (2), 197–209.
 - Merck & Co., I. 2007. *The Merck Manual — Home Health Handbook*. Whitehouse Station: Merck Sharp & Dohme Corp, 72-76.
 - Metcalfe, P.D., Thomas, S. 2010. Challenges in the prediction and modeling of oral absorption and bioavailability. *Curr Opin Drug Discovery Dev*, 13, 104-110.
 - Miller-Chou, B.A., Koenig, J.L. 2003. A review of polymer dissolution. *Prog Polym Sci*, 28,1223–1270
 - Mizrahi, B and Domb, A.J. 2008. Mucoadhesive polymers for delivery of drugs to the oral cavity. *Recent Pat Drug Deliv Formul*, 2(2), 108-19.

- Miyajima, M., Koshika, A., Okada, J., Kusai, A. & Ikeda, M. 1998. Factors influencing the diffusion-controlled release of papaverine from poly (L-lactic acid) matrix. *J Control Release*, 56, 85-94.
- Morales, J.O., McConville, J.T. 2011. Manufacture and characterization of mucoadhesive buccal films. *Eur J Pharm Biopharm*, 77, 187–199.
- Mueller, R.L. 2002. Relevant Applications of Scanning Electron Microscopy in a Pharmaceutical Development Laboratory. Physical Sciences Symposia - Microscopy, Microanalysis and Image Analysis in the Pharmaceutical Industry. *Cambridge J (online)*, 8, 142-143.
- Murdande, S.B., Pikal, M.J., Shanker, R.M., Bogner, R.H. 2010. Solubility Advantage of Amorphous Pharmaceuticals: I. A Thermodynamic Analysis. *J Pharm Sci*, 99, 1254-1264.
- Nail, S.L., Jiang, S., Chongprasert, S., Knopp, S.A. 2002. Fundamentals of freeze-drying. *Pharm Biotechnol*, 14, 281-360.
- Nair, M.K., Chien, Y.W. 1996. Development of anticandidal delivery systems: (II) mucoadhesive devices for prolonged drug delivery in the oral cavity. *Drug Dev Ind Pharm*. 22, 243–253.
- Nangia, A. 2008b. Biorod- bioadhesive based oral delivery system for targeted delivery. *Drug Deliv Tech*, 8, 42-49.
- Newa, M., Bhandari, K.H., Li, D.X., Kim, J.O., Yoo, D.S., Kim, J.A., Yoo, B.K., Woo, J. S., Choi, H.G., Yong, C.S. 2008. Preparation and evaluation of immediate release ibuprofen solid dispersions using polyethylene glycol 4000. *Bio Pharm Bull*, 31, 939-945.
- Nunthanid, J., Huanbutta, K., Luangtana-Anan, M., Sriamornsak, P., Limmatvapirat, S., Puttipipatkachorn, S. 2007. Development of time-, pH-, and enzyme-controlled colonic drug delivery using spray-dried chitosan acetate and hydroxypropyl methylcellulose. *Eur J Pharm Biopharm*, 68(2), 253-9.
- Oh, J.K., Drumright, R., Siegwart, D.J., Matyjaszewski, K. 2008. The development of microgels/nanogels for drug delivery applications. *Prog Polym Sci*, 33, 448-477.
- Passerini, N., Craig D.Q. 2001. An investigation into the effects of residual water on the glass transition temperature of polylactide microspheres using modulated temperature DSC. *J Control Release*, 73(1), 111-115.

- Park, K., Shabaly, H., Park, H. 1993. Biodegradable hydrogels for drug delivery. *Lancaster: Technomic Publishing Company Inc*, p13- 100.
- Prausnitz, M. 2004. Transdermal Micro-needle Drug Delivery System. *Adv Drug Deliv Rev*, 56 (5), 581-587.
- Patel, R.S., Poddar, S.S. 2009. Development and Characterization of Mucoadhesive Buccal Patches of Salbutamol Sulphate. *Curr Drug Deliv*, 6, 140-144.
- Patil, S.B., Sawant, K. K. 2008a. Mucoadhesive Microspheres: A Promising Tool in Drug Delivery. *Curr Drug Deliv*, 5, 312-318.
- Paediatrics, A. O. 2007. Alternative Routes of Drug Administration Advantages and Disadvantages (Subject Review). USA: AAP Publications Retired and Reaffirmed, 5-9.
- Perioli, L., Ambrogi, A., Angelici, F., Ricci, M., Giovagnoli, S., Capuccella, M., Rossi, C. 2004. Development of mucoadhesive patches for buccal administration of IBU. *J Control Release*, 99, 73-82.
- Perumal, V.A., Lutchman, D., Mackraj, I., Govender, T. 2008. Formulation of monolayered films with drug and polymers of opposing solubilities. *Int J Pharm*, 358, 184-191.
- Qi, S., Avalle, P., Saklatvala, R., Craig, D.Q.M. 2008. An investigation into the effects of thermal history on the crystallisation behaviour of amorphous PM. *Eur J Pharm Biopharm*, 69, 364-371.
- Rajput, G.C., Majmudar, F.D., Patel, J.K., Patel, K.N., Thakor, R.S., Patel, B.P., Rajgor, N.B. 2010. Stomach specific mucoadhesive tablets as controlled drug delivery system – A review work. *Int J Pharm Bio Research*, 1(1), 30-41.
- Ranade, V. 1990. Drug delivery systems.3A. Role of polymers in drug delivery. *J Clin Pharmacol*, 30, 10-23.
- Rao, K J. 2002. *Structural chemistry of glasses*. Oxford: Elsevier Science Ltd, 16-25.
- Rathbone, M. J., Michael S. Roberts, M. S., Hadgraft, J. 2007. *Modified-Release Drug Delivery Technology*. London: Informa Healthcare, p38-51.
- Read, B.E. 2004. Viscoelastic behavior of amorphous polymers in the glass-rubber transition region: Birefringence studies. *Polym Eng Sci*, 23, 835-843.
- Reed, K., Lavchak, M. & Scheafer, J. 1994. *Thermogravimetric apparatus*. USA patent application 067355 filed on 05/26/1993.

- Repka, M.A., Gerding, T.G., Repka, S.L., McGinity, J.W. 1999. Influence of plasticizers and drugs on the physical-mechanical properties of hydroxypropylcellulose films prepared by hot melt extrusion. *Drug Dev Ind Pharm*, 25, 625-633.
- Riggelman, R.A., Douglas, J.F., De Pablo, J.J. 2007. Tuning polymer melt fragility with anti-plasticizer additives. *J Chem Phys*, 126.
- Rodríguez-Spong, B., Price, C.P., Jayasankar, A., Adam, J., Rodríguez-Hornedo, M.N. 2004. General principles of pharmaceutical solid polymorphism: a supramolecular perspective. *Adv Drug Deliv Rev*, 56, 241– 274.
- Roy, S., Pal, K., Anis, A., Pramanik, K and Prabhakar, B. 2009. Polymers in Mucoadhesive Drug Delivery System: A Brief Note. *Des Monomers Polym*, 12, 483-495.
- Royall, P.G., Craig, D.Q.M., Doherty, C. 1998. Characterisation of the glass transition of an amorphous drug using modulated DSC. *Pharm Res*, 15, 1117-1121.
- Ruiz, G., Ghaly, E. 2006. Mucoadhesive delivery systems using carrageenan and eudragit RLPO. *Vitae*, 13, 1-2.
- Sabau, A.S., Porter, W.D. 2007. Analysis of a heat-flux differential scanning calorimetry instrument. *Metal Mater Trans B*, 38A, 1546-1554.
- Sarbach, C., Yagoubi, N., Sauzieres, J., Renaux, C., Ferrier, D., Postaire, E. 1996. Migration of impurities from a multilayer plastics container into a parenteral infusion fluid. *Int J Pharm*, 140, 169-174.
- Sarsfield, B. A., Davidovich, M., Desikan, S., Fakes, M., Futernik, S., Hilden, J. L., J. Tan., Yin, S., Young, G., Vakkalagadda, B and, Volk, K. 2006. Powder X-ray diffraction of crystalline phases in amorphous pharmaceuticals, The International Centre for Diffraction Data, [online] Available at <http://www.icdd.com/resources/axa/vol49/V49_47.pdf> [Accessed 12 February 2012].
- Sasaki, S., Koumi, S., Sato, R., Murata, M., Nagasawa, K., Sakurai, E., Hikichi, N. Hayakawa, H. 1998. Kinetics of buccal absorption of propafenone single oral loading dose in healthy humans. *Gen Pharmacol*, 31, 589-591.
- Sato, T., Araki, M., Nakajima, N., Omori, K., Nakamura, T. 2010. Biodegradable polymer coating promotes the epithelisation of tissue-engineered airway prostheses. *J Thorac Cardiovasc Surg*, 139, 26-31.
- Sawatari, C., Kondo, T. 1999. Interchain Hydrogen Bonds in Blend Films of Poly (vinyl

- alcohol) and Its Derivatives with Poly(ethylene oxide). *Macromolecules*, 32, 1949-1955.
- Saxena, P., Salhan, S. Sarda, N. 2004. Comparison between the sublingual and oral route of misoprostol for pre-abortion cervical priming in first trimester abortions. *Hum Reprod*, 19, 77-80.
 - Schneid, S., Gieseler, H. 2009. An overview of the annealing process and rational design of thermal treatment steps in freeze-drying. [online] April 2009 ed. Division of Pharmaceutics, University of Erlangen.
 - Schmidt, A.G., Wartewig, S., Picker, K.M. 2003. Potential of carrageenans to protect drugs from polymorphic transformation. *Eur J Pharm Biopharm*, 56, 101-110.
 - Schwegman, J. 2010. Basic Cycle Development Techniques for Lyophilized Products. [Technical note] 2 April 2009 ed. VirTis / FTS company.
 - Schwegman, J. 2009. Understanding the physical properties of properties of materials in freeze-dried products. [Online] 18 November. Available at: <www.pharmaceuticalonline.com/article.mvc/Basic-Cycle-Development-Techniques-For-Lyophi-0001> [Accessed on 28 August 2011].
 - Semalty, M., Semalty, A., Kumar, G. 2008. Formulation and Characterization of Mucoadhesive Buccal Films of Glipizide. *Ind J Pharm Sci*, 70(1), 43–48.
 - Serra, L., Doménech, J., Peppas, N. 2010. Engineering Design and Molecular Dynamics of Mucoadhesive Drug Delivery Systems as Targeting Agents. *Eur J Pharm Biopharm*, 71(3), 519–528.
 - Shah, B., Kakumanu, V.K., Bansal, A.K. 2006. Analytical techniques for quantification of amorphous/crystalline phases in pharmaceutical solids. *J Pharm Sci*, 95, 1641-1665.
 - Shah, D., Gaud, R.S., Misra A.N., Parikh, R. 2010. Formulation of a water soluble mucoadhesive film of lycopene for treatment of leukoplakia. *Int J Pharm Sci Rev Res*, 2, 6-10.
 - Shaikh, R., Raj Singh, T.R., Garland, M.J., Woolfson, D.A., Donnelly, R.F., 2011. Mucoadhesive drug delivery systems. *J Pharm Bioallied Sci*, 3, 89-100.
 - Siemann, U. 2005. Solvent cast technology – a versatile tool for thin film production. *Progr Colloid Polym Sci*, 130, 1–14.
 - Siepmann, J., Peppas, N.A. 2001. Modeling of drug release from delivery systems based on hydroxypropyl methylcellulose (HPMC), *Adv Drug Deliv Rev*, 48, 139–157.

- Sigurdsson, H., Loftsson, T., Lehr, C. 2006. Assessment of mucoadhesion by a resonant mirror biosensor. *Int J Pharm*, 325, 75-81.
- Singh, A., Singh, S and Puthli, S., Ladas & Parry LLP., 2009. Transmucosal composition. New York. USA. Pat. 10023.
- Skoog, D. A., Holler, F.J., Crouch. S.R. 2006. Principles of instrumental analysis. 6th Ed. Andover: Cengage Learning, p36-83.
- Smart, J.D. 2005. Buccal drug delivery, *Expert Opin Ther Pat*, 2(3), 507-17.
- Smart, J.D. 2005. The basics and underlying mechanisms of mucoadhesion, *Adv Drug Deliv Rev*, 57, 1556– 1568.
- Stephenson, G.A., Forbes, R.A., Reutzel-Edens, S.M. 2001. Characterization of the solid state: quantitative issues. *Adv Drug Deliv Rev*, 48, 67-90.
- Sudhakar, Y., Kuotsu, K and Bandyopadhyay. 2006. Buccal bioadhesive drug delivery-A promising option for orally less efficient drugs. *J Control Release*, 114, 15-40.
- Sun, G.M., Zhang, X.Z. Chu, C.C. 2007. Formulation and characterization of chitosan-based hydrogel films having both temperature and pH sensitivity. *J Mater Sci-Mater M*, 18, 1563-1577.
- Suzuki, S., Lim, JK. 1994. Microencapsulation with carrageenan-locust bean gum mixture in a multiphase emulsification technique for sustained drug release. *J Microencapsul*, 11(2), 197-203.
- Tang, X., Pikal, M. 2004. Design of freeze-drying processes for pharmaceuticals: practical advice. *Pharm. Res*, 21,191–200.
- Tsinontides, S.C., Rajniak, P., Pham, D., Hunke, W.A., Placek, J., Reynolds, S.D. 2004. Freeze drying—principles and practice for successful scale-up to manufacturing. *Int J Pharm*, 280, 1–16.
- Thommes, M. Kleinebudde, P. 2006. Use of kappa-carrageenan as alternative pelletisation aid to microcrystalline cellulose in extrusion/spheronisation. II. Influence of drug and filler type. *Eur J Pharm Biopharm*, 63, 68-75.
- Thommes, M. Kleinebudde, P. 2008. The behavior of different carrageenans in pelletization by extrusion/spheronization. *Pharm Dev Technol*, 13, 27-35.
- Tatavarti, A.S., Dollimore, D., Alexander, K.S. 2002. A Thermogravimetric Analysis of Non-polymeric Pharmaceutical Plasticizers: Kinetic Analysis, Method Validation, and

- Thermal Stability Evaluation. *AAPS PharmSci*, 4 (4), 1-12.
- Varelas, C.G., Dixon, D.G and Steiner, C. 1995. Zero-order release from biphasic polymer hydrogels. *J Control Release*, 34,185–192.
 - Vippagunta, S.R., Brittain, H.G. Grant, D. J. W. 2001. Crystalline solids. *Adv Drug Deliv Rev*, 48, 3-26.
 - Vogelson, T. 2001. Advances in drug delivery systems. *ACP publications*.
 - Watkinson, R.M., Herkenneb, C., Guy, R.H., Hadgraft, J., Oliveirad, G., Lane, M.E., 2009. Influence of Ethanol on the Solubility, Ionization and Permeation Characteristics of IBU in Silicone and Human Skin. *Skin Pharmacol Physiol*, 22, 15–21.
 - Werle, M., Makhlof, A., Takeuchi, H. 2009. Oral protein delivery: a patent review of academic and industrial approaches. *Recent Pat Drug Deliv Formul*, 3, 94-104.
 - Weuts, L., Van Dycke, F., Voorspoels, J., De Corti, S., Stokbroekx, S., Leemans, R., Brewster, M. E., Xu, D., Segmuller, B., Turner, Y., Roberts, M., Davies, M., Qi, S., Duncan Q.C., Reading, M. 2010. Physicochemical properties of the amorphous drug cast films and spray dried powders to predict formulation probability of success for solid dispersions: etravirine, *J Pharm Sci*, 100, 260-274.
 - www.panalytical.com/index.cfm?pid=135.
 - Wu, C., McGinity, J.W. 2001. Influence of ibuprofen as a Solid-State Plasticizer in Eudragit RS 30 D on the Physicochemical Properties of Coated Beads. *AAPS PharmSci Tech*, 2(4), 1-9.
 - Wu, J., Wei, W., Wang, L.Y., Su, Z.G., Ma, G.H. 2007. A thermosensitive hydrogel based on quaternized chitosan and poly (ethylene glycol) for nasal drug delivery system. *Biomater*, 28, 2220-2232.
 - Wu, J., Huang, G., Qu, L., Jing, Z. 2009. Correlations between dynamic fragility and dynamic mechanical properties of several amorphous polymers. *J Non-Cryst Solids*, 355, 1755-1759
 - www.ruthduncan.co.uk/#/recent-lectures/4551764748.
 - www.azonano.com/article.aspx?ArticleID=1538.
 - www.pharmainfo.net/reviews/current-status-buccal-drug-delivery-system.
 - www.vetmed.vt.edu/education/curriculum/vm8054/labs/Lab25/lab25.htm.
 - <http://www.fda.gov/cder/guidance.htm>.

- Yang, L., Alexandridis, P. 2000. Controlled Release from Ordered Microstructures Formed by Poloxamer Block Copolymers. *Contr Drug Deliv.* 752, 364–374.
- Yu, L. 2001. Amorphous pharmaceutical solids: preparation, characterization and stabilization. *Adv Drug Deliv Rev*, 48, 27-42.
- Yuguchi, Y., Thu Thuy, T.T., Urakawa, H., Kajiwara, K. 2002. Structural characteristics of carrageenan gels: temperature and concentration dependence. *Food Hydrocolloids*, 16, 515-522.
- Yuksel, N., Kanik, A.E., Baykara, T. 2000. Comparison of in vitro dissolution profiles by ANOVA-based, model-dependent and -independent methods, *Int J Pharm*, 209, 56–67.

Chapter 9 : Appendix

9.1 Published Manuscripts

1. Farnoosh Kianfar, Babur Chowdhry, Milan Antonijevic, Joshua Boateng. 2011. "Formulation development of a carrageenan based delivery system for buccal drug delivery using IBU as a model drug. *Journal of Biomaterials and Nanobiotechnology*. 1. 2 (5A). 582-595.
2. Farnoosh Kianfar, Babur Z. Chowdhry, Milan D. Antonijevic, Joshua S. Boateng. 2011. Novel films for drug delivery via the buccal mucosa using model soluble and insoluble drugs. *Drug Development and Industrial Pharmacy* DOI: 10.3109/03639045.2011.644294.
3. Farnoosh Kianfar, Babur Chowdhry, Milan Antonijevic, Joshua Boateng. 2011. "Development of stable polymeric lyophilised wafers for mucosal drug delivery using thermal annealing (DSC, freeze-drying)". *AAPS Journal*. 2011, 13(S2). W4274.
4. Farnoosh Kianfar, Babur Chowdhry, Milan Antonijevic, Joshua Boateng. 2011. Carrageenan freeze-dried wafers incorporating PM or IND for mucosal delivery. *AAPS Journal*. 2011, 13(S2). W5357.
5. Farnoosh Kianfar, Babur Z. Chowdhry, Milan D. Antonijevic and Joshua S. Boateng. 2010. Design and formulation of novel polymer-based buccal film, *Journal of Pharmacy and Pharmacology*, 62, 1259.
6. Farnoosh Kianfar, Babur Z. Chowdhry, Joshua S. Boateng and Milan D. Antonijevic. 2010. Investigation of the interaction between poloxamer 407 and poly (ethylene glycol) 600, *Journal of Pharmacy and Pharmacology*, 62, 1341.

9.2 Oral presentations

1. 20th January 2010: "Novel Polymer Based Systems for the Delivery of Drugs via Mucosal Surfaces" at University of Greenwich.
2. 2nd September 2010: "Investigation of the interaction between poloxamer 407 and poly (ethylene glycol) 600" at APS UKPHARMSCI Conference.

9.3 Conference posters

Development of polymeric films incorporating amorphous drug

F. Kianfar, B. Chowdhry, J. Boateng, M.D. Antonijevic
School of Science, University of Greenwich at Medway, Chatham Maritime, ME44TB, UK



Introduction & aim

Incorporation of amorphous drugs in formulations can help address current solubility challenges in drug delivery [1, 2]. The aim of the current study was to develop novel polymeric films for buccal drug delivery and to investigate their ability to incorporate and stabilize an amorphous drug.

Materials & Methods

Materials. carrageenan 911 (gift from BASF originally and received from UK distributor Honeywill & Stein LTD), poloxamer 407 from Aldrich, poly ethylene glycol 600 (PEG) and ibuprofen from Sigma.

Film formulation. Aqueous gels containing carrageenan 911 (2.5%), poloxamer 407 (4%), PEG600 (5.5%) and ibuprofen (0.4% (w/w) were dried in an oven at 60°C for 24 hours to prepare the films.

Analytical techniques. DSC Q2000 instrument (TA Instruments, Crawley, UK) was employed to detect the glass transition and other thermal behaviour of formulated film. Also D8 Advance XRPD instrument (Bruker instruments, Coventry, UK) was employed to conduct crystallographic studies.

Analytical method. DSC experiments involved method was consisting of heating from -80 to 200°C at the rate of 10°C/min before cooling the system rapidly to maintain temperature at -40°C. The second heating cycle was the same process as the first heating cycle and were conducted to evaluate the stability of the ibuprofen in the film. XRPD studies performed from 5 to 60, 2-theta range.

Results & Discussion

DSC as the most practical method to detect glass transition of amorphous compounds is employed to prove the presence of amorphous ibuprofen. DSC results (Fig. 1) confirmed the availability of amorphous form ($T_g = -45^\circ\text{C}$) [3] within the film matrix. In addition, definite absence of the sharp melting point peak belong to crystalline form of ibuprofen ($T_m = 74^\circ\text{C}$) is referenced as a considerable evidence. To confirm the DSC result, XRPD (a crystallographic technique) was employed and proved DSC results (Fig. 2).

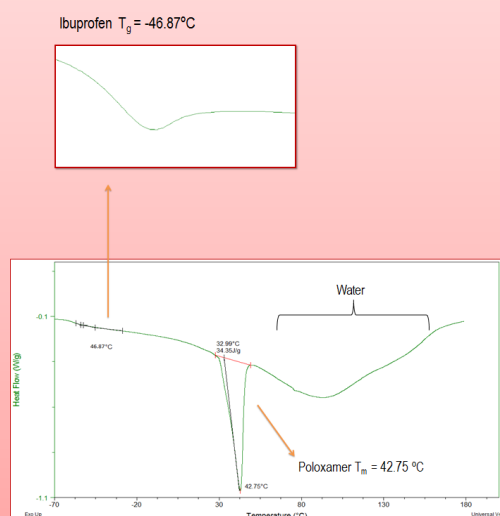


Fig.1. DSC results for film containing ibuprofen

As carrageenan is available in amorphous form the background spectrum was subtracted from the original curve (top one). The absence of the main peak for ibuprofen at about 16.2, 2-theta confirms the DSC results.

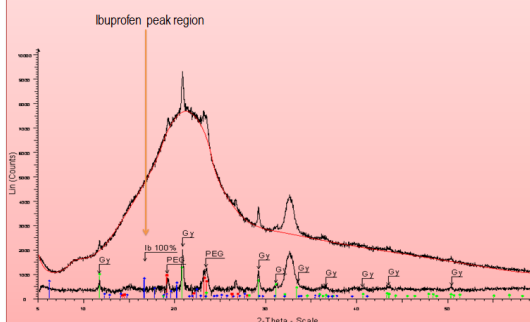


Fig.2. XRPD results for film containing ibuprofen

Conclusions

According to the DSC and XRPD results which confirmed the presence of ibuprofen in the amorphous form in the film, the main aim of the study that was development a novel film to incorporate amorphous ibuprofen and overcome the solubility challenges is achieved. Furthermore, DSC and XRPD nominated as practical techniques to characterise the physico-chemical properties of developed film. Studies are ongoing to assess the stability of the formulation during storage.

Acknowledgment

The authors would like to thank Dr Ian Slipper for his help with XRPD experiments. Also BASF for providing us carrageenan.

References

- [1] R. P. Dixit, and S. P. Puthil, "Oral strip technology: Overview and future potential". *J. Control. Release*, **139** (2009) 94-107.
- [2] B. C. Hancock and M. Parks, "What is the true solubility advantage for amorphous pharmaceuticals?" *Pharm. Res.*, **17** (2000) 397-404.
- [3] E. Dudognon, F. Danède, M. Descamps and N. Correia, "Evidence for a new crystalline phase of racemic ibuprofen." *Pharm. Res.*, **25** (2008) 2853-2858 here.

Contact detail

Farnoosh Kianfar
University of Greenwich at Medway
School of science (Grenville building)

Central Avenue
Chatham Maritime
Kent ME4 4TB

T: 020-8331-7570
F:020-8331-9805
E: Farnoosh1354@gmail.com

Design and formulation of a novel polymer based buccal film

F. Kianfar, B.Z. Chowdhry, M.D. Antonijevic, J.S. Boateng
School of Science, University of Greenwich at Medway, Chatham Maritime, ME4 4TB, UK



Aim and Introduction

The aim of this work was to develop a novel film for delivering drugs into the systemic circulation via the buccal mucosa. The advantage of the buccal mucosa over the sublingual, such as better systemic effects, has led to its exploration as a functional administration route [1]. Buccal formulations can be developed as films and freeze-dried wafers [2] which are suitable alternatives to deliver drugs promptly and safely.

Materials & Methods

Materials: Poloxamer 407 and different polymer grades (911, 379, and 812) of carrageenan known for its bioadhesive viscous modifying properties, were used to select the most appropriate grade for drug loading and PEG 600 and glycerol were used as plasticisers. Model soluble (paracetamol) and insoluble (ibuprofen and indomethacin) drugs known to exhibit polymorphism and with different log P values were chosen for investigating stable amorphous drug formation.

Method: Gels were prepared by dispersing carrageenan in deionised water for 24 hours to allow complete hydration before homogenization and poloxamer added. Films were obtained by pouring the gels into petri dishes and dried in an oven at 60°C for 24 hours. Two sets of films (diameter 90 mm) both containing poloxamer, PEG and carrageenan 911 with or without drug were evaluated for tensile properties in triplicate by Texture Analysis (Stable Microsystems) to select optimum amounts and type of film components.

Results & Discussion

The results from formulation development demonstrated that the best condition for gel formation was to incubate carrageenan in aqueous solution for 24 hours to allow for complete hydration and uniform gel formation which doesn't contain trapped air bubbles or have very high viscosity (Fig.1.).

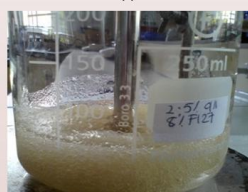


Fig.1. Gel with entrapped air bubbles



Fig.2. Developed buccal film

Carrageenan 911 was used to produce films with no entrapped air bubbles, and of acceptable transparency as well as flexibility (Fig. 2). These characteristics were achieved by the addition of an appropriate plasticizer to obtain strong but reasonably flexible films, as shown by the tensile results. The most suitable choice of plasticizer, which also allowed an enhancement in the amount of drug incorporated, was PEG 600 (PEG 600:carrageenan 11:5). This ratio produced the required films with appropriate balance between flexibility and strength which are essential for physical stability of films during handling.

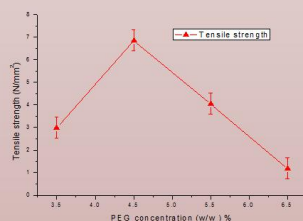


Fig. 3. Tensile testing : the effects of PEG 600 concentration on the film's tensile strength (n=3).

The data in Fig. 4 demonstrates the differences in elastic modulus as a function of concentration of PEG 600. There were significant reproducible differences in elastic properties of the films.

Examination of the plots of PEG 600 concentration against film elongation and elastic modulus showed that 5.5 % w/w PEG 600 was the optimum formulation with an elastic modulus value approximately 2.5 N/mm² (Fig. 4). Generally increasing drug content resulted in slight reduction in elastic modulus but not significantly.

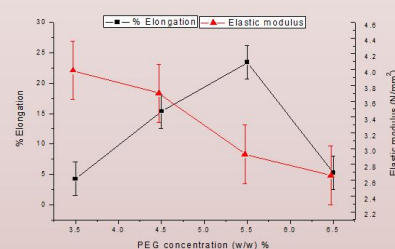


Fig. 4. Tensile testing: the effects of PEG 600 concentration on the film's elastic modulus and elongation (n=3).

Optimized ratios of the starting materials in the initial gel used to prepare the polymer films were 2.5% carrageenan 911, 5.5% PEG 600 and 4% (w/w) poloxamer 407 as well as one of the following drugs: 1.6% paracetamol, 0.4% ibuprofen, and 0.3% (w/w) indomethacin.

Conclusions

Solvent cast swellable buccal films containing optimized ratios of poloxamer, carrageenan and PEG have been designed and developed. The optimum combinations of the above polymers helped maximise drug loading and produced films with ideal mechanical properties (right balance of strength and flexibility).

References

- [1] R. P. Dixit, and S. P. Puthil, "Oral strip technology: Overview and future potential". *J. Control. Release*, **139** (2009) 94-107.
- [2] A.M. Hillery, A. W. Lloyd, J. Swarbrick, "Drug delivery and targeting for pharmacists and pharmaceutical scientists". London, Taylor and Francis, 2001, 7. 186-206.

Contact detail

Farnoosh Kianfar
University of Greenwich at Medway
School of science (Grenville Building)

Central Avenue
Chatham Maritime
Kent ME4 4TB

T: 020-8331-7570
F: 020-8331-9805
E: fk30@gre.ac.uk

Investigation of the interaction between poloxamer 407 and poly(ethylene glycol) 600

F. Kianfar, B.Z. Chowdhry, J.S. Boateng, M.D. Antonijevic,



UNIVERSITY
of
GREENWICH

1 Introduction

The aim of this study was to evaluate the interactions between poly (ethylene glycol) (PEG) 600 and poloxamer 407 prior to their use in a pharmaceutical formulation.

Chemical interactions between various ingredients can alter the stability of pharmaceutical product [1]. Investigating the interaction between starting materials is a pre-requisite to develop a stable high quality pharmaceutical formulation. Changes in melting point [2] directly influence the stability of a product. One of the fundamental changes that might modify the melting point of a compound and consequently alter the stability of the system is the interaction between excipient(s) and API(s). The formation of a mixture following, the interaction between component compounds, influences the characteristics of the system which therefore need to be determined.

2 Methods

Materials: Poloxamer 407 (a block copolymer of ethylene oxide and propylene oxide with molecular weight (MW) between 9,760 to 13,200 and melting point of 56°C) and PEG (average MW about 570 to 600 and melting point between 20 and 25°C).

Analytical techniques: A Q2000 DSC instrument (TA Instruments, Crawley, UK) was employed to investigate the interaction between PEG 600 and poloxamer 407. Samples were prepared by physical mixing of PEG 600 and poloxamer 407 at ratios of (0/100) up to (100/0 %w/w) of PEG/poloxamer at 10% increments followed by solidification. The parameters for the DSC experiments were as follows:

1st heating -40°C to 80°C @ 10°C/min
2nd heating -40°C to 80°C @ 10°C/min
3rd heating -40°C to 80°C @ 10°C/min
Cooling after each heating cycle was at 40°C/min

References

- [1] W. R. Young, "Accelerated Temperature Pharmaceutical Product Stability Determinations" *Drug Dev. Ind. Pharmacy*, **16** (1990) 551-569.
[2] J. R. Davis, "Handbook of Thermal Spray Technology" in thermal technology, ASM International, Material Park, Ohio, 2004, Ch 1, pp 1-36.

4 Conclusion

The results of the DSC analyses showed significant changes in melting point values between the individual samples of PEG 600 and poloxamer and the mixture. This finding confirms that an interaction occurred between the two polymers. However, the extent of interaction varies and depends on the ratios of two compounds in the various mixtures.

3 Result & discussion

Figure 1 shows the melting point values for a series of PEG/poloxamer mixtures. It is evident that with an increase in percentage of poloxamer, the melting point of PEG is decreased from 14.2°C to 0.7°C for pure PEG and 10/90 mixture (PEG/poloxamer), respectively. However, the same effect was not observed with the change in melting point of poloxamer. After addition of 20% of PEG, poloxamer reaches its minimum melting point of 41.2°C and remains fairly constant with further increase of PEG/poloxamer ratio. The most interesting finding is the formation of what is believed to be a complex (mixture) of PEG/poloxamer at ratios of 30/70; 40/60 up to 80/20 with the melting point of the complex being relatively uniform (26.7°C). This additional transition confirms that the two compounds not only physically interact but also form a unique entity that has characteristic properties i.e. melting behaviour.

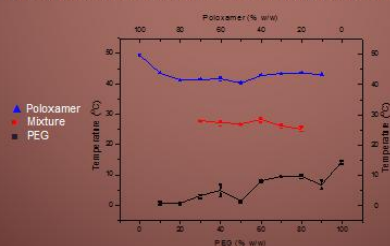


Fig.1. DSC transition onset values for mixture of 0/100 (%w/w) to 100/0 (%w/w) of PEG/ poloxamer.

Contacts:

Farnoosh Kianfar
University of Greenwich at Medway
School of Science (Grenville building)
Central Avenue, Chatham Maritime,
Kent ME4 4TB
T: 020-8331-7570
F: 020-8331-9805
E: fk30@gre.ac.uk

Developing a mucoadhesive freeze-dried wafer as a matrix to deliver drugs through mucosal surfaces



F.Kianfar, B.Z. Chowdhry, M.A. Antonijevic, J.S. Boateng
University of Greenwich, Medway Campus, Chatham Maritime, Kent ME4 4TB, UK

Introduction

The aim of this study was to develop a freeze-dried wafer to deliver drugs via mucosal surfaces. The advantage of freeze-dried wafers over other mucosal dosage forms is their ability to hydrate in body fluids and maintain drug stability due to milder freeze-drying conditions [1].

Materials and methods

Materials: Poloxamer 407 and PEG 600 were purchased from Sigma-Aldrich (Gillingham, UK). κ -Carrageenan 911 (bioadhesive) was a gift from BASF (Cheshire, UK).

Method: Gels, prepared by dispersing κ -carrageenan 911 (CAR), poloxamer 407 (POL) and PEG 600 in deionised water for 24 hours to allow complete hydration, were poured into Petri dishes and placed in a freeze dryer for 42 hours. Wafers were produced with POL and different concentrations of CAR and PEG (plasticizer). Work of compression and mucoadhesivity were evaluated for triplicate samples by texture analysis (Stable Microsystems, UK). Wafer swelling was investigated by placing them in PBS media (pH 6.2) for 2 hours and weight changes measured every 20 minutes.



Fig. 1. Lyophilized wafers.

Contact

Farnoosh Kianfar
University of Greenwich at Medway
School of Science (Grenville building)
Central Avenue, Chatham Maritime, Kent ME4 4TB
T: 020-8331-7570 , E-mail: fk30@gre.ac.uk

Results and discussion

The parameters tested are known to affect the performance characteristics of mucosal formulations. Fig. 1 shows that although the 1st, 3rd and 5th formulations are plasticized to the same extent (CAR:PEG ratio of 1:2.2) and expected to have comparable work of compression, this was not the case due to differences in POL:PEG ratios. The work of compression profiles confirmed that wafers containing 2.5% w/w CAR, 4% w/w POL and 5.5% w/w PEG did not exhibit appropriate flexibility and also had the lowest % swelling capacity (Fig. 3).

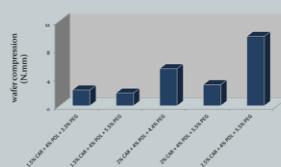


Fig. 2. Compression profile of wafers.

Increasing the ratio of CAR produced wafers which hydrated significantly more slowly and maintained the swollen formulation for a longer period of time hence, potentially applicable for sustained release drug delivery purposes (Fig. 2). Increasing the percentage of PEG however did not have a significant effect on the percentage swelling profiles. The "optimum" wafer with the highest mucoadhesive force contained 2% w/w CAR, 4% w/w POL and 4.4% w/w PEG within the original gel (Fig. 4). This formulation had an ideal work of compression profile 5.24 N.mm (flexible and tough) as shown in Fig. 2.

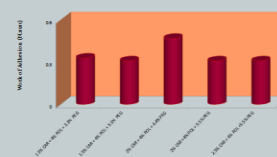


Fig. 3. Work of adhesion of wafers.

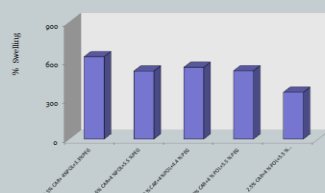


Fig. 3. Swelling profile of wafers.

Conclusion

The optimum formulation is one with a balance between flexibility, swelling capacity and mucoadhesivity to enable longer contact time and patient convenience during handling and application. This optimum wafer contained 2% w/w CAR, 4% w/w POL and 4.4 % w/w PEG. Wafers with higher CAR content remained longer on mucosal surface due to lower swelling rate. A reduction of CAR relative to PEG therefore produced desirable wafers.

References

- [1] R. Ossawa, M. S. Kamat and P. Deluca, "Hygroscopicity of cefazolin sodium: application to evaluate the crystallinity of freeze-dried product" *Pharm. Res.*, 5 (1988) 421-428.

Comparison between swelling and in vitro drug dissolution properties of mucosal films and freeze-dried wafers containing indomethacin



UNIVERSITY
of
GREENWICH

F. Kianfar, B.Z. Chowdhry, M.A. Antonijevic, J.S. Boateng

University of Greenwich, Chatham Maritime, UK



UNIVERSITY
of
GREENWICH

Introduction

The aim of this study was to investigate the differences between the swelling and dissolution properties of solvent cast films and freeze-dried wafers as buccal drug delivery systems. Buccal drug delivery dosage forms have gained increased attention in recent years due to advantages such as bypassing first pass liver metabolism and avoiding GI enzymatic degradation particularly of protein based drugs. They can be formulated as tablets, films or freeze-dried wafers [1]. Films and wafers are prepared by solvent casting or freeze-drying respectively, aqueous gels of polymer(s) of interest. The films form a continuous sheet while wafers form a porous polymeric inter-connecting network.

Material and Methods

Materials: Poloxamer 407, PEG 600 and indomethacin were purchased from Sigma-Aldrich (Gillingham, UK). κ -carrageenan 911 was a gift from BASF (Cheshire, UK).

Method: Gels comprising carrageenan 911 (CAR), poloxamer 407 (POL), PEG 600 and indomethacin were prepared by dispersing in deionised water with vigorous stirring at 50–60°C. The wafers and films were obtained by respectively freeze-drying or drying in an oven (60°C) the gels for 24 hours. The swelling of both formulations was investigated by weighing them initially and placing in PBS media (pH 6.2) for 2 hours and weight changes measured every 20 minutes. In vitro dissolution studies were conducted in the same media and the indomethacin released was detected by UV spectrophotometer at 5 minute intervals.

Result and Discussion

The swelling studies showed that swelling of wafers was significantly higher than the films. According to Fig. 1 the maximum swelling capacities of the blank and indomethacin loaded wafers were approximately 650 % and 680 % of the initial weight respectively. The indomethacin loaded films on the other hand showed maximum swelling capacity of around 470%. Interestingly, blank films showed higher swelling capacity (similar to wafers) when compared with indomethacin loaded equivalent, with complete hydration occurring in 100 minutes, which is 1.5 times longer than the time required for the corresponding drug loaded films.

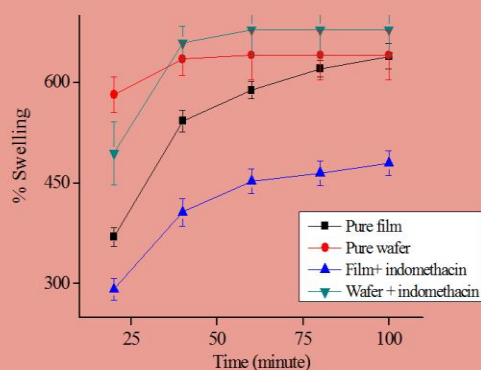


Fig. 1. Swelling profile of wafers and films

Result and Discussion

In addition, the maximum swelling for the wafers occurred within 40 minutes whereas films reached a maximum swelling after 80 minutes. These differences in rate of swelling can be attributed to the differences in the physical micro-structures of the wafers and films. The wafers which are porous allowed a faster rate of water hydration compared to the non-porous films.

The dissolution profiles (Fig. 2) showed that wafers released indomethacin faster than the films in the first 10 minutes. However, the overall release from the wafer within 60 minutes was lower than film.

This may relate to the presence of more drug particles on films' surface compared to the wafers. Both film and wafer dissolution showed a near constant release during the first 30 minutes followed by a slower rate of release (change in gradient of the curves) till 60 minutes. This could be due to the initial swelling of the polymer to form a gel and subsequent maintenance of the in vitro drug levels by diffusion from the swollen gel.

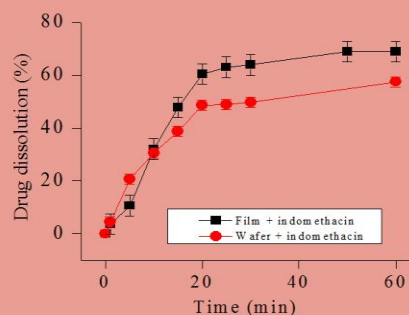


Fig. 2. Dissolution profiles of wafers and films

Conclusion

The swelling and dissolution studies show significant differences in swelling and dissolution properties of the CAR wafers and films. These differences could be exploited in different drug delivery (release mechanisms) applications to mucosal surfaces such the buccal mucosa.

References

[1] A.M. Hillery, A. W. Lloyd, J. Swarbrick, "Drug delivery and targeting for pharmacists and pharmaceutical scientists". London, Taylor and Francis, 2001, 7. 186-206.

Contacts

Farnoosh Kianfar
University of Greenwich at Medway
School of Science (Grenville building)
Central Avenue, Chatham Maritime, Kent ME4 4TB
T: 020-8331-7570
F:020-8331-9805
E: fk30@gre.ac.uk

Carrageenan freeze-dried wafers incorporating paracetamol or indomethacin for mucosal delivery

F. Kianfar, B. Chowdhry, M. Antonijevic, J. Boateng
University of Greenwich, UK



Purpose

Development of mucosal freeze-dried wafers containing κ -carrageenan, poloxamer 407 and PEG with optimum mechanical properties and drug loading capacity.

Material s

Poloxamer 407, PEG 600, paracetamol and indomethacin were purchased from Sigma-Aldrich (Gillingham, UK). κ -carrageenan 911 (bioadhesive) was a gift from BASF (Cheshire, UK).

Methods

Optimized wafers were prepared by hydration of 2.5% κ -carrageenan 911, 4% poloxamer 407 and 5.5% (w/w) PEG 600 in deionized water for 24 hours and heated to 70°C with stirring at 200 rpm for 10 minutes. Two model drugs (indomethacin, paracetamol) were individually added to the gel mixture and dispersed by continuous stirring.

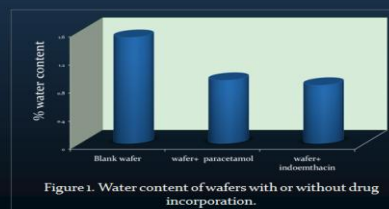
The ratio of drug to polymer in the mixture was gradually increased to determine the optimum amounts of each drug in the formulations.

Gels were freeze-dried to produce wafers with annealing (temperature cycled up and down) or without annealing (continuous freezing and drying). Wafers were characterized for water content (TGA), physical form of model drugs (DSC), morphology (SEM) and mechanical strength (texture analysis).

Results

The results demonstrated that the formulation formed using annealing contained approximately 1.5% of residual water and produced amorphous forms of the model drugs (DSC data) which were stable over six months storage. The SEM results verified formation of a porous wafer (Fig. 2a) and texture analysis confirmed adequate work of compression (data not shown) for ease of handling and application. In contrast, the wafers produced without annealing contained about 4% water and did not demonstrate appropriate porosity and work of compression due to the higher residual water within the wafer (Fig. 2b).

The observed differences in the porosity of the wafer were due to production of larger ice crystals in the annealing method, which sublimated more steadily during the secondary drying process and resulted in large pores compared to the "leafy" texture of the unannealed wafers which were also more plasticized. The maximum amounts of paracetamol and indomethacin incorporated within the matrix were 13% and 4% (w/w), respectively and attributed to differences in their aqueous solubility.



Figures

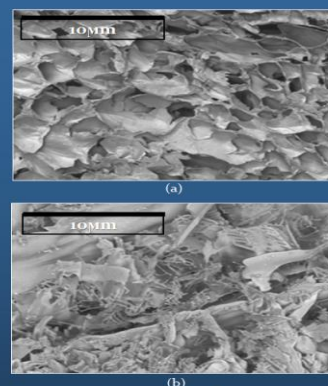


Figure 2. SEM of (a) annealed and (b) unannealed wafers.

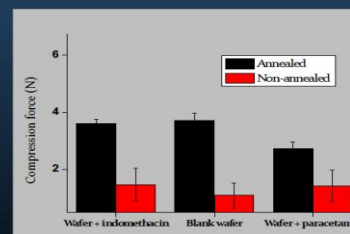


Figure 3. Work of compression profile for annealed wafer.

Conclusion

Annealing is a promising approach for the production of κ -carrageenan 911, poloxamer and PEG 600 wafers, with potential for delivering amorphous forms of either hydrophilic or hydrophobic drugs via mucosal routes.

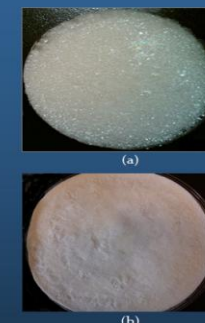


Figure 4. Blank freeze-dried wafers produce by (a) annealing (b) non-annealing process.

Contacts

Farnoosh Kianfar
University of Greenwich at Medway
School of Science (Grenville building)
Central Avenue, Chatham Maritime, Kent
ME4 4TB
T: 020-8331-7570
F:020-8331-9805
E: farnoosh1354@gmail.com

Development of stable polymeric lyophilised wafers for mucosal drug delivery using thermal annealing (DSC, freeze-drying)

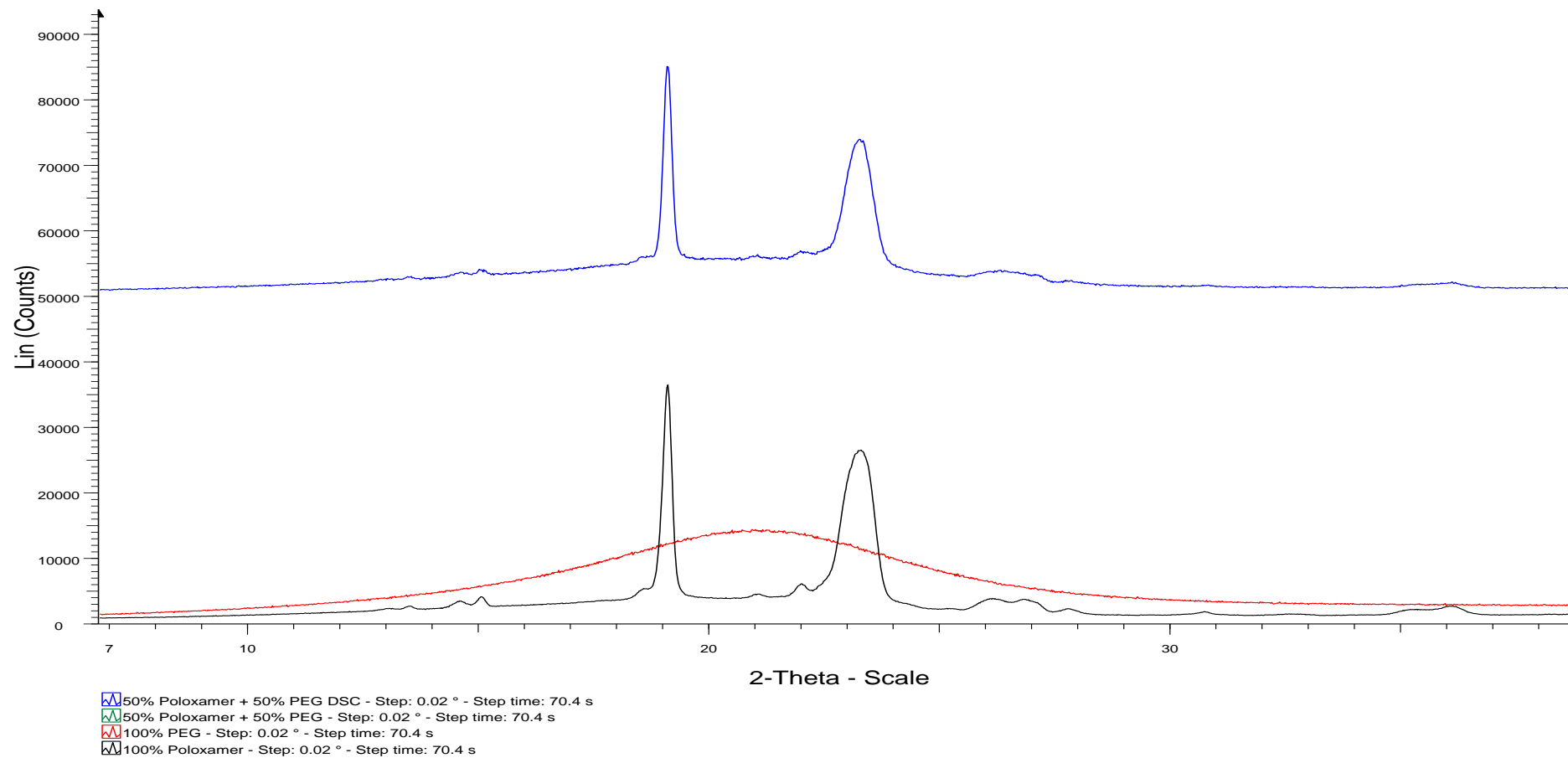
F. Kianfar, B. Chowdhry, M. Antonijevic, J. Boateng
University of Greenwich, UK

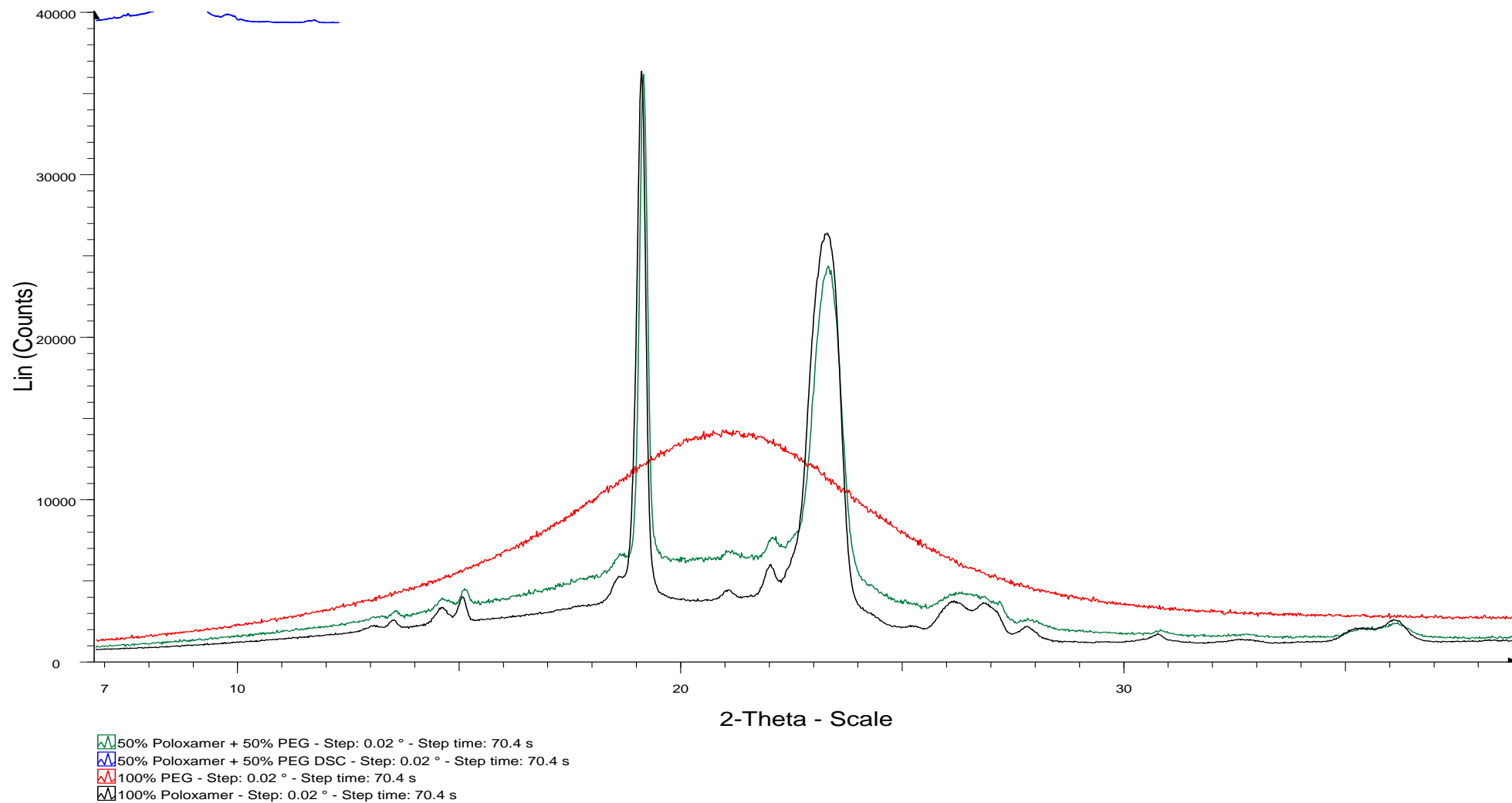


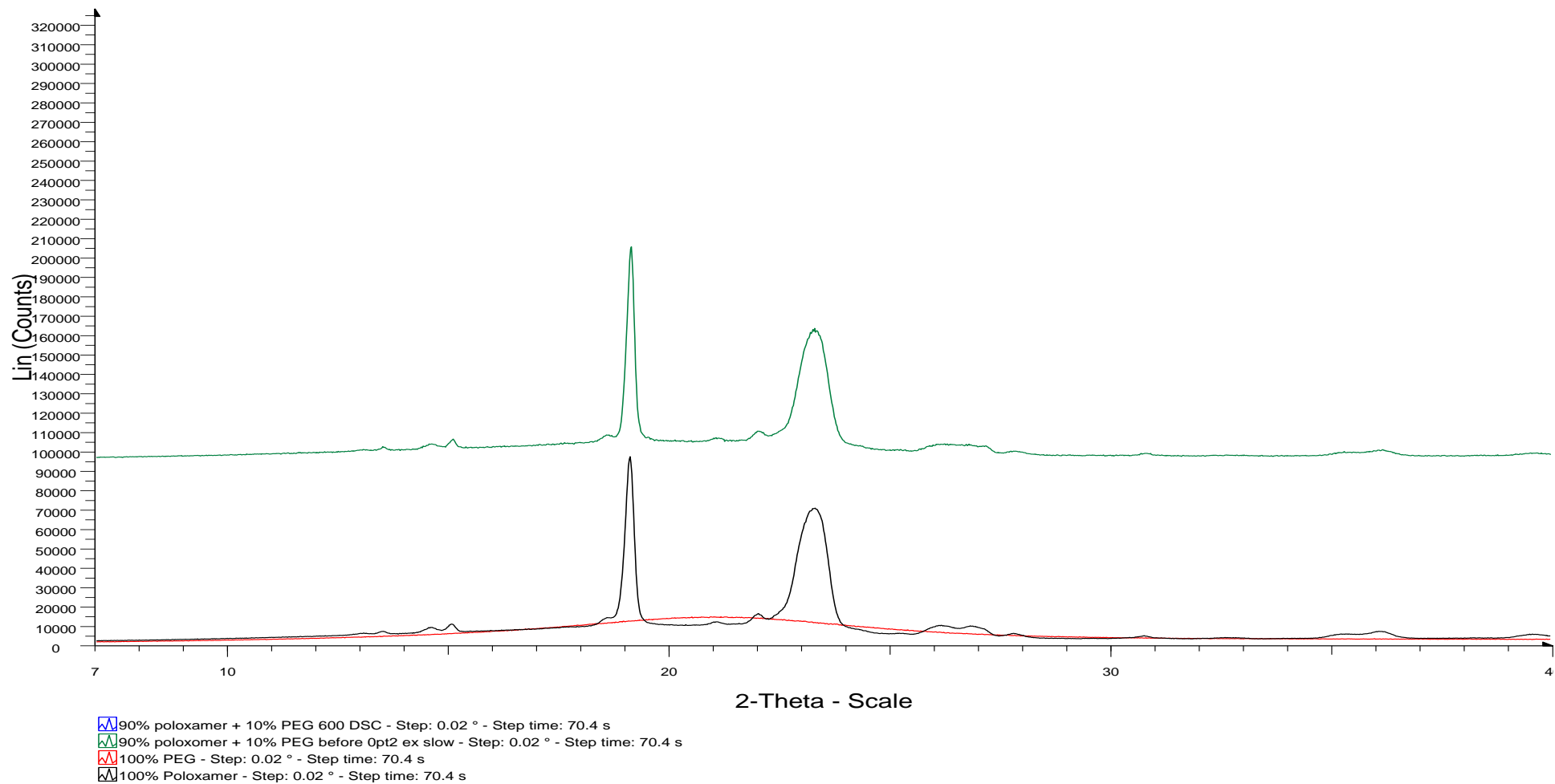
Purpose	Methods	Results	Results	Conclusion
<p>The aim was to develop an optimum freeze-drying cycle incorporating annealing to produce wafers from gels comprising κ-carrageenan, poloxamer 407 and PEG 600 with ibuprofen as a model drug. The effects of the annealing process and ibuprofen concentration on water content and mechanical properties of the wafers were also investigated.</p>	<p>10°C/min to detect the eutectic point after which gels were freeze-dried for 42 hours. The wafers obtained were compressed to a depth of 2 mm and the work of compression determined by texture analysis. 3-10mg of wafer was packed in TGA aluminium pans and heated to 150°C in order to determine the residual water content.</p>	<p>DSC analysis determined T_g values for the gel components and eutectic point of the mixture. The initial freeze-drying cycle involved cooling gels to -55°C (10°C below the minimum T_g of the compounds). Subsequently, annealing was performed by increasing the temperature to -35°C, returning to the initial temperature and maintaining for 2 hours (Fig 1). During primary drying the temperature was increased from -55°C to 0°C (5°C lower than the</p>	<p>eutectic point) to prevent melt back and preserve the stability of all the components. The TGA results showed water content of 1.0-1.4% and 5.2-5.5% for annealed and non-annealed wafers, respectively. The wafer's compressibility was directly affected by the annealing process and addition of ibuprofen to the system. Fig 2 shows ibuprofen loaded wafers with desirable mechanical characteristics.</p>	<p>An annealing process was developed to produce wafers from gels containing 2% carrageenan, 4% poloxamer 407, 4.4% PEG 600 and 0.8% w/w ibuprofen with improved compression characteristics in comparison with non-annealed wafers.</p>
<p style="text-align: center;">Methods</p> <p>Gels were prepared by dispersing 2% κ-carrageenan and 4% poloxamer in deionised water for 24 hours to allow complete hydration before homogenization with PEG 600 and ibuprofen, poured into six well plates. 3-10 mg of gel was also loaded into T-zero pans and analysed using a Q2000-DSC from -80 to 100°C at a rate of</p>	<p style="text-align: center;">Contacts</p> <p>Farnoosh Kianfar University of Greenwich Chatham Maritime, UK E.mail:fk30@gre.ac.uk Tel: +44 -7897593856</p>	<div style="text-align: center;"> </div> <p>Fig 1. Details of the freeze-drying process comprising freezing and primary/secondary drying processes.</p>		
<div style="text-align: center;"> </div> <p>Fig 2. Compression profile for annealed and non-annealed wafers.</p>				

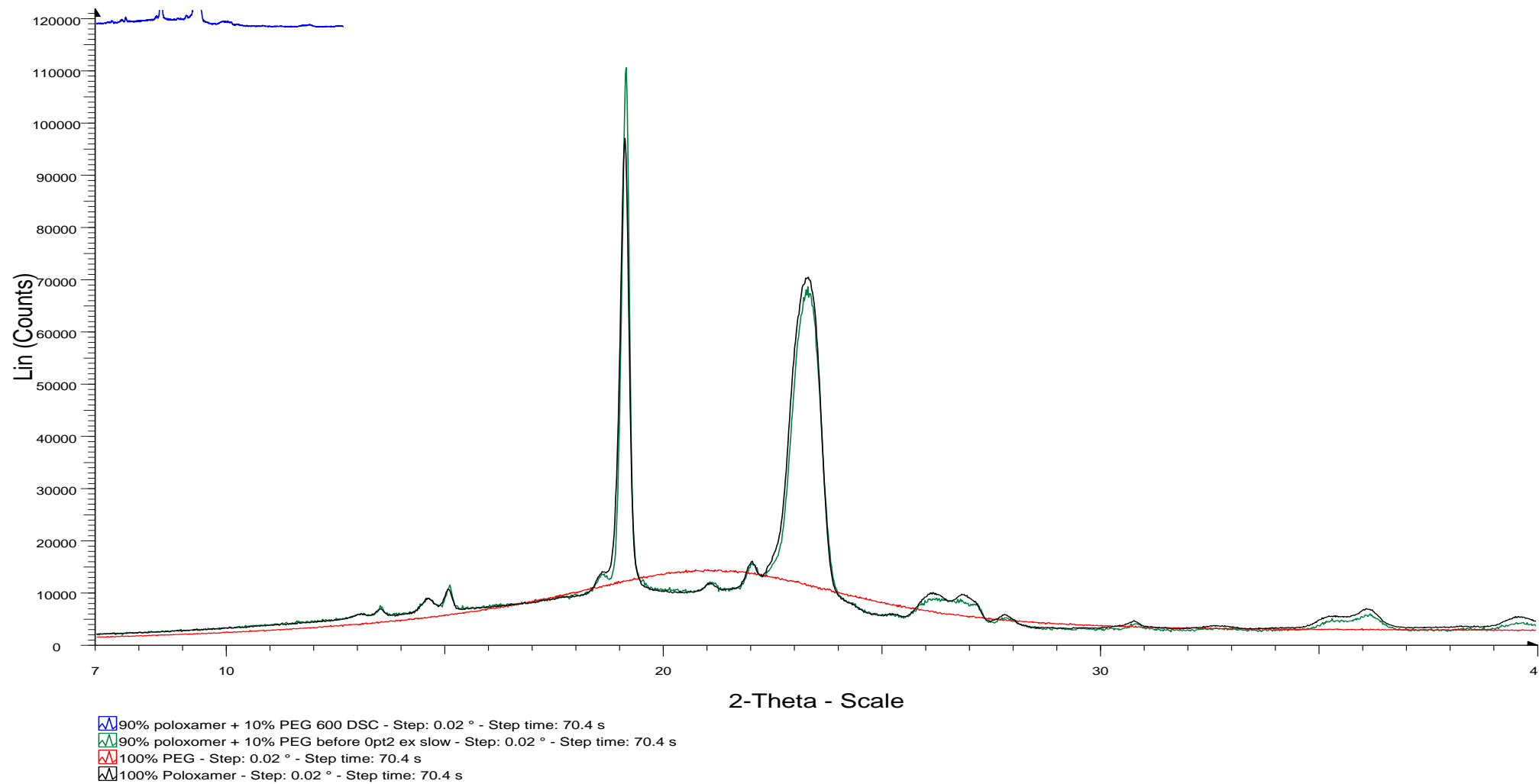
9.4 Supplementary results

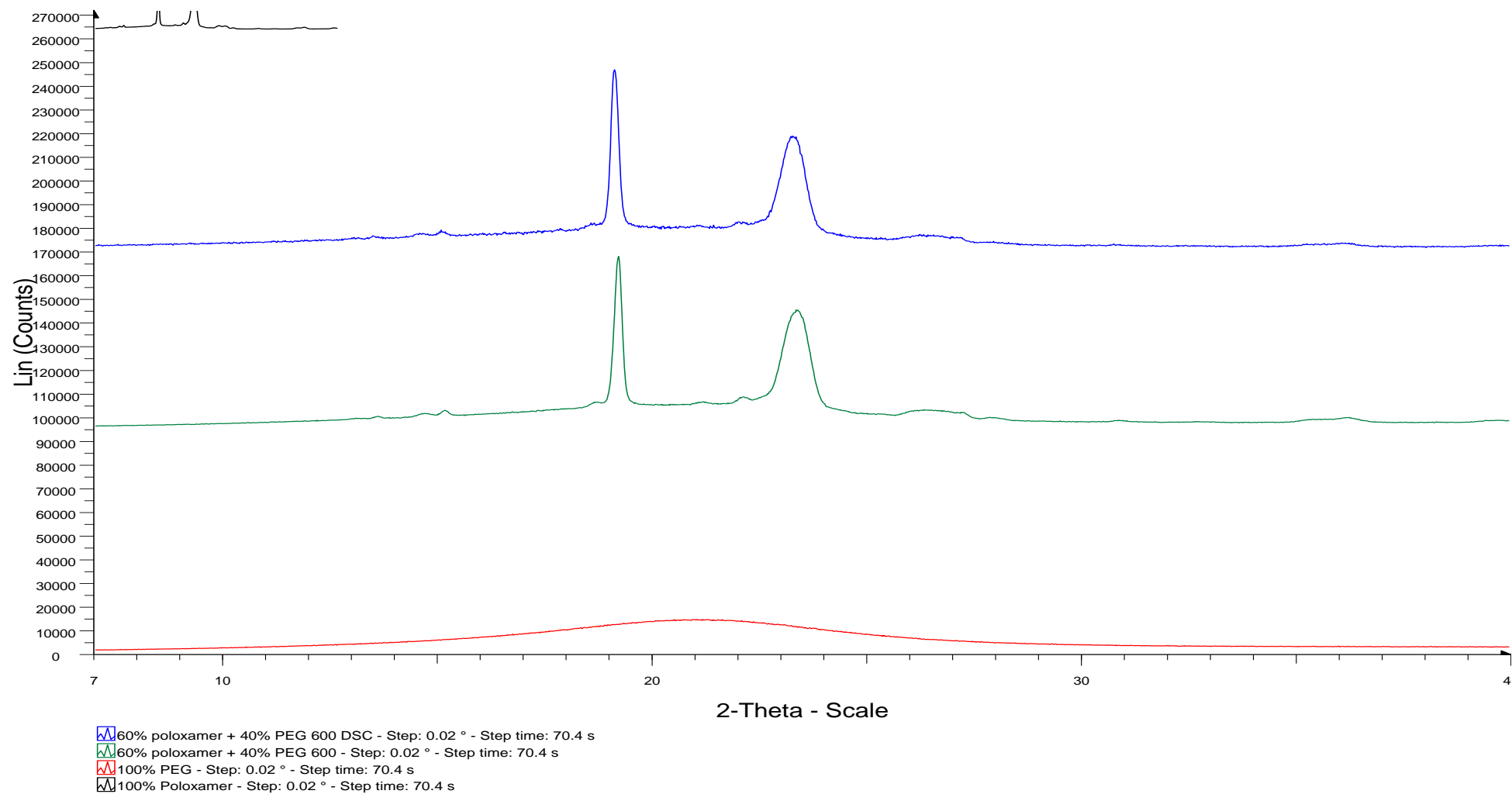
XRPD results for physical mixture of 50% P407 and 50% PEG 600 after DSC run

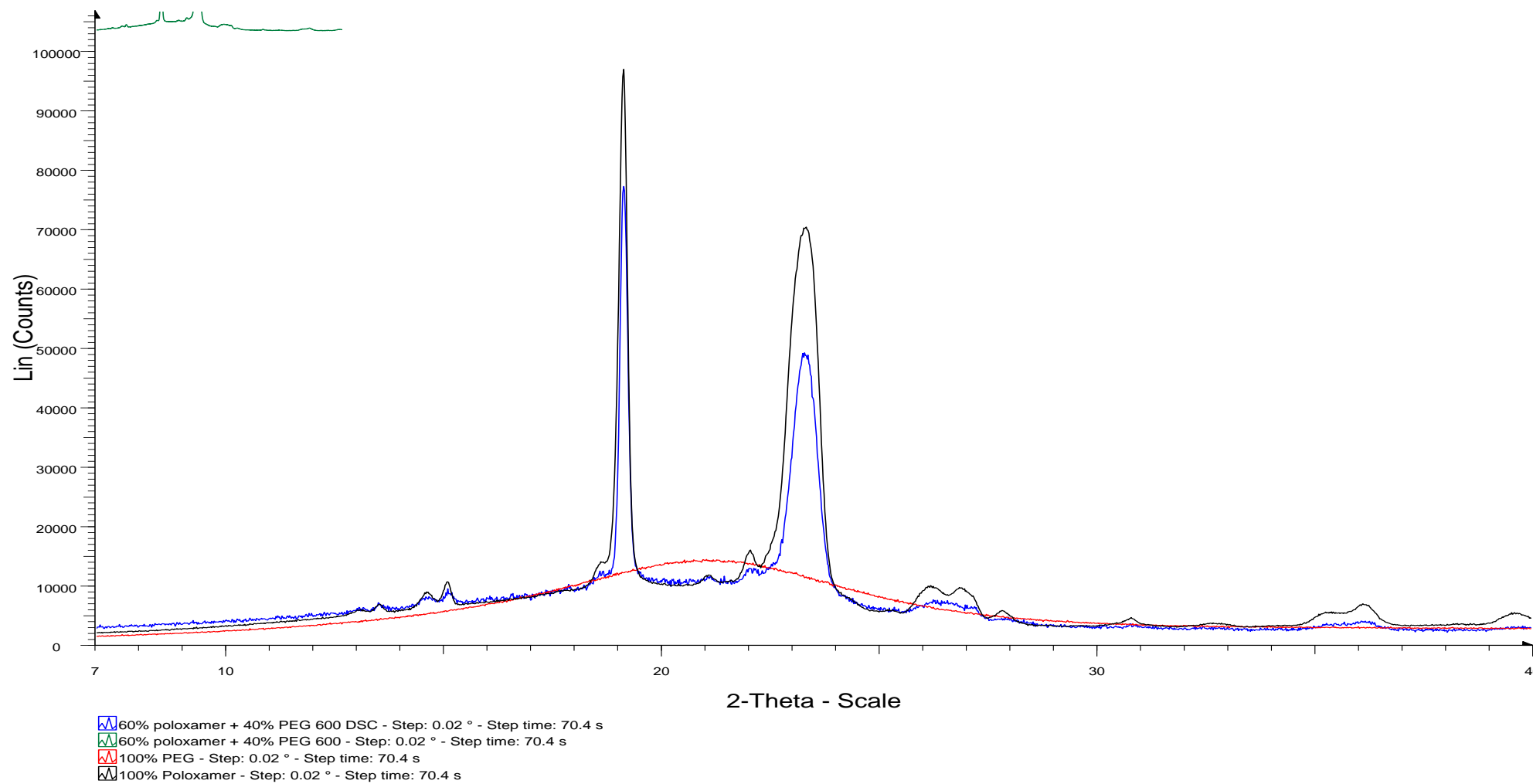


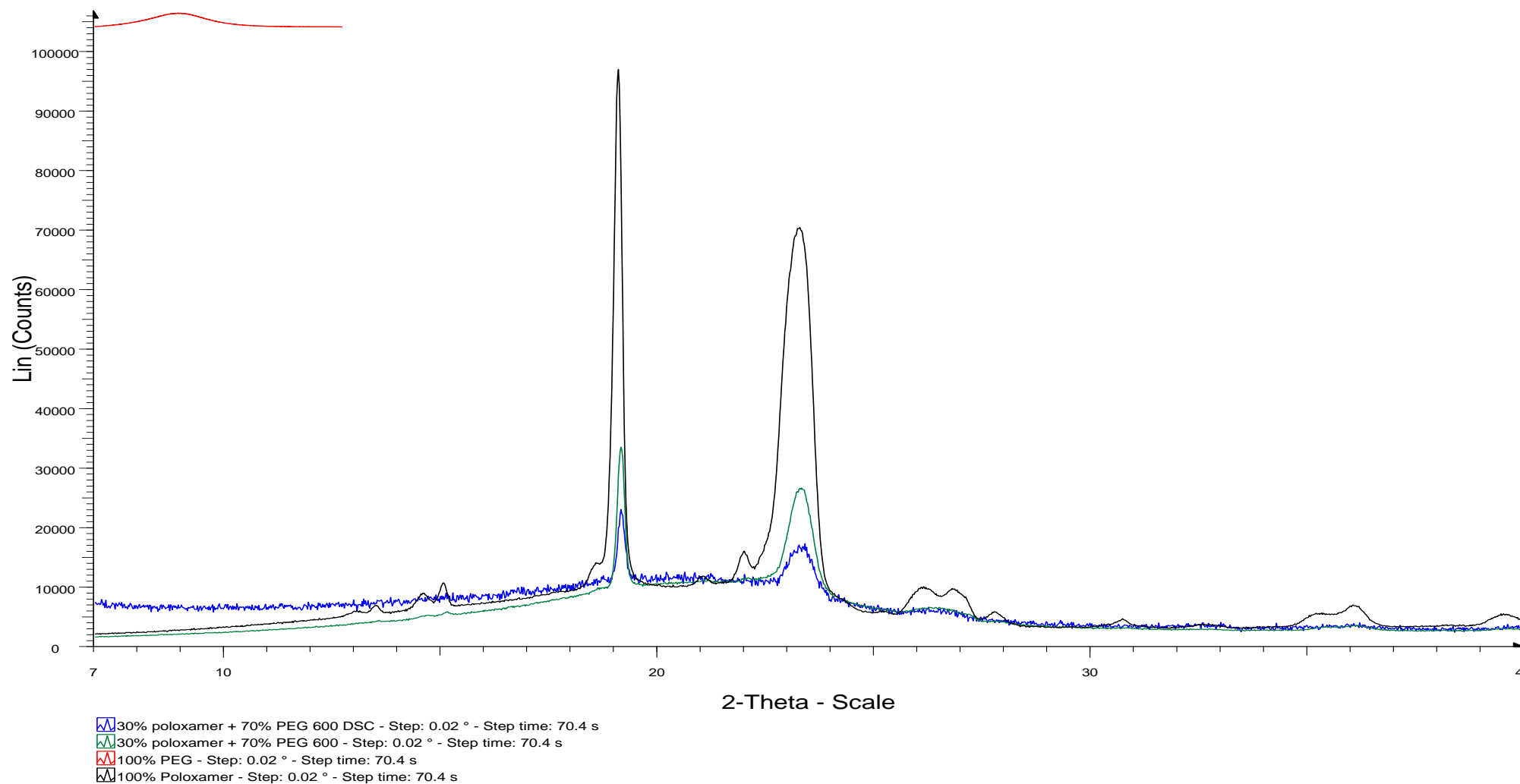
XRPD results for physical mixture of 50 % P407 and 50% PEG 600 before DSC run

XRPD results for physical mixture of 90% P407 and 10% PEG 600 after DSC run

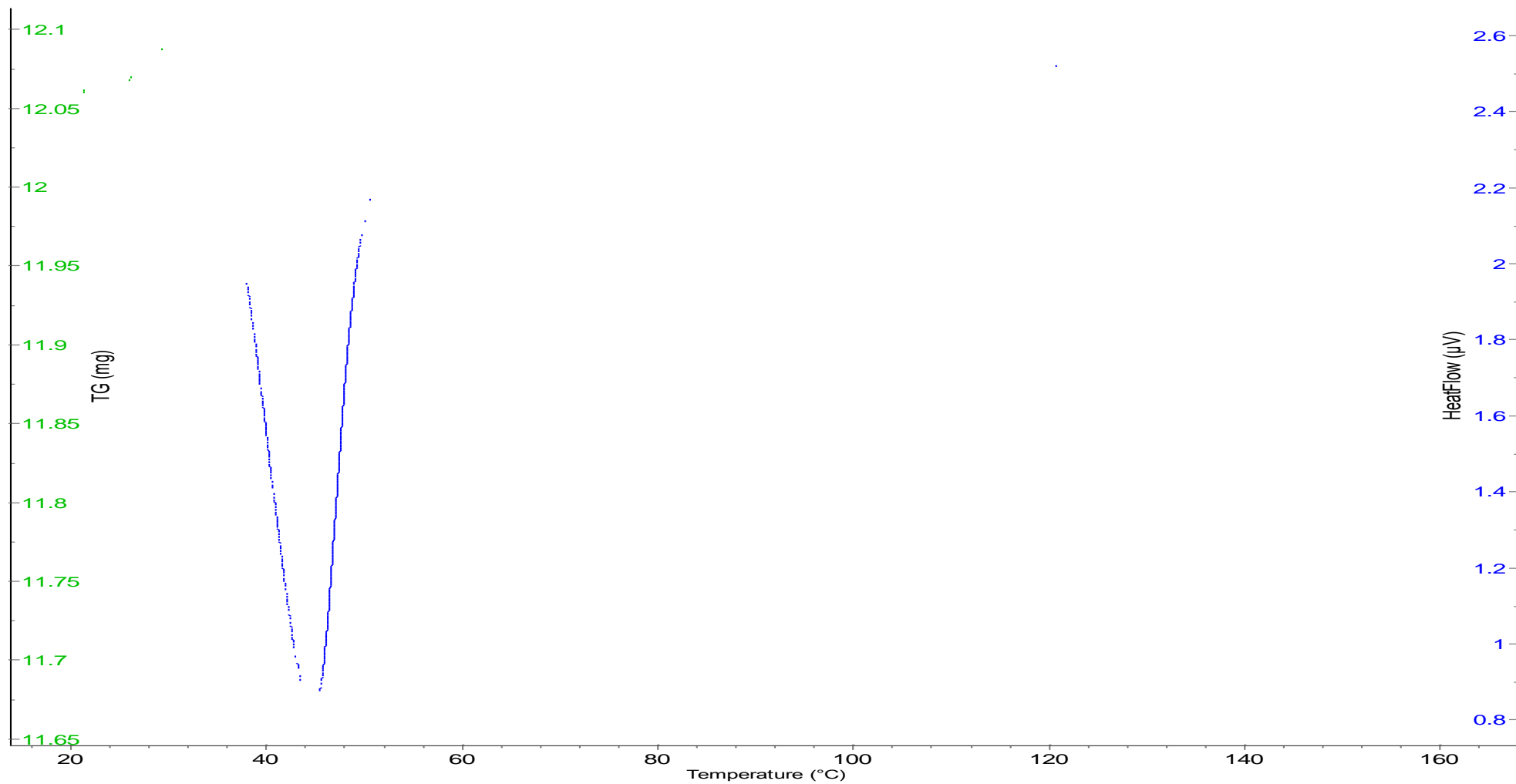
XRPD results for physical mixture of 90% P407 and 10% PEG 600 after DSC run

XRPD results for physical mixture of 60% P407 and 40% PEG 600 after DSC run

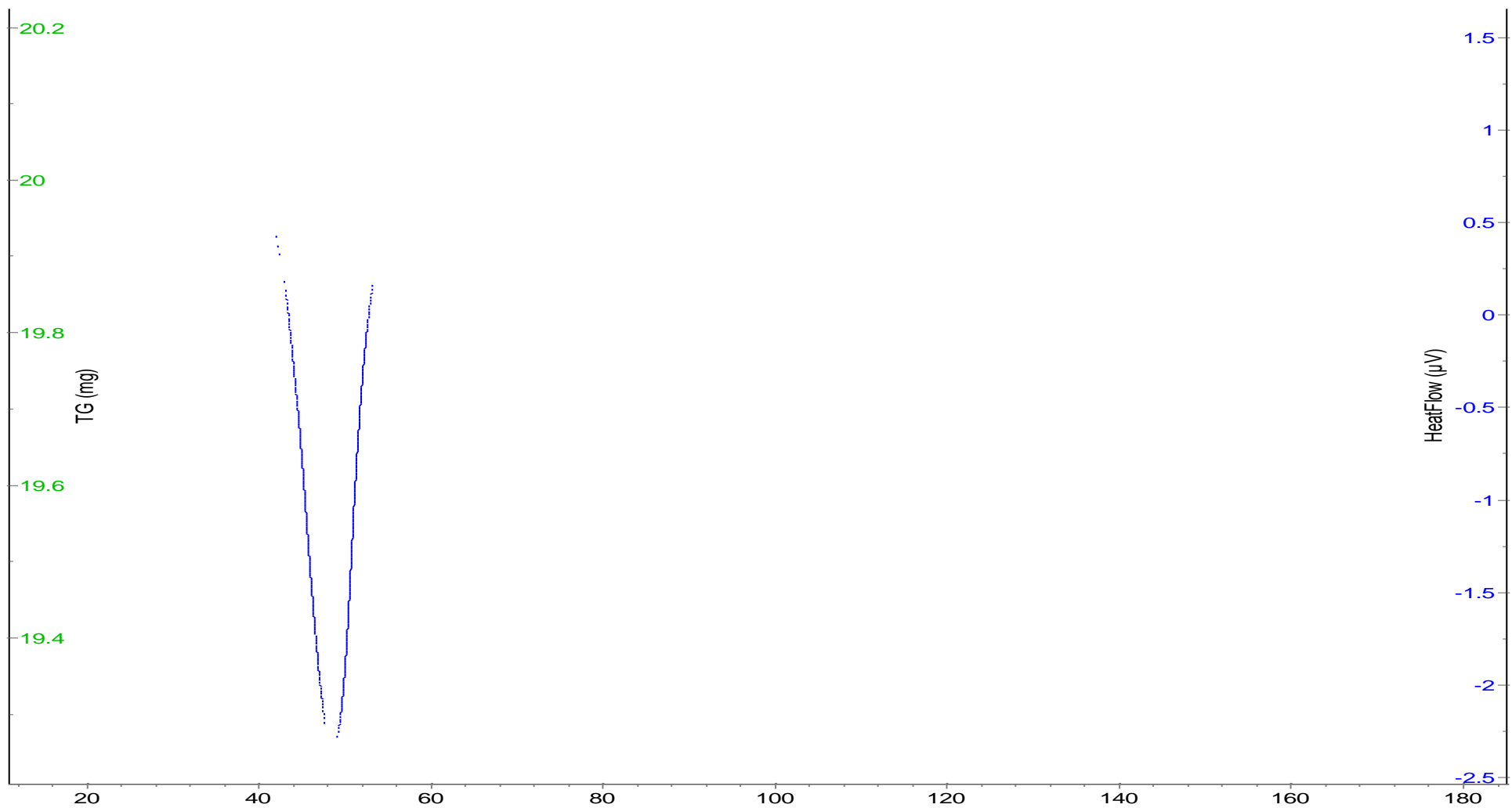
XRPD results for physical mixture of 90% P407 and 10% PEG 600 after DSC run

XRPD results for physical mixture of 30% P407 and 70%PEG 600 after DSC run

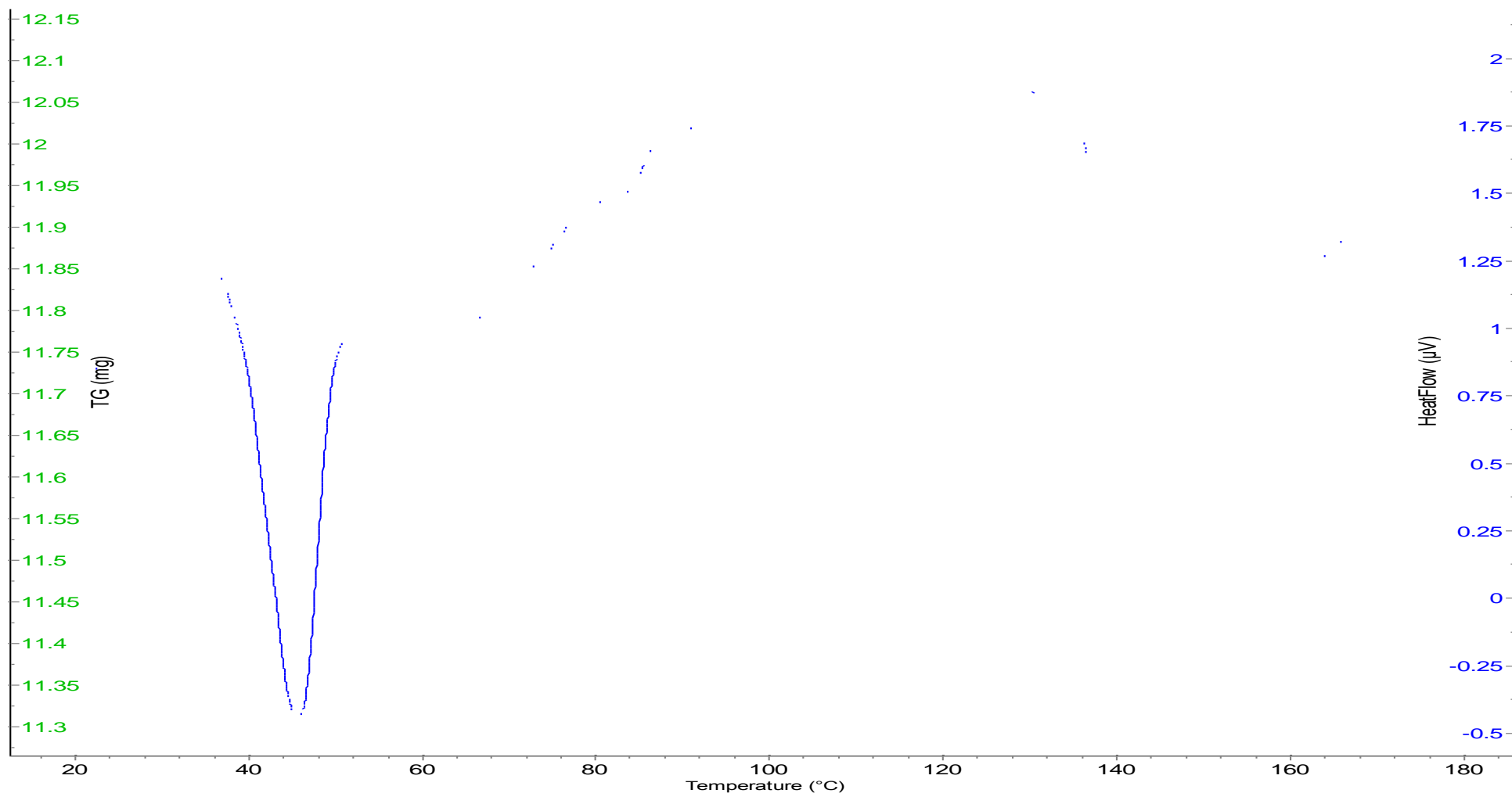
TGA result for PM loaded films and wafers stored for 1 month



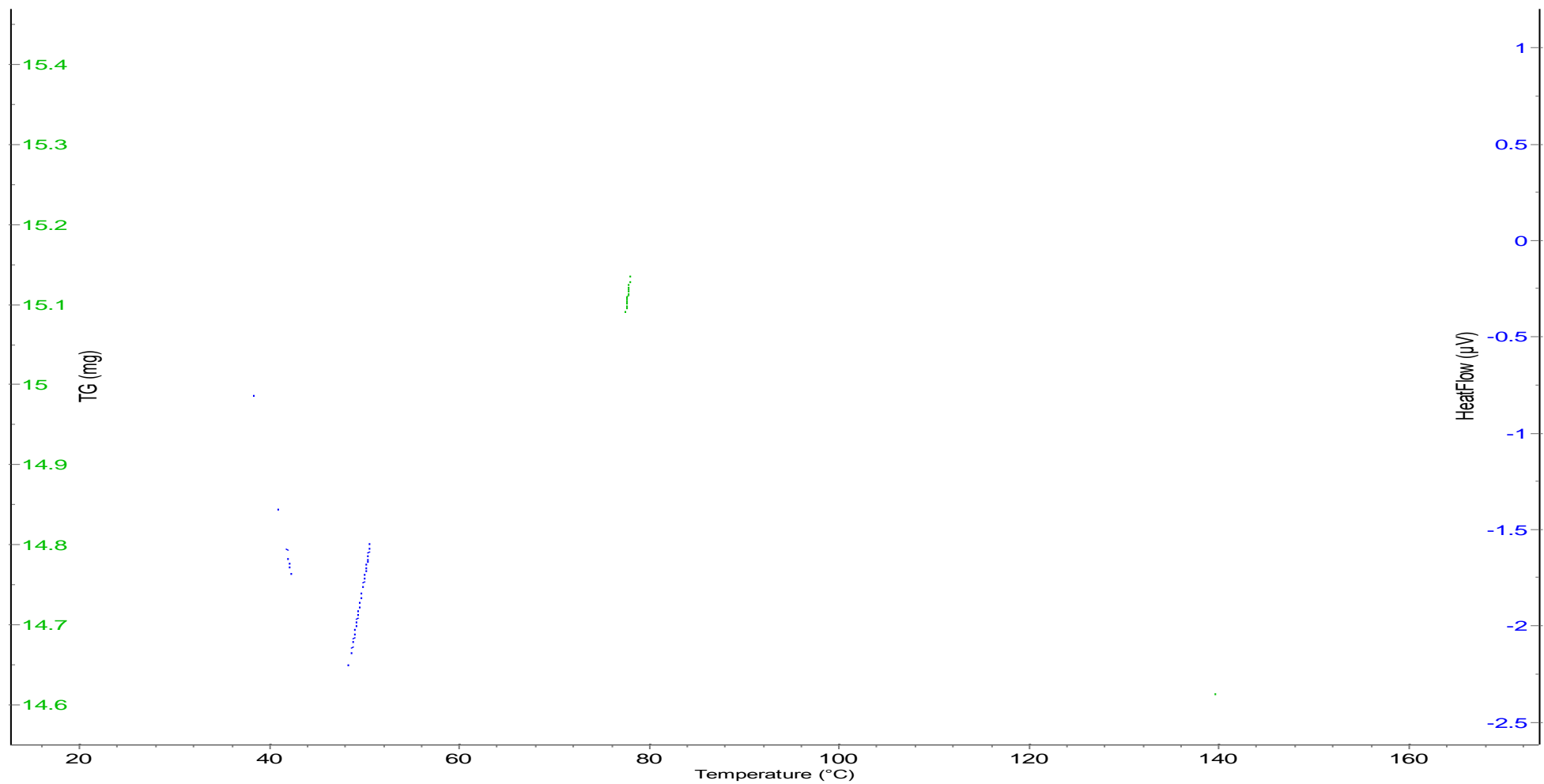
TGA results for IND loaded films stored for 1 month



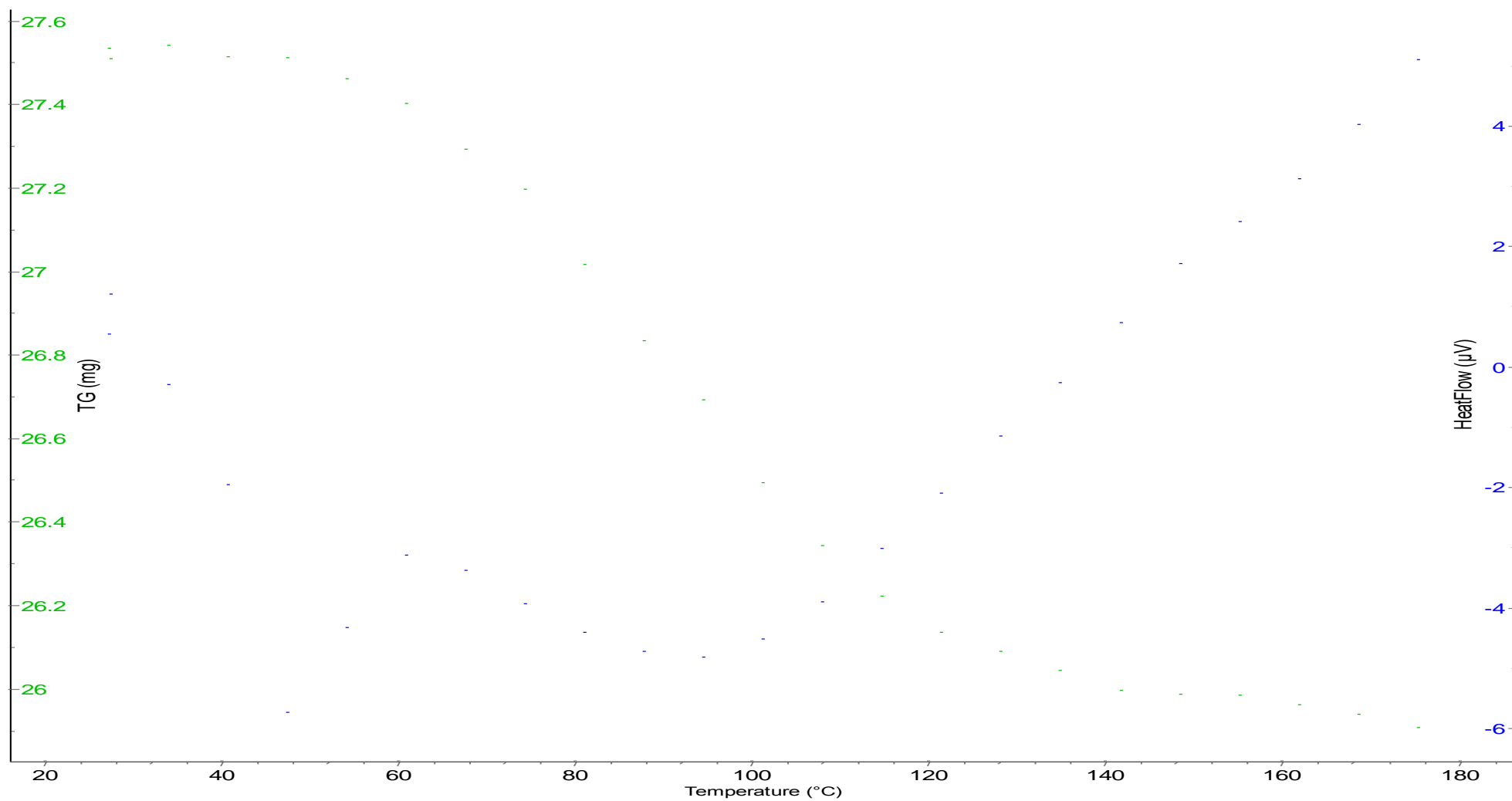
TGA results for IBU loaded films and wafers stored for 1 month



TGA results for PM loaded films and wafers stored for 6 months



TGA results for IND loaded films and wafers stored for 6 months



TGA results for IBU loaded films and wafers stored for 6 months

